

## SEMI-ANNUAL REPORT

DEVELOPMENT OF COMPRESSOR END SEALS,  
STATOR INTERSTAGE SEALS, AND STATOR PIVOT  
SEALS IN ADVANCED AIR BREATHING  
PROPULSION SYSTEMS

Prepared for

NATIONAL AERONAUTICS AND SPACE ADMINISTRATION

January 20, 1966

CONTRACT NAS3-7605

Technical Management  
NASA Lewis Research Center  
Cleveland, Ohio  
Spacecraft Technology DivisionD. P. Townsend  
Project ManagerL. P. Ludwig  
Research Advisor

Written by:

R. M. HawkinsR. M. Hawkins  
Assistant Program ManagerC. A. KnappC. A. Knapp  
Program Manager

Approved by:

D. B. Waring  
D. B. Waring *10/4/66*  
Development Engineer

Pratt &amp; Whitney Aircraft

DIVISION OF UNITED AIRCRAFT CORPORATION

U  
A

E A S T   H A R T F O R D   •   C O N N E C T I C U T

## PREFACE

This report describes the progress of work conducted between 29 June and 31 December 1965 by the Pratt & Whitney Aircraft Division of United Aircraft Corporation, East Hartford, Connecticut on Contract NAS3-7605, Development of Compressor End Seals, Stator Interstage Seals, and Stator Pivot Seals in Advanced Air Breathing Propulsion Systems, for the Lewis Research Center of the National Aeronautics and Space Administration.

Charles A. Knapp is Project Manager for Pratt & Whitney Aircraft for this program.

The following National Aeronautics and Space Administration personnel have been assigned to this project:

|                        |   |                |
|------------------------|---|----------------|
| Contracting Officer    | - | J. B. Vance    |
| Contracting Officer    | - | J. H. DeFord   |
| Project Manager        | - | D. P. Townsend |
| Research Advisor       | - | L. P. Ludwig   |
| Contract Administrator | - | T. J. Charney  |

## SUMMARY

This report describes the work completed during the first six months of an analytical, design, and experimental program directed at developing compressor end seals, stator interstage seals, and stator pivot seals for advanced air breathing propulsion systems.

The objective of this contract is to achieve a means of increasing compressor efficiency by providing compressor seals with significantly lower air leakage rates than those currently in use while not incurring undue penalties in reliability and weight.

The program involves a screening study of all potential types of seals and a detailed feasibility analysis of those recommended for further evaluation. This feasibility analysis is to be followed by design and procurement of seals for rig evaluation. Test rigs simulating advanced engine construction, where applicable, will be procured for evaluation of these seals under specified operating conditions. Mechanical Technology Incorporated, under subcontract to Pratt & Whitney Aircraft, is to conduct an analytical program contributing to the feasibility analysis (Tasks I and III) of the prime contract.

Pratt & Whitney Aircraft is supplying MTI with information required to evaluate engine application of various seal concepts and is monitoring MTI's efforts through periodic meetings, as required under terms of the prime contract.

NASA approval was obtained for the screening studies of compressor seal concepts required under Task I and Task III.

Work was initiated by MTI on a detailed feasibility analysis of four compressor end seal, four stator interstage seal, and two stator pivot seal concepts, with the major emphasis placed upon the analysis of primary seal faces.

A two and one half month extension of the prime contract was requested by Pratt & Whitney Aircraft, as a result of a reschedule of the MTI analytical effort. A supplemental agreement, effective 13 December 1965, was received from NASA extending the Period of Performance from twenty-four (24) months to twenty-six and one-half (26 1/2) months.

Preliminary design work was initiated on Task II and Task IV test rigs in which Task I compressor end seal and stator interstage seal and Task III stator pivot seal experimental evaluation will be conducted.

Milestone charts are presented at the end of this report as Figures 87 and 88.

## TABLE OF CONTENTS

|  | <u>Page No.</u> |
|--|-----------------|
| PREFACE  | ii              |
| SUMMARY  | iii             |
| LIST OF ILLUSTRATIONS  | vii             |
| LIST OF TABLES   | xiii            |
| INTRODUCTION   | 1               |
| <u>TASK I - CONCEPT FEASIBILITY ANALYSIS PROGRAMS</u><br><u>FOR COMPRESSOR END SEALS AND FOR STATOR</u><br><u>INTERSTAGE SEALS</u> | 2               |
| MTI SCREENING STUDY  | 2               |
| SUMMARY OF SCREENING STUDY   | 3               |
| Concept I - One-Sided Floated Shoe   | 5               |
| Concept II - Two-Sided Floated Shoe  | 5               |
| Concept III - Thin Strip Plus Piston Ring  | 5               |
| Concept IV - Thin Strip Plus C Diaphragm   | 5               |
| Concept V - Thin Strip Plus C Diaphragm (Radial)   | 5               |
| PRELIMINARY CONSIDERATIONS   | 6               |
| Basic Leakage Rate   | 6               |
| Film Thickness for Minimum Power Loss  | 9               |
| Thermal Distortion   | 11              |
| Tracking Dynamics  | 16              |
| Primary and Secondary Seals  | 19              |
| PRIMARY SEAL BEHAVIOR  | 20              |
| Hydrostatic-Step Seal  | 20              |
| Hydrostatic-Orific Compensated Seal  | 24              |
| Hydrostatic-Labyrinth Seal   | 27              |
| Hydrodynamic-Convergent Film   | 30              |
| Hydrodynamic-Spiral Groove Seal  | 32              |
| Hybrid Hydrostatic-Hydrodynamic Seal   | 33              |
| Hybrid Hydrostatic Pad-Labyrinth Seal  | 34              |
| COMPARISON OF PRIMARY SEAL CONCEPTS  | 34              |

## TABLE OF CONTENTS (Cont'd)

|   | <u>Page No.</u> |
|---|-----------------|
| SECONDARY SEAL BEHAVIOR   | 36              |
| Hydrostatic   | 37              |
| Bellows   | 38              |
| Piston Rings  | 38              |
| Diaphragm   | 38              |
| SCREENING OF SUGGESTED END AND INTER-STAGE SEAL DESIGNS                                 | 40              |
| General Discussion  | 40              |
| Description of Seal Concepts  | 52              |
| MTI FEASIBILITY ANALYSIS  | 59              |
| SUMMARY OF FEASIBILITY ANALYSIS   | 59              |
| Primary Seal Analysis   | 59              |
| Seal Response   | 60              |
| Seal Design   | 60              |
| PRIMARY SEAL FEASIBILITY ANALYSIS   | 60              |
| The Hydrostatic Step Seal   | 61              |
| Spiral Groove Hydrodynamic Seals  | 77              |
| Rayleigh Step   | 82              |
| Hydrostatic Orifice Compensated Seal  | 82              |
| Hydrostatic Labyrinth Seal  | 90              |
| Multiple-Pad Designs With Thin Strip Seal   | 91              |
| Seal Response   | 98              |
| SEAL DESIGN   | 112             |
| Review of Concept V   | 112             |
| Primary Seal For Hydrostatic Floated - Shoe Designs                                     | 113             |
| PRATT & WHITNEY AIRCRAFT PROGRAM  | 115             |
| Approval of Screen Study Seal Concepts  | 115             |
| Dimensional Variance Considerations   | 123             |
| Analytical Program  | 124             |
| <u>TASK II - COMPRESSOR END SEAL AND STATOR INTERSTAGE SEAL EXPERIMENTAL EVALUATION</u> | 125             |

## TABLE OF CONTENTS (Cont'd)

|  | <u>Page No.</u> |
|--|-----------------|
| <u>TASK III - COMPRESSOR STATOR PIVOT BUSHING<br/>AND SEAL CONCEPT FEASIBILITY ANALYSIS</u>                    | 126             |
| MTI SCREENING OF VANE PIVOT SEAL DESIGNS   | 126             |
| Screening  | 130             |
| Screening Chart  | 133             |
| MTI VANE-PIVOT SEAL FEASIBILITY ANALYSIS   | 135             |
| PRATT & WHITNEY AIRCRAFT PROGRAM   | 138             |
| <u>TASK IV - PIVOT BUSHING AND SEAL EXPERIMENTAL<br/>EVALUATION</u>  | 142             |
| PROGRAM SCHEDULE & MILESTONE CHART   | 144             |
| APPENDIX A - FILM THICKNESS OPTIMIZATION STUDY   | 146             |
| APPENDIX B - SOLUTION OF A HYBRID LUBRICATION<br>PROBLEM WITH RAYLEIGH STEPS AND<br>CYCLIC BOUNDARY CONDITIONS | 152             |
| APPENDIX C - CENTER OF PRESSURE, HYDROSTATIC<br>STEP-COMPUTER PROGRAM  | 167             |
| APPENDIX D - PRESSURE AND FLOW, SPIRAL GROOVE<br>SEAL - COMPUTER PROGRAM                                       | 169             |
| BIBLIOGRAPHY   | 170             |
| REFERENCES   | 171             |
| DISTRIBUTION LIST  | 172             |

## LIST OF ILLUSTRATIONS

| Figure No. | Title  | Page No. |
|------------|--|----------|
| 1          | Leakage Rate vs Film Thickness for a Typical Seal  | 9        |
| 2          | Optimization of Compressor Power Due to Leakage vs Drag Power Loss for Take-Off Conditions | 10       |
| 3          | Optimization of Compressor Power Due to Leakage vs Drag Power Loss for Cruise Conditions   | 11       |
| 4          | Model for Simple Thermal Analysis  | 12       |
| 5          | Calculated Temperatures for a Floated Shoe Design  | 12       |
| 6          | Calculated Temperatures for a Floated Shoe Design Using Thermal Shunts                     | 13       |
| 7          | Distorted Seal Segment   | 13       |
| 8          | Simplified One-Dimensional Vibration Model for Seal Segment and Rotor System               | 17       |
| 9          | Basic Primary Seal Concepts  | 20       |
| 10         | The Hydrostatic Step Seal  | 21       |
| 11         | The Hydrostatic Orifice Compensated Seal   | 24       |
| 12         | Flow Through an Orifice  | 26       |
| 13         | The Hydrostatic Labyrinth Seal   | 28       |
| 14         | Flow Through a Double Knife Edge Labyrinth   | 29       |
| 15         | Inclined Slider Seal Segment   | 30       |
| 16         | Spiral Groove Hydrodynamic Seal  | 32       |
| 17         | Hybrid Hydrostatic Step-Hydrodynamic Seal  | 33       |
| 18         | Comparison of Seal Leakage Rates for Cruise Operation                                      | 35       |

## LIST OF ILLUSTRATIONS (Cont'd)

| Figure No. | Title   | Page No. |
|------------|---|----------|
| 19         | Comparison of Load-Film Thickness Seal Characteristics            | 35       |
| 20         | Types of Secondary Seal   | 36       |
| 21         | Hydrostatic Secondary Seal  | 37       |
| 22         | Diaphragm-Type Secondary Seal                                     | 39       |
| 23         | Load Curve-Hydrostatic Step, $\bar{b}_1 = .75$                    | 62       |
| 24         | Load Curve-Hydrostatic Step, $\bar{b}_1 = .5$                     | 63       |
| 25         | Load Curve-Hydrostatic Step, $\bar{b}_1 = .35$                    | 65       |
| 26         | Load Curve-Hydrostatic Step, $\bar{b}_1 = .25$                    | 64       |
| 27         | Load Curve-Hydrostatic Step, $\bar{b}_1 = .125$                   | 64       |
| 28         | Center of Pressure-Hydrostatic Step, $\bar{b}_1 = .125$           | 65       |
| 29         | Center of Pressure-Hydrostatic Step, $\bar{b}_1 = .25$            | 65       |
| 30         | Center of Pressure-Hydrostatic Step, $\bar{b}_1 = .35$            | 66       |
| 31         | Center of Pressure-Hydrostatic Step, $\bar{b}_1 = .5$             | 66       |
| 32         | Center of Pressure-Hydrostatic Step, $\bar{b}_1 = .75$            | 67       |
| 33         | Dimensionless Film Stiffness-Hydrostatic Step, $\bar{b}_1 = .125$ | 69       |
| 34         | Dimensionless Film Stiffness-Hydrostatic Step, $\bar{b}_1 = .25$  | 70       |
| 35         | Dimensionless Film Stiffness-Hydrostatic Step, $\bar{b}_1 = .35$  | 70       |
| 36         | Dimensionless Film Stiffness-Hydrostatic Step, $\bar{b}_1 = .5$   | 71       |
| 37         | Dimensionless Film Stiffness-Hydrostatic Step, $\bar{b}_1 = .75$  | 71       |



## LIST OF ILLUSTRATIONS (Cont'd)

| Figure No. | Title   | Page No. |
|------------|---|----------|
| 38         | Dimensionless Mass Flow-Hydrostatic Step,<br>$\bar{b}_1 = .125$   | 74       |
| 39         | Dimensionless Mass Flow-Hydrostatic Step,<br>$\bar{b}_1 = .25$  | 75       |
| 40         | Dimensionless Mass Flow-Hydrostatic Step,<br>$\bar{b}_1 = .35$  | 75       |
| 41         | Dimensionless Mass Flow-Hydrostatic Step,<br>$\bar{b}_1 = .5$   | 76       |
| 42         | Dimensionless Mass Flow-Hydrostatic Step,<br>$\bar{b}_1 = .75$  | 76       |
| 43         | Hydrodynamic, Spiral-Grooved Seal   | 77       |
| 44         | Dimensionless Flow vs Pressure Ratio<br>Spiral-Grooved Seal   | 80       |
| 45         | Dimensionless Flow vs Pressure Ratio<br>Spiral-Grooved Seal   | 81       |
| 46         | Coefficients $K_1$ and $K_2$ for Spiral-Grooved Seal  | 81       |
| 47         | Hydrostatic Orifice-Load  | 86       |
| 48         | Hydrostatic Orifice-Load  | 86       |
| 49         | Hydrostatic Orifice-Load  | 87       |
| 50         | Hydrostatic Orifice-Flow  | 87       |
| 51         | Hydrostatic Orifice-Stiffness   | 88       |
| 52         | Hydrostatic Orifice-Stiffness   | 88       |
| 53         | Hydrostatic Orifice-Stiffness   | 89       |
| 54         | Discharge Coefficient for Orifices. Experi-<br>mental Data to Generate this Curve were Taken<br>From Reference 3. | 89       |
| 55         | Hydrostatic Labyrinth-Load Curves   | 90       |

## LIST OF ILLUSTRATIONS (Cont'd)

| Figure No. | Title  | Page No. |
|------------|--|----------|
| 56         | Angular Displacement of Thin Strip Seal  | 91       |
| 57         | Double Orifice Primary Seal with Spiral Grooves  | 94       |
| 58         | Cross-Section of a Double-Orifice Design   | 95       |
| 59         | Double Pad Seals with Central Vent Groove  | 96       |
| 60         | Tilting of Double Pad Seal   | 97       |
| 61         | Dynamic Response Ratio   | 98       |
| 62         | Dynamic Response Ratio - Enlarged Scale  | 99       |
| 63         | Thin Strip Seal Ring   | 99       |
| 64         | Diagram Showing Unwrapped Seal Ring Deflection Curve and Rotor Contour                         | 100      |
| 65         | Force and Moment Diagram of a Seal Ring Segment  | 101      |
| 66         | Force Distribution Across Tilted Seal  | 103      |
| 67         | Twist of Seal Section  | 104      |
| 68         | Thin Strip Radial Seal   | 112      |
| 69         | Comparison of Stiffness for Orifice and Step Hydrostatic Seals                                 | 113      |
| 70         | Stiffness Flow Criterion vs Width Ratio  | 114      |
| 71         | Compressor End Seal Concept Scheme A -<br>Ref PWA Drawing No. L-67714 Ref MTI<br>Sketch-D-2116 | 115      |
| 72         | Compressor End Seal Concept Scheme C -<br>Ref PWA Drawing No. L-67714 Ref MTI<br>Sketch-D-2134 | 116      |
| 73         | Compressor End Seal Concept Scheme D -<br>Ref PWA Drawing No. L-67714 Ref MTI<br>Sketch-D-2132 | 117      |

## LIST OF ILLUSTRATIONS (Cont'd)

| Figure No. | Title  | Page No. |
|------------|--|----------|
| 74         | Compressor End Seal Concept Scheme E -<br>Ref PWA Drawing No. L-67714 Ref MTI<br>Sketch-D-2118                 | 118      |
| 75         | Stator Interstage Seal Concept Scheme A -<br>Ref PWA Drawing No. L-67713 Ref MTI<br>Sketch-D-2116              | 119      |
| 76         | Stator Interstage Seal Concept Scheme B -<br>Ref PWA Drawing No. L-67713 Ref MTI<br>Sketch-D-2119              | 120      |
| 77         | Stator Interstage Seal Concept Scheme C -<br>Ref PWA Drawing No. L-67713 Ref MTI<br>Sketch-D-2134              | 121      |
| 78         | Stator Interstage Seal Concept Scheme D -<br>Ref PWA Drawing No. L-67713 Ref MTI<br>Sketch-D-2132              | 122      |
| 79         | Vane Pivot Seal Test Rig   | 127      |
| 80         | Vane Pivot Seal Concepts   | 129      |
| 81         | Single Bellows Seal  | 136      |
| 82         | Single Bellows Seal, Sealol Design   | 136      |
| 83         | Single Bellows Seal, Relocated Thrust Face   | 137      |
| 84         | Stator Pivot Seal Concept Scheme A - Ref<br>PWA Drawing No. L-67563 Ref MTI Sketch<br>of 9-14-65 by H. Jones   | 139      |
| 85         | Stator Pivot Seal Concept Scheme B - Ref<br>PWA Drawing No. L-67563 Ref MTI Sketch<br>of 9-1-65 by E. Belawski | 140      |
| 86         | Stator Pivot Seal Concept Scheme C - Ref<br>PWA Drawing No. L-67563 Ref MTI Sketch<br>of 9-5-65 by E. Belawski | 141      |

## LIST OF ILLUSTRATIONS (Cont'd)

| Figure<br>No. | Title   | Page No. |
|---------------|---|----------|
| 87            | Compressor Seal Development Program<br>Schedule and Milestone Chart     | 144      |
| 88            | Compressor Seal Development Program<br>Schedule and Milestone Chart     | 145      |
| 89            | Schematic of Leakage Area Slit Assumed for<br>Leakage Flow Computations | 146      |

## LIST OF TABLES

| Table No. | Title   | Page No. |
|-----------|---|----------|
| I         | Comparison of Performance of Primary Seal Concepts                        | 36       |
| II        | Comparison of Secondary Seal Concepts                                     | 40       |
| III       | Matrix Chart for Seal Concepts HSS-1, HSS-2, HS-1, HS-2, HS-3 and HS-4    | 43       |
| IV        | Matrix Chart for Seal Concepts HS-5, HS-6, HS-7 and HS-8                  | 44       |
| V         | Matrix Chart for Seal Concepts HD-1, HD-2, HD-3, HD-4, SG-1, and SG-2     | 45       |
| VI        | Matrix Chart for Seal Concepts HS-L-1, HS-L-2, HS-L-3, HS-L-4, VL and F-1 | 46       |
| VII       | Matrix Chart for Seal Concepts F-2, F-3, D-1, D-2, D-3 and D-3A           | 47       |
| VIII      | Matrix Chart for Seal Concepts D-4, D-5, and D-6                          | 48       |
| IX        | Matrix Chart for Seal Concepts HS-9, HS-10, and HS-11                     | 49       |
| X         | Second Screening for End and Interstage Seal Concepts                     | 50       |
| XI        | Results of the Screening Study of End and Interstage Seals                | 51       |
| XII       | Comparison of Vane Pivot Seal Concepts                                    | 133      |
| XIII      | Physical Dimensions - Compressor End Seal                                 | 151      |

## INTRODUCTION

High performance, modern multistage axial flow compressors built with state-of-the-art features, incorporate several air leak paths which are detrimental to compressor performance. Elimination or significant reduction of these leaks would result in a compressor of higher efficiency and possibly smaller size. Some typical areas of leak paths with estimates of percent air loss and potential effect on compressor performance are:

|   | <u>% air loss</u> | <u>effect on compressor efficiency</u> |
|---|-------------------|--|
| End Seal                                | 0.6%              | 1.0%                                   |
| Interstage Stator Seals<br>(ten stages) | 0.9%              | 1.0%                                   |
| Vane Pivot Seals<br>(variable stator)   | 0.2% per<br>stage | 0.2% per<br>stage                      |

Increases in compressor efficiency are traditionally sought by means of compressor geometry redesign. A few extra points in efficiency often mean the difference between a successful or an unsuccessful engine design. These increases as a result of geometry change are always very expensive and not always successful. On the other hand, the losses to efficiency as a result of air leaks are strikingly large and real gains are within reach at a relatively low cost. The gains in efficiency however, must be balanced against any detrimental effect that improved sealing may have on the engine, such as lower reliability or increased weight.

This program will provide for a research, analytical, and test program having as its goal the development of compressor end seals, stator interstage seals, and vane pivot seals which exhibit lower air leakage rates than those currently in use. This will be accomplished using components of such size, materials, and designs as to be considered applicable to compressors for engines capable of supersonic aircraft propulsion.

TASK I - CONCEPT FEASIBILITY ANALYSIS  
PROGRAMS FOR COMPRESSOR END SEALS  
AND FOR COMPRESSOR STATOR  
INTERSTAGE SEALS.

A feasibility analysis program is being conducted on seals for application in stator interstage and end seal systems. The first phase of this program is a preliminary analysis and screening of various seal concepts prior to the selection of concepts for the detailed feasibility analysis. The analytical effort includes a comparison of the selected concepts to current practice and all calculations, analyses, and drawings necessary to establish feasibility of these selected concepts. This analytical effort is subcontracted to Mechanical Technology Inc. (MTI) of Latham, New York and is being monitored by Pratt & Whitney Aircraft as required under the terms of the NASA contract.

The screening study of compressor end seal and stator interstage seal concepts conducted by MTI is presented in this section of the report. The material presented in this section was prepared by Dr. H. S. Cheng, Dr. D. F. Wilcock, and J. Bjerklie.

#### MTI SCREENING STUDY

Present jet engine designs employ labyrinth seals at the high pressure end of the compressor and between compressor stages. Because they must not rub severely during transient periods when temperatures are changing, they operate with clearances as large as 0.030 during normal operation. As a result, air flow through the seals is large, and may amount to a loss of as much as 2 to 3 percent of engine power.

Reduction of this power loss resulting from seal leakage is the end objective of the NASA program of which this study is a part. A design is sought which will have one tenth, or less, of the seal leakage that occurs when using the current labyrinth seal design approach. At the same time it is desired that the new design be adaptable to current engine design and manufacturing techniques, extremely reliable, light in weight, and manufacturable by presently available processes.

Numerous concepts for new seal designs had been suggested. It has been the objective of that portion of the study that is covered by the screening phase of this report to analyze the potential performance of each of these concepts and of additional concepts developed during the study, and to select no more than four compressor end seal designs and no more than four interstage seal designs for a further feasibility analysis. The objective of the feasibility analysis is to develop two

designs of each seal to the point where prototypes can be built for evaluation on a seal test rig.

Typical engine conditions were established to be used in comparing seal concepts and in analyzing seal performance for the screening study.

A seal diameter of 27 inches was selected as "standard" for this study, and current Pratt & Whitney Aircraft large engine configurations have been used as the framework within which each design should operate. Pratt & Whitney Aircraft experience indicates that the end seal leakage rate is two to four pounds per second using labyrinth seals, thus establishing the goal for a new end seal design as less than 0.4 pounds per second.

Additional information from Pratt & Whitney Aircraft has indicated that for face seals, a total axial excursion, due to tolerance build-up and thermal growth and transients, of 0.4 inches must be accommodated. The FIR (Full Indicated Reading) for face wobble may be as high as 0.005 inches FIR, while the deviation of the runner face from a plane can be expected to be no more than 0.0005 inches FIR. For cylindrical seals, the motions are larger, and the FIR may be as large as 0.016 inches. An axial motion of 0.4 inches must also be accommodated.

The authors wish to acknowledge the major efforts in the screening study by Ralph Hooker and Henry Jones. Important contributions in terms of understanding the relationship of the seal to the engine, and the nature of engine parameters and tolerances, have been made by C.A. Knapp, A.H. McKibbin, H.L. Northup, and R.M. Hawkins of Pratt & Whitney Aircraft.

### Summary of Screening Study

It was determined early in the study that analysis of the seal concepts required separate examination of the primary and secondary seal configurations. The primary seal is defined as that portion of the seal adjacent to the high velocity mating surface. Since, in a close-running seal, the primary seal must follow all motions of the runner surface, it must be flexibly mounted. The means for flexibly mounting the primary seal in such a way that leakage around it is prevented or minimized is termed the secondary seal.

Since several basic types of primary seals can be combined with each of several types of secondary seal, many combinations are possible. As a result, many concepts have been suggested for considera-



tion, sometimes several variations on a particular combination. It has been helpful, therefore, to consider the primary and secondary seal functions separately as a preliminary to the screening process.

Consideration of the basic processes at the high speed primary seal interface leads to the following conclusions:

1. To achieve the desired order of magnitude reduction in leakage rate, the film thickness between runner and seal element should be in the range of 0.5 to 1.0 mils.
2. The film thickness for minimum total power loss (compression power plus shear loss in the film) is in the same range.
3. At these film thicknesses, the major portion of the heat generated in the film must flow out through the runner structure for eventual transfer to cooling air; the runner surface will run about 100 F above the ambient.
4. In order to minimize thermal distortion, the seal element must be thermally isolated and may require thermal shunting in its design in order to approach an isothermal condition.
5. The Primary seal element must be light in weight in order to permit tracking runner motions without diminishing film thickness excessively. The key quantity is  $\omega^* = n^2 \omega^2 m / k_f$ , the ratio of dynamic load to film stiffness, which must be less than 0.3 to avoid more than a 30 percent reduction in film thickness for a disturbance amplitude three times the film thickness.
6. Because of problems of thermal growth and of tracking imperfect surfaces at a small separation distance, it appears necessary that the primary seal be either segmented if it is rigid, or highly flexible under the stress of reasonable fluid film forces.

From an examination of several types of hydrostatic and hydrodynamic Primary Seals, it appears that hydrostatic design is required to maintain the desired clearances, but that supplementary hydrodynamic action may assist by providing high film stiffness at the small film thickness where hydrostatic stiffness falls off.

An examination of secondary seal types indicates that the bellows is impractical at the large diameters and for the large pressure dif-

ferences involved. Hydrostatic, piston ring, and flexible diaphragm constructions have sufficient merit to warrant further study in the Feasibility Analysis Phase.

Following a detailed screening analysis based on considerations of operational capability, leakage rate, seal weight, and reliability; five concepts were selected for the Feasibility Analysis Phase. These are:

#### Concept I - One-Sided Floated Shoe

An axial or face seal, in which rigid primary seal segments are held by the sealed pressure against a locating surface. Hydrostatic seal action is used at the primary seal surface and at the locating surface. The segments are carried in a spring-floated secondary seal carrier.

#### Concept II - Two-Sided Floated Shoe

A radial or circumferential seal, in which rigid primary seal segments are pressure loaded against the rotating runner and are held in place by hydrostatic seal action between locating surfaces on either side of the segments.

#### Concept III - Thin Strip Plus Piston Ring

An axial or face seal, in which the primary seal element is a continuous flexible ring ( $R_2 - R \gg t$ ) with hydrostatic seal action at the primary seal face. Moment balance is achieved by an integral ridge carrying a piston ring for the secondary seal to a spring-loaded carrier.

#### Concept IV - Thin Strip Plus C Diaphragm

An axial or face seal similar to Concept III, except that the secondary seal is accomplished by a C-shaped flexible diaphragm instead of a piston ring between the thin strip and the spring-floated carrier.

#### Concept V - Thin Strip Plus C Diaphragm (Radial)

A radial or circumferential seal, otherwise similar to Concept IV.

This radial version of the thin strip plus C diaphragm design is felt to be impractical because it appears impossible to attain a pressure-balanced design, because of the compound curvature of the C diaphragm, and because the thin strip must be discontinuous to accommodate thermal expansion and must be sealed at the discontinuity.

## Preliminary Consideration

### Basic Leakage Rate

Leakage of a high pressure fluid into a low pressure ambient through the clearance between rotating and stationary machine surfaces can be minimized by use of an orifice-type annular restrictor, by the viscous resistance between surfaces separated by small clearances, or by dry rubbing contact. The present jet engine compressor end and interstage seals are of the labyrinth type which rely on an annular orifice to resist the flow. Clearances of these seals are usually large and leakage rates are high. The present study seeks to replace them with an improved design having a substantially lower leakage rate.

Most of the seal concepts proposed for this study are of the viscous type because sealing by viscous action can provide the largest reduction in leakage rates. In order to determine the thickness at which the sealing by viscous action becomes active, consider the leakage rate through an infinitely wide gap with a finite leakage path. The mass flow rate per inch of width can be derived as follows.

The simplified Stokes Equation gives

$$\frac{\partial^2 u}{\partial y^2} = \frac{1}{\mu} \frac{\partial p}{\partial x} \quad (1)$$

Integrating  $u$  with respect to  $y$ , and using the boundary conditions

$$\begin{aligned} y = 0, \quad u &= 0 \\ y = h, \quad u &= 0, \end{aligned}$$

One obtains

$$u = \frac{1}{2\mu} \left( \frac{\partial p}{\partial x} \right) y (y - h) \quad (1a)$$

The mass flow ratio per inch of width becomes

$$m = \int_0^h \rho u \, dy \quad (1b)$$

Substituting (1a) in (1b) and carrying out the integration, one obtains

$$m = - \frac{h^3 \rho}{12 \mu} \frac{\partial p}{\partial x} \quad (1c)$$

Since the mass flow through any given section is constant, it follows that

$$\frac{dm}{dx} = 0 \quad (2)$$

Therefore, for an isothermal film where  $\rho = \left(\frac{p_o}{p_o}\right) p$

$$\frac{d}{dx} \left( h^3 \frac{dp^2}{dx} \right) = 0 \quad (3)$$

For a parallel film where  $h$  is constant,

$$\frac{d^2}{dx^2} (p^2) = 0 \quad (4)$$

Integrating  $p^2$  with respect to  $x$  between limits of 0 and  $b$ , and using the boundry conditions

$$\begin{aligned} x = 0, p &= p_2 \\ x = b, p &= p_1 \end{aligned}$$

the pressure distribution is given by

$$p = p_2 \left[ 1 - \left( 1 - \frac{p_1^2}{p_2^2} \right) \frac{x}{b} \right]^{1/2} \quad (5)$$

The leakage rate can be obtained from Equations (1) and (5) giving

$$m = \frac{h^3}{24 \mu b} p_2 p_1 \left[ 1 - \left( \frac{p_1}{p_2} \right)^2 \right] \quad (6)$$

|       |          |                                    |                               |
|-------|----------|------------------------------------|-------------------------------|
| Where | $m$      | = mass flow rate per unit width    | $\text{lb-sec/in}^2$          |
|       | $\rho_2$ | = mass density of the upstream gas | $\text{lb-sec}^2/\text{in}^4$ |
|       | $p_2$    | = pressure of the upstream gas     | $\text{lb/in}^2$              |
|       | $p_1$    | = pressure of the downstream gas   | $\text{lb/in}^2$              |
|       | $h$      | = gap film thickness               | inches                        |
|       | $\mu$    | = viscosity of the upstream gas    | $\text{lb-sec/in}^2$          |
|       | $b$      | = leakage path length              | inches                        |

The leakage rate due to viscous flow increases with the cube of the film thickness. However, Equation (6) is only valid up to a certain thickness. At greater thicknesses, sealing by viscous action is not effective and flow rate is more accurately determined by the orifice formula. Figure 1 shows the basic leakage curves for a circumferential or face type seal with the following two conditions:

|           | <u>Take-Off</u>      | <u>Cruise</u>        |   |
|-----------|----------------------|----------------------|---|
| $p_2$     | 350                  | 200                  | psi   |
| $p_1$     | 200                  | 120                  | psi   |
| $T_2$     | 685                  | 1200                 | °F  |
| $\mu$     | $4.5 \times 10^{-9}$ | $5.9 \times 10^{-9}$ | $\frac{\text{lb}}{\text{in}^2} \text{ sec}$ |
| $b$       | 1/2                  | 1/2                  | inches                                      |
| $L=\pi D$ | 86.5                 | 86.5                 | inches                                      |

For each condition, two curves are shown. The upper curve is based on orifice flow and the lower curve on laminar or viscous flow.

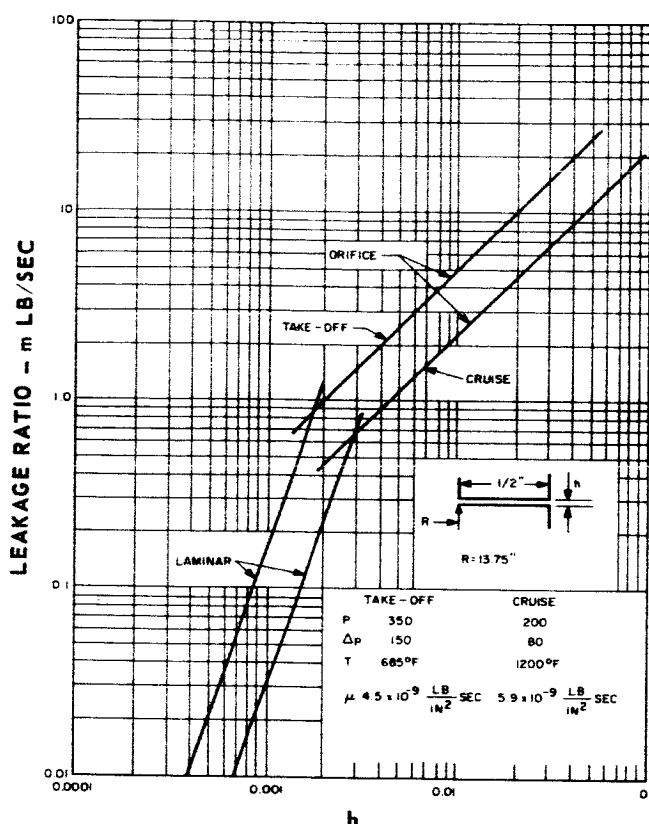


Figure 1 Leakage Rate vs Film Thickness for a Typical Seal

In the neighborhood of  $h = 0.001$  inches, the flow is definitely governed by the viscous flow and for  $h \sim 0.01$  inches, the orifice curves are more representative. In the region where the two lines intersect, the actual leakage will be slightly lower than is indicated by either line. Note that viscous sealing becomes active at 0.003 inches and 0.0018 inches for the cruise and take-off conditions respectively. Furthermore, to obtain a substantial leakage reduction compared to the present seal, the new seal must operate in the region of about 0.001. These two conclusions, although calculated from these simple relations, are extremely significant in providing direction for the screening study and in developing new concepts.

#### Film Thickness for Minimum Power Loss

If the compressor seal operates at a large film thickness, the excessive leakage will require excess compressor power and reduce engine efficiency. On the other hand, if the film thickness becomes extremely small, the power loss due to seal frictional drag will go up rapidly and become predominant. Consequently, it is desirable to maintain an intermediate film thickness at which these power losses are near a minimum.

Figure 2 shows the results of an optimization study for the take-off condition. A detailed account of this study is presented in Appendix A. Two sets of curves are represented in this figure; one for the end seal and the other for the last interstage seal. For each set, there are three curves. The rapidly decaying curve shows the seal drag loss being inversely proportional to the film thickness and the right curve is the calculated power loss due to the leakage of high pressure air. In calculating the compression power loss it was assumed that none of the energy in the leakage air would be recovered. By adding these two power losses, one obtains the middle curve which shows a minimum power loss at a film thickness equal to 0.0004 inches for the end seal and 0.0011 inches for the interstage seal. Similar curves are also shown in Figure 3 for the cruise condition. The optimized film thicknesses for this condition are slightly higher than for the take-off condition; they are 0.0006 inches and 0.0016 inches for the end and interstage seals respectively.

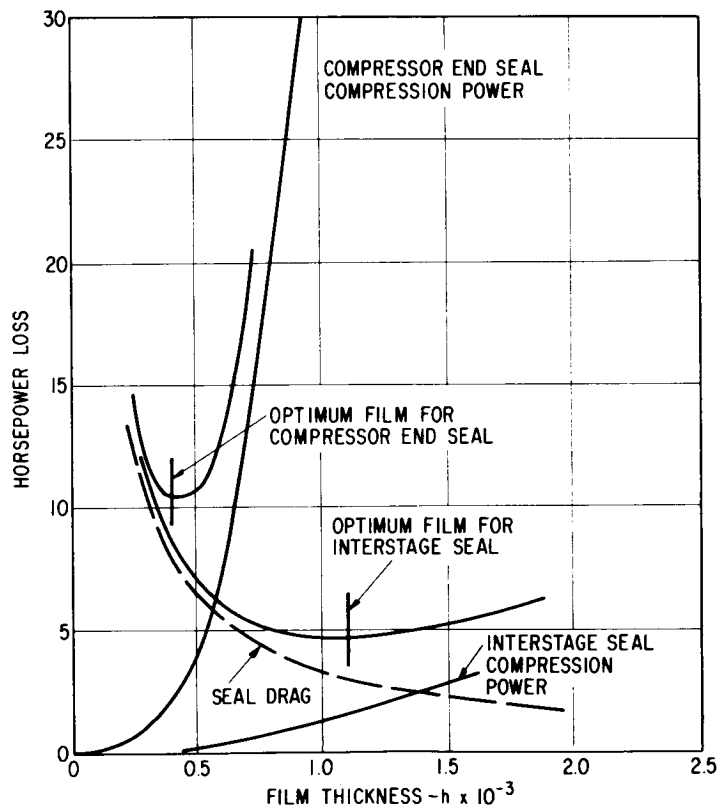


Figure 2 Optimization of Compressor Power Due to Leakage vs Drag Power Loss for Take-Off Conditions

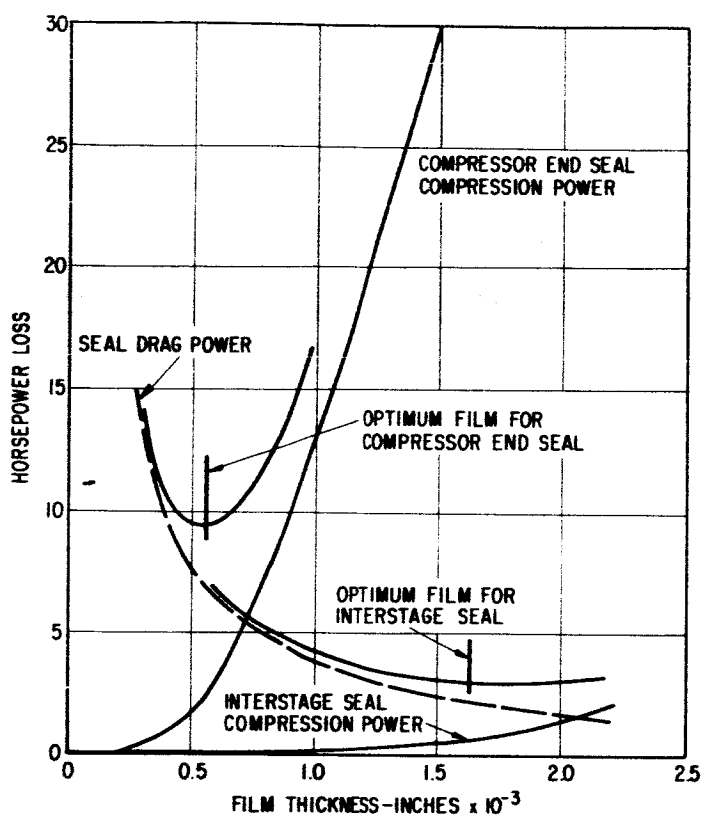


Figure 3 Optimization of Compressor Power Due to Leakage vs Drag Power Loss for Cruise Conditions

### Thermal Distortion

Thermal Map - Assuming that there is no temperature gradient in the circumferential direction, a steady-state analysis of the temperature distribution for a typical segment of a circumferential seal has been performed using a discrete model. The geometry of this section and the conditions used are shown in Figure 4. Results for a 1/2-inch square segment riding on a gas film of 0.0006-inch film thickness are shown in Figure 5. It is seen that a substantial thermal gradient can be developed in the axial as well as radial direction due to the heat generated by shearing of the air film. The same analysis was used to investigate the effect of a thermal shunt to improve the thermal gradient in the axial direction. As seen in Figure 6, the gradient in the axial direction is reduced by more than 50 percent in the seal segment as well as in the rotor.



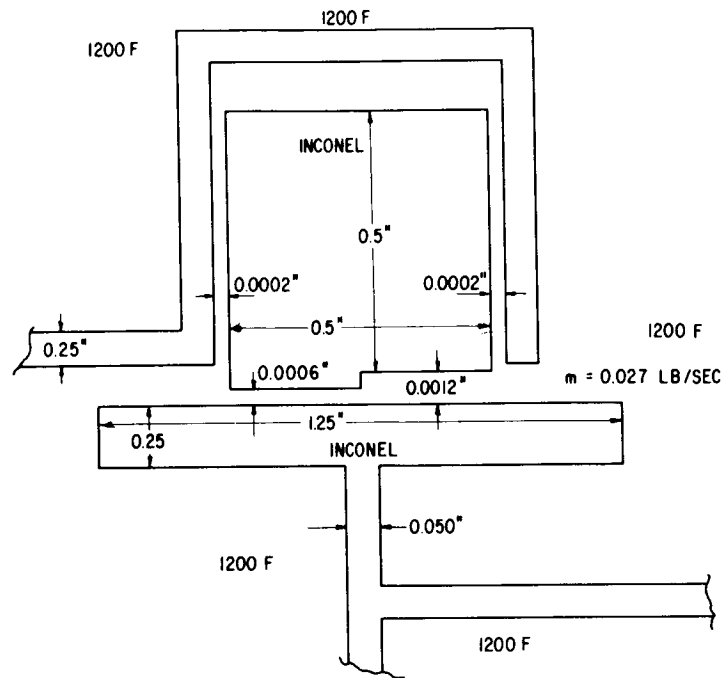


Figure 4 Model for Simple Thermal Analysis

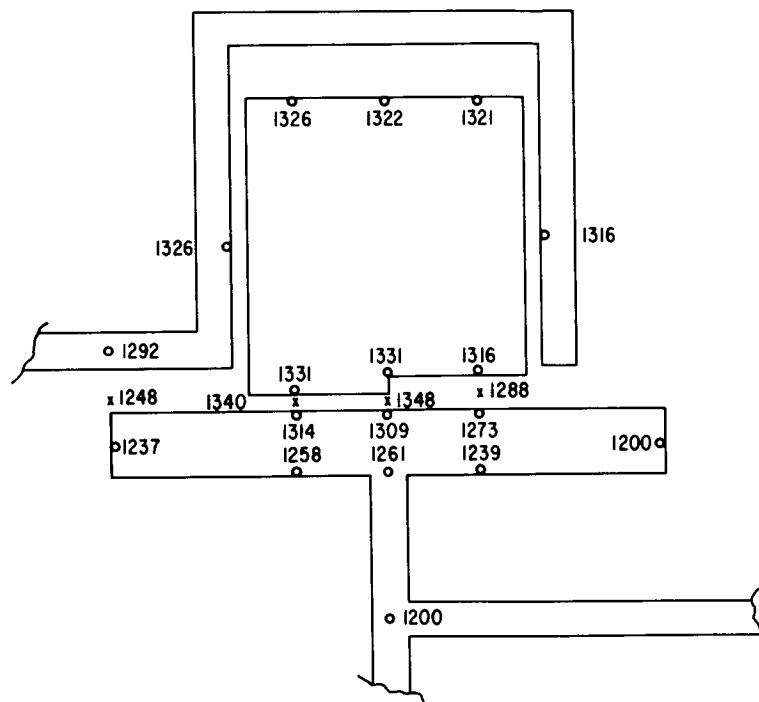


Figure 5 Calculated Temperatures for a Floated Shoe Design

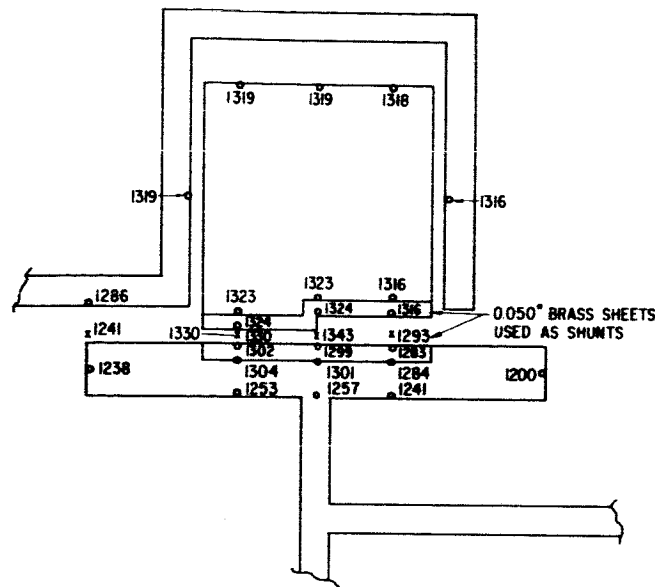


Figure 6 Calculated Temperatures for a Floated Shoe Design Using Thermal Shunts

Distortion of a Circumferential Seal Segment - When a seal ring segment and the rotor drum are subjected to a high temperature environment and heating from the shearing of the air film, the radius undergoes considerable thermal distortion. It is important to determine whether there still remains enough radius conformity between the seal segment and the drum to insure an adequate hydrostatic gas film.

Figure 7 shows an exaggerated picture of the distorted drum and seal segment under a steady-state condition.

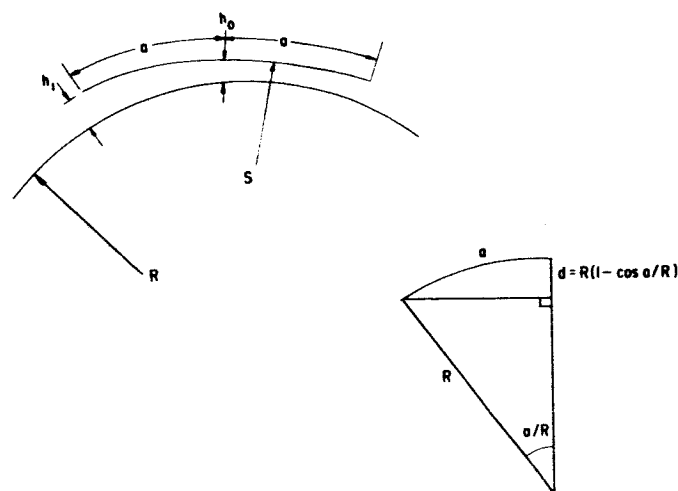


Figure 7 Distorted Seal Segment

The film thickness  $h_1$  at the end of a segment where the center film thickness is  $h_o$ , is given by

$$h_1 = \frac{1}{\cos \frac{a}{R}} \left[ h_o + \left( 1 - \cos \frac{a}{R} \right) C \right] \quad (7)$$

where  $C$  is the difference in radii,

$$C = S - R.$$

The rotor radius  $R$  will increase due to centrifugal force and temperature increase. The segment radius will increase due to temperature increase and thermal gradient bowing.

If we let:

$C_m$  = radial clearance as manufactured

$\delta_c$  = centrifugal growth,

$\delta_t$  = differential growth due to temperature and material difference

$\delta_b$  = radius increase due to thermal bowing

$$h_1 = \frac{1}{\cos \frac{a}{R}} \left[ h_o + \left( 1 - \cos \frac{a}{R} \right) \left( C_m - \delta_c + \delta_t + \delta_b \right) \right] \quad (8)$$

The rotor centrifugal growth is estimated by

$$\delta_c = 0.4\rho \left( \frac{2\pi NR}{60} \right)^2 \frac{R}{E} \quad (9)$$

where 0.4 represents an experience factor accounting for the restraint of the hub (steel assumed).

The differential thermal growth is

$$\delta_t = R \left( \alpha_s T_s - \alpha_r T_r \right) \quad (10)$$

The thermal bowing radial change is given by

$$\delta_b = \alpha R^2 \frac{\Delta T}{t} \quad (11)$$

where

$E$  = modulus of elasticity, psi

$\alpha_s$  = thermal expansion coefficient of segment, in/in °F

$\alpha_r$  = thermal expansion coefficient of rotor, in/in °F

$T_s$  = surface temperature of segment, °F

$T_r$  = surface temperature of rotor, °F

$\Delta T$  = temperature change across  $t$ , °F

$N$  = rotor speed, rpm

$t$  = radial depth of segment, inches

$\rho$  = mass density, lb.-sec<sup>2</sup>/in<sup>4</sup>

If we assume  $N = 8000$ ,  $(T_r - T_s) = 25$  F,  $t = 1/2$ ,  $\Delta T = 20$  F,  
 $\alpha = 7.5 \times 10^{-6}$ ,  $E = 30 \times 10^6$ ,  $R = 13.75$ ,  $C_m = 0.001$ ,  $h_o = 0.001$

and using the same material for segment and rotor

$$\delta_c = 0.4 \times \frac{.283}{386} \left( \frac{2\pi \times 8000 \times 13.75}{60} \right)^2 \times \frac{13.75}{30 \times 10^6} = 0.0178$$

$$\delta_t = 7.5 \times 10^{-6} \times 13.75 \times 25 = 0.00257$$

$$\delta_b = 7.5 \times 10^{-6} \times (13.75)^2 \times \frac{20}{0.5} = 0.0568$$

$$\frac{a}{R} = \frac{2}{13.75} = 0.1455 \text{ rad.} \quad \cos \frac{a}{R} = 0.9894$$

Inserting these values into Equation (3)

$$h_1 = \frac{1}{0.9894} \left[ 0.001 + 0.0106 (0.001 - .0178 + 0.0026 + 0.0568) \right]$$

$$= 0.00146$$

and

$$h_1 - h_o = 0.00046$$

The above calculation shows clearly that bowing of the segment due to thermal distortion caused by radial temperature gradients is a major cause of film thickness variation under a segment, and that these effects can be large in proportion to the desired film thickness. Under these conditions, heating will be concentrated at the smaller film thickness regions and may further aggravate the film distortion. Whether this effect will result in thermal instability will be examined during the Feasibility Analysis Phase.

Distortion of a Seal Ring - The thermal distortion of a complete ring is different from that of the segments. Under an axial temperature gradient, a free ring will bend thermally into a spherical surface and for, a ring of 1/2 inch square section,  $\alpha = 7.5 \times 10^{-6}$ ,  $\Delta T = 20$ , the rotation,  $\delta$ , of the cross section due to the axial thermal gradient is found to be

$$\delta = R \left( \frac{\alpha \Delta T}{t} \right) = \frac{13.75 \times 7.5 \times 10^{-6} \times 20}{1/2} = .0041 \text{ rad.}$$

This degree of angular rotation (4 mils per inch) would cause rubbing contact for the one mil film thickness desired for the seal. Therefore, either the temperature gradient must be made much smaller, for example by thermal shunting, or the tendency to rotate must be countered by the angular moment stiffness of the air film in the seal.

### Tracking Dynamics

One of the most important aspects of seal performance is conformity or tracking of the seal ring or seal segments to the irregular motion of the rotor due to the runout, initial warping and elastic or thermal distortion of the runner. To determine the exact motion of the seal ring in the presence of these irregular excitations, it is necessary to carry out a vibration analysis for the segment considering it as

a rigid body capable of moving in all unrestrained directions. For a continuous seal ring, it is necessary to treat the problem as an elastic ring resting on the gas film which may be considered as an elastic foundation. However, the more exact vibration study is too involved to be considered in the screening stage; it is more useful to consider a simplified analysis to indicate whether the film stiffness is adequate to allow the seal ring to follow the rotor face. To this end, a simplified one-dimensional vibration model for the seal segment and rotor system is chosen and shown in Figure 8.

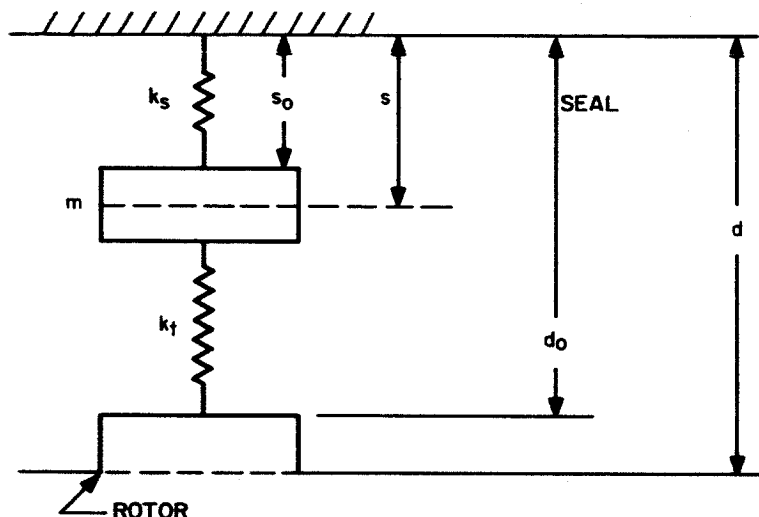


Figure 8 Simplified One-Dimensional Vibration Model for Seal Segment and Rotor System

The equation of motion of this system is

$$m\ddot{s} + C\dot{s} + (k_s + k_f)(s - s_o) = (d - d_o)k_f \quad (11a)$$

where

$k_s$  = stiffness of the seal back-up springs

$k_f$  = stiffness of the fluid film

$m$  = mass of the seal

$C$  = combined viscous damping constant

$$\dot{s} = \frac{\partial s}{\partial t}, \quad \ddot{s} = \frac{\partial^2 s}{\partial t^2}$$

The term  $(d-d_0)$  represents the motion of the rotor face which includes the runout, wobbling, initial warping, or waviness. Of course,  $(d-d_0)$  is a function of time and, in general can be represented mathematically by a Fourier series as follows:

$$d - d_0 = \sum_{n=0}^{\infty} f_n \cos n\omega t \quad (11b)$$

To determine the response of the seal element within the framework of linear vibration theory, the motion of the seal element,  $s-s_0$ , when subjected to a single component,  $f_n \cos n\omega t$ , can be put into the form,

$$s - s_0 = A_n e^{in\omega t}, \quad (11c)$$

where  $A_n$  is the complex amplitude.

Substituting (11c and 11b) into (11a) and collecting the terms containing  $e^{in\omega t}$ , one obtains

$$\frac{A_n}{f_n} = \frac{1}{\left[ \left( 1 + \frac{k_s}{k_f} - \frac{mn^2 \omega^2}{k_f} \right) + \frac{n\omega c}{k_f} i \right]} \quad (11d)$$

It follows that the magnitude of  $A_n$  can be expressed as

$$|A_n| = \frac{f_n}{\left[ \left( 1 + \frac{k_s}{k_f} - \frac{mn^2 \omega^2}{k_f} \right)^2 + \left( \frac{n\omega c}{k_f} \right)^2 \right]^{1/2}} \quad (11e)$$

For the seals considered in this investigation, the value of  $k_s$  is in the order of 2 lb/in/in of seal segment, and the value of  $k_f$  will be shown later to be in the neighborhood of 10,000 lb/in/in. Consequently, the term  $k_s/k_f$  can be ignored in Equation (11e). Furthermore, the damping of a fully floated segment is believed to be small so that the damping term can be ignored in estimating the response. Using these arguments, Equation (11e) becomes

$$|A_n| = \frac{f_n}{1 - \omega_n^*} \quad (11f)$$

where

$$\omega_n^* = \frac{mn^2 \omega^2}{k_f}$$

The satisfactory tracking of the seal ring can be measured by the ratio,  $\delta/h$ , where  $\delta$  is equal to  $|A_n| - f_n$  representing the difference between the seal motion and the rotor motion and  $h$  is the fluid film thickness. In terms of the quantity  $\omega^*$ , the ratio  $\delta/h$  can be written as

$$\begin{aligned} \frac{|A_n| - f_n}{h} &= \frac{\delta}{h} \\ &= \frac{f_n}{h} \left( \frac{1}{1 - \omega^*} - 1 \right) \\ &= \frac{f_n}{h} \left( \frac{\omega^*}{1 - \omega^*} \right) \end{aligned} \quad (11g)$$

When this ratio is below 0.3 (a design experience factor), the tracking is considered to be satisfactory. This criterion is used later in the screening study for all proposed seal concepts. Rewriting (11g),

$$\omega^* = \frac{\frac{\delta}{h}}{\frac{\delta}{h} + \frac{f_n}{h}} = \frac{1}{1 + \frac{f_n}{\delta}} \quad (11h)$$

### Primary and Secondary Seals

Examination of the requirements for a low-leakage seal and of the dynamic as well as transient motions it must accommodate shows that, in addition to the primary seal behavior at the high speed interface, one must also be concerned with some form of flexible or adjustable support for the primary seal. Thus, motion of the primary seal requires that a secondary seal be made to avoid static leakage behind the primary seal. By definition (in this report) the primary seal supporting and sealing structure is termed the secondary seal.



These requirements for both small running clearance and dynamic motions due to runout, irregular surfaces, and thermal and elastic growth, dictate that the primary seal must itself be flexible for small motions. For these reasons, rigid one-piece primary seals appear impractical. Rather, the primary seal must either be very flexible or it must be segmented to accommodate small motions.

### Primary Seal Behavior

Five basic primary seal concepts and two hybrid concepts have been considered. The configurations of these concepts are shown in Figure 9. Descriptions and principles of these concepts are discussed in the following sections. Analyses for these concepts are also made based on the assumption of an isothermal and parallel film thickness.

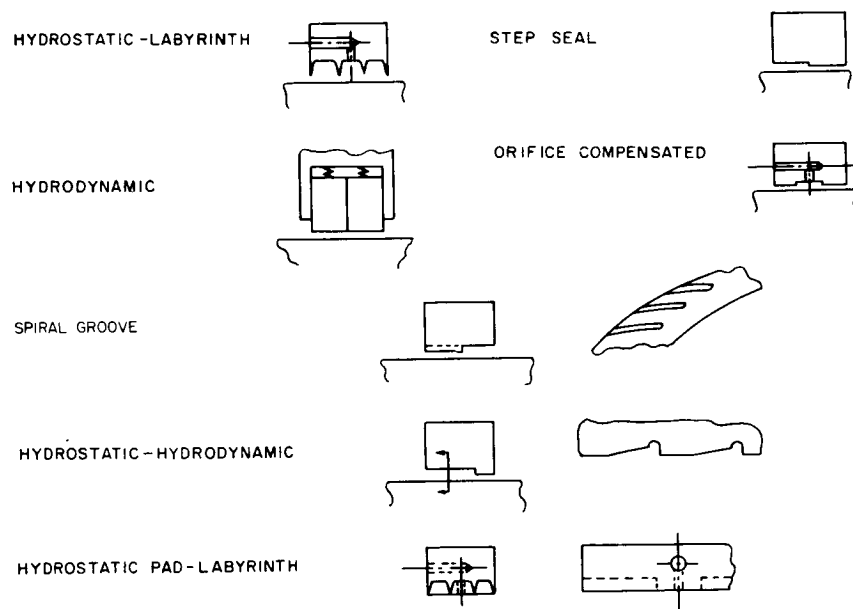


Figure 9 Basic Primary Seal Concepts

### Hydrostatic-Step Seal

In this concept, a step in the sealing surface is located at the high pressure, ( $p_2$ ), side of the seal as shown in Figure 10. As the gap decreases, the resistance to flow in the smaller film increases and causes the pressure to build up in the larger film, providing a positive stiffness for the gas film. Several pressure profiles across the seal for various film thicknesses are depicted in Figure 10.

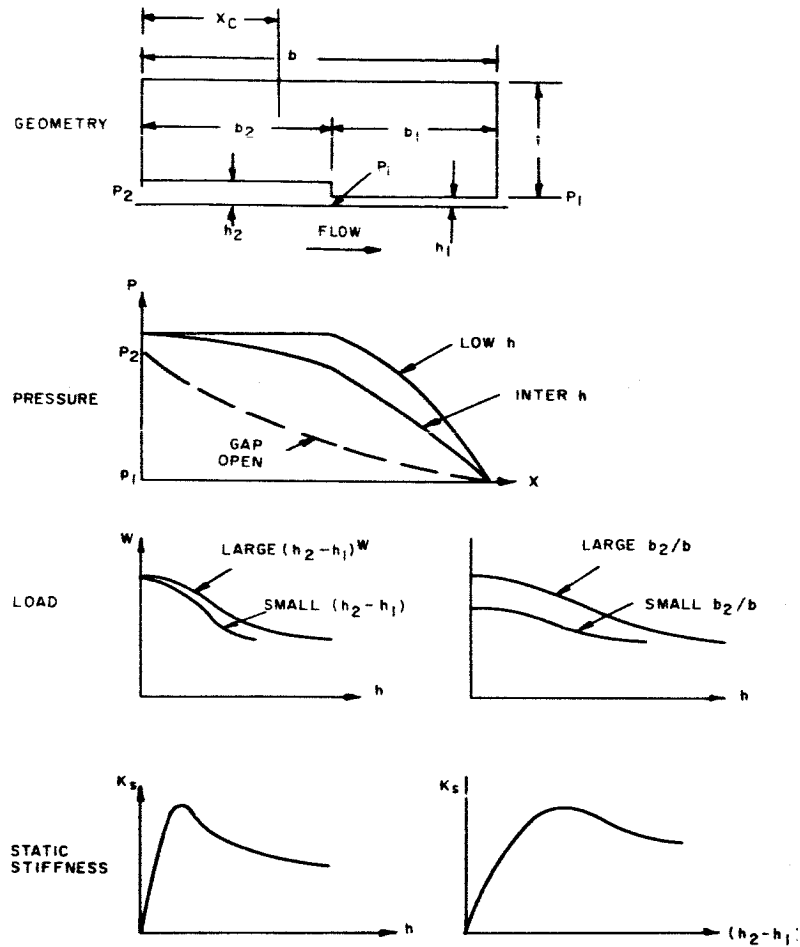


Figure 10 The Hydrostatic Step Seal

The pressure distribution in the step seal can be determined by matching the flow through the step as follows. If the intermediate pressure at the step is designated by  $p_i$ , the flow in the upstream section can be expressed (see Equation (6)), by

$$m = \frac{h_2^3}{24\mu b_2} \rho_2 p_2 \left[ 1 - \left( \frac{p_i}{p_2} \right)^2 \right] \quad (12)$$

and likewise, in the downstream section by

$$m = \frac{h_1^3}{24\mu b_1} \rho_i p_i \left[ 1 - \left( \frac{p_1}{p_i} \right)^2 \right] \quad (13)$$

where

|                  |  |                               |
|------------------|--|-------------------------------|
| $m$              | = flow rate per unit circumferential length                | $\text{lb-sec/in}^2$          |
| $h_2, h_1$       | = film thicknesses of the upstream and downstream sections | inches                        |
| $p_2, p_1$       | = upstream and downstream pressure                         | $\text{lb/in}^2$              |
| $b_1, b_2$       | = widths of the sealing surface (see Fig. 9)               | inches                        |
| $\rho_2, \rho_i$ | = densities at the upstream and downstream entrance        | $\text{lb-sec}^2/\text{in}^4$ |

Equating (12) and (13), one obtains

$$p_i = p_2 \left[ \frac{\left(\frac{h_1}{h_2}\right)^3 \left(\frac{b_2}{b_1}\right) \left(\frac{p_1}{p_2}\right)^2 + 1}{\left(\frac{h_1}{h_2}\right)^3 \left(\frac{b_2}{b_1}\right) + 1} \right]^{1/2} \quad (14)$$

Letting  $r_{ij} = \frac{p_i}{p_j}$ , and following equation (5),

the pressure in the upstream section becomes

$$p = p_2 \left[ 1 - \left(1 - r_{i2}^2\right) \frac{x}{b_2} \right]^{1/2} \quad (15)$$

and likewise, the pressure in the downstream section can be expressed as

$$p = p_2 \left[ r_{i2}^2 - \left(r_{i2}^2 - r_{12}^2\right) \frac{x-b_2}{b_1} \right]^{1/2} \quad (16)$$

Defining the dimensionless load  $\bar{W}$  by

$$\bar{W} = \frac{\int_0^b (p - p_1) dx}{(p_2 - p_1) b}, \quad (17)$$

and substituting (15) and (16) into (17), one obtains

$$\begin{aligned} \bar{W} = & \frac{1}{(1 - r_{12})^b} \left[ \int_0^{b_2} \left\{ \left[ 1 - \left( 1 - r_{i2}^2 \right) \frac{x}{b_2} \right]^{1/2} - r_{12} \right\} dx \right. \\ & \left. + \int_{b_2}^b \left\{ \left[ r_{i2}^2 - \left( r_{i2}^2 - r_{12}^2 \right) \frac{(x-b_2)}{b_1} \right]^{1/2} - r_{12} \right\} dx \right] \quad (18) \end{aligned}$$

Integrating with respect to  $x$ , one obtains the following expression for the load parameter

$$\begin{aligned} \bar{W} = & \frac{1}{1 - r_{12}} \left\{ \frac{b_2}{b} \left[ \frac{2 \left( r_{i2}^2 + r_{i2} + 1 \right)}{3 \left( r_{i2} + 1 \right)} - r_{12} \right] \right. \\ & \left. + \frac{b_1 r_{i2}}{b} \left[ \frac{2 \left( r_{li}^2 + r_{li} + 1 \right)}{3 \left( r_{li} + 1 \right)} - r_{li} \right] \right\} \quad (18a) \end{aligned}$$

The actual load per inch of length of seal is, therefore,

$$W = b (p_2 - p_1) \bar{W} \quad (19)$$

Once the intermediate pressure is determined by Equation (14), the leakage rate and load can be readily calculated from Equations (13) and (18). The film stiffness can be obtained by differentiating the load parameter with respect to the film thickness. One may define a gas film stiffness,  $K_s$ , as the change of average film pressure with respect to the film thickness, and it can be expressed as

$$K_s = \frac{d \left( \frac{W}{b} \right)}{dh_1} = \frac{d\bar{W}}{dh_1} (p_2 - p_1), \quad (20)$$

The derivative  $\frac{d\bar{W}}{dh_1}$  is derived in the Hydrostatic step section of the Feasibility Analysis.

The variation of the load and stiffness with respect to the step geometry can be seen qualitatively in Figure 10. Optimization of the step geometry as well as other primary seal concepts will be carried out in the detailed feasibility analysis.

### Hydrostatic-Orifice Compensated Seal

The cross section of an orifice-compensated seal is shown in Figure 11. High pressure air is fed into a groove of width (d) through a series of orifices of radius (a) and spaced at a distance (ℓ). Either the upstream gas or an external gas supply can be used as the high pressure source. The pressure in the groove increases with a decrease of the film thickness because of the lower flow rate and consequently lower pressure drop across the orifice, and thereby provides a positive film stiffness. The pressure distribution at different levels of film thickness is seen in Figure 11.

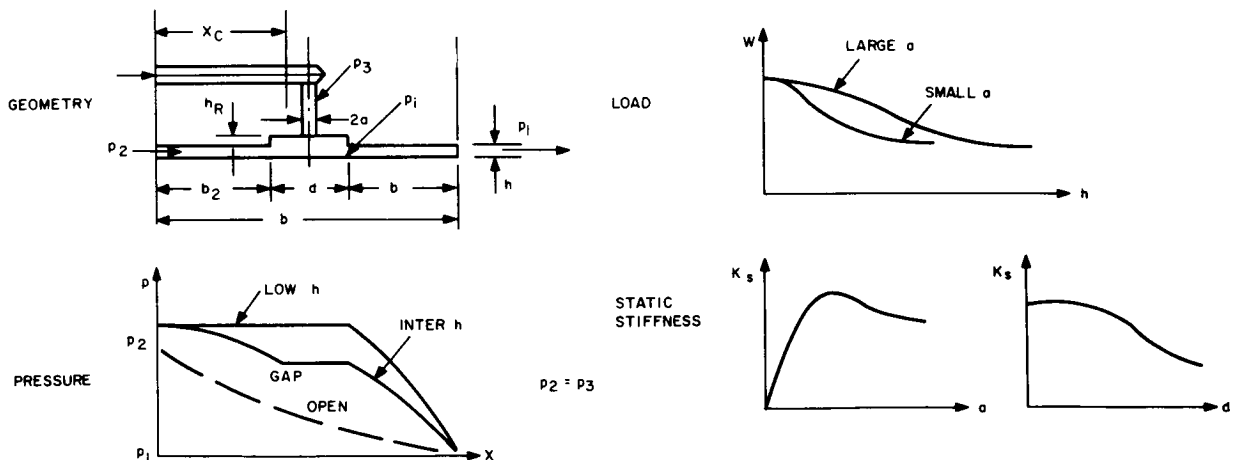


Figure 11 The Hydrostatic Orifice Compensated Seal

The pressure in the sealing area can be determined by matching the flows through the orifice and through the sealing passages. Letting  $m_1$  and  $m_2$  denote the mass flow rate through the downstream and upstream sections per orifice, and  $m_3$  the flow through the orifice, the flow quantities can be expressed in the following forms:

$$m_1 = \frac{h^3}{24\mu b_1} \rho_i p_i (1 - r_{i1}^2) \ell \quad (21)$$

$$m_2 = \frac{h^3}{24\mu b_2} \rho_2 p_2 (1 - r_{i2}^2) \ell \quad (22)$$

$$m_3 = C_D \frac{\pi a^2}{\sqrt{RT}} p_3 G(r_{i3}) \quad (23)$$

where

$$G(r_{i3}) = v \sqrt{\frac{2k}{k-1}} r_{i3}^{1/k} \left[ 1 - r_{i3}^{\frac{k-1}{k}} \right]^{1/2} \quad (24)$$

$$\text{for } r_{i3} > \left( \frac{2}{k+1} \right)^{\frac{k}{k-1}}$$

$$G(r_{i3}) = v \sqrt{\frac{2k}{k+1}} \left( \frac{2}{k+1} \right)^{\frac{1}{k-1}} \quad (25)$$

$$\text{for } r_{i3} < \left( \frac{2}{k+1} \right)^{\frac{k}{k-1}}$$

$C_D$  is the discharge coefficient of the orifice and  $v$  is the vena contracta coefficient. A graphical representation of the flow function  $G(r_{ij})$  represents the value of  $G$  in Figure 12 for the pressure ratio  $p_i/p_j$ .

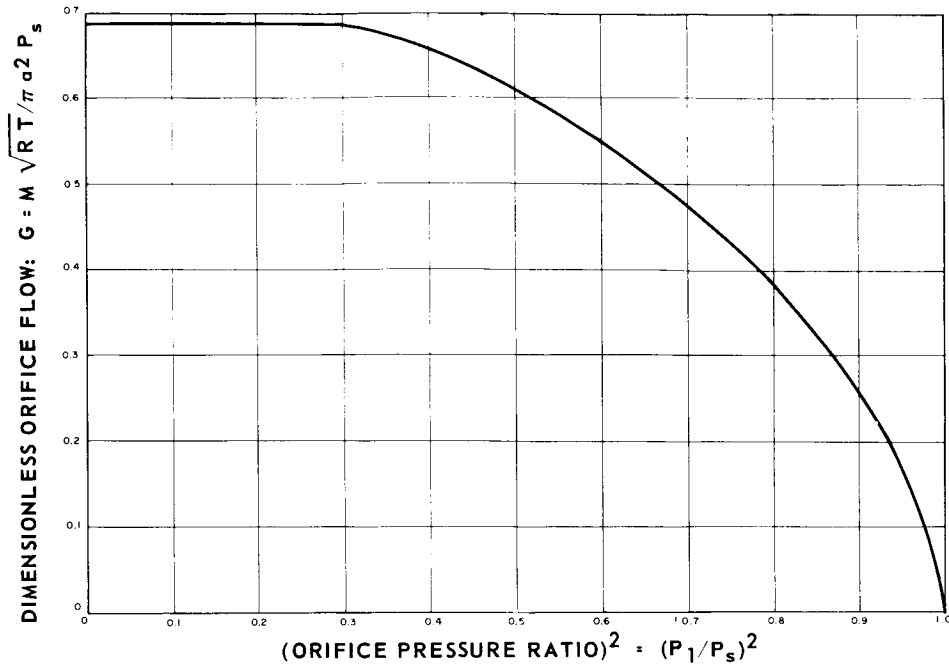


Figure 12 Flow Through an Orifice

For continuity of flow,

$$m_1 = m_2 + m_3 \quad (26)$$

Substituting (21), (22), and (23) into (26), one obtains

$$\begin{aligned} \frac{h^3 \ell \rho_2 p_2}{24 \mu b} \left[ \left( \frac{b}{b_1} \right) (r_{i2}^2 - r_{12}^2) - \left( \frac{b}{b_2} \right) (1 - r_{i2}^2) \right] \\ = C_D \frac{\pi a^2 p_3}{\sqrt{RT_3}} G(r_{i3}) \end{aligned} \quad (27)$$

which can be solved graphically or numerically for the intermediate pressure  $p_i$ . It should be pointed out that the units of the gas constant,  $R$ , are  $\text{in}^2/\text{sec}^2 \text{ } ^\circ\text{R}$  ( $R$  for air is  $2.47 \times 10^5 \text{ in}^2/\text{sec}^2 \text{ } ^\circ\text{R}$ ).

Once  $p_i$  or  $r_{i2}$  is determined, the leakage rate can be readily calculated by (21), and the dimensionless load as defined by

$$\bar{W} = \frac{\int_0^b (p - p_1) dx}{(p_2 - p_1) b} \quad (28)$$

can be readily integrated in the same manner as the hydrostatic step seal, using Equations (15) and (16). The resulting formula is

$$\begin{aligned} \bar{W} = & \frac{b_2}{b(1-r_{12})} \left[ \frac{2}{3} \left( \frac{r_{i2}^2 + r_{i2} + 1}{r_{i2} + 1} \right) - r_{i2} \right] \\ & + \frac{d}{b} \left( \frac{r_{i2} - r_{12}}{1 - r_{12}} \right) \\ & + \frac{b_1}{b} \frac{r_{i2}}{1 - r_{12}} \left[ \frac{2}{3} \left( \frac{r_{li}^2 + r_{li} + 1}{r_{li} + 1} \right) - r_{li} \right] \end{aligned} \quad (29)$$

The gas film stiffness can be readily obtained by numerical differentiation of  $\bar{W}$  with respect to  $h$  and it can be expressed by

$$K_s = \frac{d(W/b)}{dh} = \left( \frac{d\bar{W}}{dh} \right) (p_2 - p_1) \quad (30)$$

The variations of the load and stiffness with respect to changes of the geometrical dimensions "a" and "d" are also qualitatively depicted in Figure 11.

#### Hydrostatic-Labyrinth Seal

The hydrostatic-labyrinth seal relies on a series of knife edges to restrict the flow as shown in Figure 13. The clearance between the knife edge and the opposite ring is controlled by feeding a high-pressure gas into the center of the seal ring. Like the orifice-compensated seal, this high-pressure gas could be taken directly from the upstream gas or from a separate source. Two pressure profiles are shown in Figure 13 for two different film thicknesses. At a low film thickness, the high pressure region extends further towards the exit end and gives a higher load capacity. The pressure at the center cavity between the knife edges can be determined in the same manner as the orifice-compensated seal except that the viscous passages are now replaced by orifice restrictors.



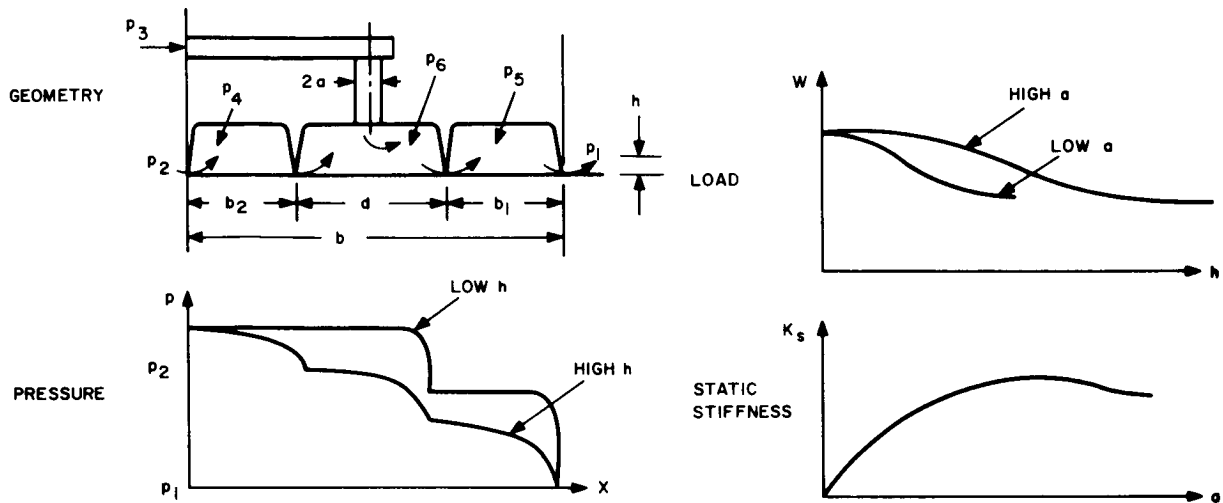


Figure 13 The Hydrostatic Labyrinth Seal

Letting the flow through the upstream knife edges be denoted by  $m_2$ , through the downstream knife edges by  $m_1$ , and through the orifice by  $m_3$ , the expressions for  $m_1$ ,  $m_2$  and  $m_3$  can be written as

$$m_2 = \frac{Chlp_2}{\sqrt{RT_2}} g \left( \frac{p_6}{p_2} \right) \quad (31)$$

$$m_1 = \frac{Chlp_6}{\sqrt{RT_6}} g \left( \frac{p_1}{p_6} \right) \quad (32)$$

$$m_3 = C_D \frac{\pi a^2}{\sqrt{RT_3}} p_3 G \left( \frac{p_6}{p_3} \right) \quad (33)$$

Where the function  $G$  represents the flow through the orifice (shown in Figure 12). The flow function  $g$  represents the mass flow through the double knife edges and is shown in an empirical curve in Figure 14.  $C$  is the discharge coefficient of the labyrinth. Again the units for  $R$  are  $\text{in}^2/\text{sec}^2 \text{ } ^\circ\text{R}$ .

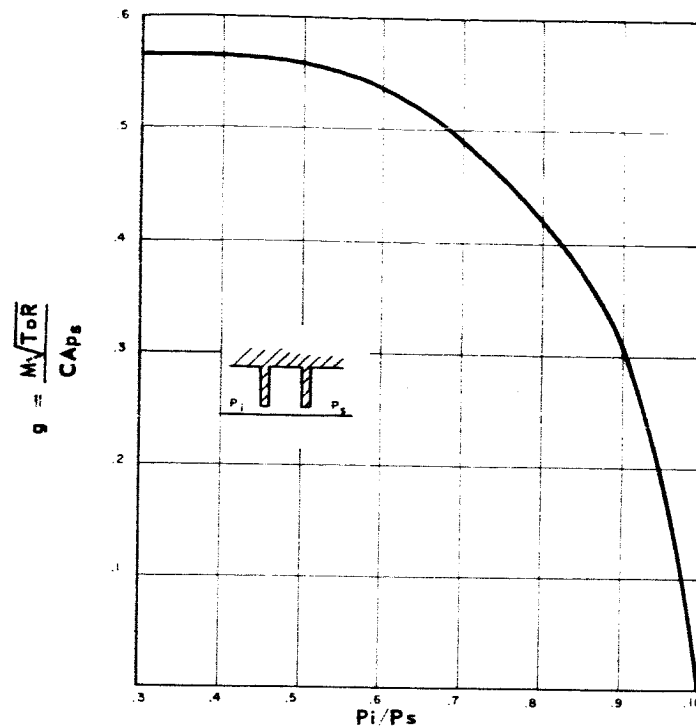


Figure 14 Flow Through a Double Knife Edge Labyrinth

Matching the flow, one obtains the following equation,

$$C_D \frac{\pi a^2}{\sqrt{RT_3}} \left( \frac{P_3}{P_2} \right) G \left( \frac{P_6}{P_3} \right) + \frac{Ch\ell}{\sqrt{RT_2}} g \left( \frac{P_6}{P_2} \right) = \frac{Ch\ell}{\sqrt{RT_6}} \left( \frac{P_6}{P_2} \right) g \left( \frac{P_1}{P_6} \right) \quad (34)$$

Equation (34) can be solved graphically by using Figures 12 and 14 for  $p_6$ , and once  $p_6$  is known, the intermediate pressures between knife edges can be determined by

$$\frac{P_4}{P_2} = \left[ \frac{1 + \left( \frac{P_6}{P_2} \right)^2}{2} \right]^{1/2} \quad (35)$$

$$\frac{P_5}{P_6} = \left[ \frac{1 + \left( \frac{P_1}{P_6} \right)^2}{2} \right]^{1/2} \quad (36)$$

With  $p_4$ ,  $p_5$  and  $p_6$  known, the dimensionless load becomes

$$\begin{aligned}\bar{W} &= \frac{\int_0^b (p - p_1) dx}{(p_2 - p_1)^b} \\ &= \frac{1}{1 - r_{12}} \left[ \frac{b_2}{b} (r_{42} - r_{12}) + \frac{d}{b} r_{62} + \frac{b_1}{b} (r_{52} - r_{12}) \right]\end{aligned}\quad (37)$$

and the gas film stiffness can be calculated by differentiating  $\bar{W}$  with respect to  $h$  numerically according to the following expression,

$$K_s = \frac{d\bar{W}}{dh} (p_2 - p_1) \quad (38)$$

The effect of changing the orifice on the load and the static stiffness is qualitatively shown in Figure 13.

#### Hydrodynamic-Convergent Film

Figure 15 shows a typical segment of a hydrodynamic seal operating on the principle of an inclined slider. During operation, a convergent film is formed and gives rise to circumferential and radial pressure profiles as shown in Figure 15.

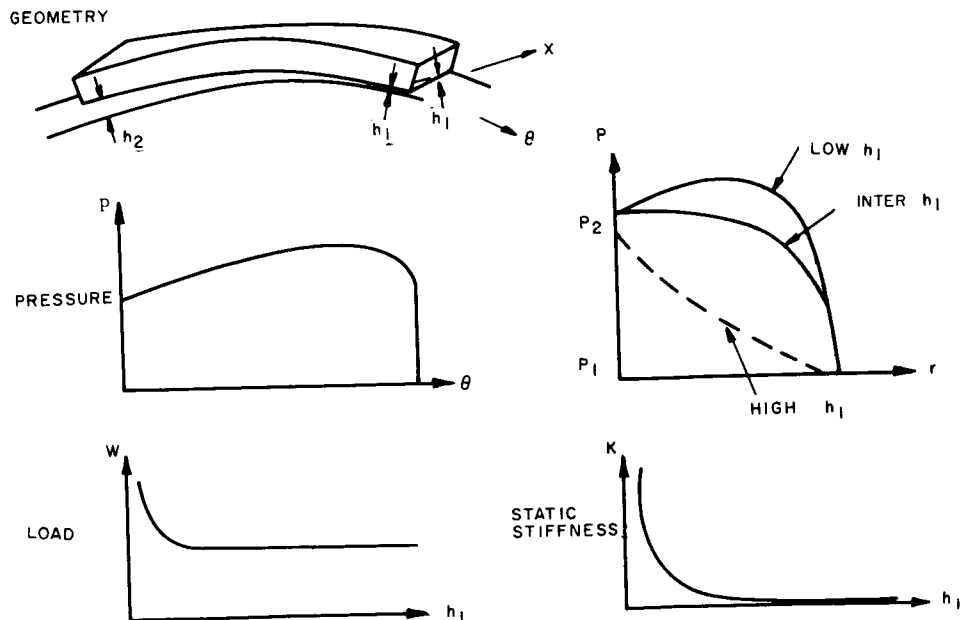


Figure 15 Inclined Slider Seal Segment

In order to estimate the film thickness at which hydrodynamic pressure becomes significant, a solution to the pressure is obtained based on the short bearing equation for an incompressible fluid; the additional load generated by the hydrodynamic action can be calculated by

$$\Delta \bar{W} = \frac{1}{32} \frac{1}{(1-r)} \frac{6\mu U}{p_2} \left(\frac{b}{h_1}\right)^2 \frac{1}{\ell} \left(\frac{h_2 - h_1}{h_1}\right) \quad (39)$$

Assuming that the hydrodynamic effect upon the leakage is negligible, the leakage across each segment can be obtained by integrating the local leakage for differential element according to Equation (3). The resulting expression for each segment of length  $\ell$  is

$$m = \frac{h_1^3 \ell}{96\mu b} p_2 p_2 \left(1 - r_{12}^2\right) \left(\frac{h_2}{h_1}\right)^4 - 1 \quad (40)$$

The static stiffness can be estimated by

$$K_s = \frac{d(\Delta \bar{W})}{dh_1} (p_2 - p_1) = \frac{2\Delta \bar{W} (p_2 - p_1)}{h_1} \quad (41)$$

Using the following data:

|                  |                                     |   |
|------------------|-------------------------------------|---|
| $\mu$            | = viscosity = $5.96 \times 10^{-9}$ | $\frac{\text{lb}}{\text{in}^2} \text{ sec}$ |
| $U$              | = surface velocity = 10,000         | in/sec                                      |
| $b$              | = width of the seal segment = 0.5   | inches                                      |
| $\ell$           | = length of the seal segment = 2.0  | inches                                      |
| $h_1$            | = smaller film thickness = 0.0005   | inches                                      |
| $h_2$            | = larger film thickness = 0.001     | inches                                      |
| $p_1$            | = 200 psi                           |   |
| $p_2$            | = 350 psi                           |   |
| $\Delta \bar{W}$ | = 0.0378                            |   |

the leakage and static stiffness were found respectively to be 0.0506 lb/sec and 22,600 lb/in<sup>3</sup>. In Figure 15, the variation of load and static stiffness with respect to  $h_1$  is also depicted qualitatively. Note the extra load capacity at extremely low film thickness which indicates the desirability of using hydrodynamic action as a protection from bottoming.

### Hydrodynamic-Spiral Groove Seal

The hydrodynamic action in this seal concept can be achieved by a band of spiral grooves located at the low pressure side of the seal. By virtue of the viscous action of the gas, the groove geometry, as oriented in Figure 16, creates a pumping action which increases the resistance of the gas flow from the high pressure to the low pressure side. At a higher film thickness, the pumping is ineffective, so that the seal operates like a step seal as indicated by the pressure profile "b" in Figure 16. The pumping action becomes effective as the film gradually decreases, in that there may exist a film thickness where the pressure gradient in the smooth surface region becomes zero, so that perfect sealing will result as indicated by the pressure profile "c". Further decrease of the film thickness will cause the groove region to act as a compressor and produce negative leakage.

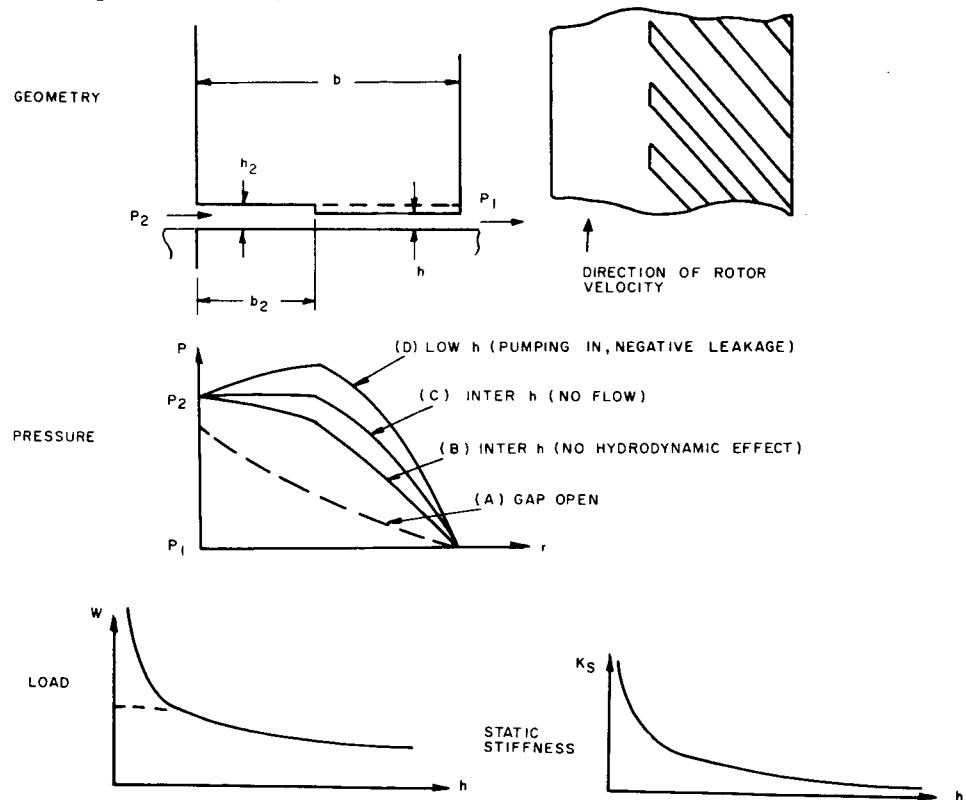


Figure 16 Spiral Groove Hydrodynamic Seal

It is desirable to determine the film thickness at which no flow will take place. For the velocity of 10,000 in/sec, a groove width of 1/4 inch and a gas viscosity of  $5.96 \times 10^{-9}$  (lb. sec)/in<sup>2</sup> this film thickness was found to be 263 microinches. This indicates that the spiral groove seal can be made effective only at an extremely small film thickness. Numerical programs are available to determine the performance of the spiral groove seal and this calculation will be made in the detailed feasibility analysis.

### Hybrid Hydrostatic-Hydrodynamic Seal

This concept combines the design of a hydrostatic-step seal and a hydrodynamic seal. The geometry of this seal concept is shown in Figure 17. The sealing is accomplished by a narrow gap at the low pressure side. On the high pressure side, intermittent pockets are provided to form a series of circumferential step bearings. At a higher film thickness, the pressure generated by the hydrodynamic step bearing is negligible, and the seal operates like a step seal. When the film thickness decreases, the hydrodynamic action becomes effective and the extra load capacity protects it from bottoming.

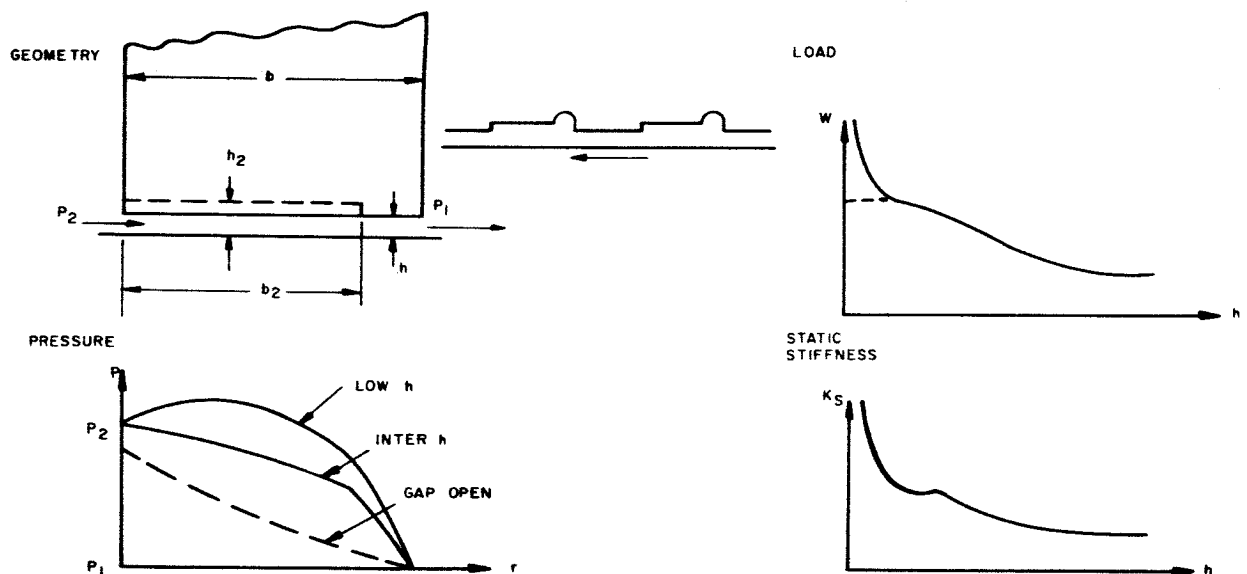


Figure 17 Hybrid Hydrostatic Step-Hydrodynamic Seal

To date, there is no exact analysis to predict the performance of this geometry, but a rough estimate of the load capacity can be made by using the infinite step bearing theory. It was found that an additional mean pressure of 30 psi can be obtained at  $h = 0.0005$  inches based on the infinite theory. For a finite seal geometry, the load capacity will be considerably less than this estimate.

A detailed calculation of the performance by modifying the present computer program for the partial arc bearing will be carried out for further comparison with other seal concepts.

### Hybrid Hydrostatic Pad-Labyrinth Seal

The last primary seal concept is also a hybrid type which consists of a labyrinth seal with intermittent hydrostatic pads for the purpose of controlling the clearance of the labyrinth and at the same time providing the necessary dynamic stiffness for satisfactory tracking. The basic performance of this seal concept is quite similar to that of the hydrostatic-labyrinth seal with the exception that the response of this seal will be more favorable than the plain labyrinth seal on account of the higher dynamic stiffness.

The analyses developed for the orifice compensated seal and hydrostatic-labyrinth seal can be directly used here to estimate the load, static stiffness and leakage of this hybrid concept.

### Comparison of Primary Seal Concepts

Load and leakage curves were calculated for a typical geometry of the hydrostatic-step, the hydrostatic-pocket (also called orifice-compensated), and the hydrostatic-labyrinth seal concepts. These results are plotted in Figure 18 and 19. The hydrostatic-pocket concept appears to have the best stiffness. The leakage curves shown in Figure 18 are only for the cruise condition. For the hydrostatic-step and the hydrostatic-pocket concepts, the leakage in the thin film region is governed by laminar flow, and in the thick film region it is governed by orifice flow. The leakage for the hydrostatic-labyrinth seal is always of the orifice type and it is represented by a single curve in which the leakage is directly proportional to the film thickness.

Table I shows a comparison of all primary seal concepts based on their leakage, film thickness level, tracking capability, and reliability. An individual rating is given to each of these considerations; some of the reasons on which the rating is based are listed after the table. The total ratings of these concepts indicate that no one basic primary seal concept has a clear-cut superiority over the others. The hybrid concepts appear to be slightly more favorable than the basic concepts. The close comparison in the total ratings suggests that a more detailed analysis of each concept is necessary in order to make the final selection of the primary seal concept for the test rig.

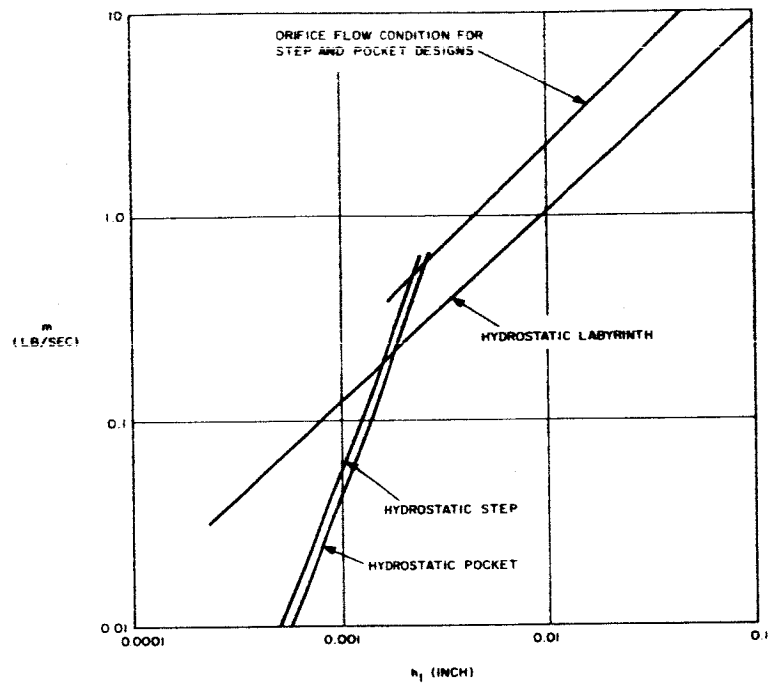


Figure 18 Comparison of Seal Leakage Rates for Cruise Operation

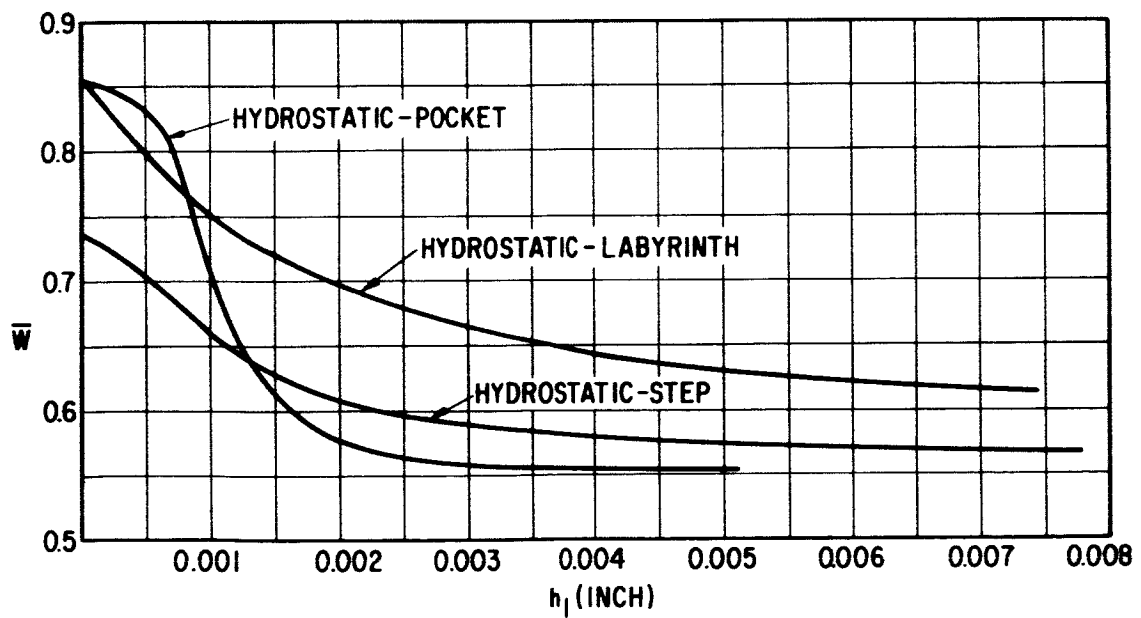


Figure 19 Comparison of Load-Film Thickness Seal Characteristics



TABLE I  
COMPARISON OF PERFORMANCE OF PRIMARY SEAL CONCEPTS  
(Based on Segmented Design)

|                              | Leakage lb/sec. |            | Film Thickness<br>h in. | Rating | Radial or<br>Axial lb<br>Track. in <sup>3</sup> | Rating | Angular<br>Tracking | Rating | Stability   | Rating | Tolerance<br>to Dirt<br>& Rubbing | Rating | Final<br>Rating |      |
|------------------------------|-----------------|------------|-------------------------|--------|---|--------|---------------------|--------|-------------|--------|-----------------------------------|--------|-----------------|------|
|                              | (Cruise)        | (Take-Off) |                         |        |   |        |                     |        |             |        |                                   |        | (E)             | (I)  |
| Step Seal                    | 0.044           | 0.25       | 0.001                   | 7      | $\delta/h=0.24$ (E)<br>$=2.0$ (I)               | 5      | Low                 | 2      | Low         | 2      | Low                               | 2      | .09             | .02  |
| Orifice<br>Compensated       | 0.038           | 0.22       | 0.001                   | 7      | $\delta/h=0.056$ (E)<br>$=0.51$ (I)             | 7      | Low                 | 2      | Low         | 2      | Low                               | 2      | .13             | .04  |
| Hydrostatic<br>Labyrinth     | 0.126           | 0.350      | 0.001                   | 4      | Very Low  | 1      | Very<br>Low         | 1      | High        | 8      | Medium                            | 5      | .05             | .05  |
| Hydrodynamic                 | 0.02            | 0.1        | 0.0005                  | 9      | $\delta/h=0.128$ (E)<br>$=1.4$ (I)              | 6      | Medium              | 5      | Very<br>Low | 1      | Low                               | 2      | .18             | .03  |
| Spiral<br>Groove             | 0.0             | 0.0        | 0.0003                  | 9      | $\delta/h=0.21$ (E)<br>$=2.2$ (I)               | 5      | Medium              | 5      | Very<br>Low | 1      | Low                               | 2      | .15             | .03  |
| Hydrostatic<br>Hydrodynamic  | 0.01            | 0.05       | 0.0003                  | 10     | $\delta/h=0.21$ (E)<br>$=2.2$ (I)               | 5      | Medium              | 5      | Very<br>Low | 1      | Low                               | 2      | .16             | .033 |
| Hydrostatic<br>Pad Labyrinth | 0.126           | 0.30       | 0.001                   | 4      | $\delta/h=0.22$ (E)<br>$=2.0$ (I)               | 5      | Low                 | 2      | Medium      | 5      | Medium                            | 5      | .32             | .07  |

(E) - End

(I) - Inter

$\delta$  - Amplitude of seal vibration relative to the rotor  
based on a rotor radial amplitude of 0.016 TIR

### Secondary Seal Behavior

The secondary seal concepts suggested for screening study can be classified into four types as shown in Figure 20. The operation and principle of each concept are described in the following paragraphs.

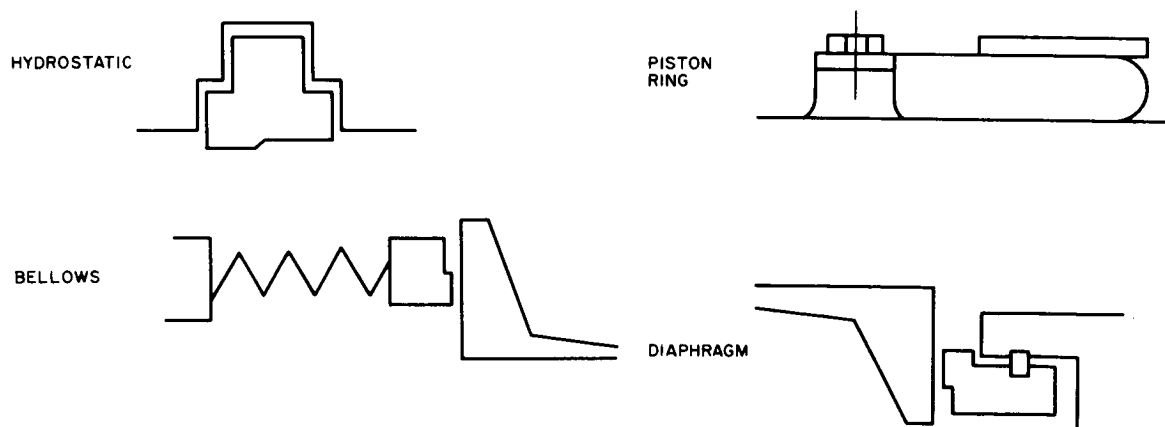


Figure 20 Types of Secondary Seal

## Hydrostatic

As shown in Figure 21, the principal feature of this concept is that both sides of the seal segments are floated frictionlessly by hydrostatic bearings. This action allows the seal segments to track the rotor motion freely.

Vertical forces are balanced by limiting the horizontal surface over which  $p_2$  acts, and by applying the downstream pressure  $p_1$  to the two shoulders. Horizontal forces are likewise balanced by the insertion of the low pressure zone on the right-hand vertical face, and the high pressure zone on the lower left-hand vertical face. Moment balance may be achieved by adjusting the shoulder width  $b_4$  and the shoulder heights  $d$  and  $g$ . Each vertical face has a restoring force generated by a hydrostatic step. While orifice compensation could be used, the step construction appears more simple and straightforward in this case.

The clearances of these secondary sealing surfaces should be held at 0.0003 to 0.0005 inch in order to keep the secondary leakage at a minimum.

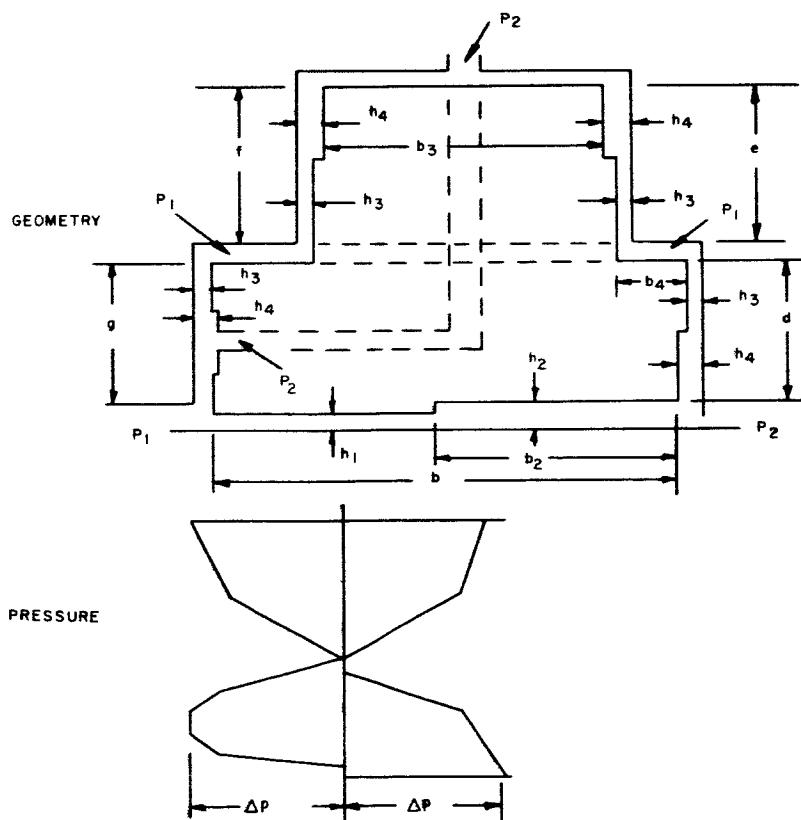


Figure 21 Hydrostatic Secondary Seal

## Bellows

The bellows has a unique feature as a secondary seal, namely that it acts as a seal as well as a spring. But so far, successful applications of bellows have been limited to smaller diameters, low temperatures and moderate pressures. When the requirements become more severe, the walls of the bellows may buckle under the pressure unbalance between sections. Advice from Sealol, Inc., indicates also that the necessary radial dimension is about two inches, a figure too large for compact design. For these reasons, it is doubtful that a satisfactory bellows can be designed for the present seal application.

## Piston Ring

The piston ring and spring type of secondary seal construction is the most commonly used design, at least in all face-type seals. Either one or two piston rings can be used to provide secondary sealing between the frame and a carrier on which the primary seal ring is mounted. The piston ring is usually pressure-balanced to yield low friction across the secondary sealing surface. Minimizing frictional force is important since it may prevent satisfactory tracking of the runner under rotor vibration.

Successful results have been reported by Pratt & Whitney Aircraft in using the piston and spring design on jet engine main bearing seals. No great difficulty is anticipated in manufacturing large diameter piston rings for the compressor and interstage seals, so that the piston ring design is a strong contender among the list of secondary seal concepts.

## Diaphragm

The function of a diaphragm secondary seal is very similar to that of the bellows. It is a flexible connector between the primary seal and the carrier. Figure 22 shows a typical schematic of a primary seal mounted on a "U" shaped diaphragm. The flexibility of the diaphragm allows the primary seal strip to conform to any movement of the rotor caused by runout, transverse or axial vibration, and thermal expansion. Free body diagrams showing the forces acting on the seal strip and the diaphragm can be found in the lower half of Figure 22. The primary sealing surface is illustrated as the hydrostatic-step type and is located on the bottom of the strip. The pressure in the sealing area is balanced by the full pressure acting on the top face of the strip extending to where the diaphragm begins. In the horizontal direction, the forces acting on the strip are balanced by a tension member anchored to the frame. This tension member is located in such a way as to insure a moment balance of all forces on the strip.

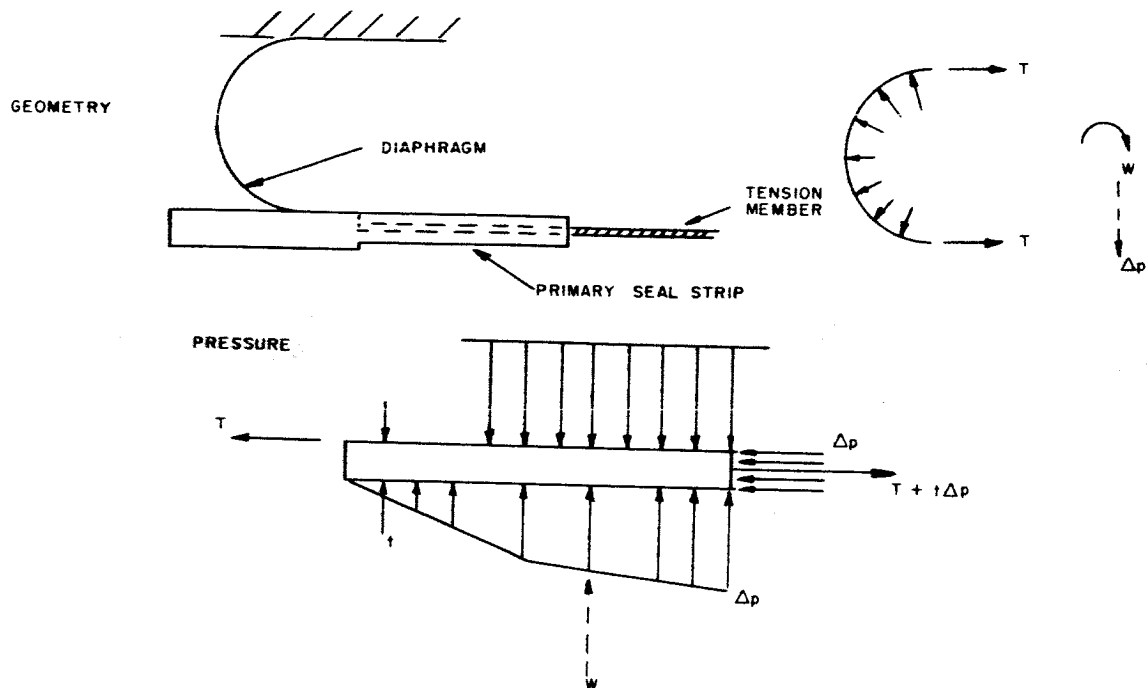


Figure 22 Diaphragm-Type Secondary Seal

The diaphragm seal is applicable for both circumferential and face seals. For circumferential applications, it may be necessary to provide radial slots in the diaphragm to increase its flexibility. Secondary foils will be overlayed between slots to prevent leakage through slots. For radial face seals, a single-piece diaphragm will be governed mainly by the bending stress caused by a maximum movement of the primary seal and the direct stress produced by the hydrostatic pressure.

The one-piece diaphragm appears to be attractive from the standpoint of leakage, friction, and simplicity but the slotted diaphragm with secondary foil will definitely introduce complications to the seal system. From the standpoint of dimensional stability and reliability, the diaphragm secondary seal is not desirable because of its extremely thin structure.

Table II shows a qualitative comparison of all secondary seal concepts. On balance, the hydrostatic and piston-ring types appear more practical than the flexible-diaphragm seals.

TABLE II  
COMPARISON OF SECONDARY SEAL CONCEPTS

|             | <u>Leakages</u> | <u>r</u> | <u>Friction</u> | <u>r</u> | <u>Simplicity</u> | <u>r</u> | <u>Dimensional<br/>Stability</u> | <u>r</u> | <u>Reliability</u> | <u>r</u> | <u>Total<br/>Rating</u> |
|-------------|-----------------|----------|-----------------|----------|-------------------|----------|----------------------------------|----------|--------------------|----------|-------------------------|
| Hydrostatic | Medium          | 5        | Very Low        | 9        | Simple            | 9        | Medium                           | 5        | Medium             | 5        | 3.24                    |
| Piston      | Medium          | 5        | Medium          | 5        | Simple            | 9        | Medium                           | 5        | Medium             | 5        | 1.8                     |
| Diaphragm   | Low             | 7        | Medium          | 5        | Medium            | 5        | Low                              | 2        | Low                | 2        | .224                    |
| Bellows     | Very<br>Low     | 9        | Very Low        | 9        | Medium            | 5        | Very<br>Low                      | 1        | Very<br>Low        | 1        | .130                    |

r = Individual rating

### Screening of Suggested End and Interstage Seal Designs

#### General Discussion

Altogether, 34 seal designs have been collected for screening. These seal designs include those contained in the request for proposal and in the Pratt & Whitney Aircraft proposal, those suggested by Stein Seal Co., and those conceived by MTI during the course of the preliminary screening study.

A brief scanning of the suggested designs revealed that emphasis had been placed on the primary seal design. In most cases, the bellows were used as a symbol for the secondary seal and little or no consideration was given to the secondary seal friction and balancing. Subsequent preliminary analyses of film thickness level, leakage rate, heat generation, and thermal distortion all indicated that secondary sealing design is of utmost importance. It has a major influence upon the static and dynamic performance, particularly for a segmented design. For this reason, the designs conceived later during this investigation have given more considerations to the secondary seal design.

Each design has been given a code number according to the type of primary seal concept. The abbreviations used are the following:

HSS - Hydrostatic-Step  
HS - Hydrostatic-Pocket  
HD - Hydrodynamic  
SG - Spiral Groove  
HSL - Hydrostatic-Labyrinth  
VL - Vortex Labyrinth  
D - Diaphragm  
F - Foil

In this screening study these designs have been compared against the following criteria:

| <u>Criteria</u>                                | <u>Rating</u> |
|--|---------------|
| 1. Leakage rate, both primary and secondary    | 2             |
| 2. Compensation ability                        |               |
| a. Primary seal tracking                       | 2             |
| b. Secondary seal friction and balancing       | 2             |
| c. Thermal distortion                          | 2             |
| 3. Gas film stability                          | 2             |
| 4. Dimensional stability                       | 2             |
| 5. Reliability                                 |               |
| a. Fail safe ability                           | 1             |
| b. Tolerance to start, stop and high speed rub | 1             |
| c. Tolerance to foreign particles              | 1             |
| d. Off-design operation (tracking), at         |               |
| 1. take-off                                    | 1             |
| 2. idling                                      | 1             |
| 3. windmilling                                 | 1             |
| 4. response to rapid maneuver of aircraft      | 1             |

Each design is given an individual rating from 0-10 for each criterion. A value of 5 is considered average, above 5 favorable and below 5 unfavorable.

Since many of the criteria are essential, in that a low rating must rule out a design poor in that respect, the total rating has been formulated as a multiplicative rather than an additive combination of the individual ratings. The most important factors are given an exponent of 2. Following this approach,

$$\text{TOTAL RATING} = \pi_0^n (r_i)^{e_i}$$

where

$e_i$  = exponents for  $r_i$

$r_i$  = individual rating

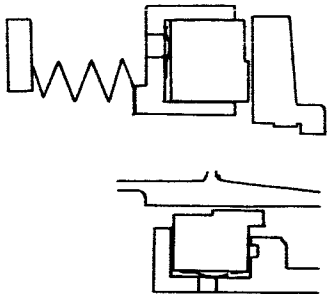
$n$  = number of criteria considered

The result of this screening is expected to yield sufficient information to select four designs for further detailed feasibility study. The weight, space and costing factors were not included in the screening criteria. These factors are considered as secondary at this stage and would have been only if the screening study based on the primary essential criteria yielded insufficient reason for selection.

The screening is accomplished in two stages. In the first stage, careful considerations and individual ratings are given to each seal concept against the first half of the screening criteria. Results of this screening study are shown as matrix charts in Tables III through IX. The first ten interstage and end seal concepts are selected for further screening against the second half of the screening criteria. Results of the second screening are tabulated in Table X. Based on the results of the second screening, the first four designs of the end as well as interstage seal concepts are selected and recommended for further feasibility study. A summary of these results is shown in Table XI.

HSS-1

CONCEPT



| Type of Primary Seal           | Hydrostatic-Step (Segmented) |
|--------------------------------|------------------------------|
| Type of Secondary Seal         | Bellows or Piston            |
| Type of Seal Ring Construction | Face or Circumferential      |

|              |              |       |         |   |
|--------------|--------------|-------|---------|---|
| LEAKAGE RATE | a. Primary   | 0.004 | lb/sec. | 7 |
|              | b. Secondary | 0.005 |         |   |

|                       |  |   |
|-----------------------|--|---|
| PRIMARY SEAL TRACKING | $\frac{\delta}{h} = .084$ (End, Face)  | 7 |
|                       | $\frac{\delta}{h} = .65$ (Inter, Face) | 2 |

|                                       |      |   |
|---------------------------------------|------|---|
| SECONDARY SEAL FRICTION AND BALANCING | Poor | 3 |
|---------------------------------------|------|---|

|                    |                                      |   |
|--------------------|--------------------------------------|---|
| THERMAL DISTORTION | Can be controlled by segment length. | 5 |
|--------------------|--------------------------------------|---|

|                    |   |   |
|--------------------|---|---|
| ELASTIC DISTORTION | Can be controlled by segment thickness. | 6 |
|--------------------|---|---|

|                    |        |   |
|--------------------|--------|---|
| GAS FILM STABILITY | Stable | 8 |
|--------------------|--------|---|

|                       |                       |   |
|-----------------------|-----------------------|---|
| DIMENSIONAL STABILITY | Low tolerance to wear | 5 |
|-----------------------|-----------------------|---|

INTERMEDIATE RATING (End)  
(Inter)

1.768 x 10<sup>5</sup>  
.50 x 10<sup>5</sup>

↑  
Selected  
for further  
screening

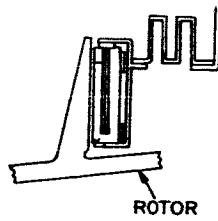
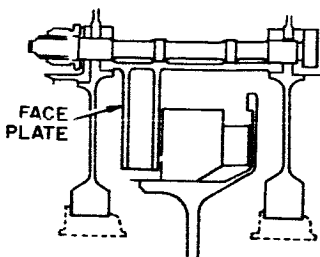


TABLE III

## MATRIX CHART FOR SEAL CONCEPTS HSS-1, HS

HSS-2

HS-1



SPRING

| Hydrostatic-Step (Segmented)<br>Spring & Hydrostatic<br>Face |   | Hydrostatic-Face<br>Bellows<br>Solid Ring   |   | Hydrostatic-Face<br>Bellows<br>Solid Ring |
|--|---|---|---|---|
| 0.044  | 7 | 0.038   | 8 | 0.038                                     |
| 0.05   |   | 0.0   |   | 0.001                                     |
| $\frac{\delta}{h} = 0.084$ (End)                             | 7 | $\frac{\delta}{h} = .02$ (End)  | 9 | $\frac{\delta}{h} = .02$                  |
| $\frac{\delta}{h} = 0.65$ (Inter)                            | 2 | $\frac{\delta}{h} = .16$ (Inter)  | 6 | $\frac{\delta}{h} = .16$                  |
| Friction Very High   | 1 | Friction Low,<br>but balancing<br>is difficult<br>for bellows.                          | 1 | Friction<br>Balancing<br>difficult        |
| Same as HSS-1  | 5 | Thermal coning 5<br>is severe but<br>can be compen-<br>sated by elastic<br>deformation. |   | Coning                                    |
| Same as HSS-1  | 6 | Twist of<br>section is<br>severe, can<br>be controlled.                                 | 6 | Small                                     |
| Stable   | 8 | Stable if<br>orifice is<br>properly<br>designed.  | 6 | Stable                                    |
| Low tolerance to wear  | 5 |   | 8 |   |

$$1.753 \times 10^5$$

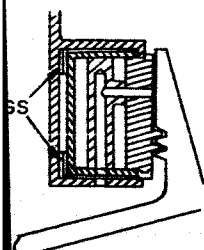
$$0.211 \times 10^5$$

$$\begin{matrix} 1.038 \times 10^5 \\ 0.692 \times 10^5 \end{matrix}$$

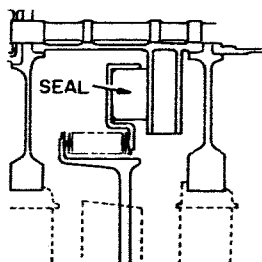
↑  
Selected  
for further  
screening

2

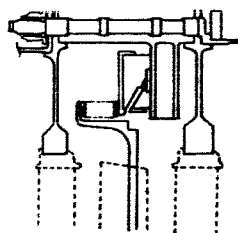
HS-2



HS-3



HS-4



Static-Self Locating  
Static  
ing, Face

Low-Unbalanced Face  
Bellows  
Rubbing Seal, Face

Hydrostatic-Pocket  
Bellows  
Solid Ring-Face

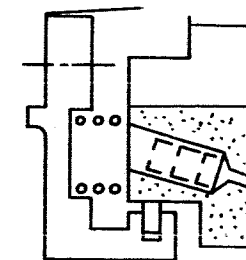
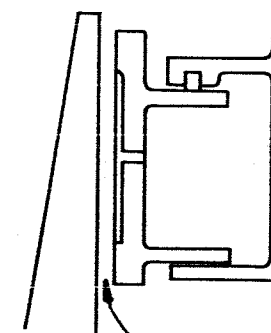
|                       |                     |  |     |   |                    |
|-----------------------|---------------------|--|-----|---|--------------------|
|                       | 8                   | Nearly Zero  | 10  | 0.038<br>0.0  | 8                  |
| (End)                 | 9                   | Volume of Pockets  |     | $\frac{\delta}{h} = .02$ (End)                          | 9                  |
| (Inter)               | 6                   | must be small  |     | $\frac{\delta}{h} = .16$ (Inter)                        | 6                  |
| n Low,<br>ng is<br>t. | 2                   |  |     | Same as HS-1  | 1                  |
| is severe             | 1                   | Seal Power Loss<br>is estimated at<br>76 hp thermal<br>distortion and<br>temperature rise<br>is excessive. | 0.0 | Coning is<br>severe, cannot<br>be compensated.          | 1                  |
|                       | 7                   |  | 0.0 | Twist of section<br>is severe but<br>can be controlled. | 6                  |
|                       | 6                   |  | 0.0 | Strong likeli-<br>hood to hammer.                       | 2                  |
|                       | 8                   |  | 0.0 |   | 8                  |
|                       | $0.484 \times 10^5$ |  | 0.0 |   | $.069 \times 10^5$ |
|                       | $0.323 \times 10^5$ |  |     |   | $.046 \times 10^5$ |

## MATRIX CHART FOR SEAL CONCE

HS-5

HS-6

CONCEPT



Type of Primary Seal  
Type of Secondary Seal  
Type of Seal Ring Construction

Hydrostatic-Pocket  
Piston  
Solid Ring, Face

Hydrostatic-Pocket  
Piston  
Solid-Ring, Face

LEAKAGE RATE a. Primary  
b. Secondary

0.038 8  
0.0

0.038  
0.0

PRIMARY SEAL TRACKING

$\frac{\delta}{h} = 0.02$  (End) 9  
.16 (Inter) 6

Same as HS-5

SECONDARY SEAL FRICTION  
AND BALANCING

Piston friction 3  
is high

Same as HS-5

THERMAL DISTORTION

Thermal coning 2  
is large

Coning is  
severe

ELASTIC DISTORTION

Can be controlled 6

Can be controlled

GAS FILM STABILITY

Strong likeli- 2  
hood to hammer

Same as HS-5

DIMENSIONAL STABILITY

8

INTERMEDIATE RATING (End)

$0.415 \times 10^5$

0.207

(Inter)

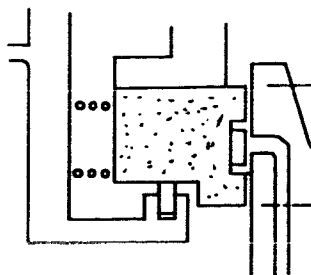
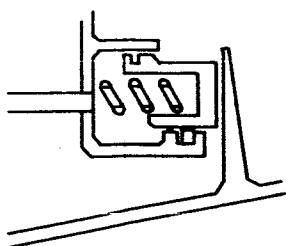
$0.277 \times 10^5$

0.138

CPTS HS-5, HS-6, HS-7, AND HS-8

HS-7

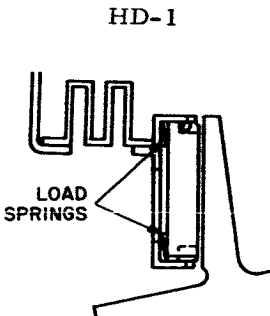
HS-8



| et            |   | Hydrostatic-Externally Press.<br>Piston<br>Solid Ring | Hydrostatic-Externally Press.<br>Piston<br>Solid Ring, Face |
|---------------|---|---|---|
| 8             | 0.07<br>0.0                             | 6   | 0.07<br>0.0   |
| 9             | Same as HS-5                            | 9   | Same as HS-5  |
| 6             |   | 9   |   |
| 3             | Piston friction is<br>very high         | 4   | Same as HS-5  |
| 1             | Coning is severe                        | 1   | Coning is severe  |
| 6             | Twist of seal ring<br>can be controlled | 6   | Twist can be<br>controlled                                  |
| 2             | Very strong likeli-<br>hood to hammer   | 2   | Same as HS-7  |
| 8             |   | 8   |   |
| $\times 10^5$ |   | $0.207 \times 10^5$                                   | $0.311 \times 10^5$   |
| $\times 10^5$ |   | $0.207 \times 10^5$                                   | $0.311 \times 10^5$   |

2

CONCEPT



| Type of Primary Seal                     | Hydrostatic-Shoe   | Hydr                                |                        |              |
|--|--|-------------------------------------|------------------------|--------------|
| Type of Secondary Seal                   | Bellows  | Dry                                 |                        |              |
| Type of Seal Ring Construction           | Segmented, Face  | Segm                                |                        |              |
| LEAKAGE RATE                             | a. Primary<br>b. Secondary   | 0.02 at 0.0005"<br>0.005 at 0.0003" | 9<br>9                 | 0.02<br>0.00 |
| PRIMARY SEAL TRACKING                    | $\frac{\delta}{h} = .04$ (End)<br>$\frac{\delta}{h} = .32$ (Inter) | 8<br>5                              | $\frac{\delta}{h} = 1$ |              |
| SECONDARY SEAL FRICTION<br>AND BALANCING | Friction is low<br>balancing for<br>bellows is<br>sensitive        | 1                                   | Fric<br>high           |              |
| THERMAL DISTORTION                       | Can be con-<br>trolled by vary-<br>ing length of<br>segments       | 5                                   | Same                   |              |
| ELASTIC DISTORTION                       | Severe but can<br>be controlled                                    | 6                                   | Less                   |              |
| GAS FILM STABILITY                       | Stable   | 8                                   | Stabl                  |              |
| DIMENSIONAL STABILITY                    |  | 8                                   |                        |              |

INTERMEDIATE RATING (End)  
(Inter)

1.38 x 10<sup>5</sup>  
0.862 x 10<sup>5</sup>

↑  
Selected for further screening

TABLE V

RT FOR SEAL CONCEPTS HD-1, HD-2, HD-3, HD-4, SG-1, AND SG-2

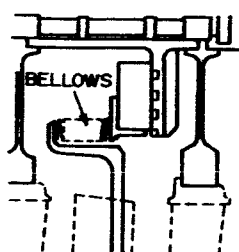
| HD-2   | HD-3  | HD-4   |
|--|---|--|
|  |   |  |
| Hydrodynamic-Shoe<br>Dry Rub<br>Segmented, Circum. | Hydrodynamic-Shoe<br>Dry Rub<br>Segmented, Face   | Hydrostatic-Hydro<br>Dry Rubbing<br>Segmented, Circum      |
| at 0.0005" 9<br>at 0.0003"                         | 0.02 at 0.0005" 9<br>0.005 at 0.0003"   | 0.01 at 0.0003"<br>0.0                                     |
| .12 (End) 6<br>.10 (Inter) 0.0                     | $\frac{\delta}{h} = .04$ (End) 8<br>$\frac{\delta}{h} = .32$ (Inter) 5  | $\frac{\delta}{h} = .18$ (End)<br>$\frac{\delta}{h} = 1.5$ |
| Friction very 0.5                                  | Friction very 0.5<br>high   | Friction very<br>high                                      |
| Same as HD-1 5                                     | Same as HD-2 5  | Severe but can be<br>controlled                            |
| Severe 7   | Less severe 7   | Small  |
| 8  | Stable 8  | Stable   |
| 8  | 8   |  |
| $0.605 \times 10^5$<br>0.0                         | <div data-bbox="507 1680 694 1782" style="border: 1px solid black; padding: 5px; display: inline-block;"> <math>0.805 \times 10^5</math><br/> <math>0.504 \times 10^5</math> </div> | $0.405 \times 10^5$<br>0.0                                 |

Selected  
for further  
screening

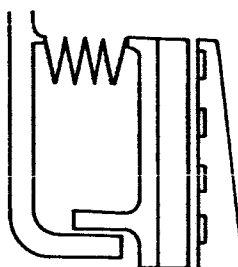
2

-2

SG-1



SG-2



Dynamic

n.

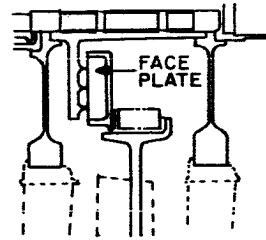
Spiral Groove  
Bellows  
Solid Ring, Face

Spiral Groove  
Bellows  
Solid Ring, Face

|        |                                     |     |                                |     |
|--------|-------------------------------------|-----|--------------------------------|-----|
| 9      | 0.0 at 0.0003"                      | 10  | 0.0                            | 10' |
| 6      | $\frac{\delta}{h} = .06$ (End)      | 8   | $\frac{\delta}{h} = .06$ (End) | 8   |
| 0.0    | 0.5 (Inter)                         | 3   | 0.5 (Inter)                    | 3   |
| 0.5    | Balancing<br>difficult              | 1   | Balancing<br>difficult         | 1   |
| 5      | Thermal<br>coning is<br>very severe | 0.5 | Very severe                    | 0.5 |
| 7.5    | Less severe                         | 8   | Severe                         | 8   |
| 8      | Stable                              | 8   | Stable                         | 8   |
| 5      |                                     | 5   |                                | 5   |
| $10^5$ | $0.128 \times 10^5$                 |     | $0.128 \times 10^5$            |     |
|        | $0.048 \times 10^5$                 |     | $0.048 \times 10^5$            |     |

HS-L-1

## CONCEPT



| Type of Primary Seals<br>Type of Secondary Seals<br>Type of Seal Ring Construction | Hydrostatic-Labyrinth<br>Bellows<br>Solid Ring, Face                     |   |                     |
|--|--|---|---------------------|
| LEAKAGE RATE a. Primary<br>b. Secondary  | 0.11 at 0.001"<br>0.0  | 5 | 0<br>0              |
| PRIMARY SEAL TRACKING  | Tracking poor<br>because of low<br>dynamic stiffness                     | 1 | R<br>b<br>d         |
| SECONDARY SEAL FRICTION<br>AND BALANCING   | Balancing<br>difficult   | 1 | F                   |
| THERMAL DISTORTION   | Face coning is<br>less severe  | 6 | T<br>is<br>b<br>c   |
| ELASTIC DISTORTION   | Less severe  | 8 | L                   |
| GAS FILM STABILITY   | Most likely un-<br>stable but hammer-<br>ing amplitude might<br>be small | 3 | Sa                  |
| DIMENSIONAL STABILITY  |  | 8 |                     |
| INTERMEDIATE RATING (End)<br>(Inter)   |  |   |                     |
|  |  |   | $.0576 \times 10^5$ |

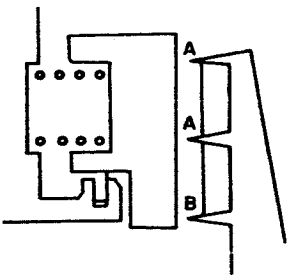
1



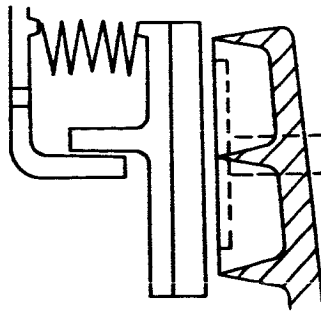
TABLE VI

IX CHART FOR SEAL CONCEPTS HS-L-1, HS-L-2, HS-L-3, HS-L-4,

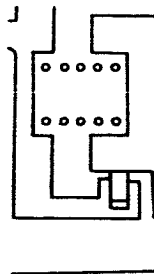
HS-L-2



HS-L-3



HS-L-4



Hydrostatic-Labyrinth  
Piston  
Solid Ring, Face

0.11 at .001" 5  
0.0

Response is poor 1  
because of low  
dynamic stiffness

Friction is high 6

Thermal coning 6  
less severe  
it cannot be  
compensated

Less severe 8

Same as HS-L-1 3

8

$.346 \times 10^5$

Hydrost. Pocket-Labyrinth  
Bellows  
Solid Ring, Face

0.108 at 0.001" 4  
0.0

With hydrostatic pads 5  
dynamic stiffness is  
adequate

Bellow balancing is 1  
difficult

Thermal distortion 4  
can be significant

Less severe 8

Same as HS-L-1 3

8

$.153 \times 10^5$

Hydrost. Po  
Piston  
Solid Ring,

0.126 at 0.0  
0.0

Response is  
because of  
dynamic sti

Friction is

Same as HS

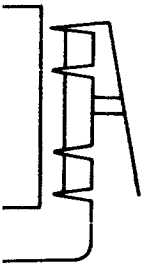
Less severe

Same as HS

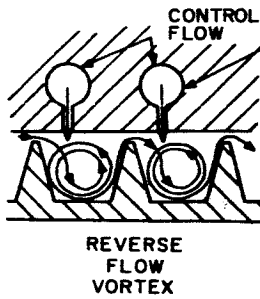
2

V1, AND F-1

L-4



VL



F-1

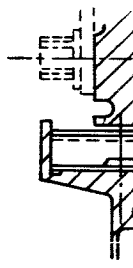
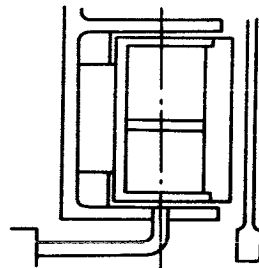


| Bucket-Labyrinth    |   | Vortex Labyrinth   |       | Centrifugal Activ. Foil  |   |
|---------------------|---|--------------------|-------|--|---|
| Face                |   | Circumferential    |       | Not shown<br>Foil, Face  |   |
| 01"                 | 4 | 1.0                | 0.005 | 0.038 at 0.001"  | 8 |
| poor<br>ow<br>fness | 1 |                    | 10    | Local film stiffness<br>is adequate  | 5 |
| high                | 6 |                    | 10    |  | 5 |
| L-1                 | 6 | Not severe         | 8     | Coning of seal ring<br>is severe but can be<br>compensated by foil                           | 5 |
|                     | 8 | Not severe         |       | Foil has no rigidity<br>in radial direction.<br>Local deformation is<br>difficult to control | 1 |
| L-1                 | 3 | Stable             | 10    | Foil might flutter   | 3 |
|                     | 8 |                    | 10    |  | 3 |
| $.276 \times 10^5$  |   | $.320 \times 10^5$ |       | $.09 \times 10^5$  |   |

3

F-2

CONCEPT

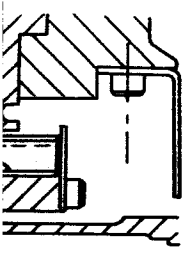
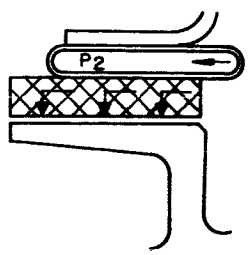
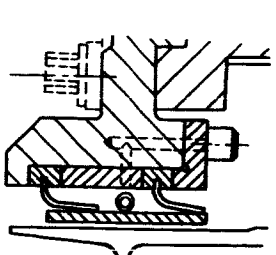


| Type of Primary Seal      | Type of Secondary Seal | Type of Seal Ring Construction | Foil-Hydrostatic   | Hydrostatic | Solid Ring, Face | Foil-Sp                | Foil | Circum |
|---------------------------|------------------------|--------------------------------|--------------------|-------------|------------------|------------------------|------|--------|
| LEAKAGE                   | a. Primary             |                                | 0.038 at 0.001"    | 8           |                  | 0.02 at                |      |        |
|                           | b. Secondary           |                                | 0.005 at 0.0003"   |             |                  | 0.0                    |      |        |
| PRIMARY SEAL TRACKING     |                        |                                | Local film stiff-  | 5           |                  | Same a                 |      |        |
|                           |                        |                                | ness is adequate   |             |                  |                        |      |        |
| SECONDARY SEAL FRICTION   |                        |                                | Very low           | 9           |                  | Frictio                |      |        |
| AND BALANCING             |                        |                                |                    |             |                  | tolerab                |      |        |
| THERMAL DISTORTION        |                        |                                | Coning is severe   | 5           |                  | Severe                 |      |        |
|                           |                        |                                | but can be com-    |             |                  | comper                 |      |        |
|                           |                        |                                | pensated           |             |                  | elastic                |      |        |
|                           |                        |                                |                    |             |                  | tion                   |      |        |
| ELASTIC DISTORTION        |                        |                                | Foil local de-     | 1           |                  | Foil lo                |      |        |
|                           |                        |                                | formation is       |             |                  | format                 |      |        |
|                           |                        |                                | difficult to       |             |                  | difficul               |      |        |
|                           |                        |                                | control            |             |                  | control                |      |        |
| GAS FILM STABILITY        |                        |                                | Foil might flutter | 3           |                  | Foil m                 |      |        |
| DIMENSIONAL STABILITY     |                        |                                |                    | 3           |                  |                        |      |        |
| INTERMEDIATE RATING (End) |                        |                                |                    |             |                  | .162 x 10 <sup>5</sup> |      |        |
| (Inter)                   |                        |                                |                    |             |                  | .162 x 10 <sup>5</sup> |      |        |

1

TABLE VII

RIX CHART FOR SEAL CONCEPTS F-2, F-3, D-1, D-2, D-3, and D

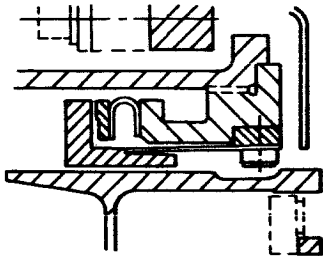
| F-3   |   | D-1  |   | D-2   |   |
|---|---|--|---|---|---|
|  |   |   |   |  |   |
| Spiral Groove<br>Differential   |   | Hydrostatic-Porous Pads<br>Diaphragm<br>Solid Ring, Circum.  |   | Hydrostatic<br>Diaphragm<br>Segmented, Circum.                                    |   |
| 0.0005"   | 9 | 0.019<br>0.0   | 9 | 0.019<br>0.0  | 9 |
| s F-2   | 5 | $\frac{\delta}{h} = .06$ (End) 8<br>.5 (Inter) 3   |   | $\frac{\delta}{h} = .06$ (End) 8<br>.5 (Inter) 3                                  |   |
| n is<br>le  | 8 | Friction is very low but side thrust is not balanced   | 3 | Friction is medium side pressure is not balanced                                  | 1 |
| but is<br>sated by<br>deforma-  | 5 | Severe but it is compensated by elastic deformation  | 5 | Severe but it is compensated by elastic deformation                               | 5 |
| cal de-<br>on is<br>t to  | 1 | Severe but controllable  | 5 | Severe controllable   | 6 |
| ght flutter   | 3 | Stability can be controlled by pore size   | 3 | Stable  | 6 |
|   | 3 |  | 5 |   | 5 |
| .162 x 10 <sup>5</sup>  |   | <div style="border: 1px solid black; padding: 5px; display: inline-block;"> .81 x 10<sup>5</sup><br/> .304 x 10<sup>5</sup> </div> |   | .648 x 10 <sup>5</sup><br>.225 x 10 <sup>5</sup>                                  |   |
| .162 x 10 <sup>5</sup>  |   |  |   |   |   |
|   |   | <div style="text-align: center;"> ↑<br/> Selected for<br/> further screening </div>  |   |   |   |

2

-3A.

D-3

D-3A



Same as D-3  
with Piston  
Ring replacing  
Diaphragm Ring

| Hydrostatic-Hydrodynamic<br>Diaphragm<br>Segmented, Circum. |   | Hydrostatic-Hydrodynamic<br>Piston<br>Segmented, Circum. |     |
|---|---|--|-----|
| 0.044 at 0.001"   | 7 | 0.044 at 0.001"  | 7   |
| 0.015 at 0.0003"  |   | 0.015 at 0.0003"   |     |
| $\frac{\delta}{h} = .25$ (End)                              | 5 | Same as D-3  | 5   |
| $\frac{\delta}{h} = 2.1$ (Inter)                            | 0 |  | 0   |
| Friction is low<br>balancing is good                        | 9 | Friction is high<br>balancing is good                    | 6   |
| Can be controlled<br>by length of<br>segments               | 5 | Can be controlled<br>by length of<br>segments            | 5   |
| Less severe   | 8 | Less severe  | 8   |
| Stable  | 8 | Stable   | 7.5 |
| 0.5   |   | 0.5  |     |
| $.502 \times 10^5$  |   | $.315 \times 10^5$                                       |     |
| 0   |   | 0  |     |

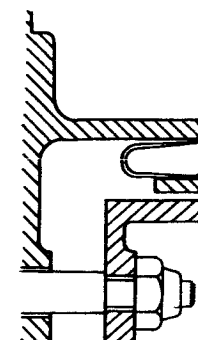
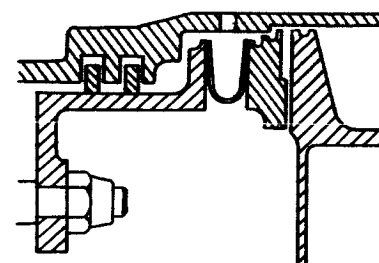
3

TABLE VII

MATRIX CHART FOR SEAL CONCEPT

D-4

CONCEPT



| Type of Primary Seal                     | Type of Secondary Seal     | Type of Seal Ring Construction | Hydrostatic<br>Piston-Diaphragm<br>Flexible-Ring, Face | Hydrostatic<br>Diaphragm<br>Flexible-Ring |
|--|----------------------------|--------------------------------|--|---|
| LEAKAGE RATE                             | a. Primary<br>b. Secondary |                                | 0.038 at 0.001"<br>0.005 at 0.0003"                    | 8<br>0.038 at<br>0.01 at                  |
| PRIMARY SEAL TRACKING                    |                            |                                | $\frac{\delta}{h} = .02$ (End)<br>.16 (Inter)          | 9<br>6<br>Same as                         |
| SECONDARY SEAL FRICTION<br>AND BALANCING |                            |                                | Friction can be<br>high. Balancing<br>is good          | 6<br>Friction<br>Balancing                |
| THERMAL DISTORTION                       |                            |                                | Severe but can be<br>compensated                       | 5<br>Same as                              |
| ELASTIC DISTORTION                       |                            |                                | Severe but con-<br>trollable                           | 4<br>Same as                              |
| GAS FILM STABILITY                       |                            |                                | Stable   | 8<br>Stable                               |
| DIMENSIONAL STABILITY                    |                            |                                |  | 5   |
| 1st SCREENING RATING (End)<br>(Inter)    |                            |                                |  |   |

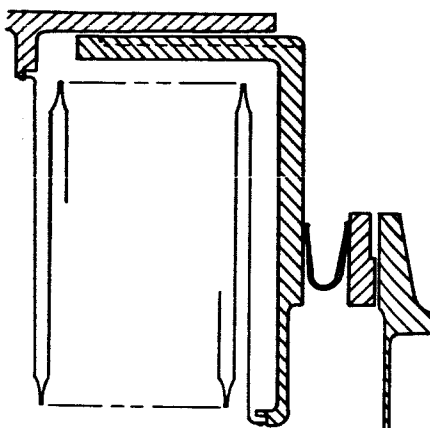
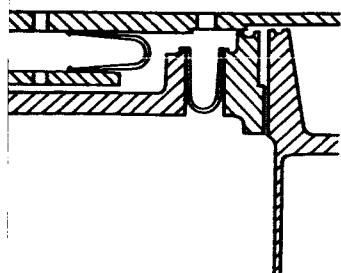
3.45 x 10<sup>5</sup>  
2.30 x 10<sup>5</sup>

Selected for  
further screening

EPTS D-4, D-5 and D-6.

D-5

D-6



atic  
gm-Hydrostatic  
-Ring, Face

Hydrostatic  
Diaphragm-Bellows  
Flexible-Ring, Face

|                |   |                                    |   |
|----------------|---|------------------------------------|---|
| 0.001"         | 8 | 0.038                              | 8 |
| 0.0005"        |   | 0.0                                |   |
| D-4            | 9 | Same as D-4                        | 9 |
|                | 6 |                                    | 6 |
| is low         | 2 | Friction is low                    | 1 |
| ing inadequate |   | Balancing is difficult for bellows |   |
| D-4            | 5 | Same as D-4                        | 5 |
| D-4            | 6 | Same as D-4                        | 6 |
|                | 8 | Stable                             | 8 |
|                | 5 |                                    | 5 |

1.15 x 10<sup>5</sup>  
0.767 x 10<sup>5</sup>

0.575 x 10<sup>5</sup>  
0.383 x 10<sup>5</sup>

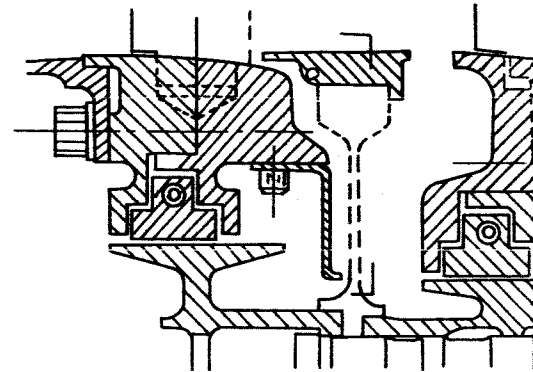
Selected for  
further screening

2

MATRIX CHART FOR

HS-9

CONCEPT



| Type of Primary Seal                     | Hydrostatic  |  |
|--|--|--|
| Type of Secondary Seal                   | Fully Floating Hydrostatic   |  |
| Type of Seal Ring Construction           | Segmented, Circumferential   |  |
| LEAKAGE RATE                             | a. Primary<br>b. Secondary   | 0.044 at 0.001"<br>0.03 at 0.0003"               |
| PRIMARY SEAL TRACKING                    | $\frac{\delta}{h} = .06$ (End)<br>$\frac{\delta}{h} = .5$ (Inter)                  | 8<br>3   |
| SECONDARY SEAL FRICTION<br>AND BALANCING | Friction is low<br>Balancing is good   | 9  |
| THERMAL DISTORTION                       | Adequate for primary<br>seal tracking but<br>severe for secondary<br>seal tracking | 4  |
| ELASTIC DISTORTION                       | Less severe  | 8  |
| GAS FILM STABILITY                       | Stable   | 8  |
| DIMENSIONAL STABILITY                    |  | 5  |
| 1st SCREENING RATING (End)<br>(Inter)    |  | 6.45 x 10 <sup>6</sup><br>2.42 x 10 <sup>6</sup> |

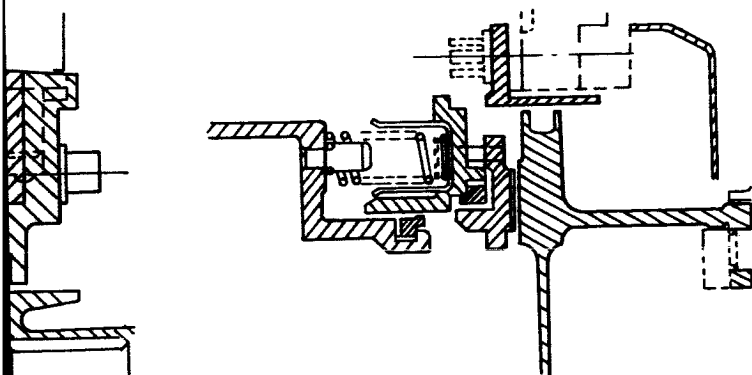
Selected for  
further sc



TABLE IX

SEAL CONCEPTS HS-9, HS-10, and HS-11.

HS-10



Hydrostatic  
Piston  
Flexible Ring, Face

Hy  
Pis  
Seg

0.038 at 0.001" 8  
0.001

0.0  
0.0

$\frac{\delta}{h} = .02$  (End) 9  
 $\frac{\delta}{h} = .16$  (Inter) 6

$\frac{\delta}{h}$

Friction is high 6

Fr  
Me  
se

Coning is severe 5  
but can be con-  
trolled

Ca  
by

Not severe 8

No

Stable 8

St

5

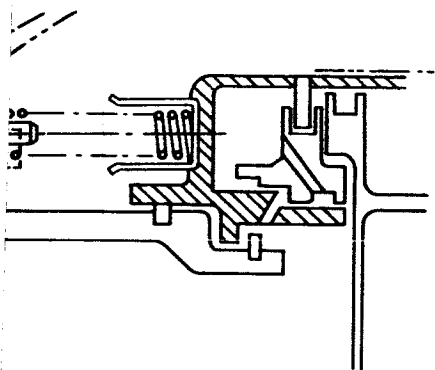
$6.9 \times 10^5$   
 $4.6 \times 10^5$



Selected for  
further screening

2

HS-11



Hydrostatic  
ton  
Segmented Ring, Face

038 at 0.001" 7  
005

.02 (End) 9  
.16 (Inter) 6

Friction is high 4  
Segment balance of  
segment is sensitive

Can be controlled 4  
segment length

Not severe 8

able 8

5

$3.22 \times 10^5$   
 $2.15 \times 10^5$



Selected for  
further screening

3

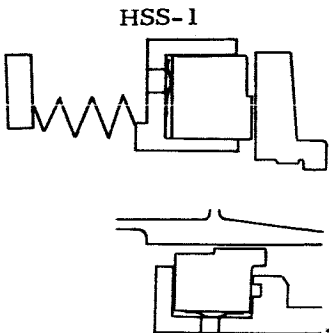
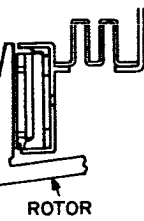
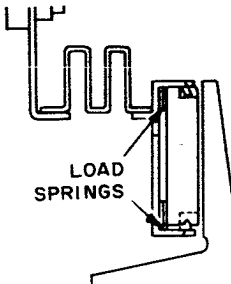
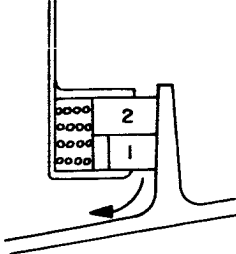

|  |  |                         |                                 |        |
|--|--|-------------------------|---------------------------------|--------|
| CONCEPT  |  |                         |                                 |        |
|  | Type of Primary Seal   | Hydrostatic-Step (Seg.) |                                 | Hydro  |
|  | Type of Secondary Seal   | Bellows or Piston       |                                 | Bellow |
|  | Type of Seal Ring Construction   | Face or Circum.         |                                 | Solid  |
| FAIL SAFE ABILITY                              | Very Low   | 1                       | Very                            |        |
| TOLERANCE TO START, STOP<br>AND HIGH SPEED RUB | Low  | 2                       | Low                             |        |
| TOLERANCE TO FOREIGN<br>PARTICLES              | Low  | 2                       | Very                            |        |
| TAKE-OFF & IDLING (sea<br>level) TRACKING      | $\frac{\delta}{h} = 0.03$ (End)<br>$= 0.3$ (Inter)                                 | 8<br>5                  | $\frac{\delta}{h} = .$<br>$= .$ |        |
| RESPONSE TO RAPID<br>MANEUVER OF AIRCRAFT      | Transient tracking<br>is adequate  | 6                       | Trans<br>tracki<br>adequa       |        |
| 2nd SCREENING RATING (End)                     |  | $.192 \times 10^3$      |                                 |        |
| (Inter)  |  | $.12 \times 10^3$       |                                 |        |

TABLE X.

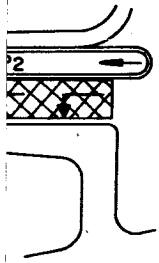
TABLE X

## SECOND SCREENING FOR END AND INTERSTAGE SEALS

| HS-1   |   | HD-1  |   | HD-3  |   |  |
|--|---|---|---|---|---|--|
|  |   |  |   |  |   |  |
| Static-Face vs Ring  |   | Hydrostatic-Shoe Bellows Segmented, Face  |   | Hydrodynamic-Shoe Dry Rub Segmented, Face   |   | Hydrostatic Diaphragm Solid Ring   |
| Low  | 1 | Very Low  | 1 | Low   | 2 | Low  |
|  | 2 | Hydrodynamic action provides slightly more protection                             | 3 | Same as HD-1  | 3 | Low  |
| Low  | 1 | Very Low  | 1 | Very Low  | 1 | Dirt may pick up pores low   |
| 01 (End)   | 9 | $\frac{\delta}{h} = .02$ (End)  | 9 | Same as HD-1  | 9 | $\frac{\delta}{h} = .03$   |
| 073(Inter)   | 6 | $= .14$ (Inter)   | 6 |   | 6 | $= .2$   |
| Transient tracking is adequate   | 4 | Transient tracking is adequate  | 6 | Same as HD-1  | 6 | Transient tracking inadequate  |
| $.072 \times 10^3$   |   | $.162 \times 10^3$  |   | $.324 \times 10^3$  |   |  |
| $.056 \times 10^3$   |   | $.108 \times 10^3$  |   | $.216 \times 10^3$  |   |  |

AL CONCEPTS

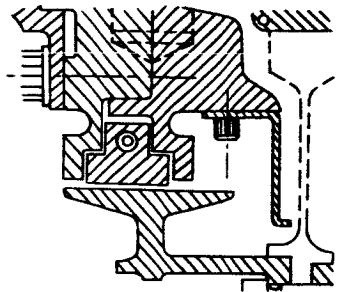
D-1



D-4, D-5  
HS-10, HS-11

See Table VIII  
and Table IX

HS-9



tic-Porous Pads  
m  
g, Circum.

See Table IX  
and Table VIII

Hydrostatic  
Fully Floating Hydrostatic  
Segmented, Circum.

|                |                    |                                |                    |                                |                   |
|----------------|--------------------|--------------------------------|--------------------|--------------------------------|-------------------|
|                | 2                  | Low                            | 2                  | Very Low                       | 1                 |
|                | 2                  | Medium                         | 5                  | Medium                         | 5                 |
| plug<br>, very | 1                  | Low                            | 2                  | Low                            | 2                 |
| (End)          | 8                  | $\frac{\delta}{h} = .01$ (End) | 9                  | $\frac{\delta}{h} = .03$ (End) | 8                 |
| (Inter)        | 5                  | $= .073$ (Inter)               | 7                  | $= .21$ (Inter)                | 5                 |
| ut<br>is<br>te | 2                  | Adequate                       | 6                  | Adequate                       | 6                 |
|                | $.064 \times 10^3$ |                                | $1.08 \times 10^3$ |                                | $.48 \times 10^3$ |
|                | $.04 \times 10^3$  |                                | $.836 \times 10^3$ |                                | $.30 \times 10^3$ |

3

| Seal<br>Concepts | Type of Seal & Seal Ring Co |    |
|------------------|-----------------------------|----|
|                  | Secondary Seal              |    |
| HSS-1            | Bellows or Piston           | Hy |
|                  | Face or Circum.             |    |
| HS-1             | Bellows                     | Hy |
|                  | Solid Ring                  |    |
| HD-1             | Bellows                     | Hy |
|                  | Segmented, Face             |    |
| HD-3             | Dry Rub                     | Hy |
|                  | Segmented, Face             |    |
| D-1              | Diaphragm                   | Hy |
|                  | Solid Ring, Circum.         |    |
| D-4              | Piston-Diaphragm            | Hy |
|                  | Flexible-Ring, Face         |    |
| D-5              | Diaphragm-Hydrostatic       | Hy |
|                  | Flexible-Ring, Face         |    |
| HS-9             | Fully-Float. Hydrostatic    | F  |
|                  | Segmented, Circum.          |    |
| HS-10            | Piston                      | F  |
|                  | Flexible-Ring, Face         |    |
| HS-11            | Piston                      | F  |
|                  | Segmented Ring, Face        |    |

$$*R_t = R_I^2 R_{II}$$

#Selected for Feasibility Analysis

/

TABLE XI

5 OF THE SCREENING STUDY OF END AND INTERSTAGE

| Configuration<br>Primary Seal | Schematic<br>Drawing | First<br>Screening<br>Rating $R_I$ |                    |
|-------------------------------|----------------------|------------------------------------|--------------------|
|                               |                      | End                                | Inter              |
| Hydrostatic-step (Seg)        | See Table X          | $1.78 \times 10^5$                 | $.5 \times 10^5$   |
| Hydrostatic-Face              | See Table X          | $1.038 \times 10^5$                | $.692 \times 10^5$ |
| Hydrostatic-Shoe              | See Table X          | $1.38 \times 10^5$                 | $.862 \times 10^5$ |
| Hydrostatic-Shoe              | See Table X          | $0.805 \times 10^5$                | $.504 \times 10^5$ |
| Hydrostatic-Porous Pads       | See Table X          | $.81 \times 10^5$                  | $.304 \times 10^5$ |
| Hydrostatic                   | See Table VIII       | $3.45 \times 10^5$                 | $2.30 \times 10^5$ |
| Hydrostatic                   | See Table VIII       | $1.15 \times 10^5$                 | $.767 \times 10^5$ |
| Hydrostatic                   | See Table IX         | $6.45 \times 10^5$                 | $2.42 \times 10^5$ |
| Hydrostatic                   | See Table IX         | $6.9 \times 10^5$                  | $4.6 \times 10^5$  |
| Hydrostatic                   | See Table IX         | $3.22 \times 10^5$                 | $2.15 \times 10^5$ |

2

## SEALS

|                 | Second<br>Screening<br>Rating R <sub>II</sub> |                      | *Total Screening R <sub>t</sub><br>Rating x 10 <sup>-13</sup> |              |
|-----------------|---|----------------------|---|--------------|
|                 | <u>End</u>                                    | <u>Inter</u>         | <u>End</u>  | <u>Inter</u> |
|                 | .192x10 <sup>3</sup>                          | .12x10 <sup>3</sup>  | .608  | .03          |
| 10 <sup>5</sup> | .072x10 <sup>3</sup>                          | .056x10 <sup>3</sup> | .0776   | .0268        |
| 10 <sup>5</sup> | .162x10 <sup>3</sup>                          | .108x10 <sup>3</sup> | .308  | .080         |
| 10 <sup>5</sup> | .324x10 <sup>5</sup>                          | .216x10 <sup>3</sup> | .21   | .0548        |
| 10 <sup>5</sup> | .064x10 <sup>3</sup>                          | .04x10 <sup>3</sup>  | .042  | .006         |
| 10 <sup>5</sup> | 1.08x10 <sup>3</sup>                          | .836x10 <sup>3</sup> | 12.9  | 4.42 #       |
| 10 <sup>5</sup> | 1.08x10 <sup>3</sup>                          | .836x10 <sup>3</sup> | 1.43  | .494         |
| 10 <sup>5</sup> | .48x10 <sup>3</sup>                           | .30x10 <sup>3</sup>  | 20.0  | 1.75 #       |
| 10 <sup>5</sup> | 1.08x10 <sup>3</sup>                          | .836x10 <sup>3</sup> | 51.4  | 17.7 #       |
| 10 <sup>5</sup> | 1.08x10 <sup>3</sup>                          | .836x10 <sup>3</sup> | 11.2  | 3.86 #       |

3



## Description of Seal Concepts

HSS-1, HSS-2 - Hydrostatic-Step - These two concepts represent the basic hydrostatic step seal. The primary seal ring is segmented in order to satisfactorily follow the irregular motion of the rotor. The seal segments pressure balanced in the axial direction but not in the radial direction. They are contained in a solid ring carrier which is flexibly-mounted on a bellows or on a spring and piston type of support. Leakage rate is quite favorable and is about 1/20 of that of the present labyrinth design. Primary seal tracking is satisfactory for the end seal but may be unsatisfactory for the interstage design because of lower stiffness at the low pressure difference. The thermal distortion of the seal segment is severe according to preliminary analysis but it can be reduced to a safe level by shortening the segment; the elastic distortion can be controlled in the same manner. The elastic distortion can also be effectively controlled by increasing the moment of inertia of the cross section. For off-design operations, the most important consideration is the primary seal tracking. The pressure difference during take-off is higher than that during cruising and therefore gives a more satisfactory tracking. During idle operation, pressure is much reduced, but the speed is also lower and the end result gives a response identical to take-off. During windmilling, the pressure may reverse its direction; it may be necessary to retract the seal ring away from the rotor for this condition. For sudden change of operating condition or maneuver, the tracking of primary seal ring might become difficult because of the sudden change of the thermal environment. Detailed studies will be performed to insure satisfactory performance during sudden maneuvering. The gas film should be stable since there is no air pocket in the system. Dimensional stability is marginal since any change of the step geometry due to wear will cause significant changes in performance.

HS-1, HS-2, HS-4 (Orifice Compensated) - In these designs, the air film is pressurized by the upstream high pressure air through orifices distributed evenly along the circumference. When the film thickness decreases, the flow becomes restricted and the pressure in the middle of the air film increases, causing a positive stiffness of the gas film. In the case of HS-1, there are two rows of orifices located at the inner and outer radii of the seal ring to give a stronger angular stiffness. The HS-2 design only has one row of orifices and a labyrinth back-up seal at the inner radius of the seal. The HS-4 design also has a compensating orifice and a recessed groove to provide a uniform pressure at the inlet to the viscous film. A bellows is used as the secondary seal for HS-1 and HS-4, but, for HS-2, the secondary seal is achieved by floating the sealing ring hydrostatically in the carrier. All designs use a solid ring.

From the standpoint of leakage rate and primary seal tracking, the orifice compensated seal appears to be quite attractive. However, the thermal coning problem is very severe, since they are all solid rings. The HS-1 design has a flexible ring and also has more angular stiffness to compensate for the thermal coning. The HS-2 and HS-4 designs have heavier sections and therefore have more severe problems in thermal coning. Off-design conditions appear to be satisfactory. Stability of HS-1 and HS-2 can be controlled by adjusting the orifice diameter and the recess area around the orifice, but the central grooved pocket for HS-4 contains a large high pressure reservoir and may be subject to pneumatic hammer. The geometry of these designs is such that they are less susceptible to dimensional change due to wear than are the step designs.

HS-3 - This design is an unbalanced seal in which the leakage is prevented between two contacting surfaces. A quick calculation shows that the heat generated using an extremely low unbalance factor (.05) is too excessive to be considered safe. This design is, therefore, ruled out in this screening study.

HS-5 and HS-6 - These two designs are basically the same as HS-4 except that the secondary seal is a spring and piston arrangement. HS-6 uses a cascade of orifices to restrict the flow into the pocket. Because the spring and piston design is more desirable than the bellows used for HS-4, these two concepts have a higher total rating.

HS-7 and HS-8 - The basic arrangement of these two designs is again similar to that of HS-5, with the exception that the high pressure is from an external source which can be higher than the upstream pressure. This gives considerable improvement in the static stiffness for interstage seals. Slight improvement in the tolerance to high speed can also be expected due to the high supply pressure at the orifice.

HD-1, HD-2, HD-3, and HD-4 - These designs share the common feature that the pressure loading on the back face of the seal segments is balanced by the film pressure generated hydrodynamically. In HD-1, HD-2, and HD-3 the hydrodynamic pressure is produced by the tilting action of the segments, whereas in HD-4, the pressure results from a series of steps or tapered pads. All four designs indicate a segmented approach.

A preliminary calculation shows that the hydrodynamic action will not become active until the film thickness drops below 0.0005 inch. At this low film thickness, the leakage is low, the static stiffness is

high, and the heat generation becomes considerably higher than for other designs. However, by proper control of the segment length, thermal distortion could be kept under control. The weakest point of each of these four designs lies in the high secondary seal friction caused by excessive unbalance of the side pressure exerted over the secondary sealing surface.

From the standpoint of reliability, the extra load capacity produced by the hydrodynamic action at extremely thin film thicknesses should give a higher tolerance to high speed rub during bottoming. Tracking under off-design conditions appears to be satisfactory. Film stability does not seem to be a serious problem since tilting pads have operated at speeds much higher than the proposed speed for these seals and have not experienced any instability problem.

SG-1 and SG-2 - In these two designs, the pumping action of the spiral grooves is used to generate the extra pressure to obtain a positive stiffness of the film. The characteristics and performance of the spiral groove design are very similar to other hydrodynamic seals. For this reason, they have individual ratings almost identical to the HD-series with the exception that the thermal distortion is much more severe because of the solid ring design.

HS-L-1, HS-L-2, HS-L-3 and HS-L-4 - Sealing in these designs is achieved by floating a flat face plate against several close-clearance labyrinths. The leakage rate of these concepts is expected to be much lower than the present labyrinth seals since the gaps are now controlled and kept at a very small clearance. In HS-L-1 and HS-L-2, the height of the knife edges increases slightly along the flow passage and forms a tapered gap. As the gap decreases, the restrictor becomes more effective at the exit side and raises the pressure level between the knife edges to provide a positive static stiffness for this seal. In HS-L-4, the height of the knife edges is uniform along the flow passage and the static stiffness is achieved by feeding high pressure air into the mid section of the seal. HS-L-3 is a hybrid design which uses the hydrostatic pad to control the close clearance of the labyrinths.

The major shortcoming of these designs is the lack of dynamic stiffness when subjected to high frequency excitation. The large air pockets between the knife edges act like a very soft spring and give very poor response at high frequencies. In spite of the fact that these designs have low thermal distortion, high tolerance to dirt, and reasonably little danger during occasional rubbing, the overall ratings of close clearance labyrinth seals are extremely low due to lack of tracking capability of the primary seals. The hybrid design (HS-L-3) has improved tracking capability but still shows a low overall rating compared to other designs.

VL - Perhaps this design is the most unique one among all the suggested concepts. It retains all essential features of the present labyrinth seal except that small jets are introduced between the labyrinth teeth to deflect the flow path and to induce a vortex pattern. These vortex motions can provide additional resistance to reduce the leakage rate.

A preliminary experiment was conducted using water flowing through a plastic model with the same labyrinth geometry as suggested in this design. No substantial reduction of leakage rate ( $< 10\%$ ) has been found in this preliminary test. Consequently, this design has been ruled out by an extremely small individual rating in the leakage rate consideration.

F-1, F-2 and F-3 - The fundamental principle of these concepts departs quite drastically from the other designs in that one of the sealing members is made very flexible. In all three designs, the centrifugally-activated foils have been used as the flexible member. In the design F-1, a thin annular foil is deflected to the shape of the stationary primary sealing surface. This design has no provision for axial adjustment. In F-2, the foil is kept under radial tension by the centrifugal load produced by a concentrated rim at the outer radius. The primary seal ring is floated hydrostatically in the carrier. The F-3 design is an application of a circumferential foil seal. The flexibility of the foil is oriented in the circumferential direction instead in the radial direction. These foils are made of rectangular strips whose thickness is determined by the centrifugal load required for sealing the high pressure. They are bolted on the drum and the end of each foil is overlapped by the next foil in the circumferential direction.

Leakage of these foil seals is quite favorable at a film thickness of 0.001 inch. Primary seal tracking should not be a problem because the foil has a low inertia. However, there exists one major shortcoming which is common to all foil designs, namely that the local elastic deformation under an uneven high pressure distribution or caused by variation from the design pressure difference can become excessive and cause local contact at high speeds. In addition, the thin foil may flutter at high tangential speeds. Because of these arguments, seals using extremely flexible foils have not received a high total rating.

D-1 and D-2 - These two circumferential seal concepts utilize a metallic diaphragm or pieces of diaphragms as the secondary seal. In this manner, the seal segments are free to move radially in response to the high frequency vibrations of the rotor and the thermal expansion of the frame. The design D-1 also suggests a porous material for the

primary seals. The porous structure plays the same role as the orifices described in the HS-type seals. The diaphragm has a shape of a flattened tube which can be either a complete ring or sections of tubes. In the design D-2, two half "C" shape diaphragms are used as secondary seals which are welded onto the primary seal segments. The diaphragms may contain intermittent slots to reduce the elastic stiffness in the radial direction. Leakage through the slots can be reduced by secondary thin foils on top of the slotted areas. Leakage of D-1 and D-2 is estimated to be approximately equal to that of the HS-type seals and is therefore highly favorable. Primary seal tracking is more than adequate for the end seal version but is somewhat marginal for the interstage seal version. Secondary seal side thrust is not balanced and is a major problem with this concept. The overall rating for end stage seals of this design is reasonably high compared to some of the other concepts, but it is still far from acceptable for interstage seals.

D-3 and D-3A - This design consists of a series of L-shaped segments as the primary sealing member which employ the hydrostatic and hydrodynamic seal concept described earlier. The side thrust exerted on the primary seal segments by the pressure is balanced by a tension strip anchored to the frame. The secondary seal for the D-3 design consists of a small, thin, hydrostatic-step ring backed up by a U-shaped diaphragm which is secured to the frame. The D-3A design is an alternate design which uses the hydrostatically-balanced piston as the secondary seal.

Leakage rate for this design is about the same as for the other designs. Primary seal tracking for end stage seals is considered only marginal and is definitely unsatisfactory for the interstage seals because of the low available pressure difference. Considerations of secondary seal friction and balancing, thermal distortion, off-design performance, and gas-film stability are all acceptable. However, in considering dimensional stability, these two designs received a very low rating because of the difficulty in keeping the segments aligned with the tension strips particularly, when they begin to creep at high temperatures. This is the main reason why high ratings were not given to the L-shaped design.

D-4, D-5 and D-6 - In these three designs, a flexible ring is used as the primary seal. Both the bending and torsional rigidity of the ring is kept small to allow it to follow any runout, initial waviness, or thermal twisting of the rotor. On the other hand, it has enough rigidity in the radial direction to resist excessive local deformations. It is mounted flexibly upon the seal carrier by means of a U-shaped diaphragm which must be flexible enough to allow the seal section to move a small

axial distance or to rotate through a small angle. The seal ring and carrier assembly is, in turn, flexibly-connected to the frame by a tension spring which retracts the seal when the pressure drops below a certain prescribed value. Secondary sealing of the seal carrier is achieved in three different ways. The pressure-balanced piston is used in D-4; a hydrostatically-floated shoe with diaphragm backing is employed in D-5; and a conventional bellows with a realistic dimension is used in D-6. The leakage and primary seal tracking ratings are comparable to the hydrostatic-pocket configuration. Secondary seal friction and balancing are considerably improved for the D-4 design, but are still far from acceptable for designs D-5 and D-6 due to balancing difficulty of the bellows or the floated shoes. The severeness of the elastic and thermal distortions of the primary seal ring is considerably relieved because of the flexibility. This results in much improved total ratings for these three designs compared to some of the concepts suggested earlier.

HS-9 - This particular design is designated as the two-side floated shoe, circumferential seal. The seal ring is segmented and contains hydrostatic bearings between the side walls and the housing. The objective of these bearings is to allow the segment to adjust freely for rotor vibration, runout and initial waviness. The leakage through the bearing clearance can be made acceptable by keeping the clearances below 0.0005 inch.

Initial studies indicate that the vertical and horizontal force balance as well as the moment balance can be obtained by a slight adjustment of a few key dimensions. The principal of operation for this second seal concept has been described in detail earlier.

Leakage and primary seal tracking ratings were again based on the hydrostatic pocket primary seal. The tracking rating is slightly lower because of the higher irregular motion associated with the circumferential seal. The secondary seal friction and balancing were rated very high because of the free floating action of the segments. Other ratings are comparable to those given to D-4 concepts. The total rating was found to be the highest for the endstage seal and the second highest for the interstage seal.

HS-10 and HS-11 - The HS-10 design is another version of the flexible ring face seal. The basic features are very similar to the D-4 design except that the U-shaped diaphragm is now replaced with a fully-floated piston ring. The thin strip is spring-mounted to the secondary seal carrier and is allowed to follow any runout, wobble, or initial warping of the rotor face. The seal carrier is in turn free to

move the full 0.4 inch of axial motion required for compensation of thermal expansion. It is also sealed by a second piston ring. The second order motions required of the two piston rings, arising primarily from thermal changes, will be possible due to machine vibration. A back-up labyrinth is also used when the seal ring is in its retracted position. This is a segmented face seal with the segments supported hydrostatically on one side only instead of on two sides as in the HS-9 design. The bearing surface between the seal carrier and the segments is extended below the level of the primary seal surface in order to balance the side pressure. The segments are free to follow the irregular motion of the rotor. The carrier construction is similar to that of the one-piece flexible ring design.

Since the basic construction of these two designs is similar to the D-4 design, the individual ratings are almost the same in all criteria except for secondary seal friction, balancing, and either thermal or elastic distortions. The piston ring construction in HS-10 appears to be superior to the U-shaped diaphragm due to the uncertain behavior of the thin diaphragm under high pressures. According to the total rating of HS-10, it appears to be the most favorable choice for both the end and interstage seals. The HS-11 design received a lower rating compared to HS-10 mainly because of the additional leakage through the segments and the possible rocking of the segments due to dynamically unbalanced moments.

## MTI FEASIBILITY ANALYSIS

The feasibility analysis of compressor end seal and stator inter-stage seal concepts conducted to date by MTI is presented in this section of the report. The material presented in this section was prepared by Dr. H. S. Cheng, John Bjerklie, and Dr. D. F. Wilcock. They wish to acknowledge the major contributions made by Dr. V. Castelli, Dr. T. Chiang, and Mr. C. Chow in preparing this material.

Summary of Feasibility Analysis

Typical engine conditions were used in the screening study analysis of seal performance. Since the prototype seals will be tested in an apparatus incapable of simulating engine pressure levels, practical test pressure levels have been used in the feasibility analysis computations without departing from either the letter or spirit of the specified engine conditions. The pressures, temperatures and other conditions are summarized as follows:

|                                   | <u>End Seal</u> |                 | <u>Interstage Seal</u> |                 |
|-----------------------------------|-----------------|-----------------|------------------------|-----------------|
|                                   | <u>Cruise</u>   | <u>Take-Off</u> | <u>Cruise</u>          | <u>Take-Off</u> |
| Sliding Speed, ft/sec             | 850             | 785             | 850                    | 785             |
| Air Temperature, °F               | 1200            | 680             | 1200                   | 680             |
| Pressure Differential, psi        | 80              | 150             | 25                     | 50              |
| *Air Pressure, Low Pr. Side, psi  | 20              | 20              | 20                     | 20              |
| *Air Pressure, High Pr. Side, psi | 100             | 170             | 45                     | 70              |
| *Pressure Ratio                   | 5               | 8.5             | 2.5                    | 3.5             |

\*Determined by test rig capability; does not simulate engine pressure levels.

## Primary Seal Analysis

Dimensionless variable charts are being prepared for five basic seal geometries. Included in this section of the report are (a) load, center of pressure, stiffness, and mass flow as a function of film thickness, step width ratio and pressure ratio for the hydrostatic step seal; (b) mass flow rate for the spiral groove hydrodynamic seal; (c) the computer program which will be used for the Rayleigh step seal; (d) load, stiffness, and flow for the hydrostatic orifice seal; and (e) load versus film thickness for the hydrostatic labyrinth seal.



The flexible thin strip designs listed on page 5 require that there be a restoring moment generated in the primary seal whenever the strip is not parallel to the runner at any position around the circumference. This restoring moment must overcome elastic moments due to local twisting and error moments resulting from manufacturing tolerances and varying seal positions in the secondary carrier. The resulting angular displacement must be small enough to maintain a safe film thickness. A criterion for evaluating this situation has been developed. A number of multiple pad designs are being examined for their capability in terms of angular moment stiffness.

### Seal Response

The dynamic equations permitting the determination of minimum film thickness as a function of seal mass, primary seal stiffness, shaft speed, and the frequency and magnitude of runner errors have been developed and plotted in non-dimensional form.

The criteria for evaluating the possibility of encountering self-sustained oscillations in a thin strip seal have been determined and applied to a typical seal section.

### Seal Designs

Seal designs were not undertaken during this time period pending completion of sufficient primary seal data to permit efficient detailed circulation and design.

### Primary Seal Feasibility Analysis

Since the completion of the Screening evaluation, more extensive and detailed information on primary seal performance has been required in order to permit adequate overall design calculations to be made. While these primary seal performance calculations are not completed at this stage, the following subsections summarize the information generated to date on the Hydrostatic Step Seal, the Spiral Groove Hydrodynamic Seal and the Rayleigh Step Seal. These are adequate for the floated shoe design work.

For the designs employing the flexible thin strip concept, additional primary seal work is required. The flexible strip requires a substantial transverse moment capability from the primary seal in order to balance elastic moments from small angular twist and error moments arising from manufacturing tolerances and off-design pressure conditions. Creation of this transverse moment capability in the primary seal has necessitated study of several multiple pad designs together with careful analysis of the moments to be balanced. At this writing it is not certain that a successful design can be produced.

## The Hydrostatic Step Seal

In the screening report, preliminary consideration was given to the load capability, the stiffness and the flow through a hydrostatic step seal. For the detailed design analysis, the center of pressure, or the position of the net load vector, is also required to determine moment equilibrium.

This subsection contains the design charts needed when using the hydrostatic step seal. These are expressed in terms of dimensionless quantities (combinations of dimensional variables) so that their applicability can be as broad as possible.

The principal dimensions and pressures of the hydrostatic step seal are defined as follows:

|                 |   |                                      |
|-----------------|---|--------------------------------------|
| $b_1, b_2, b$   | width,  | inches                               |
| $h_1, h_2$      | height,   | inches                               |
| $P_1, P_i, P_2$ | pressure,   | psia                                 |
| $m$             | mass flow/unit circumference,                           | $\frac{\text{lb-sec}}{\text{in}^2}$  |
| $R$             | gas constant,   | $\text{in}^2/\text{sec}^2 - R^\circ$ |
| $W$             | load/unit circumference,                                | lb/inch                              |
| $x_c$           | distance from high pressure edge to center of pressure, | inches                               |

The dimensionless quantities used in the design charts are:

$$\begin{aligned} \bar{b}_1 &= \text{step width ratio} = b_1/b \\ \bar{H} &= \text{height ratio} = h_1/(h_2 - h_1) \\ r_{12} &= \text{pressure ratio} = P_1/P_2 \\ \bar{W} &= \text{dimensionless load} = W/(P_2 - P_1)b \\ \bar{K}_s &= \text{dimensionless stiffness} = K_s \frac{h_1}{(P_2 - P_1) \bar{H}b} \\ \bar{M} &= \text{dimensionless flow} \\ &= m / \left( \frac{h_1^3}{24 \mu b} \right) \left( \frac{P_2}{RT_2} \right) \\ \bar{x}_c &= \text{dimensionless center of pressure} = \frac{x_c}{b} \end{aligned}$$

Load - The dimensionless load  $\bar{W}$  is shown in Figure 23 as a function of the height ratio  $\bar{H}$  for a step width ratio  $\bar{b}_1$  of 0.75. Curves for pressure ratios of 0.1, 0.2, 0.4 and 0.572 permit interpolation for all pressure ratios of interest. Figures 24 through 27 show similar curves for step width ratios of 0.5, 0.35, 0.25 and 0.125, respectively.

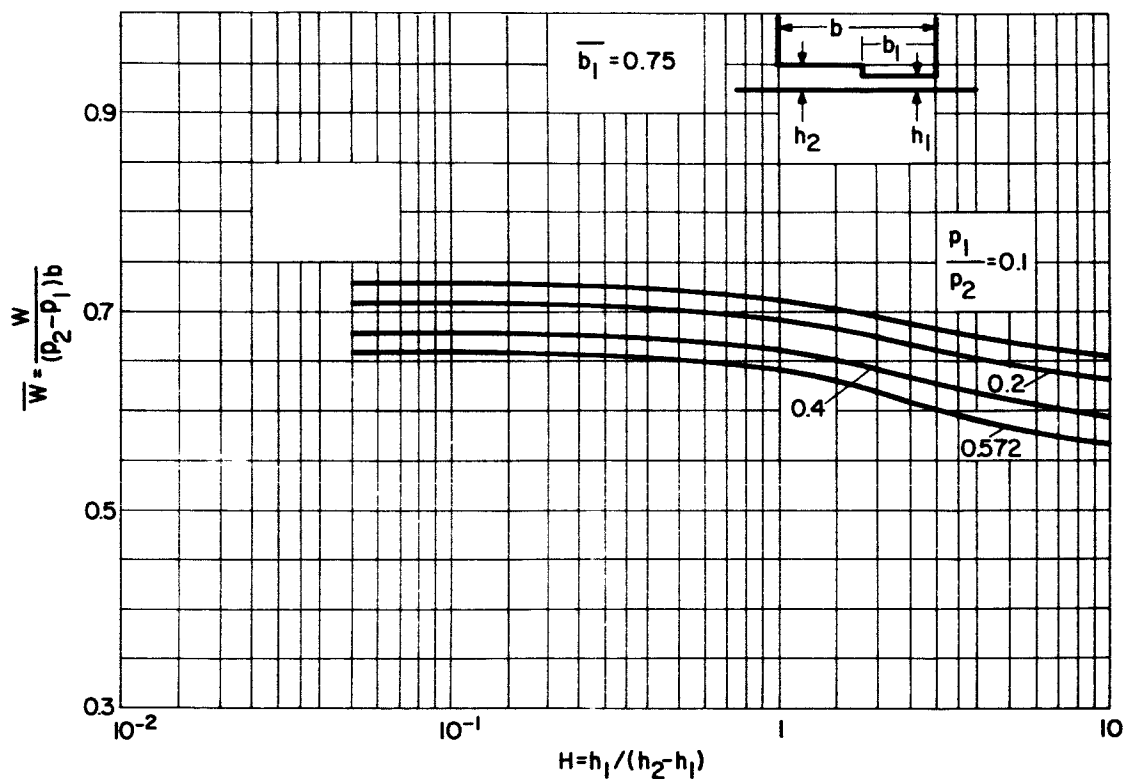


Figure 23 Load Curve-Hydrostatic Step,  $\bar{b}_1 = .75$

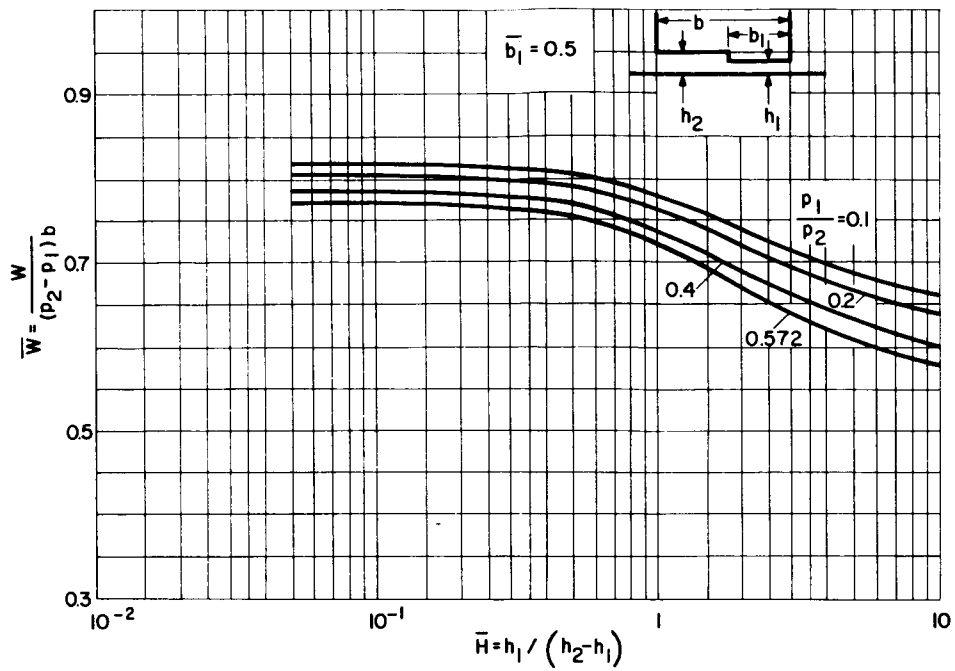


Figure 24 Load Curve-Hydrostatic Step,  $\bar{b}_1 = .5$

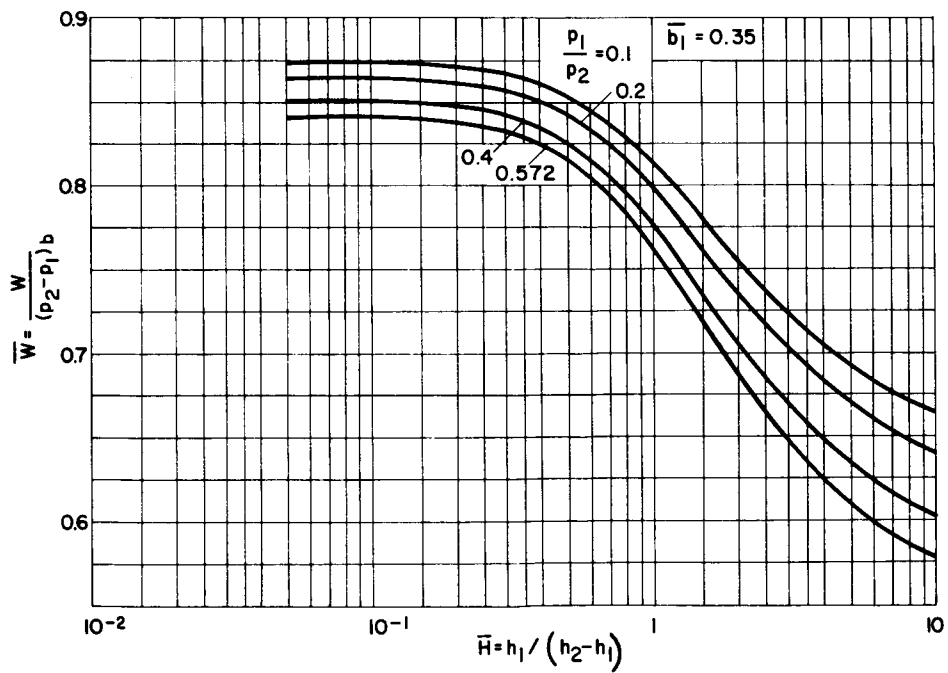


Figure 25 Load Curve-Hydrostatic Step,  $\bar{b}_1 = .35$

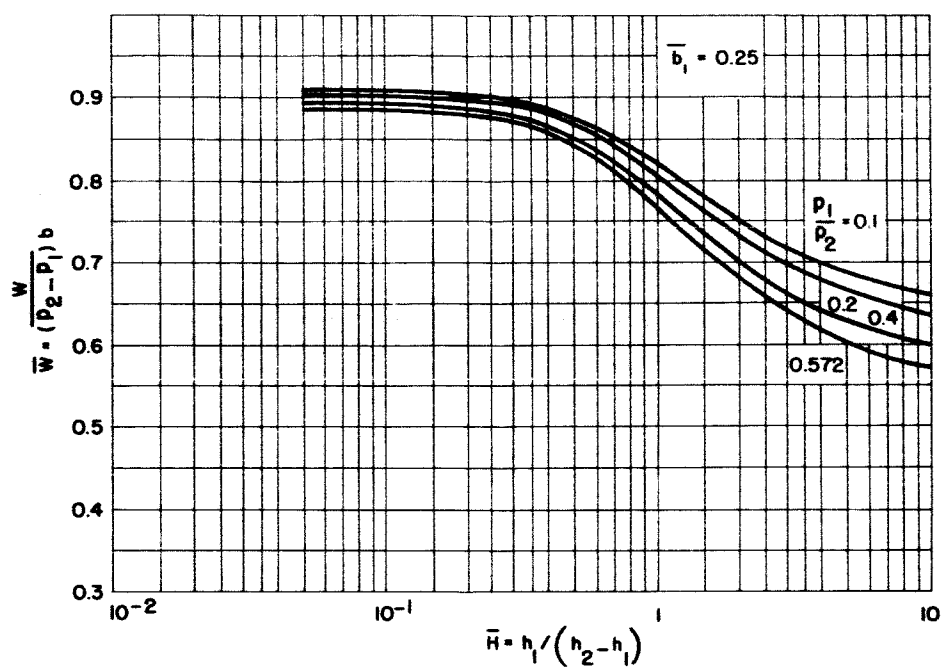


Figure 26 Load Curve-Hydrostatic Step,  $\bar{b}_1 = .25$

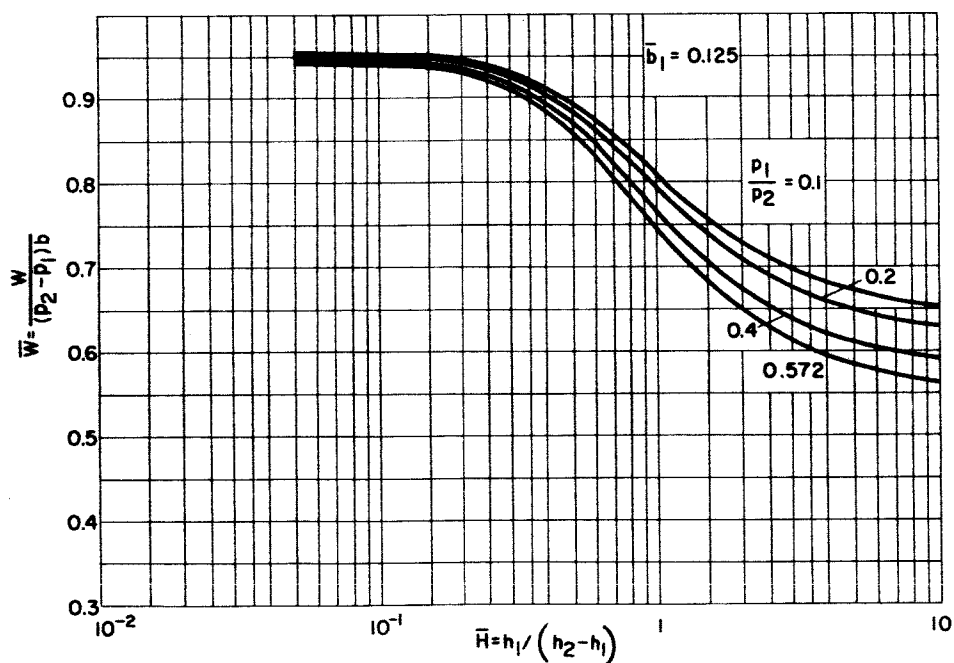


Figure 27 Load Curve-Hydrostatic Step,  $\bar{b}_1 = .125$

Center of Pressure - The dimensionless center of pressure  $\bar{x}$  is shown in Figures 28 through 32 as a function of  $\bar{H}$  for the same values of  $\bar{b}$ , and  $r_{12}$ .

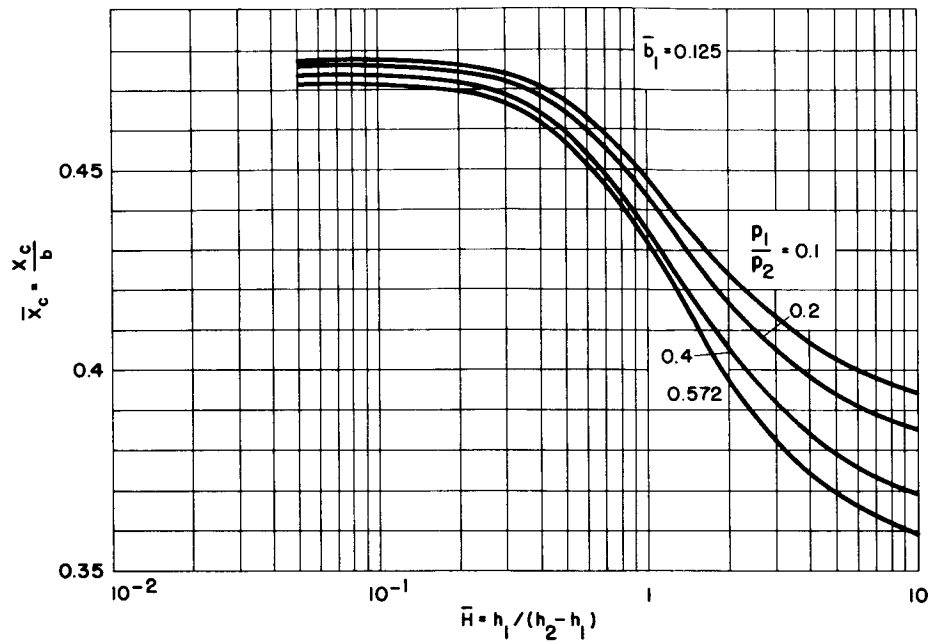


Figure 28 Center of Pressure-Hydrostatic Step,  $\bar{b}_1 = .125$

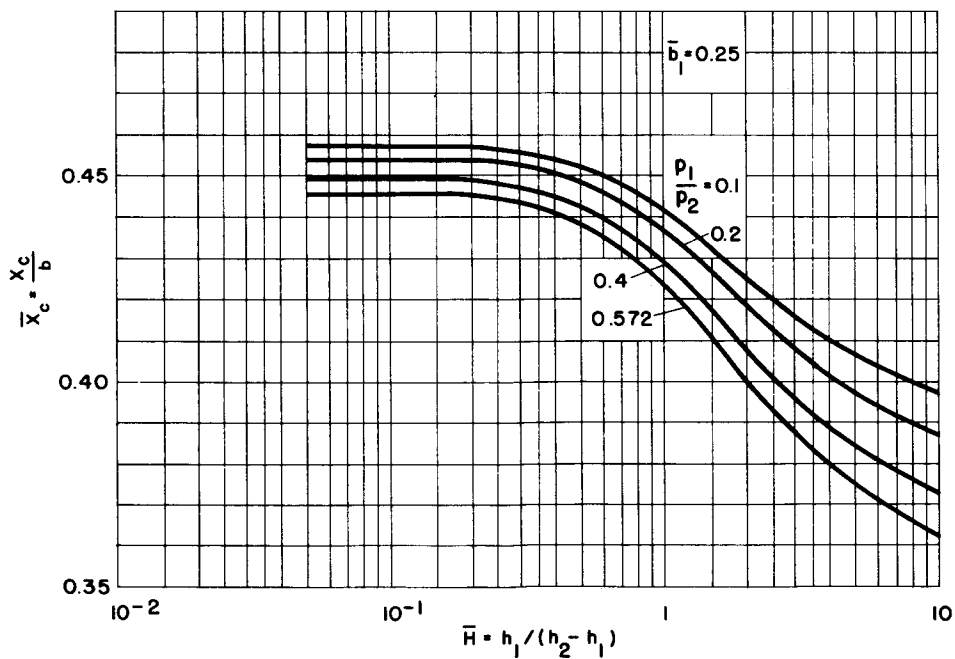


Figure 29 Center of Pressure-Hydrostatic Step,  $\bar{b}_1 = .25$

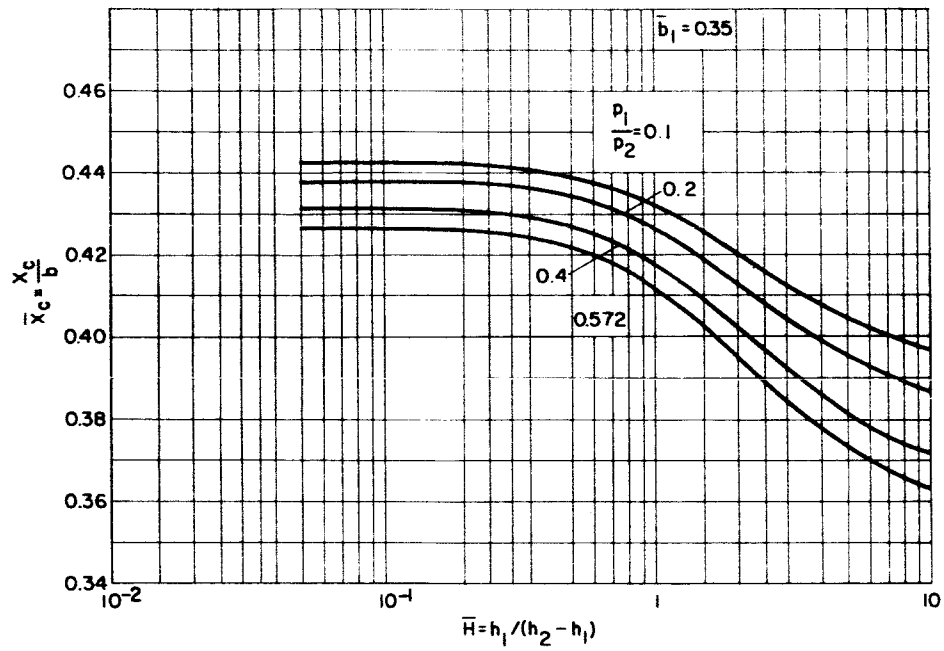


Figure 30 Center of Pressure-Hydrostatic Step,  $\bar{b}_1 = .35$

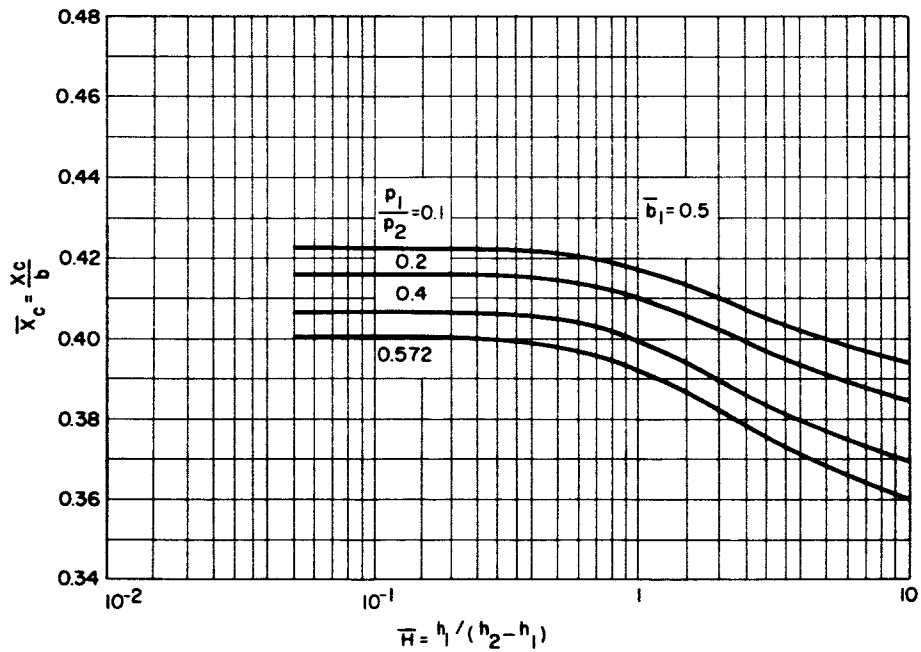


Figure 31 Center of Pressure-Hydrostatic Step,  $\bar{b}_1 = .5$

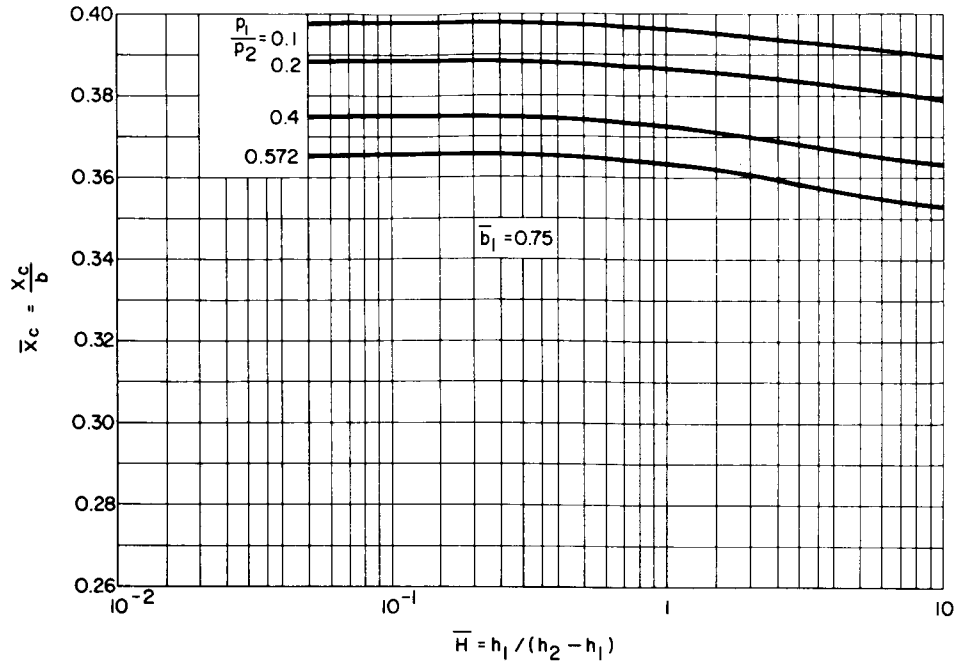


Figure 32 Center of Pressure-Hydrostatic Step,  $\bar{b}_1 = .75$

The center of pressure is found from the equation of equilibrium of the moments due to the hydrostatic pressure acting on the seal and the load. Thus, defining  $x_c$  as the center of pressure measured from the high pressure edge of the seal, one has

$$x_c = \frac{\int_0^b x(p-p_1) dx}{W} \quad (42)$$

In dimensionless form,

$$\begin{aligned} \bar{x}_c = \frac{x_c}{b} &= \frac{\int_0^1 (p-p_1) \bar{x} b d\bar{x}}{\bar{W} b (p_2-p_1)} \\ &= \frac{\int_0^1 \left(\frac{p}{p_2} - r_{12}\right) \bar{x} d\bar{x}}{\bar{W}(1-r_{12})} \\ &= \frac{\int_0^{\bar{b}_2} \left(\frac{p}{p_2} - r_{12}\right) \bar{x} d\bar{x} + \int_{\bar{b}_2}^1 \left(\frac{p}{p_2} - r_{12}\right) \bar{x} d\bar{x}}{\bar{W}(1-r_{12})} \end{aligned} \quad (43)$$



From equation (15), one has

$$\begin{aligned} \int_0^{\bar{b}_2} \left( \frac{p}{p_2} - r_{12} \right) \bar{x} d\bar{x} &= \int_0^{\bar{b}_2} \left\{ \left[ 1 - (1 - r_{i2}^2) \frac{\bar{x}}{\bar{b}_2} \right]^{1/2} - r_{12} \right\} \bar{x} d\bar{x} \\ &= \frac{2\bar{b}_2^2}{15(1 - r_{i2}^2)^2} \left[ (r_{i2}^2 - 5)r_{i2}^3 + 2 \right] - \frac{r_{12}\bar{b}_2^2}{2} \end{aligned} \quad (43a)$$

From equation (16), one has

$$\begin{aligned} \int_{\bar{b}_2}^1 \left( \frac{p}{p_2} - r_{12} \right) \bar{x} d\bar{x} &= \int_{\bar{b}_2}^1 \left\{ \left[ r_{i2}^2 - (r_{i2}^2 - r_{12}^2) \frac{(\bar{x} - \bar{b}_2)}{\bar{b}_1} \right]^{1/2} - r_{12} \right\} \bar{x} d\bar{x} \\ &= \frac{2\bar{b}_1^2}{15(r_{12}^2 - r_{i2}^2)^2} \left[ (3r_{12}^2 - 5r_{i2}^2)r_{12}^3 + 2r_{i2}^5 \right] \\ &\quad - \frac{r_{12}\bar{b}_1}{2} (2 - \bar{b}_1) + \frac{2\bar{b}_2\bar{b}_1}{3} \left( \frac{r_{i2}^2 + r_{i2}r_{12} + r_{12}^2}{r_{12} + r_{i2}} \right) \end{aligned} \quad (43b)$$

Substituting equations (43a) and (43b) in equation (43), one obtains

$$\begin{aligned} \bar{x}_c &= \frac{1}{(1 - r_{12})\bar{W}} \left\{ \frac{2}{15} \left[ \bar{b}_1^2 \frac{(3r_{12}^2 - 5r_{i2}^2)r_{12}^3 + 2r_{i2}^5}{(r_{12}^2 - r_{i2}^2)^2} \right. \right. \\ &\quad + (1 - \bar{b}_1)^2 \left[ \frac{(r_{i2}^2 - 5)r_{i2}^3 + 2}{(1 - r_{i2}^2)^2} \right] + \frac{2\bar{b}_1}{3} (1 - \bar{b}_1) \frac{r_{i2}^2 + r_{i2}r_{12} + r_{12}^2}{r_{12} + r_{i2}} \\ &\quad \left. \left. - \frac{r_{12}}{2} \right\} \end{aligned} \quad (44)$$

For the cases where  $1 - r_{12} \sim 0$ , the second term in the bracket of equation (44) is undefined. However, the pressure distribution within the region of  $0 \leq x \leq b_2$  can be made linear from equation (15) as

$$p = p_2 \left[ \frac{1 - (1 - r_{12}) \frac{\bar{x}}{\bar{b}_2}}{\bar{b}_2} \right] \quad (45)$$

Performing the integration as shown in equation (43a), one obtains the following form.

$$\frac{(1 - \bar{b}_1)^2}{6} \left[ 1 + 2 r_{12} - 3 r_{12}^2 \right]$$

$\bar{x}_c$  is plotted against  $\bar{H}$  at different  $\bar{b}_1$  and  $r_{12}$ .

The computer program used to generate the data for Figures 28 through 32 is presented in Appendix C.

Stiffness - The dimensionless stiffness  $\bar{K}_s$  is shown in Figures 33 through 37 as a function of  $\bar{H}$  for the same values of  $\bar{b}$ , and  $r_{12}$ .

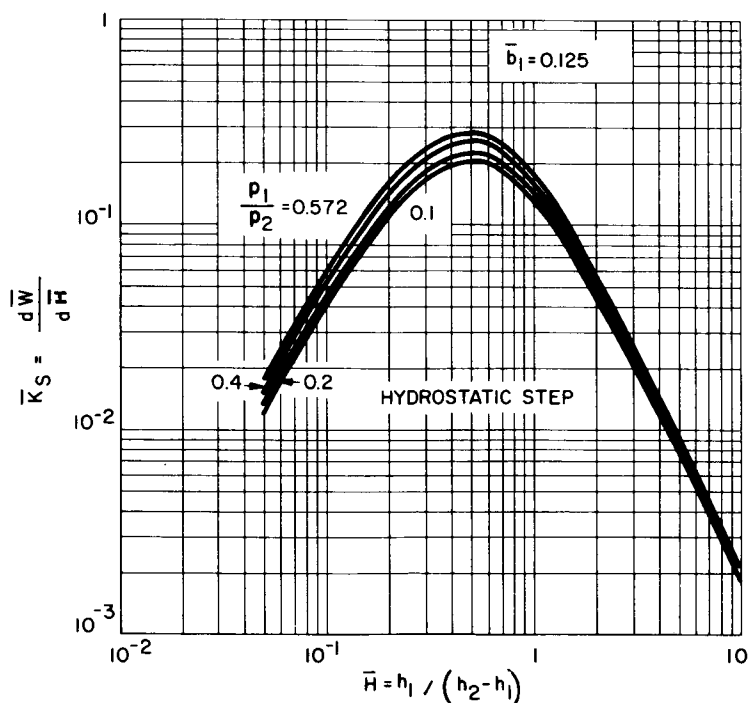


Figure 33 Dimensionless Film Stiffness-Hydrostatic Step,  $\bar{b}_1 = .125$

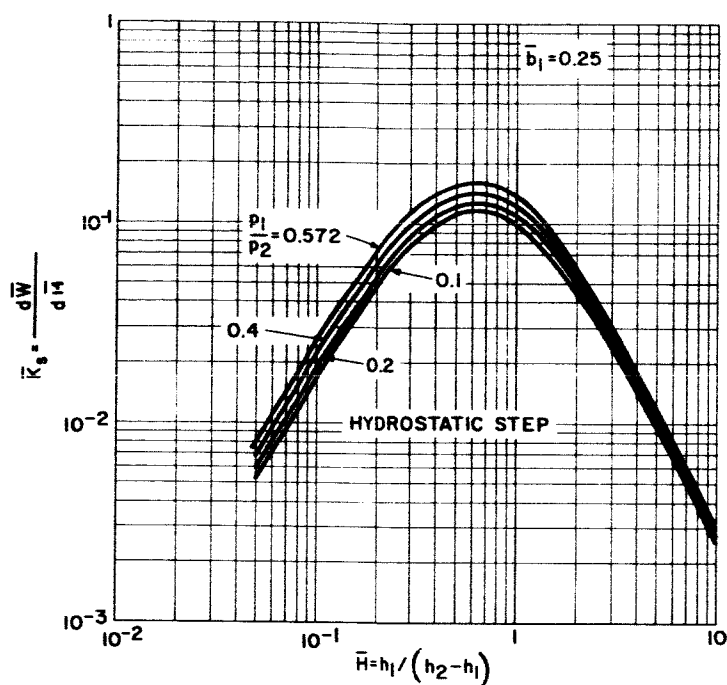


Figure 34 Dimensionless Film Stiffness-Hydrostatic Step,  $\bar{b}_1 = .25$

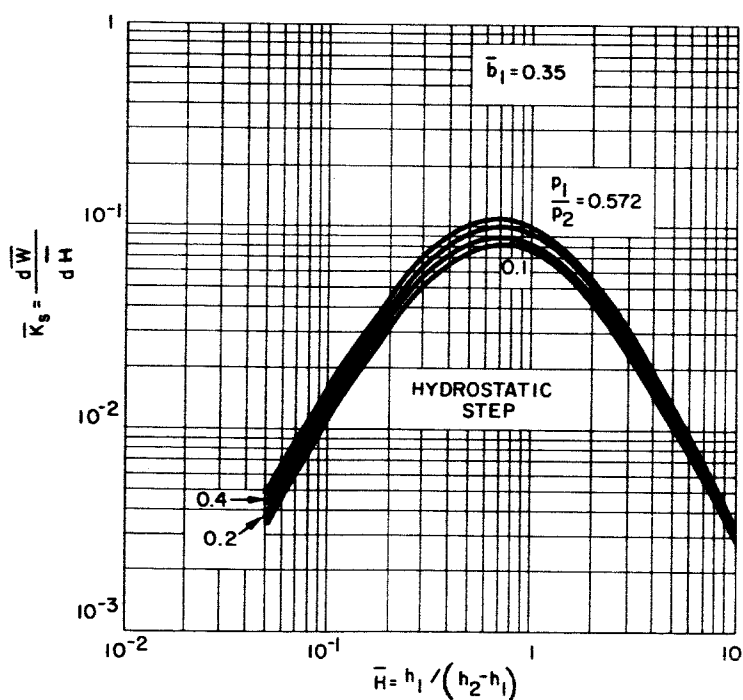


Figure 35 Dimensionless Film Stiffness-Hydrostatic Step,  $\bar{b}_1 = .35$

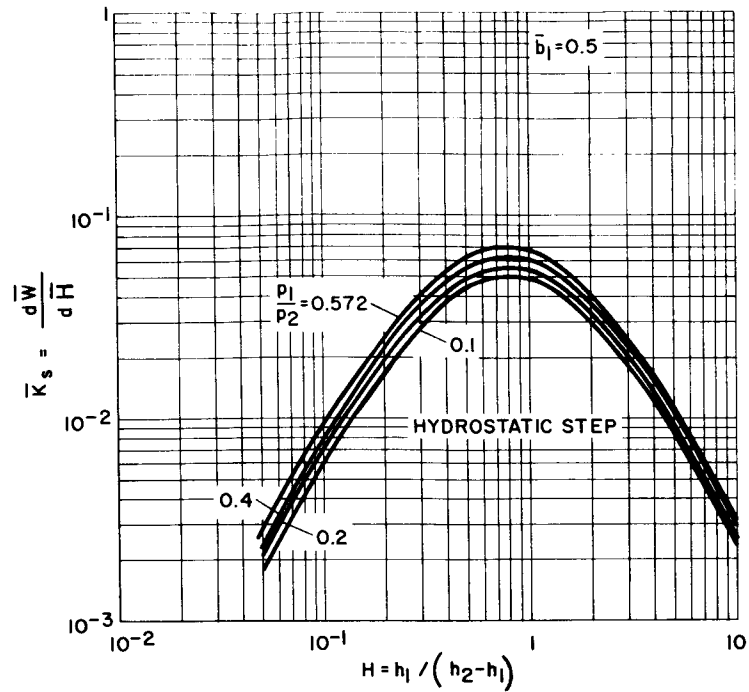


Figure 36 Dimensionless Film Stiffness-Hydrostatic Step,  $\bar{b}_1 = .5$

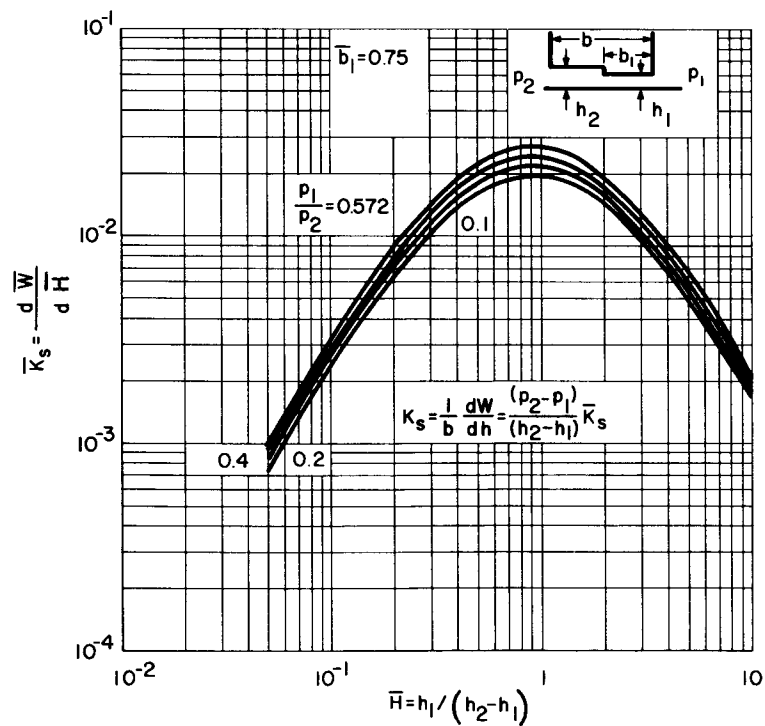


Figure 37 Dimensionless Film Stiffness-Hydrostatic Step,  $\bar{b}_1 = .75$

Referring to Equation (20) of the Screening Study, the dimensionless stiffness of a step-seal can be written as

$$\bar{K}_s = \frac{d\bar{W}}{d\bar{H}} = \frac{K_s h_1}{P_2 (1 - r_{12}) \bar{H}} \quad (46)$$

Thus, by the chain rules of differentiation,  $\bar{K}_s$  can be readily obtained from Equation (18).

$$\bar{K}_s = \left( \frac{d\bar{W}}{dr_{i2}} \right) \left( \frac{dr_{i2}}{d\bar{H}} \right) \quad (47a)$$

From Eq. (18), one obtains

$$\begin{aligned} \frac{d\bar{W}}{dr_{i2}} &= \frac{d}{dr_{i2}} \left\{ \frac{1}{1 - r_{12}} \left[ \bar{b}_2 \left[ \frac{2(r_{i2}^2 + r_{i2} + 1)}{3(r_{i2} + 1)} - r_{12} \right] \right. \right. \\ &\quad \left. \left. + \bar{b}_1 r_{i2} \left[ \frac{2(r_{1i}^2 + r_{1i} + 1)}{3(r_{1i} + 1)} - r_{1i} \right] \right] \right\} \\ &= \frac{d}{dr_{i2}} \left\{ \frac{\bar{b}_2}{1 - r_{12}} \left[ \left[ \frac{2(r_{i2}^2 + r_{i2} + 1)}{3(r_{i2} + 1)} - r_{12} \right] \right. \right. \\ &\quad \left. \left. + \frac{\bar{b}_1}{\bar{b}_2} \left[ \frac{2(r_{i2}^2 + r_{i2} r_{12} + r_{12}^2)}{3(r_{i2} + r_{12})} - r_{12} \right] \right] \right\} \\ &= \frac{2r_{i2} (1 - \bar{b}_1)}{3(1 - r_{12})} \left[ \frac{r_{i2} + 2}{(r_{i2} + 1)^2} + \frac{r_{i2} + 2r_{12}}{(r_{i2} + r_{12})^2} b_1^* \right] \quad (47b) \end{aligned}$$

Where

$$\left. \begin{aligned} \bar{b}_1 &= \frac{b_1}{b} \\ \bar{b}_2 &= \frac{b_2}{b} = 1 - \bar{b}_1 \\ \text{and} \\ b_1^* &= \frac{b_1}{b_2} \end{aligned} \right\} \quad (47c)$$

Equation (14) can be written below

$$r_{i2} = \left[ \frac{\bar{H}^3 r_{12}^2 + b_1^* (1 + \bar{H})^3}{\bar{H}^3 + b_1^* (1 + \bar{H})^3} \right]^{1/2} \quad (47d)$$

From which,

$$\begin{aligned} \frac{dr_{i2}}{d\bar{H}} &= \frac{1}{2} \left[ \frac{\bar{H}^3 r_{12}^2 + b_1^* (1 + \bar{H})^3}{\bar{H}^3 + b_1^* (1 + \bar{H})^3} \right]^{-1/2} \\ &\quad \frac{\left[ \bar{H}^3 + b_1^* (1 + \bar{H})^3 \right] \left[ 3\bar{H}^2 r_{12}^2 + 3b_1^* (1 + \bar{H})^2 \right] - \left[ \bar{H}^3 r_{12}^2 + b_1^* (1 + \bar{H})^3 \right] \left[ 3\bar{H}^2 + 3b_1^* (1 + \bar{H})^2 \right]}{\left[ \bar{H}^3 + b_1^* (1 + \bar{H})^3 \right]^2} \\ &= \frac{3}{2r_{i2}} \left[ \frac{\left[ \bar{H}^3 + b_1^* (1 + \bar{H})^3 \right] \left[ \bar{H}^2 r_{12}^2 + b_1^* (1 + \bar{H})^2 \right] - \left[ \bar{H}^3 r_{12}^2 + b_1^* (1 + \bar{H})^3 \right] \left[ \bar{H}^2 + b_1^* (1 + \bar{H})^2 \right]}{\left[ \bar{H}^3 + b_1^* (1 + \bar{H})^3 \right]^2} \right] \quad (48) \end{aligned}$$

Substituting Eqs. (47b) in (48) and the resultant into Eq. (47a), one obtains

$$\bar{K}_s = \left[ \frac{1 - \bar{b}_1}{1 - r_{12}} \left[ \frac{b_1^* (r_{i2} + 2r_{12})}{(r_{i2} + r_{12})^2} + \frac{(r_{i2} + 2)}{(r_{i2} + 1)^2} \right] \right]$$

$$\left[ \frac{[\bar{H}^3 + b_1^* (1 + \bar{H})^3] [\bar{H}^2 r_{12}^2 + b_1^* (1 + \bar{H})^2] - [\bar{H}^3 r_{12}^2 + b_1^* (1 + \bar{H})^3] [\bar{H}^2 + b_1^* (1 + \bar{H})^2]}{[\bar{H}^3 + b_1^* (1 + \bar{H})^3]^2} \right] \quad (49)$$

Mass Flow - The dimensionless mass flow  $\bar{M}$  is shown in Figures 38 through 42 as a function of  $\bar{H}$  for the same values of  $\bar{b}_1$  and  $r_{12}$ .

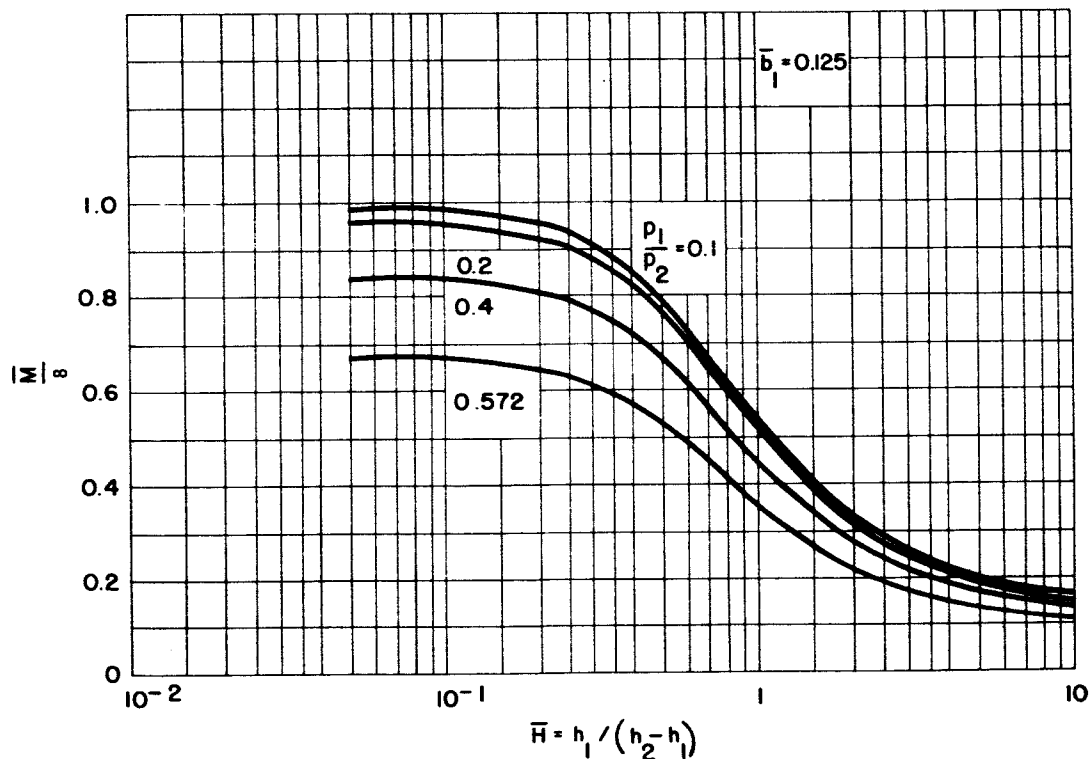


Figure 38 Dimensionless Mass Flow-Hydrostatic Step,  $\bar{b}_1 = .125$

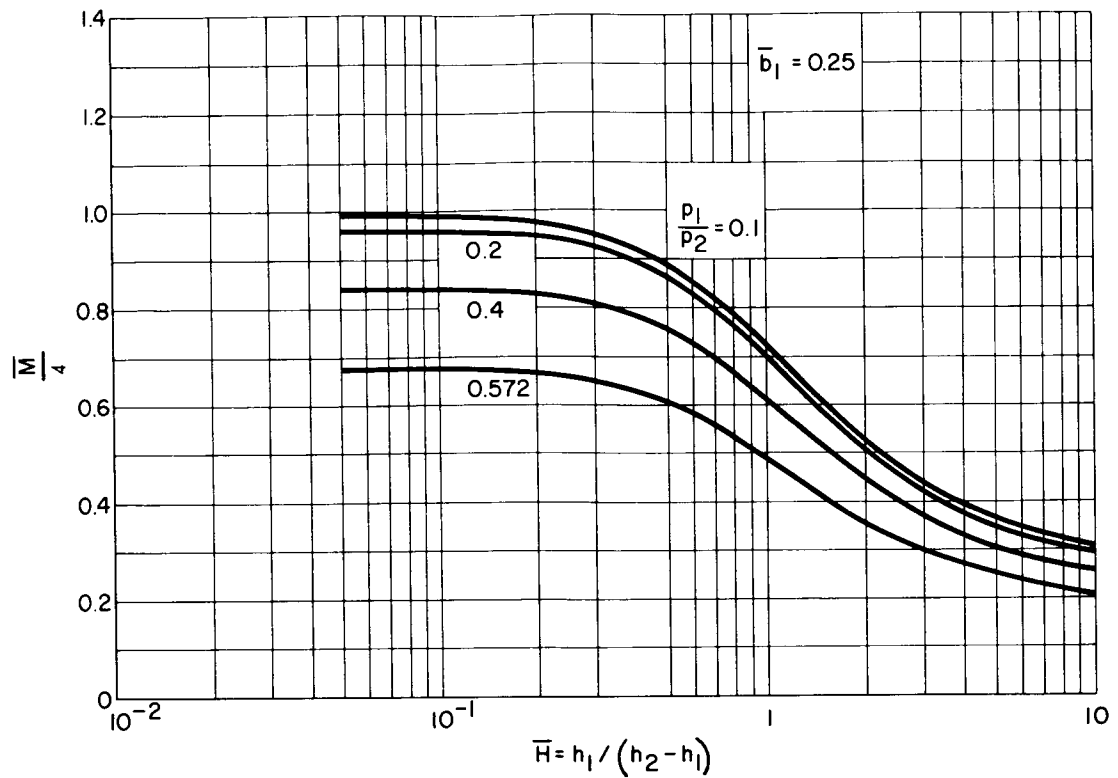


Figure 39 Dimensionless Mass Flow-Hydrostatic Step,  $\bar{b}_1 = .25$

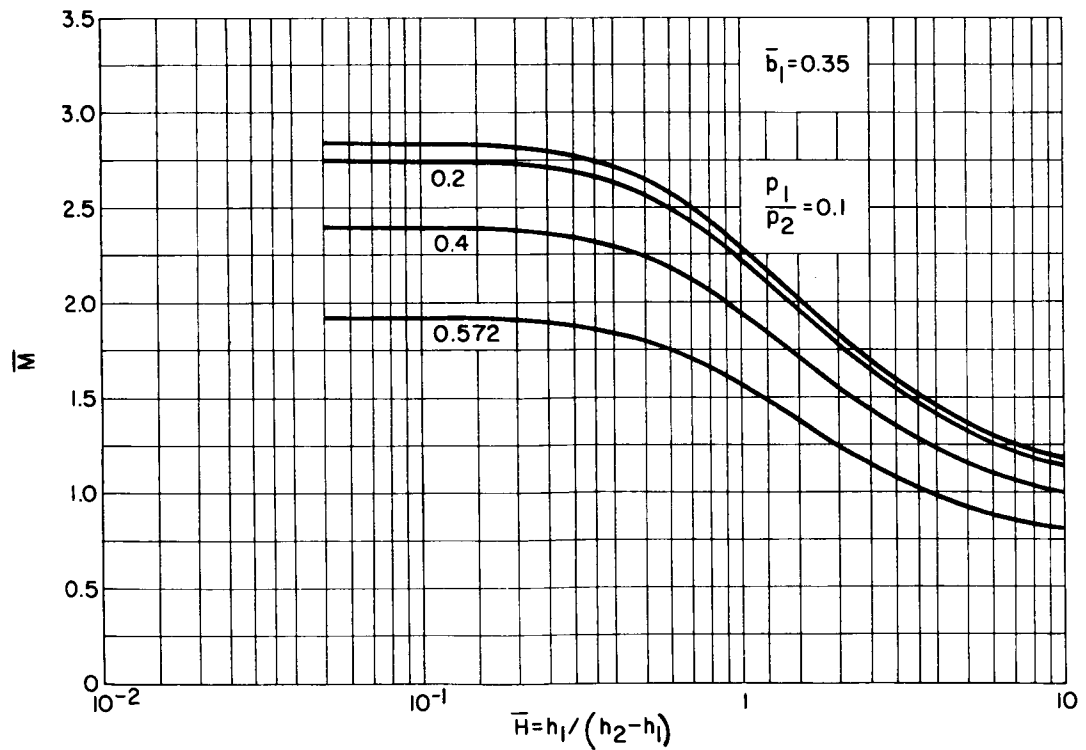


Figure 40 Dimensionless Mass Flow-Hydrostatic Step,  $\bar{b}_1 = .35$



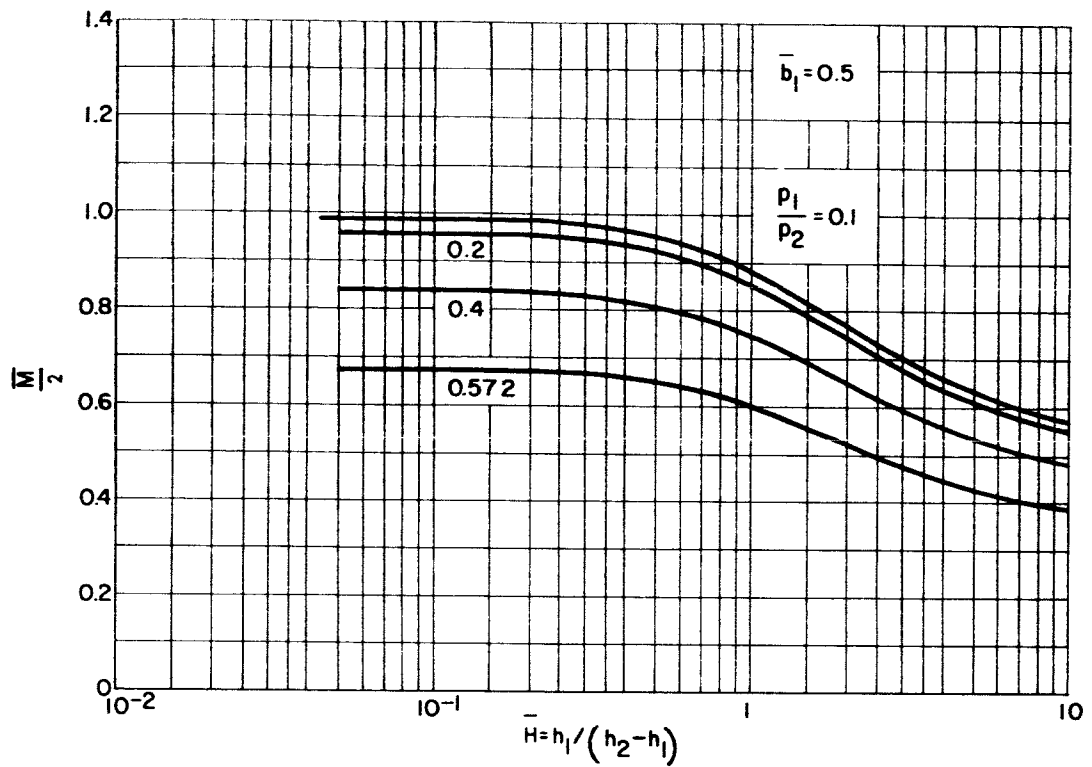


Figure 41 Dimensionless Mass Flow-Hydrostatic Step,  $\bar{b}_1 = .5$

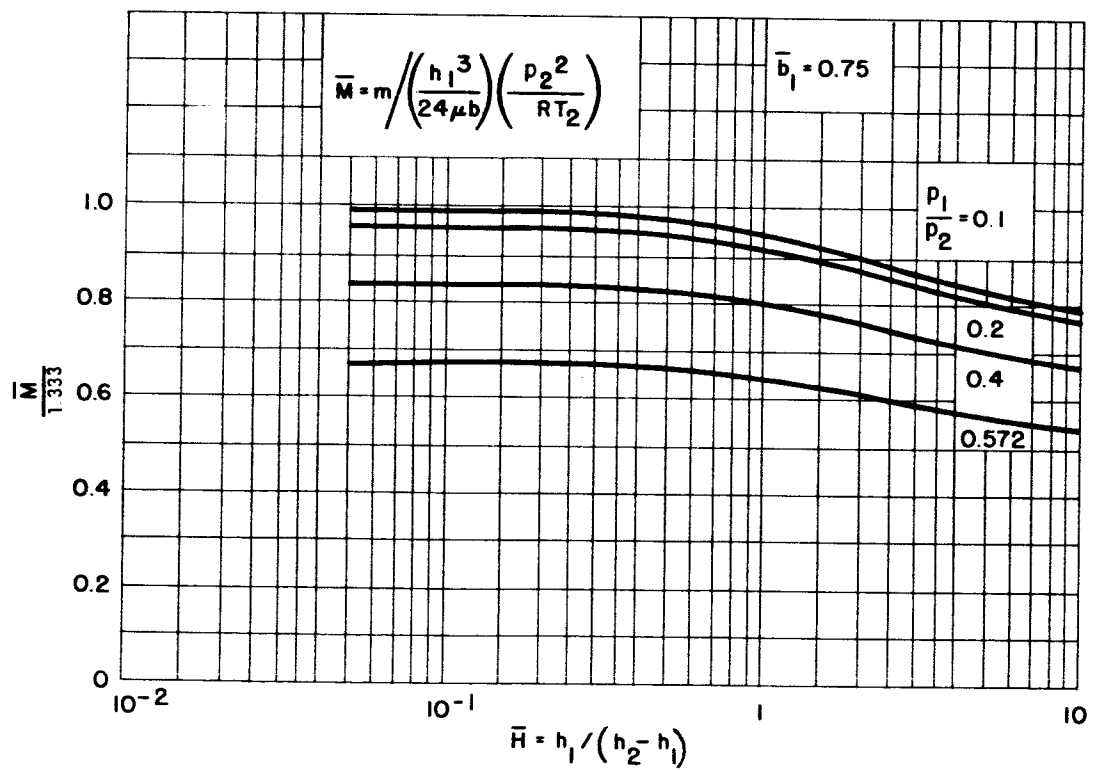


Figure 42 Dimensionless Mass Flow-Hydrostatic Step,  $\bar{b}_1 = .75$

### Spiral-Groove Hydrodynamic Seals

Description - A hydrodynamic spiral-grooved seal consists of two members, one with a smooth surface and the other provided with numerous spiral grooves as shown in Figure 43. Either one of these surfaces can be moving. In the presence of viscous shear and appropriate geometry of grooves, a viscous pumping action exists between the two edges. The pumping action creates a higher resistance to flow between the high and low pressure edges.

As mentioned previously in the Screening Report, the effect of viscous pumping action depends on the film thickness between the two seal members. The groove geometry also influences the effect of pumping. The groove parameters are the angle, the width ratio, the length ratio, the depth ratio, and the number of grooves. However, in this report, only the fully-grooved seal of narrow width with a sufficiently large number of spiral grooves is considered.

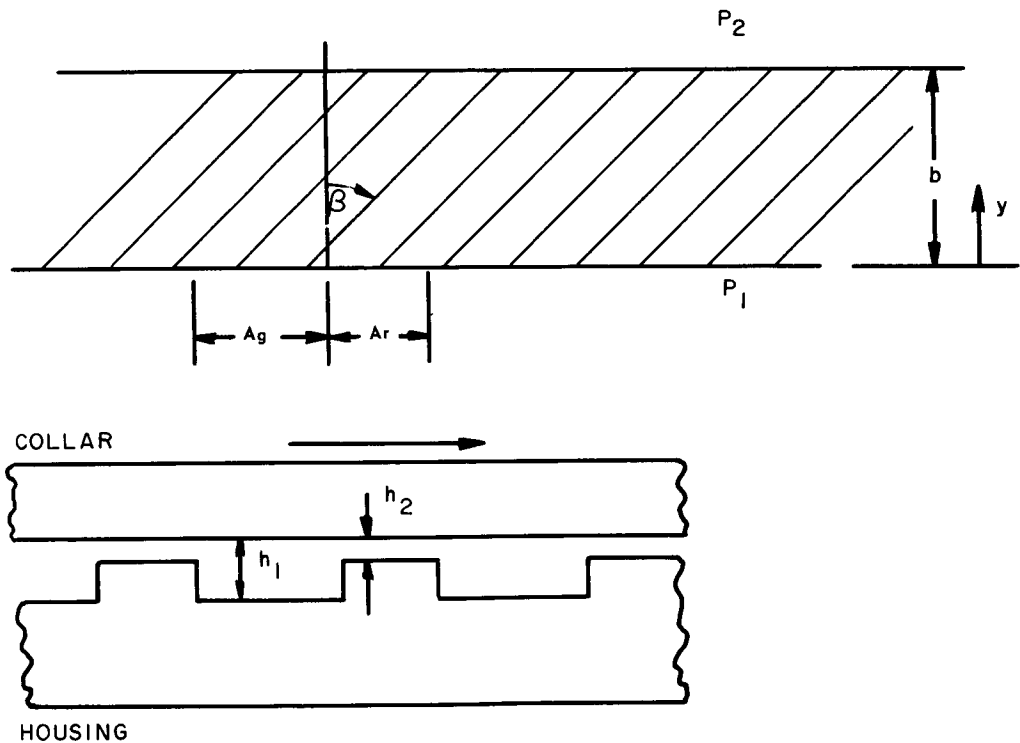


Figure 43 Hydrodynamic, Spiral-Grooved Seal

Governing Equations - A mathematical derivation of the pressure distribution in a hydrodynamic, grooved seal with an isothermal gas film may be found in Reference 1. In non-dimensional form, the Equation of pressure can be written as

$$\frac{d\bar{p}}{d\bar{y}} = \Lambda K_1 - \frac{\bar{M} K_2}{\bar{p}} \quad (50)$$

where

$$\bar{p} = p/p_1$$

$$\bar{y} = y/b$$

$$\Lambda = \frac{6\mu Ub}{p_1 h_1^2}$$

$$\bar{M} = m \frac{12\mu b}{p_1 h_1^3 \rho_1}$$

$$K_1 = \frac{(H^3 - 1)(H - 1) \sin 2\beta}{(H^3 + 1)^2 + 2H^3 (A + A^{-1}) + (H^3 - 1)^2 \cos 2\beta}$$

$$K_2 = \frac{2(1 + A^{-1})(H^3 + A)}{(H^3 + 1)^2 + 2H^3 (A + A^{-1}) + (H^3 - 1)^2 \cos 2\beta}$$

$$U = \text{mean speed, in/sec}$$

$$\mu = \text{viscosity of gas, lb-sec/in}^2$$

$$m = \text{mass flow, } \frac{\text{lb} - \text{sec}}{\text{in}^2}$$

$$\rho_1 = \text{Density of gas at } p_1, \frac{\text{lb} - \text{sec}^2}{\text{in}^4}$$

$H$  = groove height ratio =  $h_2/h_1$

$A$  = groove width ratio =  $A_g/A_r$

$\beta$  = groove angle

For a fully grooved seal, Equation (50) becomes

$$\int_1^{\bar{p}_2} \frac{\bar{p} d\bar{p}}{\bar{p} - \frac{\bar{M} K_2}{\Lambda K_1}} = \Lambda K_1 \int_0^1 d\bar{y} \quad (51)$$

therefore,

$$\Lambda K_1 = (\bar{p}_2 - 1) + \bar{M}^* \log_e \left( \frac{\bar{p}_2 - \bar{M}^*}{1 - \bar{M}^*} \right) \quad (52)$$

where

$$\bar{p}_2 = p_2/p_1$$

and

$$\bar{M}^* = \bar{M} K_2 / \Lambda K_1.$$

Discussion - The sense of mass flow ( $\bar{M}$ ) is negative when the direction of flow points toward the low pressure side. By observation of Equation (52), it is seen that, for a constant compressibility number and groove geometry:

(a)  $\bar{M} = 0$  (Condition of no flow and a perfect seal) when

$$\bar{p}_2 = \bar{p}_2^* = 1 + \Lambda K_1$$

- (b)  $\bar{M} < 0$  (the flow direction is from the high pressure side to the low pressure side) when

$$\bar{p}_2 > \bar{p}_2^*$$

- (c)  $\bar{M} > 0$  (i.e., the flow is sucked from a low pressure to a high pressure ambient), when

$$\bar{p}_2 < \bar{p}_2^*$$

Another interesting point is that, for a constant pressure ratio  $\bar{p}_2$ , the mass flow (in the absolute sense) directly increases if the compressibility number  $\Lambda$  or  $K_1$  (or both) decreases. Since the compressibility number and the dimensional flow are inversely proportional to the square and the cube of the film gap, a careful selection of film gap should be made.

Graphical Representation - Equation (52) is plotted in graphical form. Figure 44 shows the dimensionless flow vs  $\bar{p}$  at different  $K_1 \Lambda$ . Figure 45 shows the enlarged portion of Figure 44 in the low pressure zone. The values of  $K_1$  and  $K_2$  can be found from Figure 46 which is based on one particular groove-geometry (angle and width ratio).

The computer program used to evaluate eq. (52) is given in Appendix D.

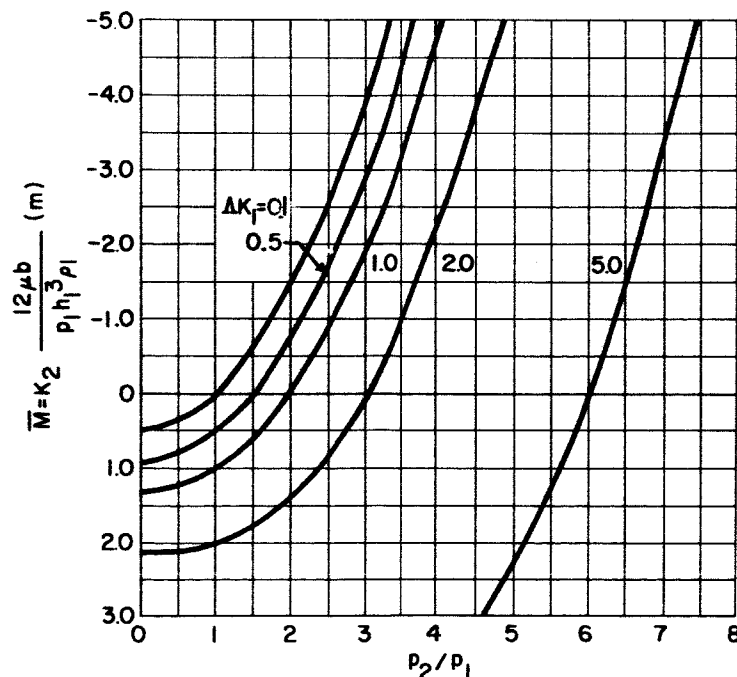


Figure 44 Dimensionless Flow vs Pressure Ratio Spiral-Grooved Seal

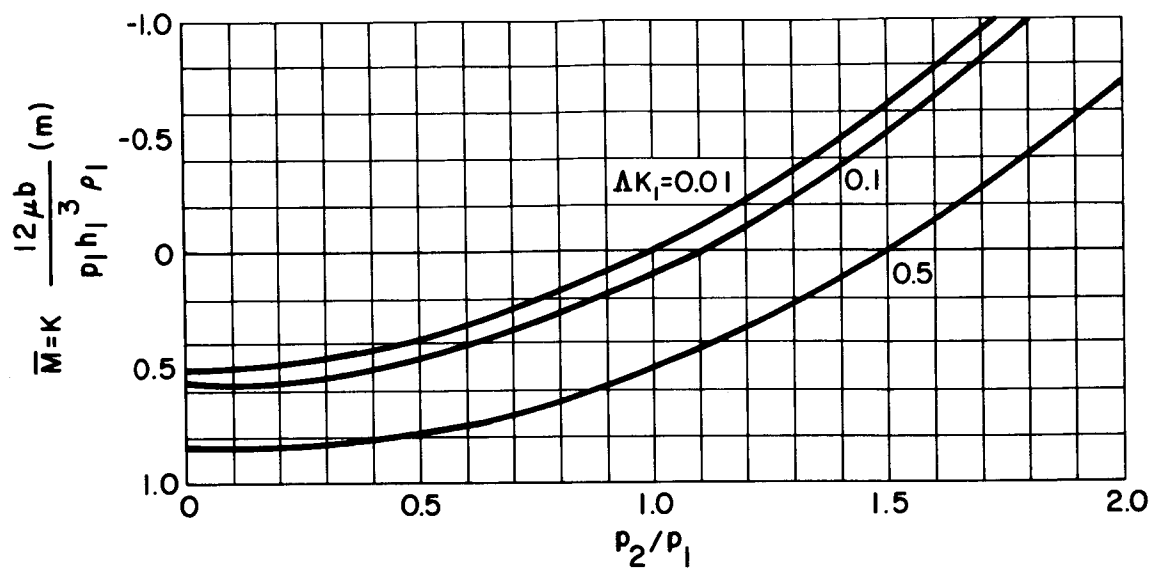
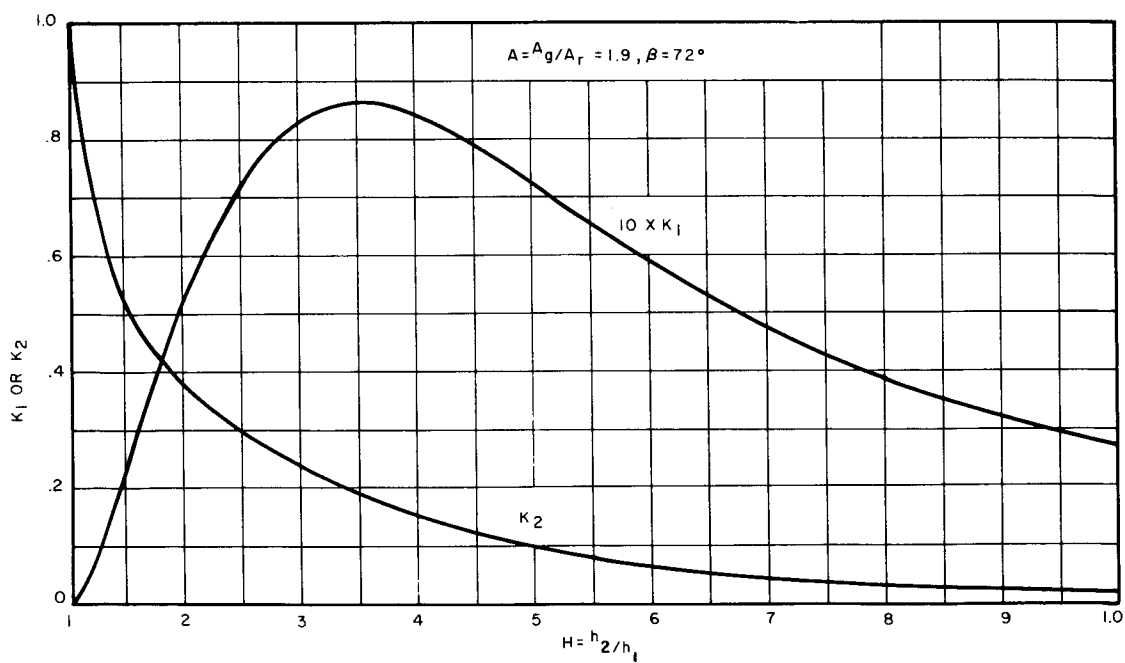


Figure 45 Dimensionless Flow vs Pressure Ratio Spiral-Grooved Seal

Figure 46 Coefficients  $K_1$  and  $K_2$  for Spiral-Grooved Seal

Charts on load, stiffness and center of pressure are not yet available. Because the spiral groove seal is basically a pump, it must be combined with a restrictor before substantial load capacity or stiffness is attained. The restrictor may be a land (at the high pressure side) or an orifice feed.

### Rayleigh Step

The Rayleigh Step (in a circumferential direction) is attractive as a means of providing additional hydrodynamic support for the primary seal. This is particularly desirable during moments of high load and reduced film thickness, such as might be experienced during transients or sudden displacements. The Rayleigh Step may be used either as a shallow pattern on the lip of a hydrostatic step seal or as the primary seal itself with a larger step.

The necessary information and charts to permit evaluation of the Rayleigh Step in comparison with other approaches are not yet complete. A new computer program was necessary to accommodate the differing boundary pressures in this application of the Rayleigh Step Pattern. The background of this program and the FORTRAN IV statement are included as Appendix B.

### Hydrostatic Orifice Compensated Seal

The expressions for the load and stiffness of hydrostatic orifice compensated design have been derived earlier in the Screening Study. The pressure distributions in the upstream and downstream section are exactly the same as the step seal given as Equations (15) and (16).

Following the procedure described earlier in the Screening Study, the intermediate pressure can be determined graphically and the dimensionless load can be readily calculated from Equation (29). Results of  $\bar{W}$  are plotted against a dimensionless film thickness defined by

$$\bar{H} = h \left( \frac{\ell p_2}{24 \mu b} \frac{\sqrt{RT_2}}{C_D \pi a^2} \right)^{1/3} \quad (53)$$

These curves are shown in Figures 47, 48, and 49 for width ratios of 1/8, 1/4 and 1/2, and pressure ratio of 0.1 and 0.2. The leakage through the seal can be calculated from the flow equation for the downstream section, Equation (21). In Figure 50, the dimensionless leakage is plotted against the dimensionless film thickness. The dimensionless leakage is defined by

$$\bar{M} = m \left[ \frac{24 \mu b}{h^3 \ell} \frac{RT_2}{p_2^2} \right] \quad (54)$$

The dimensionless stiffnesses, as defined by

$$\left. \begin{aligned} \bar{K}_s &= \frac{dW}{d\bar{H}} \\ &= \left[ \frac{d\bar{W}}{dh} (p_2 - p_1) \right] \frac{h}{\bar{H}} \left( \frac{1}{p_2 - p_1} \right) \\ &= K_s \frac{h}{\bar{H} (p_2 - p_1)} \end{aligned} \right\} \quad (55)$$

are plotted against  $\bar{H}$  in Figure 51 through 53.

To illustrate the use of these dimensionless charts, an illustration example is presented.

#### Illustration Example

The problem is to design a hydrostatic-orifice seal to operate under the following given conditions with maximum stiffness.

$$\begin{aligned} P_1/P_2 &= 0.2 \\ P_2 &= 100 \text{ psia} \\ b &= 0.75 \text{ inches} \\ b_1/b &= 0.25 \\ h &= 0.001 \text{ inches} \\ T_2 &= 1200 \text{ F} \\ R &= 2.47 \times 10^5 \frac{\text{in}^2}{\text{sec}^2 \text{ } ^\circ\text{R}} \\ \ell &= 1.0 \text{ inch} \\ u &= 5.9 \times 10^{-9} \frac{\text{lb. sec.}}{\text{in}^2} \end{aligned}$$

1. Referring to the stiffness curve for  $b_1/b = 0.25$ , Figure 52, for maximum stiffness at  $p_1/p_2 = 0.2$ ,

$$\begin{aligned} \bar{H} &= 0.56 \\ \bar{K}_s &= 0.48 \end{aligned} \quad \text{and} \quad \left\{ \begin{aligned} K_s &= \bar{K}_s \frac{\bar{H}}{h} (p_2 - p_1) \\ &= 0.48 \times \frac{0.56}{0.001} \times 80 = 21,500 \left( \frac{\text{lb}}{\text{in}^2} \right) / \text{in.} \end{aligned} \right.$$



2. Referring to the load curves for  $b_1/b = 0.25$ , Figure 48, for

$$\bar{H} = 0.56$$

$$\bar{W} = 0.81$$

3. To determine the orifice radius, one must first find  $C_D$  from Figure 54 and also calculate  $\rho_2$ .

From Figure 52, one locates  $C_D \approx 0.83$

$$\rho_2 = \frac{P_2}{RT_2} = \frac{100}{2.47 \times 10^5 \times (1200 + 460)} =$$

$$2.43 \times 10^{-7} \frac{\text{lb sec}^2}{\text{in}^4}$$

$$\frac{h}{\bar{H}} = \left( \frac{24 \mu b}{\ell \rho_2} \frac{C_D \pi a^2}{\sqrt{RT_2}} \right)^{1/3}$$

and

$$a = \left[ \frac{\ell \rho_2 \sqrt{RT_2}}{24 \mu b C_D \pi} \left( \frac{h}{\bar{H}} \right)^3 \right]^{1/2}$$

$$= \left[ \frac{1.0 \times 2.43 \times 10^{-7} \sqrt{2.47 \times 10^5 \times 1660}}{24 \times 5.9 \times 10^{-9} \times 0.75 \times 0.83 \times 3.1416} \times \left( \frac{0.001}{0.56} \right)^3 \right]^{1/2}$$

$$= 1.13 \times 10^{-2}$$

4. Referring to Figure 48, the dimensionless leakage for  $\bar{H} = 0.56$ , is found to be

$$\bar{M} = 2.78$$

$$m = \bar{M} \left[ \frac{h^3 \ell}{24 \mu b} \right] \left[ \frac{p_2^2}{RT_2} \right]$$

$$\begin{aligned} m &= 2.78 \left[ \frac{1}{24 \times 5.9 \times 0.75} \right] \left[ \frac{10^4}{2.47 \times 10^5 \times 1660} \right] \\ &= .64 \times 10^{-6} \left( \frac{\text{lb sec}}{\text{in}} \right) \end{aligned}$$

$$m = .64 \times 10^{-6} \times 386 = 2.47 \times 10^{-4} \text{ lb/sec}$$

Note that this leakage is for  $\ell = 1$  inch, so that for a complete seal this must be multiplied by  $\pi D$ .

5. The results can be summarized as below:

$$\bar{H} = 0.56$$

$$\bar{K}_s = 0.48$$

$$\bar{W} = 0.81$$

$$\bar{M} = 2.78$$

$$h = 0.001 \quad \text{inches}$$

$$K_s = 21,500 \quad (\text{lb/in}^2)/\text{in.}$$

$$m = 2.47 \times 10^{-4} \quad \text{lb/sec}$$

$$a = 1.13 \times 10^{-2} \quad \text{inches}$$

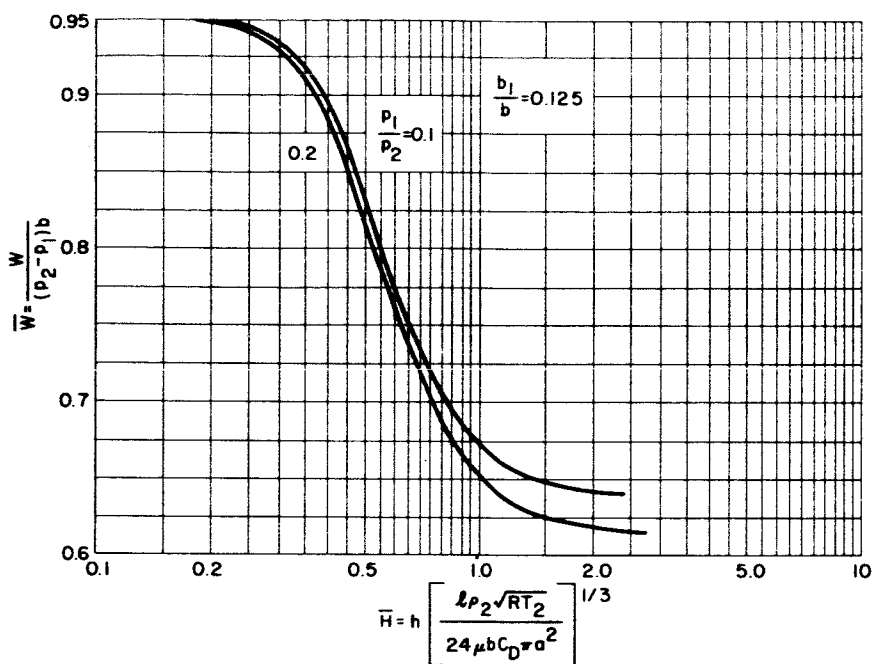


Figure 47 Hydrostatic Orifice-Load

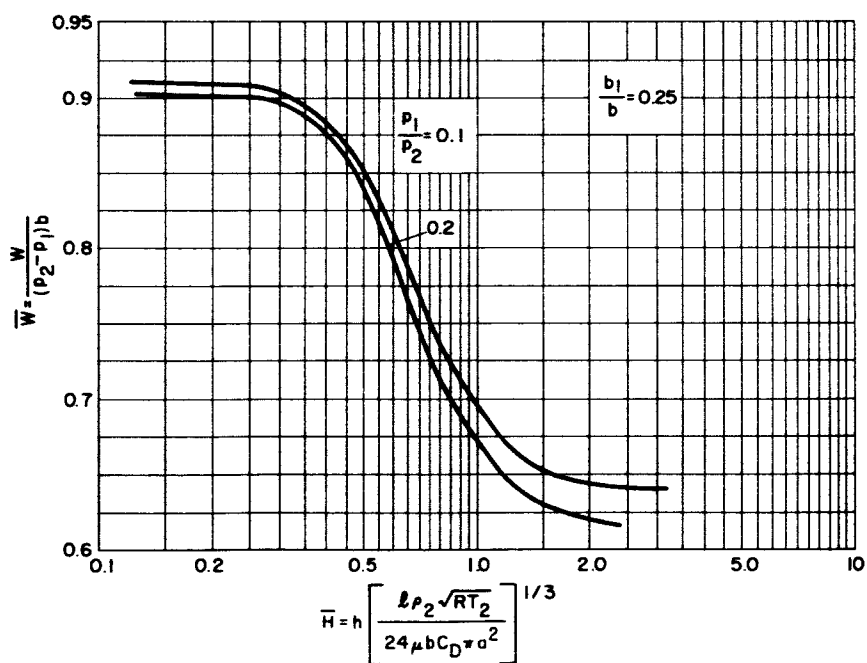


Figure 48 Hydrostatic Orifice-Load

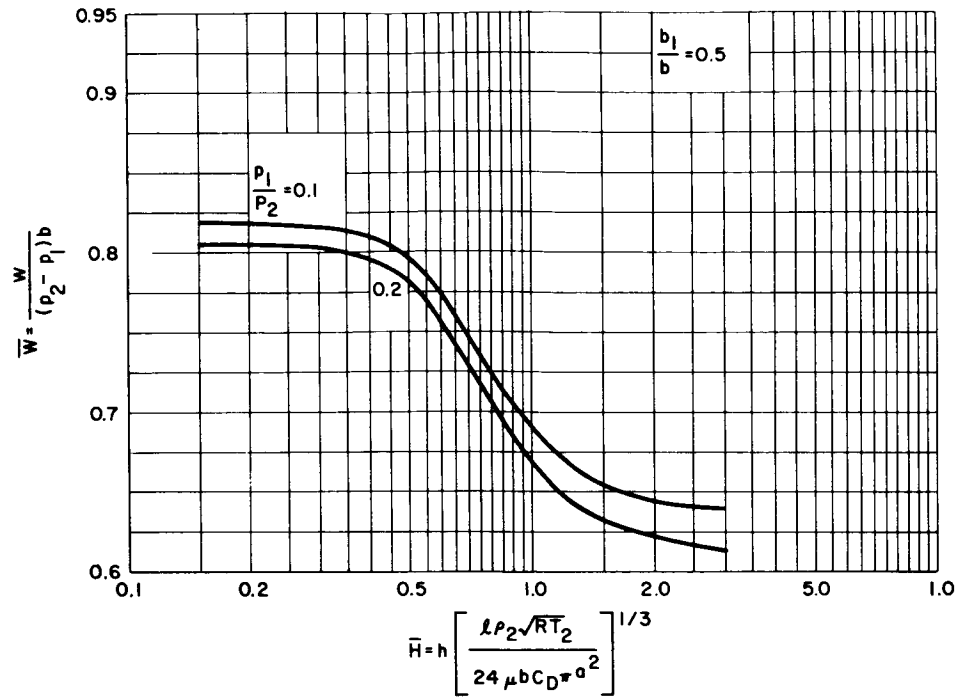


Figure 49 Hydrostatic Orifice-Load

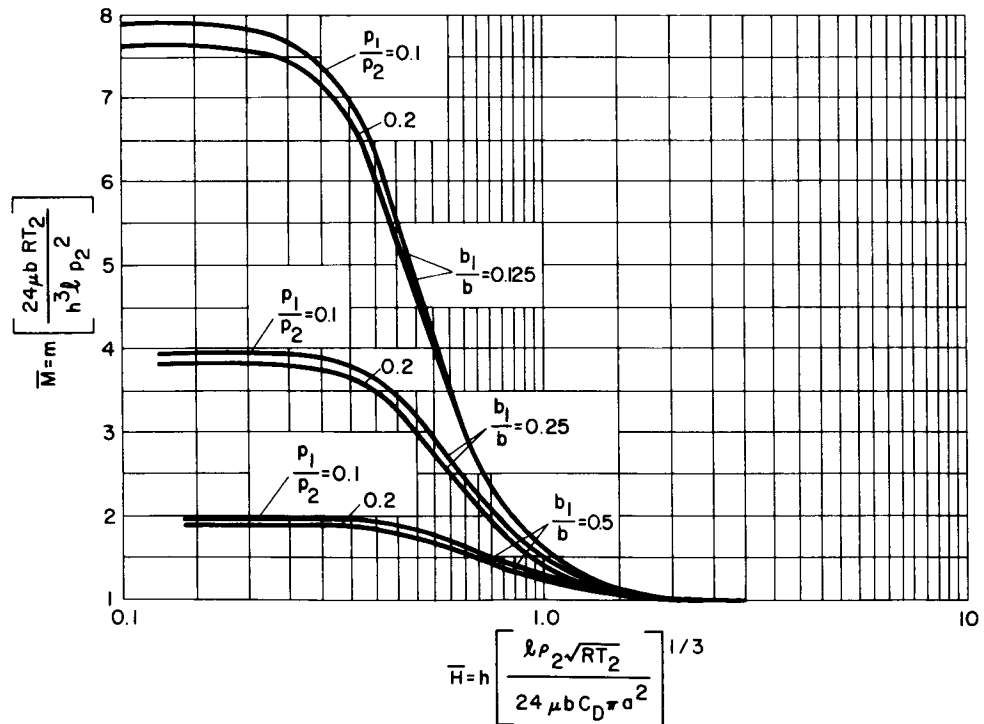


Figure 50 Hydrostatic Orifice-Flow

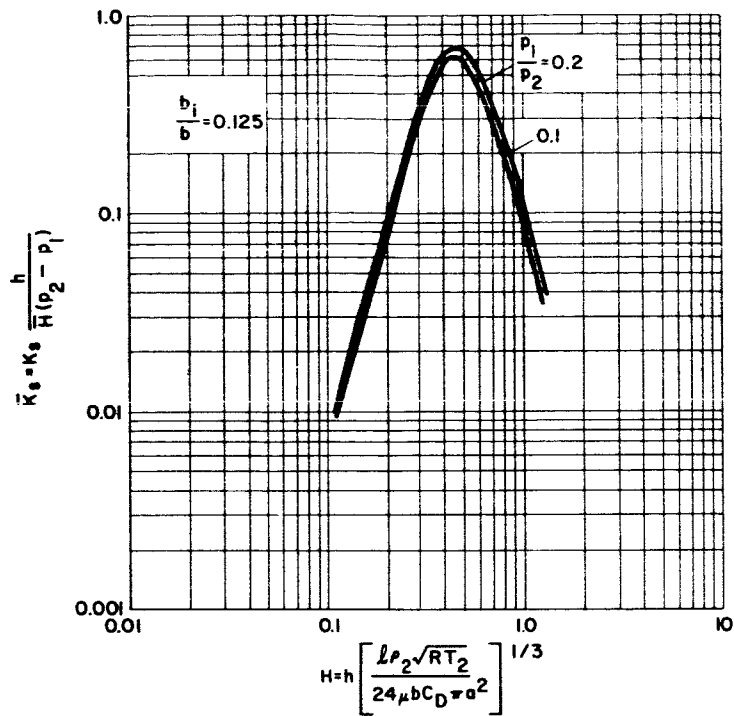


Figure 51 Hydrostatic Orifice-Stiffness

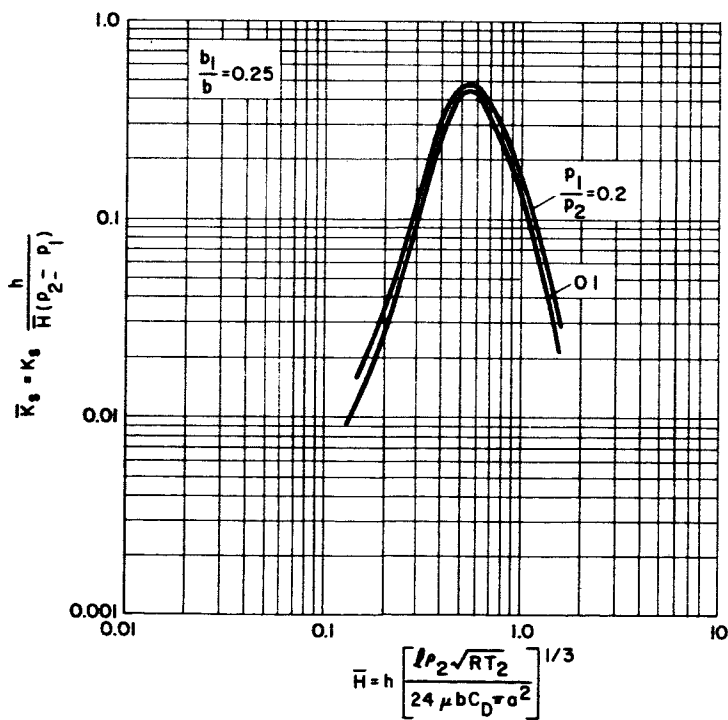


Figure 52 Hydrostatic Orifice-Stiffness

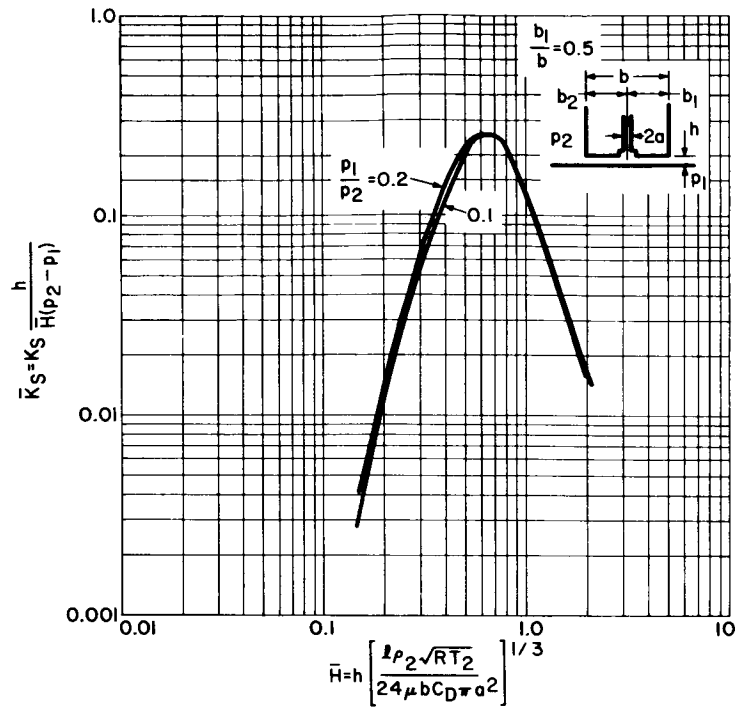


Figure 53 Hydrostatic Orifice-Stiffness

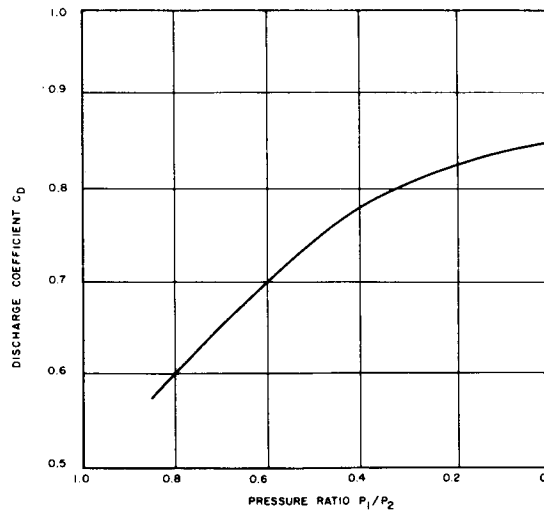


Figure 54 Discharge Coefficient for Orifices. Experimental Data to Generate this Curve were Taken From Reference 3.

### Hydrostatic Labyrinth Seal

The dimensionless load for hydrostatic labyrinth seals has been calculated according to Equation (37) for a range of pressure ratios from 0.1 to 0.572. Figure 55 shows the relationship between the load and a dimensionless film thickness defined by

$$\bar{H} = \frac{Ch\ell}{C_D \pi a^2} \quad (56)$$

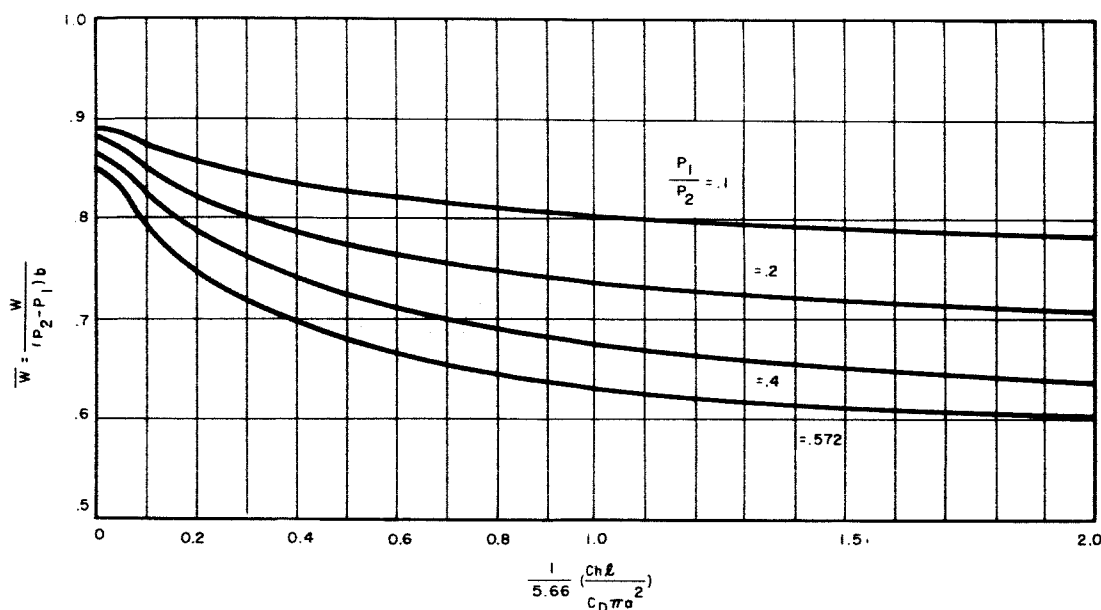


Figure 55 Hydrostatic Labyrinth-Load Curves

Where  $C$  and  $C_D$  represent the discharge coefficients for the labyrinths and orifices respectively.

The load does not vary appreciably with respect to change of the film thickness, particularly at low values of  $p_1/p_2$ . This indicates that the static stiffness of this seal concept is not as satisfactory as either the hydrostatic step or the hydrostatic orifice compensated design. In addition to the lack of static stiffness, the dynamic stiffness of this seal concept is believed to be low because of the large volume of the air pocket between labyrinths. These large pockets act as a very soft spring and give rise to poor response during any irregular motion of the rotor. For these reasons, further data on hydrostatic labyrinth seals have not been obtained.

### Multiple Pad Designs with Thin Strip Seal

Among the seal concepts proposed for further feasibility studies, two of the concepts rely upon the flexibility of a thin ring to follow any runout and wobble motion and to compensate for any thermal coning resulting from the frictional heating in the gas film. These are the thin strip-one piece design and the thin strip-C diaphragm design.

In designing this seal ring section, two important factors must be considered. First, the cross-section must have a sufficiently small section modulus in order to allow it to follow any thermal coning without resulting in excessive curvature along the radial profile. Second, the restoring moment produced by the film pressure due to relative coning between the seal ring and rotor must be sufficiently strong to cause the seal ring to twist but not to touch the rotor either at the inner or at the outer edge. On the basis of these two considerations, the directions for design are certainly towards choosing a seal ring cross-section having a minimum section modulus and a primary seal concept having a maximum restoring moment. In the next section, a simple but important design criterion is established for the purpose of determining the required section modulus and gas film restoring moment.

A Design Criterion for Thin Strip Seal - Consider a flexible seal ring as shown in Figure 56.

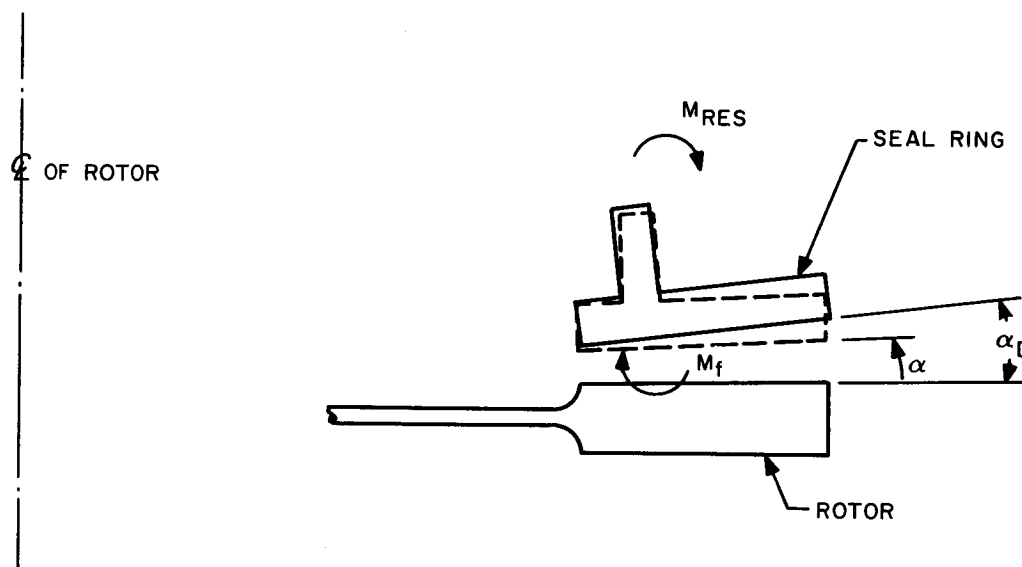


Figure 56 Angular Displacement of Thin Strip Seal



The angular twist ( $\alpha$ ), the restoring moment by the gas film, as well as other forces acting on the seal ring, are assumed to be axisymmetrical in order to arrive at the first-order design criteria. The consideration of any non-symmetrical deformations will be considered in the flexible seal ring analysis.

Let  $\alpha_D$  denote the relative angular twist between the ring and the rotor due to distortion from the axial thermal gradient or initial warping, and let  $M_{RES}$  designate the residual unbalanced moment which may arise from imperfect manufacturing, off-design operation, or inexactness in the prediction of the center of pressure. Of course, if everything is designed and made perfectly and the thermal distortion is small, then  $M_{RES}$  and  $\alpha_D$  will be negligible. But, if they are not small, then the restoring moment from the gas film must be large enough to twist the seal ring into an angle within the allowable angle of twist, which will be denoted by  $\alpha_A$ .

Let  $a_e$  be the moment required to rotate the seal ring section through one radian.

Referring to Reference 2,

$$\beta_e = \left( \frac{\Delta M}{\Delta \alpha} \right)_e = \frac{E I_c}{R^2} \quad (57)$$

where  $\Delta M$  is the increment of the moment about the centroid of the cross-section,  $\Delta \alpha$  is the increment of the angular twist in the direction of the acting moment.  $I_c$  is the area moment of inertia about an axis passing through the centroid and perpendicular to the axis of the seal ring.

Let  $\beta_f$  be the gas film angular stiffness which is defined by

$$\beta_f = \left( \frac{\Delta M_f}{\Delta \alpha} \right)_f \quad (58)$$

where  $\Delta M_f$  is the increase of the gas film moment about the centroid in the clockwise direction.

The net moment acting in the clockwise direction is

$$\beta_f \alpha + M_{RES} \quad (59)$$

For condition of equilibrium, this moment must be equal to the moment required to twist the ring from the angle  $\alpha_D$  back to  $\alpha$ . This requires

$$\beta_f \alpha + M_{RES} = \beta_e (\alpha_D - \alpha) \quad (60)$$

Solving Equation (4) for  $\alpha$ , one obtains

$$\alpha = \left[ \frac{\beta_e}{\beta_f + \beta_e} \alpha_D - \frac{M_{RES}}{\beta_f + \beta_e} \right] \quad (61)$$

If the absolute value of this angle is to be limited within a certain allowable angle  $\alpha_A$ , one obtains the following criterion

$$\left| \frac{\beta_e}{\beta_f + \beta_e} \alpha_D - \frac{M_{RES}}{\beta_f + \beta_e} \right| < \alpha_A \quad (62)$$

It is instructive to note that if  $\beta_e \rightarrow \infty$ , which is the case of a rigid ring, then the criterion reduces to

$$\alpha_D < \alpha_A \quad (63)$$

which simply means that the combined thermal and initial coning must be less than the allowable angular displacement.

On the other hand, if  $\beta_e \rightarrow 0$ , which is the case of a perfectly flexible ring, then the criterion reduces to

$$\frac{M_{RES}}{\beta_f} < \alpha_A \quad \text{or} \quad M_{RES} < \alpha_A \beta_f \quad (64)$$

which means that the residue moment be less than the allowable coning times the angular stiffness.

It should be noted that this criterion is an important, necessary one; it is by no means sufficient, since other problems associated with non-symmetrical thermal distortion, static stability, and dynamic response of the entire ring in the transverse and angular mode will add further restrictions to the design requirements.

The criterion (62) indicates that thermal coning of the seal ring and the rotor face must be kept at an absolute minimum. In the Screening Study, it was shown that a coning of 0.004 rad can be expected for the seal ring. For the rotor face, it is particularly restrained but the axial thermal gradient is expected to be higher; therefore, the coning of the rotor face might be of the same order as the seal ring. As to the residue moment, it can come from three sources: (1) inexact prediction of both the centroid of a complicated seal ring section and

the center of pressure in the gas film, (2) manufacturing tolerance, and (3) off-design operation and transient variation of pressure. This seems to indicate that even if the seal ring is made perfectly flexible, it would require considerable angular stiffness to overcome the residue moment.

Since the primary seal for the thin strip concept requires a high angular stiffness, none of the single-pad primary seal concepts considered in the Screening Report are adequate for this application. It is necessary to seek other designs having a much wider base and having more than one pad. The new designs considered for the flexible seal are discussed in the following subsections.

Double Orifice Design - This design actually is a single pad but with two rows of orifices intended to give stronger angular stiffness, and two rows of spiral grooves for prevention of high speed rub at the edges (see Figure 57). An analysis was made to solve the flow network through the orifices and spiral grooves and a computer program was written to calculate the load, stiffness and flow of this design. The details of this analysis will be reported at a later date. In addition, the load and moment for a non-parallel film was analyzed by assuming the gas film is composed of three parallel films at different levels of the film thickness.

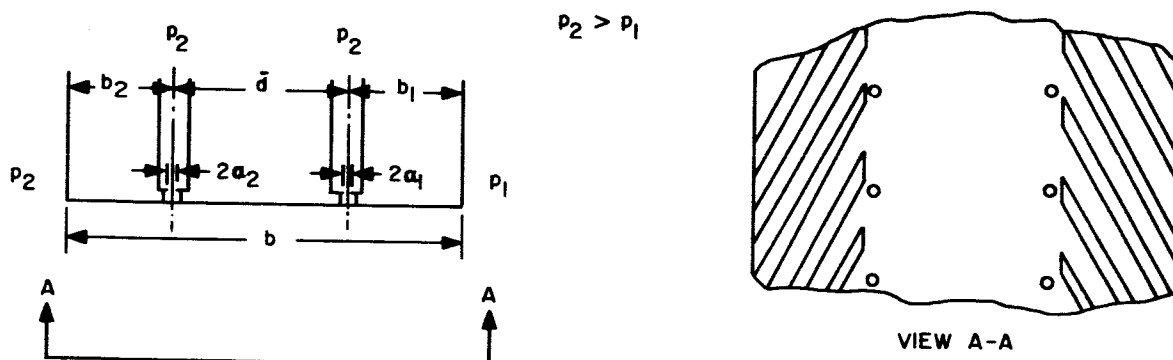


Figure 57 Double Orifice Primary Seal with Spiral Grooves

Using the following dimensions:

$$b = 3/4 \text{ inches}$$

$$b_1 = b_2 = d = 1/4 \text{ inch}$$

$$a_1 = a_2 = 0.005 \text{ inch}$$

it was found that the angular stiffness,  $\beta_f$ , at  $h = 0.0009$  inches is 460 (in lb/in)/rad.

A cross section for this design and its dimension is shown in Figure 58.

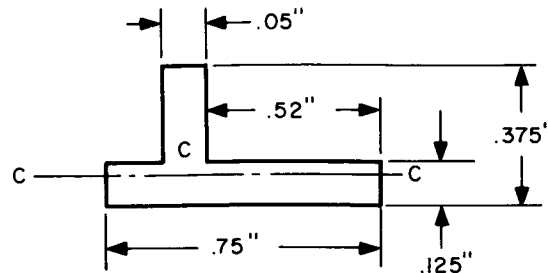


Figure 58 Cross-Section of a Double-Orifice Design

The area moment of inertia about its centroidal axis C-C is  $5.55 \times 10^{-4}$  inches<sup>4</sup>. The elastic stiffness,  $\beta_e$ , for a steel segment and a radius of 13.75 inches becomes

$$\beta_e = \frac{EI_c}{R^2} = \frac{30 \times 10^6 \times 5.55 \times 10^{-4}}{(13.75)^2} = 88 \quad \left( \frac{\text{in-lb}}{\text{in}} \right) / \text{rad}$$

If one assumes that the value of  $\alpha_D$  can be controlled to within 0.005 rad. and the allowable  $\alpha_A$  is 0.001 rad., the criterion (62) gives

$$\left( \frac{\beta_e}{\beta_f + \beta_e} \right) \alpha_D - \frac{M_{RES}}{\beta_f + \beta_e} < 0.001$$

To satisfy this criterion, the residue moment must lie within the following limits

$$- .108 < M_{RES} < 0.988 \quad \text{in-lb/in}$$

This limit is very narrow, and it indicates strongly that this design does not have adequate angular stiffness.

Double Pad Design - When a vented groove is introduced in the sealing area as shown in Figure 59, the single pad is split into two pads. The right pad functions as a seal, and the left pad becomes a thrust bearing used primarily to provide the needed angular stiffness. Of course, with this design, the leakage is expected to be much higher than the single pad design. A design compromise must be made between the angular stiffness and leakage.

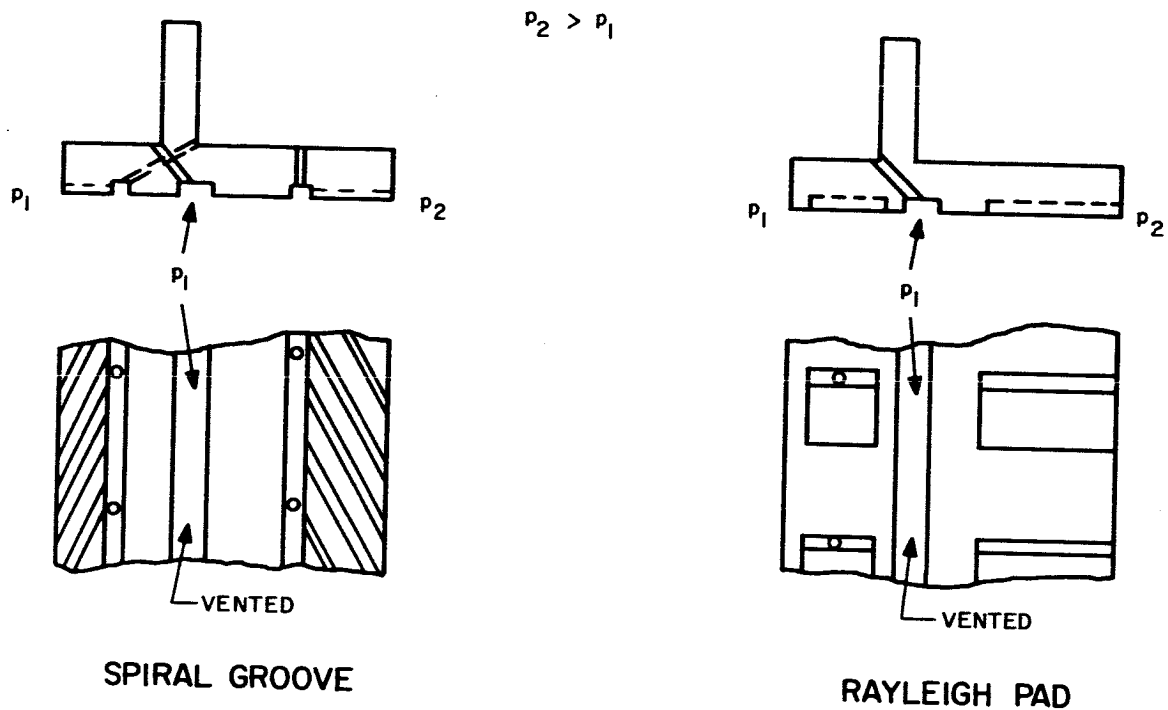


Figure 59 Double Pad Seals with Central Vent Groove

The axial stiffness of the left pad is much higher than the right pad because a thrust pad is inherently stiffer than the seal. The angular stiffness can be estimated by the following expression

$$\beta_f = k_1 b_1 \ell_1^2 + k_2 b_2 (\ell - \ell_1)^2 \quad (65)$$

Where  $k_1$  and  $k_2$  are the axial film stiffnesses in (lb/in<sup>2</sup>)/in based on the parallel film analysis,  $b_1$  and  $b_2$  are the widths of the pads; the dimensions,  $\ell$ , and  $\ell_1$  are shown in Figure 60.

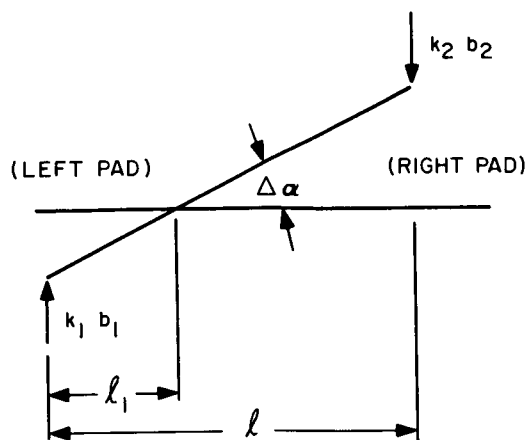


Figure 60 Tilting of Double Pad Seal

If  $k_1$  and  $k_2$  are known, the ratio of the widths can be optimized and the resulting expression is

$$\frac{b_1}{b_1 + b_2} = \frac{\sqrt{\frac{k_1}{k_2}} - 1}{\frac{k_1}{k_2} - 1} \quad (66)$$

The ratio of  $k_1/k_2$  is about 2, and using this value,  $(\frac{b_1}{b_1 + b_2})$  is found to be equal to 0.414.

The magnitude of  $k_1$  and  $k_2$  based on the previous single pad hydrostatic-orifice solution is approximately equal to 40,000 and 20,000 psi/in. Assuming these values for  $k_1$  and  $k_2$  and a total width of 1.25 inches, the calculated angular stiffness is 1,600 in lb/in. rad.

The double pad design has one disadvantage, since a wider pad would require a deeper section in the axial direction to achieve the necessary moment balance. A deeper section would increase  $\beta_e$  and may not give a significant reduction in  $\frac{\beta_e}{\beta_f + \beta_e}$ . However, the double pad design definitely increases the tolerance to residue moments since both  $\beta_f$  and  $\beta_e$  will be increased with this design.

The primary seal concept considered for these pads is the hydrostatic spiral groove concept, or the hydrostatic-hydrodynamic Rayleigh pads. The load axial stiffness, angular stiffness and the leakage of the double pad design using the primary seal concepts are currently being studied in detail; results will be reported later.

## Seal Response

Tracking - The dynamics of a seal segment within the framework of the one-dimensional theory of vibration has been studied in detail in the Screening Study. The response of the seal segment to any rotor motion is characterized by the motion of the seal segment relative to the rotor. Using Equation (11e) in the Screening Study, the seal response can be expressed as

$$\frac{\delta}{f_n} = \frac{A_n - f_n}{f_n} = \frac{1}{\left[ \left( 1 - \frac{n^2 \omega_m^2 - k_s}{k_f} \right)^2 + \left( \frac{n \omega_c}{k_f} \right)^2 \right]^{1/2}} - 1 \quad (67)$$

For the design concepts considered in this section, the only sources of damping force appear to come from the internal damping of the seal back-up spring and the gas film damping. Both of these are believed to be extremely small in affecting the response. Assuming that the damping effect is absent, the quantity  $\delta/f_n$  is calculated according to Equation (11) and plotted against the parameter  $\frac{n^2 \omega_m^2 - k_s}{k_f}$  in Figure 61.

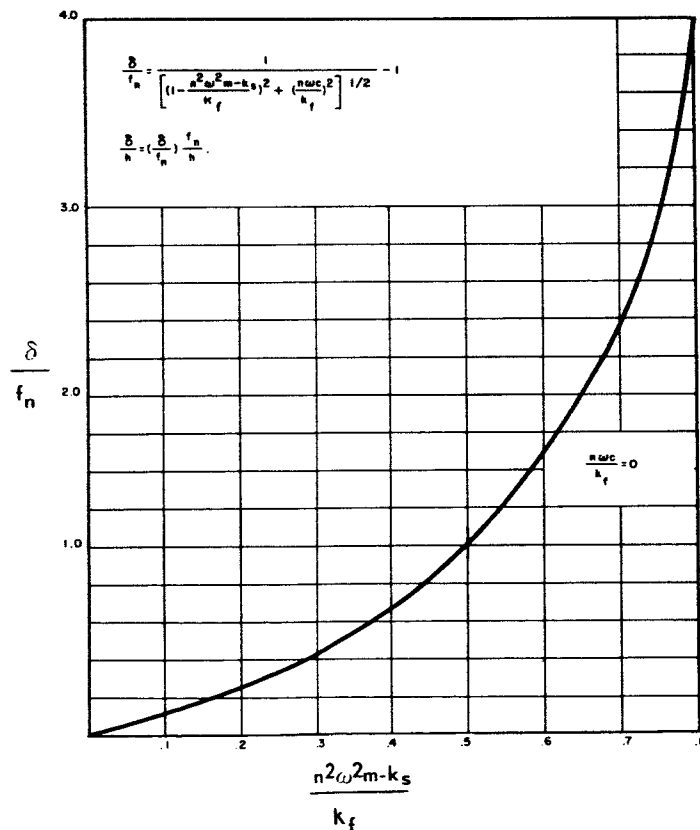


Figure 61 Dynamic Response Ratio

Figure 62 shows the portion of the curve for small values of  $\delta/f_n$  on an enlarged scale.

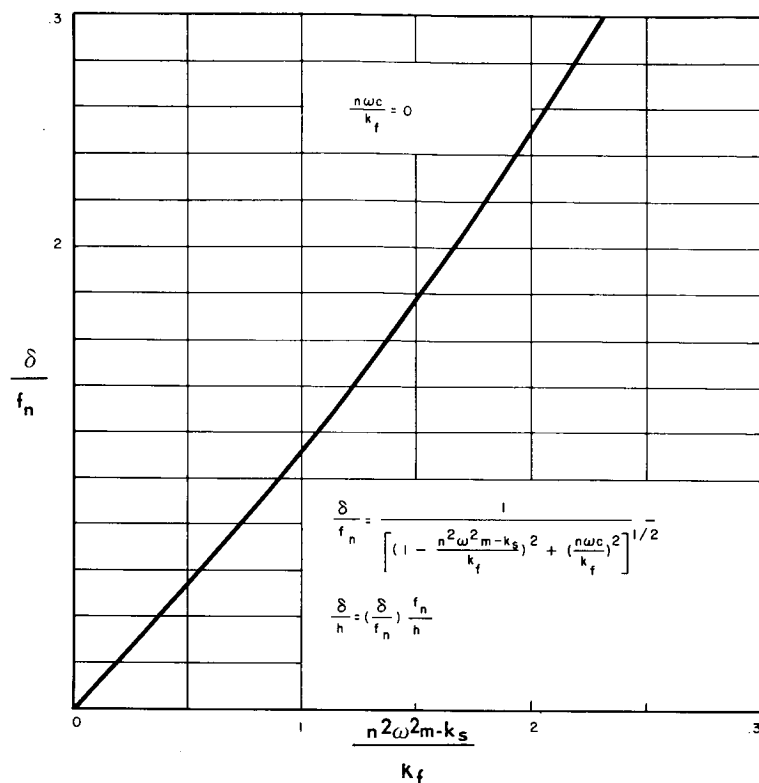


Figure 62 Dynamic Response Ratio - Enlarged Scale

Flexible Seal Ring Vibration - The vibration of a flexible seal ring supported by a gas film will be analyzed in this section. Figure 63 shows a seal ring with a mean radius  $R$  and cross-sectioned dimensions  $a$  and  $b$ .

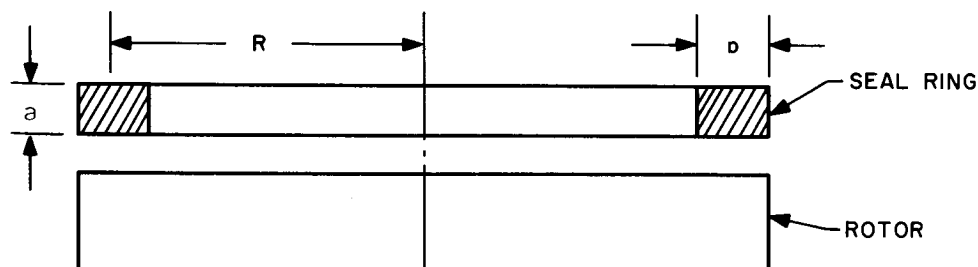


Figure 63 Thin Strip Seal Ring



Consider the situation where the rotor surface facing the seal ring is not perfectly flat and let its contour in the circumferential direction be represented by  $\delta = \delta_0 \cos \theta$ . Since the rotor is rotating at an angular speed  $\omega$ , the circumferential contour of the rotor is, at any particular instant of time

$$\delta = \delta_0 \cos 2(\theta + \omega t) \quad (68)$$

Let  $y$  be an instantaneous deflection curve of the seal ring. Then the film thickness is given by

$$h = h_m - y + \delta \quad (69)$$

where  $h_m$  = mean film thickness.

Note that both  $y$  and  $\delta$  are defined as positive in the downward direction, as shown in Figure 64.

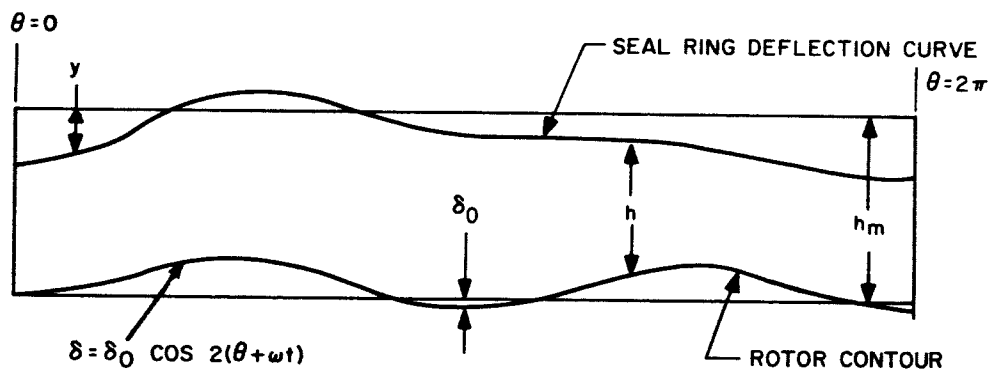


Figure 64 Diagram Showing Unwrapped Seal Ring Deflection Curve and Rotor Contour

Taking a differential segment of the ring as shown in Figure 65, the forces and moments acting on this element are shear forces  $V$ , gas film restoring force  $q$ , bending moments  $M_b$ , twisting moments  $M_t$ , and gas film restoring moment  $q\alpha$ . Double arrow head denotes vector representation (right hand system) of angular quantities. The equations of motion can be written as follows.

Transverse motion (linear translation):

$$-\frac{dV}{d\theta} d\theta - qRd\theta = (\rho ARd\theta)\ddot{y} \quad (70)$$

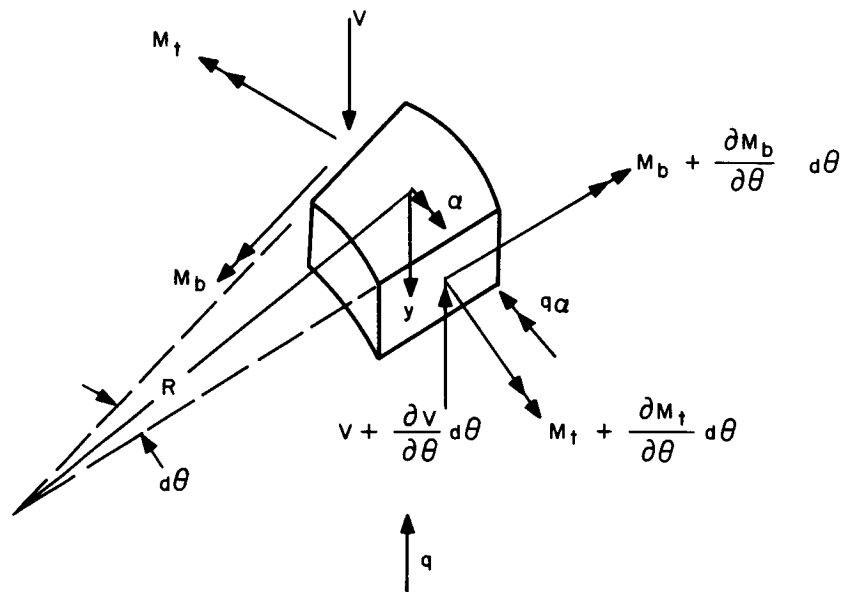


Figure 65 Force and Moment Diagram of a Seal Ring Segment

Radial equilibrium of all moments

$$\frac{\partial M_b}{\partial \theta} d\theta - M_t d\theta - VRd\theta = I_{rr} \frac{\partial \ddot{y}}{\partial \theta} \frac{1}{R} \quad (71)$$

Tangential equilibrium of all moments

$$M_b d\theta + \frac{\partial M_t}{\partial \theta} d\theta - q_\alpha R d\theta = I_{tt} \ddot{\alpha} \quad (72)$$

where

$$I_{rr} = \frac{M(R^2 d\theta^2 + a^2)}{12}$$

$$I_{tt} = \frac{M(a^2 + b^2)}{12}$$

$$\ddot{\alpha} = \frac{\partial^2 \alpha}{\partial t^2}$$

$$\ddot{y} = \frac{\partial^2 y}{\partial t^2}$$

$M$  = mass of the segment =  $\rho abR d\theta$

$\rho$  = density of seal ring

$A$  = cross-sectional area,  $ab$

$q$  = restoring force per unit length

$q_\alpha$  = restoring moment per unit length

From (68) and (69) we have

$$\begin{aligned} q &= k(y - \delta) \\ &= k(y - \delta_o \cos 2(\theta + \omega t)) \end{aligned} \quad (73)$$

where  $k$  is the linear stiffness of the gas film per unit length.

To obtain  $q_\alpha$ , refer first to Figure 66. The restoring force distribution due to an angular displacement  $\alpha$  is linear across

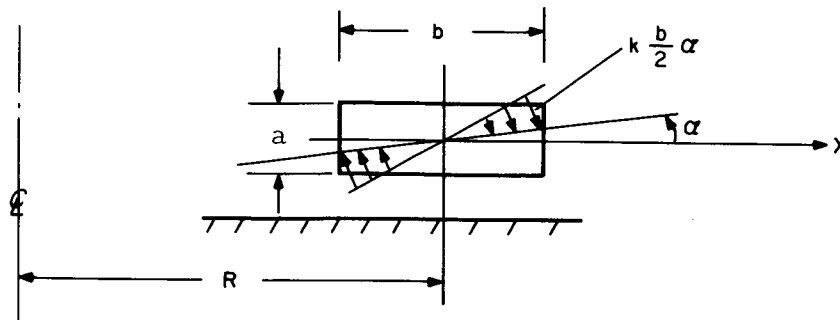


Figure 66 Force Distribution Across Tilted Seal

the width  $b$ . Integration of the moment of this distributed restoring force about the center results in

$$q_\alpha = 2 \int_0^{b/2} k x^2 \alpha \frac{dx}{b} = \frac{1}{12} k \alpha b^2 \quad (74)$$

Eliminating  $M_t$  and  $V$  from Equations (70), (71) and (72), we obtain

$$\begin{aligned} & -\frac{1}{R^2} \frac{\partial^2 M_b}{\partial \theta^2} - \frac{1}{R^2} M_b + \frac{k b^2 \alpha}{12 R} - q \\ & = \rho A \ddot{y} - \frac{1}{12} \frac{\rho A}{R} \left[ (a^2 + b^2) \ddot{\alpha} + \frac{a^2}{R} \frac{\partial^2 \ddot{y}}{\partial \theta^2} \right] \end{aligned} \quad (75)$$

Before going any further, obtain a relationship between  $M_b$  and the displacements  $y$  and  $\alpha$ . Again, take a segment of the seal ring with length  $R d\theta$ . Due to angular (twisting) displacement  $\alpha$ , the upper portion is compressed while the lower portion is stretched (See Figure 67).

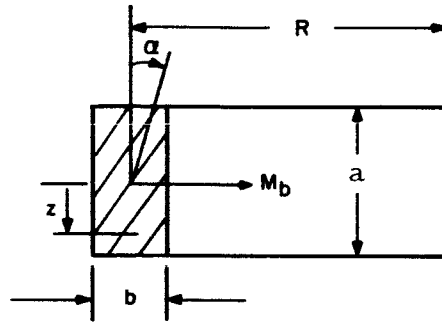


Figure 67 Twist of Seal Section

At an arbitrary location  $z$ , the stretched length of the segment  $Rd\theta$  is  $(R + z\alpha) d\theta$ . Hence

$$\text{deformation} = z\alpha d\theta$$

$$e_{\alpha} = \text{strain due to } \alpha = \frac{z\alpha d\theta}{Rd\theta} = \frac{z\alpha}{R}$$

We also know that

$$e_b = \text{strain due to bending} = \frac{z}{\bar{\rho}}$$

where

$$\bar{\rho} = \text{radius of curvature} = \left( \frac{d^2 y}{R^2 d\theta^2} \right)^{-1}$$

Hence

$$\begin{aligned} e &= \text{total strain} = e_{\alpha} + e_b \\ &= z \left( \frac{\alpha}{R} + \frac{1}{R^2} \frac{d^2 y}{d\theta^2} \right) \end{aligned} \quad (76)$$

For the particular seal ring application we have

$$b \sim a$$

and

$$\frac{b}{R} \ll 1$$

where  $\sim$  denotes "of the order of".

Also, it is reasonable to assume that

$$\alpha b \sim y \sim \frac{d^2 y}{d\theta^2}$$

Thus

$$\frac{\frac{1}{R^2} \frac{d^2 y}{d\theta^2}}{\frac{\alpha}{R}} \sim \frac{\left(\frac{1}{R^2}\right) \alpha b}{\frac{\alpha}{R}} \sim \frac{b}{R} \ll 1$$

Therefore, neglecting the strain due to bending, Equation (76) reduces to

$$e = z \frac{\alpha}{R}$$

The expression for the bending moment is readily obtained,

$$M_b = \int_{-a/2}^{a/2} E e z b dz = -E \frac{\alpha}{R} \int_{-a/2}^{a/2} z^2 b dz$$

$$\therefore M_b = -EI \frac{\alpha}{R} \quad (77)$$

Substituting (77) and (73) into (75) and neglecting terms of the order of  $(b/R)$ , we obtain

$$+ \frac{1}{R^2} \frac{EI}{R} \left( \frac{\partial^2 \alpha}{\partial \theta^2} + \alpha \right) - k [y - \delta_o \cos 2(\theta + \omega t)] = \rho A \ddot{y}$$

which is readily reduced to

$$\frac{d^2 \alpha}{d\theta^2} + \alpha - Ku - \frac{1}{f^2} \ddot{u} = -K \frac{\delta_o}{b} \cos 2(\theta + \omega t) \quad (78)$$

where

$$\left. \begin{aligned} u &= \frac{y}{b} \\ K &= \frac{k R^3 b}{EI} \\ f^2 &= \frac{EI}{\rho R^3 a b^2} \end{aligned} \right\} \quad (79)$$

Here  $u$  is the non-dimensional transverse displacement,  $K$ , a stiffness ratio, and  $f$ , a characteristic frequency.

Using the well-known formula

$$M_t = GI_p \frac{d\alpha}{Rd\theta} \quad (80)$$

with  $G$  = modulus of rigidity and  $I_p$  = section polar moment of inertia, Equation (72) becomes

$$\frac{\partial^2 \alpha}{\partial \theta^2} - \xi \left( 1 + \frac{K}{12} \frac{b}{R} \right) \alpha - \frac{1}{f^2} \ddot{\alpha} = 0 \quad (81)$$

where

$$\left. \begin{aligned} \xi &= \frac{EI}{GI_p} \\ \frac{1}{f^2} &= \frac{12}{\xi} \frac{Rb}{a^2 + b^2} \quad f^2 = \frac{G}{\rho R^2} \end{aligned} \right\} \quad (82)$$

Note that Equation (78) involves both  $u$  and  $\alpha$ , while Equation (81) is an uncoupled equation of  $\alpha$ . Therefore, we would first solve Equation (81) for  $\alpha$ . Knowing the solution  $\alpha$ , Equation (78) can be solved for  $u$ . Assume separation of variables,

$$\alpha(\theta, t) = A(\theta) T(t) \quad (83)$$

Substitution of (83) into (81) yields

$$\ddot{T} + \lambda \bar{f}^2 T = 0 \quad (84)$$

and

$$A'' - \left( \frac{K}{12} \frac{b}{R} + 1 \right) \xi A + \lambda A = 0 \quad (85)$$

where  $\lambda$  is a positive constant.

The solution of (85) is

$$\begin{aligned} A(\theta) = & a_1 \exp \left[ i \theta \sqrt{\lambda - \left( \frac{K}{12} \frac{b}{R} + 1 \right) \xi} \right] \\ & + a_2 \exp \left[ -i \theta \sqrt{\lambda - \left( \frac{K}{12} \frac{b}{R} + 1 \right) \xi} \right] \end{aligned} \quad (86)$$

where  $a_1$  and  $a_2$  are orbiting constants.

For a seal ring, the boundary conditions require that the solutions be periodic in  $\theta$ . Hence

$$\lambda - \left( \frac{K}{12} \frac{b}{R} + 1 \right) \xi \quad \text{must be integers, or}$$

$$\lambda - \left( \frac{K}{12} \frac{b}{R} + 1 \right) \xi = n \quad (n=0, 1, 2, \dots) \quad (87)$$

Thus

$$\lambda_n = \left( \frac{K}{12} \frac{b}{R} + 1 \right) \xi + n^2 \quad (n=0, 1, 2, \dots) \quad (88)$$

$\lambda_n$ 's are the eigen values of the system.

The solution of (84) is then of the form

$$T(t) = \sum_n \left\{ b_n \exp [i \nu_n t] + C_n \exp [-i \nu_n t] \right\} \quad (89)$$

where

$$\nu_n = \bar{f} \sqrt{\lambda_n}$$



Obviously,  $\nu_n = \bar{f} \sqrt{\lambda_n}$  represents the natural frequency of torsional vibration. The lowest, torsional, natural frequency is  $\bar{f} \sqrt{\lambda_o}$ .

$$\nu_o = \bar{f} \sqrt{\lambda_o} = \bar{f} \sqrt{\left(\frac{K}{12} \frac{b}{R} + 1\right) \xi} \quad (90)$$

The natural frequencies are generally very large. In a typical application, (see example at the end of this Section), even the lowest natural frequency is much higher than the rotating speed of the seal ring; thus the torsional vibration is not excited. Furthermore, there is no forcing function in the torsional vibration (see Equation (81)). We, therefore, conclude that

$$\alpha \equiv 0 \quad (91)$$

It is to be emphasized that the above result is valid if the rotating speed of the seal ring is much smaller than  $\nu_o$ .

Using (91), Equation (78) becomes

$$\frac{1}{f^2} \ddot{u} + Ku = K \frac{\delta_o}{b} \cos 2(\theta + \omega t) \quad (92)$$

This is the familiar forced vibration equation. Its steady-state oscillation solution corresponding to the forcing function is

$$u = \frac{\left(\frac{\delta_o}{b}\right) \cos 2(\theta + \omega t)}{1 - \frac{4\omega^2}{f^2 K}} \quad (93)$$

The resonance condition occurs when

$$1 - \frac{4\omega_o^2}{f^2 K} = 0$$

or

$$\omega_o = \frac{f}{2} \sqrt{K} = \text{transverse natural frequency} \quad (94)$$

When the rotating speed is approaching to  $\omega_0$ , the amplitude of transverse vibration becomes increasingly large. Hence, we conclude that, in order for a seal ring to avoid excessive vibrations (torsional or transverse) the rotating speed must be designed to differ considerably from both  $v_0$  of Equation (90) and  $\omega_0$  of Equation (94).

### Example

#### Input Data

$$R = 14 \text{ inches}$$

$$a = 3/16 \text{ inches}$$

$$b = 1/2 \text{ inch}$$

$$\text{Steel: } E = 30 \times 10^6 \text{ psi}$$

$$G = 12 \times 10^6 \text{ psi}$$

$$\rho = 0.3 \text{ lb/cu.in.}$$

$$\omega = 800 \text{ rad/sec}$$

$$k = 5000 \text{ lb/in}^2$$

$$g = 386 \text{ in/sec}^2$$

#### Compute

$$I = \frac{1}{12} b a^3 = \frac{1}{12} \frac{1}{2} \left(\frac{3}{16}\right)^3 = 2.75 \times 10^{-4} \text{ in}^4$$

$$I_p = \frac{1}{12} a b (a^2 + b^2) = 2.22 \times 10^{-3} \text{ in}^4$$

$$\xi = \frac{EI}{GI_p} = 0.308$$

$$K = \frac{k R^3 b}{EI} = \frac{5000 \times 14^3 \times 0.5}{30 \times 10^6 \times 2.75 \times 10^{-4}} = 830$$

$$f^2 = \frac{EI}{\rho R^3 ab^2} = \frac{30 \times 10^6 \times 2.75 \times 10^{-4}}{\frac{0.3}{386} \times 14^3 \times \frac{3}{16} (0.5)^2} = 8.28 \times 10^4 \frac{1}{\text{sec}^2}$$

$$\bar{f}^2 = \frac{G}{\rho R^2} = \frac{12 \times 10^6}{\frac{0.3}{386} \times 14^2} = 7.9 \times 10^7 \frac{1}{\text{sec}^2}$$

From Equation (90) we can compute the lowest torsional natural frequency

$$\begin{aligned} \nu_o &= \bar{f} \sqrt{\left( \frac{K}{12} \frac{b}{R} + 1 \right) \xi} = 8.83 \times 10^3 \sqrt{\left( \frac{830}{12} \frac{0.5}{14} + 1 \right) 0.308} \\ &= 9150 \text{ rad/sec} \end{aligned}$$

which is much greater than the rotating speed; thus the torsional vibration is not excited.

From Equation (94) the transverse natural frequency is

$$\omega_o = \frac{f}{2} \sqrt{K} = \frac{\sqrt{8.28 \times 10^4}}{2} \sqrt{830} = 4150$$

Thus,

$$u = \frac{y}{b} = 1.04 \frac{\delta_o}{b} \cos 2(\theta + \omega t)$$

#### NOMENCLATURE FOR SEAL RESPONSE SECTION

|                                 |   |
|---------------------------------|---|
| a, b                            | cross-sectional dimension                               |
| a <sub>1</sub> , a <sub>2</sub> | arbitrary constants in Equation (86)                    |
| A                               | cross-sectional area, ab                                |
| b <sub>n</sub> , C <sub>n</sub> | arbitrary constants in Equation (89)                    |
| e                               | strain  |
| e <sub>a</sub> , e <sub>b</sub> | strains due to $\alpha$ and conventional bending moment |
| E                               | Young's modulus   |

|                    |  |
|--------------------|--|
| $f, \bar{f}$       | Characteristic frequencies defined in Equation (79) and Equation (82) respectively |
| $G$                | modulus of rigidity  |
| $h$                | gas film thickness   |
| $h_m$              | mean gas film thickness  |
| $i$                | $\sqrt{-1}$  |
| $I$                | moment of inertia  |
| $I_p$              | polar moment of inertia  |
| $I_{rr}, I_{tt}$   | mass moments of inertia  |
| $k$                | gas film stiffness per unit circumferential length                                 |
| $K$                | stiffness ratio defined in Equation (79)   |
| $M$                | mass   |
| $M_b$              | bending moment   |
| $M_t$              | twisting moment  |
| $q$                | restoring force per unit circumferential length                                    |
| $q_\alpha$         | restoring moment per unit circumferential length                                   |
| $R$                | mean radius of seal ring   |
| $t$                | time   |
| $u$                | $\frac{y}{b}$  |
| $V$                | shear force  |
| $y$                | transverse displacement  |
| $z$                | coordinate in Figure 67  |
| $\alpha$           | angular (torsional) displacement   |
| $\delta, \delta_o$ | defined in Equation (68)   |
| $\theta$           | circumferential coordinate   |
| $\lambda$          | constant   |

|              |                                    |
|--------------|------------------------------------|
| $\lambda_n$  | eigen values of Equation (85)      |
| $\nu_n$      | torsional natural frequency        |
| $\nu_0$      | lowest torsional natural frequency |
| $\xi$        | $\frac{EI}{GI_p}$                  |
| $\rho$       | density                            |
| $\bar{\rho}$ | radius of curvature                |
| $\omega$     | rotating speed                     |
| $\omega_0$   | transverse natural frequency       |

### Seal Design

The work on compressor end and interstage seal design, beyond the work on the primary seal performance, has been limited. Further consideration of Concept V has led to the conclusion that it is very difficult or impractical to design. Review of primary seal performance has not yet led to a clear selection of either type for the floated shoe designs.

### Review of Concept V

One of the proposed concepts for the feasibility study is the thin strip radial seal with a C-diaphragm as the secondary seal as shown in Figure 68.

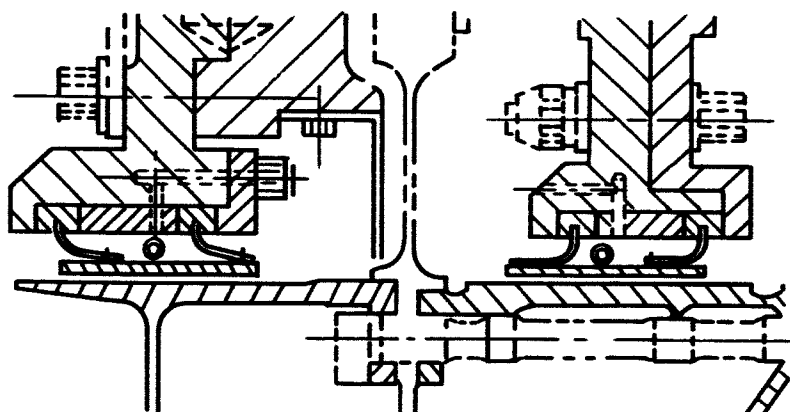


Figure 68 Thin Strip Radial Seal

Upon further examination, several serious drawbacks have been discovered in this concept. First, the C-diaphragm must be flexible enough to allow a radial displacement of 0.032 inches between the seal and the housing for transient thermal growth. A continuous construc-

tion of the diaphragm like a semi-toroid is out of the question because of its inflexibility. Consequently, the diaphragm not only has to be made in sections, but also may have to be slotted in each section to reduce the flexure stresses. Secondary sealing problems between sections of diaphragm become quite difficult. The leakage through secondary sealing surfaces is very difficult to control. Second, sectionalized diaphragms have practically no load carrying capacity in the axial direction.

It is unlikely that an effective means can be added to maintain the force balance in the axial direction.

In view of these shortcomings, the thin strip C-diaphragm radial seal has been abandoned from any further considerations.

### Primary Seal for Hydrostatic Floated Shoe Designs

A critical item for the floated shoe designs is their ability to respond to runner deviations from true without excessive reduction in film thickness. This is due to their relatively massive cross-section, and is of particular concern for the two-side floated shoe which is a radial seal and must accommodate radial motions at once per rev. of  $\pm 0.008$  inches. It is anticipated that a hollow section may be necessary.

Since response is a function of primary seal stiffness, high stiffness is desired and a comparison must be made between the hydrostatic step seal and the orifice compensated hydrostatic seal. Such a comparison is made in Figure 69 for a pressure ratio of  $R = 0.2$  and for a step width ratio of  $\bar{b}_1 = 0.35$  for the hydrostatic step, and  $\bar{b}_1 = 0.25$  for the orifice compensated design.

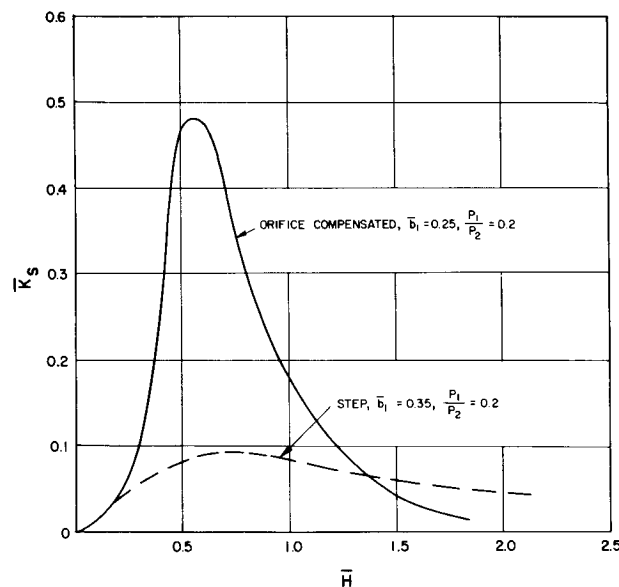


Figure 69 Comparison of Stiffness for Orifice and Step Hydrostatic Seals

Figure 70 shows an evaluation of the efficiency of each type of seal, in terms of the ratio of stiffness to mass flow, as a function of  $\bar{b}_1$ , the step width ratio. The optimum ratio for the hydrostatic step is at about  $\bar{b}_1 = 0.3$ . No optimum is indicated for the orifice compensated design, but its maximum stiffness is several times that of the hydrostatic step. The mass flows are nearly equal at equivalent  $\bar{b}_1$ .

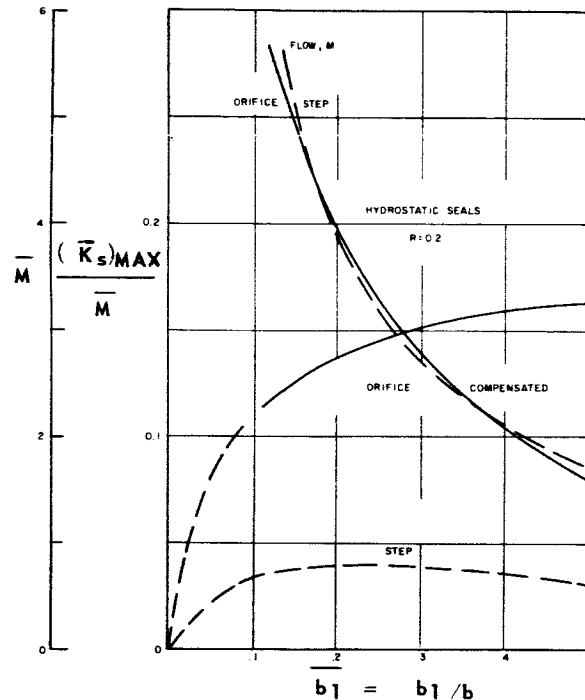


Figure 70 Stiffness Flow Criterion vs Width Ratio

Referring again to Figure 69, the stiffnesses of the two designs may be compared as a function of film thickness. The orifice compensated design is much stiffer at the design point (maximum), but falls off more steeply than the hydrostatic step design so that below 40 percent of the design film thickness, or above 225 percent, the hydrostatic step is stiffer.

The need for supplementary hydrodynamic action at small film thickness is apparent from this brief examination. As soon as corresponding data is available on the Rayleigh step design, a final selection can be made. Sensitivity of the spiral groove pattern to non-parallel surfaces makes it appear less desirable for supplementary support.

## PRATT &amp; WHITNEY AIRCRAFT PROGRAM

Approval of Screening Study Seal Concepts

Four compressor end seal and four stator interstage seal screening study concepts were presented to NASA on October 7, 1965. NASA approval was indicated in a letter dated October 11, 1965. This approval allowed the program to continue into the detailed feasibility analysis, which is expected to require approximately four and one-half months to complete. The approved seal concepts listed below are shown in actual size and in exploded views with accompanying descriptions in Figures 71 through 78.

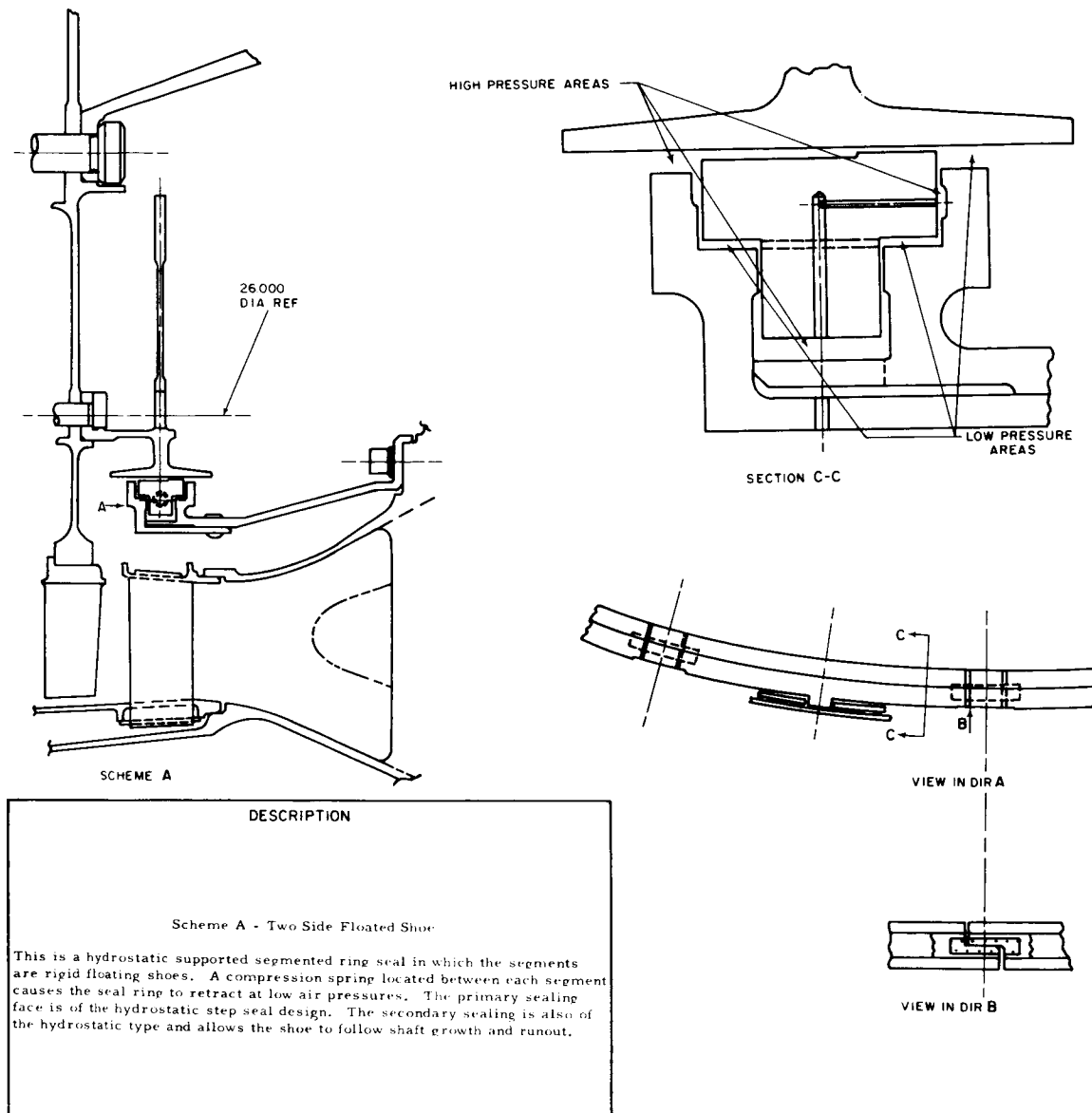
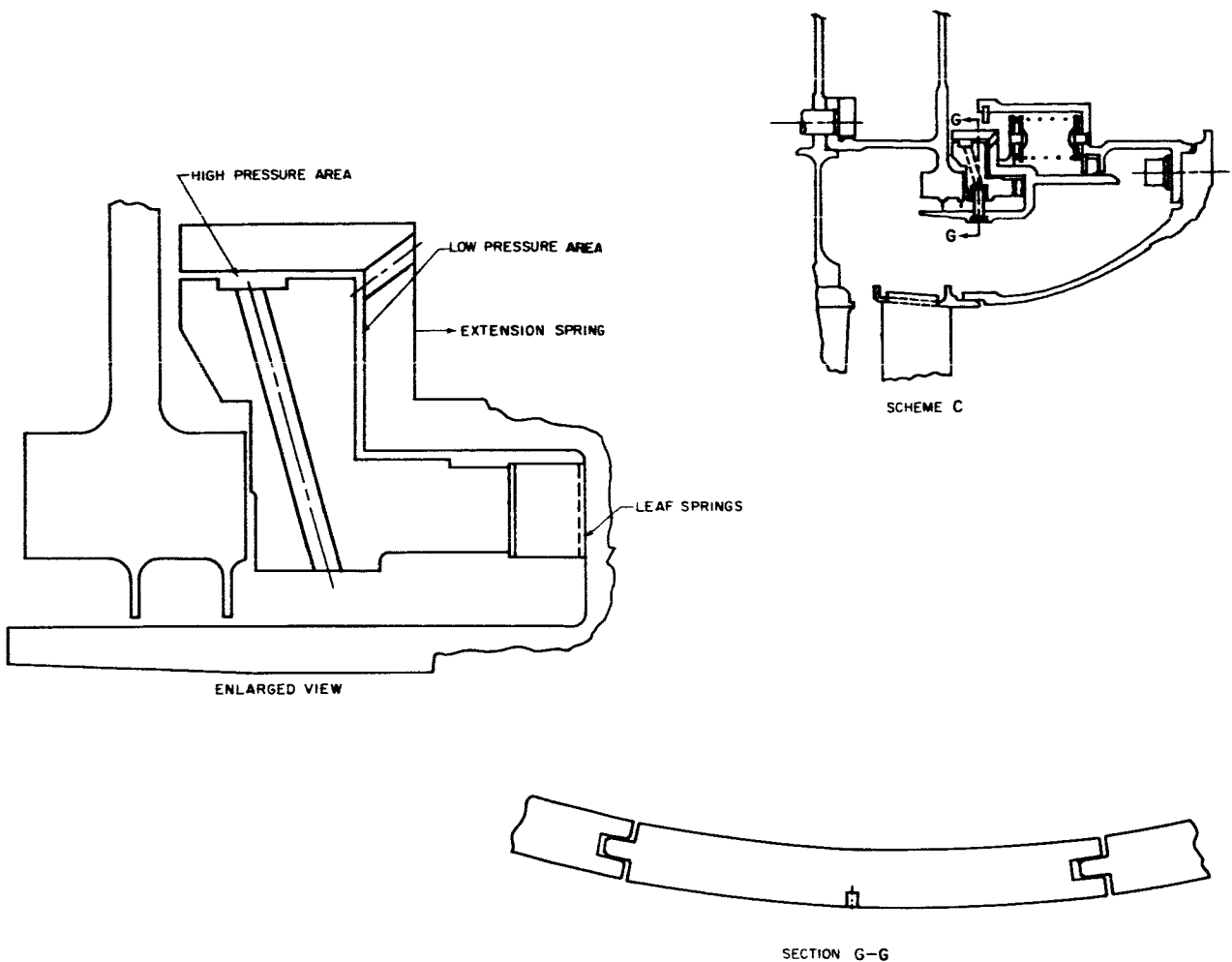


Figure 71 Compressor End Seal Concept Scheme A - Ref PWA Drawing No. L-67714 Ref MTI Sketch-D-2116



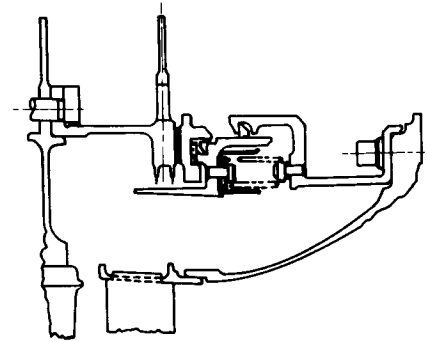
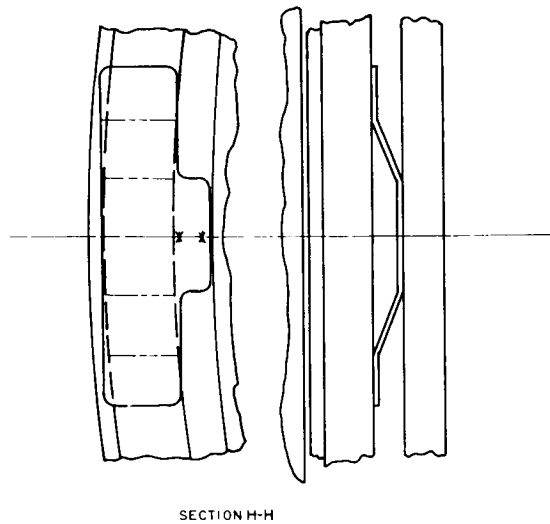


## DESCRIPTION

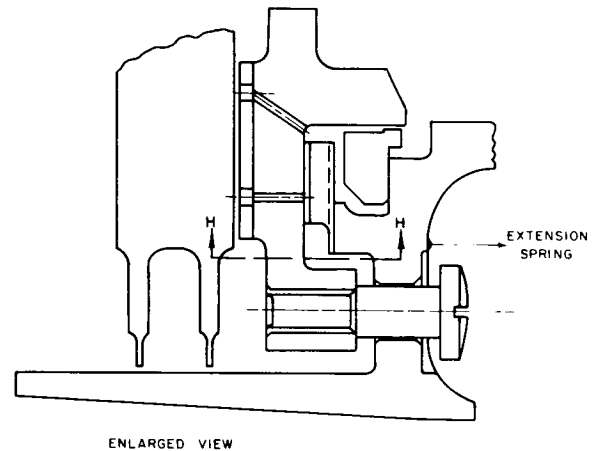
## Scheme C - One Side Floated Shoe

This seal is a hydrostatic supported segmented face seal in which the segments are rigid floating shoes. The floating shoes are retained in the seal carrier by an anti-rotation pin which also maintains a light compressive load on the leaf springs. The light duty leaf springs and hydrostatic secondary sealing between the shoe and carrier allows the shoe to follow low magnitude high frequency motion. The seal carrier which has a piston ring for the secondary seal will follow the full 0.4 inches of axial motion required. The extension spring ties the seal carrier to the fixed housing and causes the seal carrier to retract at low air pressures. When the primary seal is open a labyrinth seal produces the required pressure differential to close the seal at the desired engine operating condition.

Figure 72 Compressor End Seal Concept Scheme C - Ref PWA Drawing No. L-67714 Ref MTI Sketch-D-2134



SCHEME D

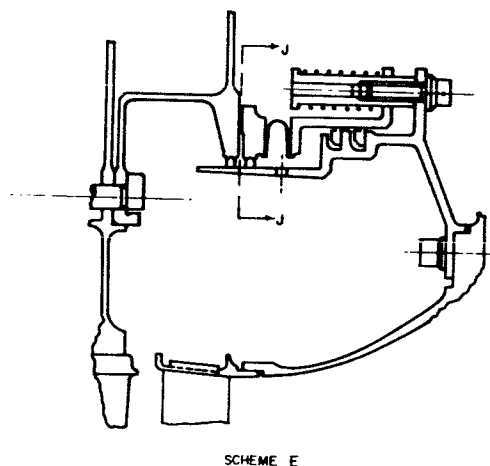
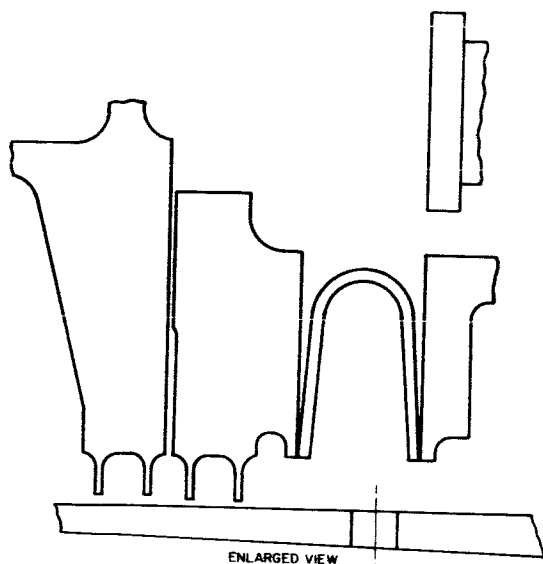


ENLARGED VIEW

**DESCRIPTION****Scheme D - Thin Strip - One Piece**

The primary seal in this design is an orifice compensated hydrostatic supported one piece continuous thin strip face seal. A leaf spring is attached to the seal carrier and exerts a compressive force on the thin strip which is attached to the seal carrier by guide pins. Secondary sealing between the thin strip and the carrier consists of a fully floated piston ring which permits the thin strip to follow any runout or wobble of the face. A coating is shown which provides a better rubbing surface in case the thin strip contacts the face. The balance of the construction is similar to the one ride floating shoe.

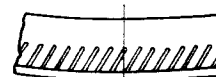
Figure 73 Compressor End Seal Concept Scheme D - Ref PWA Drawing No. L-67714 Ref MTI Sketch-D-2132



## DESCRIPTION

## Scheme E - Thin Strip - C Diaphragm

This seal is similar to the one piece thin strip seal, the method of secondary sealing being the primary change. This design utilizes a C diaphragm as the secondary seal between the thin strip and seal carrier in place of the piston ring and leaf springs. The design has been changed to incorporate compression springs in place of the extension springs used in two other face seal designs, but the operation of the seal is similar.



SECTION J-J

Figure 74 Compressor End Seal Concept Scheme E - Ref PWA Drawing No. L-67714 Ref MTI Sketch-D-2118

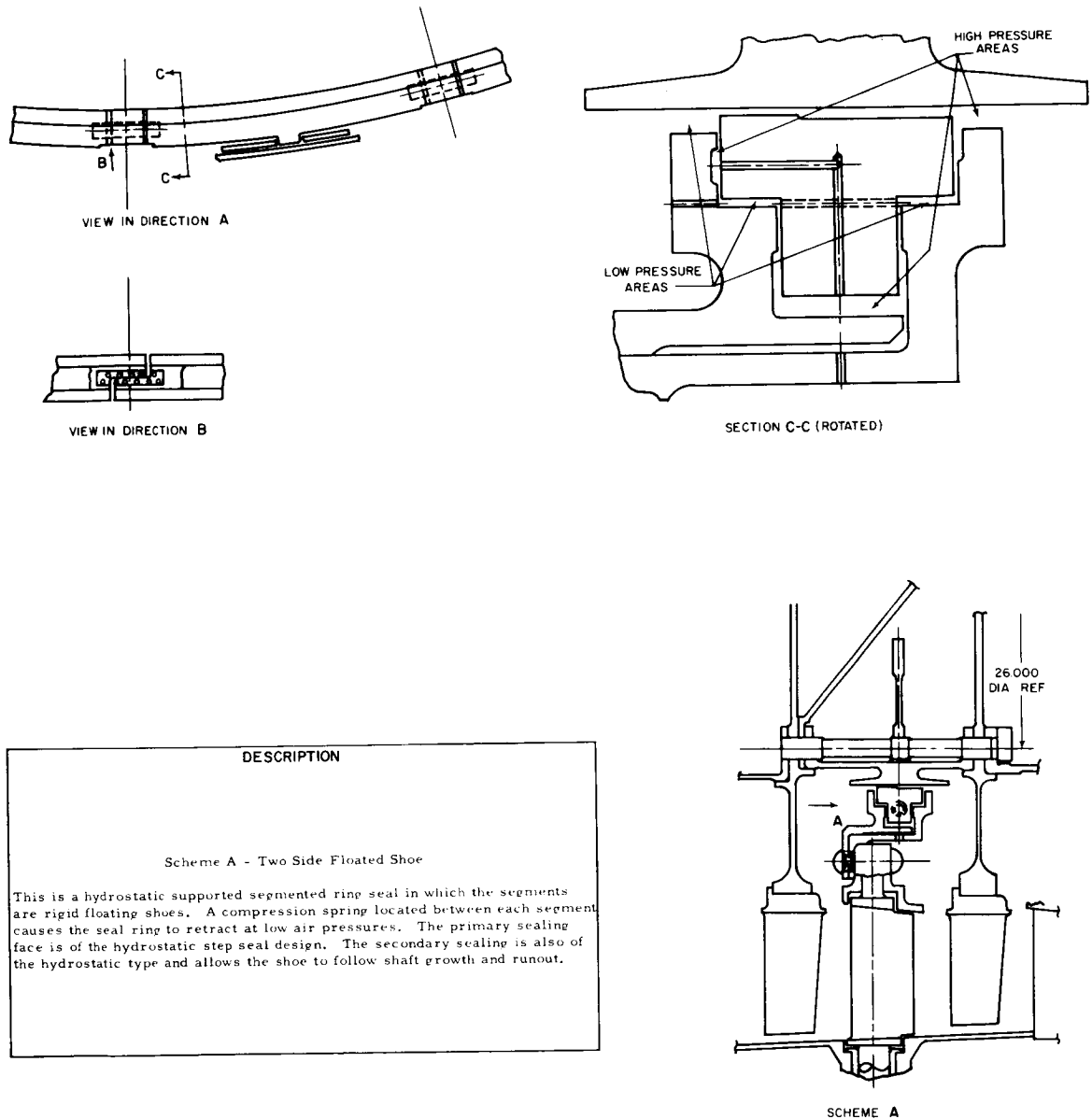
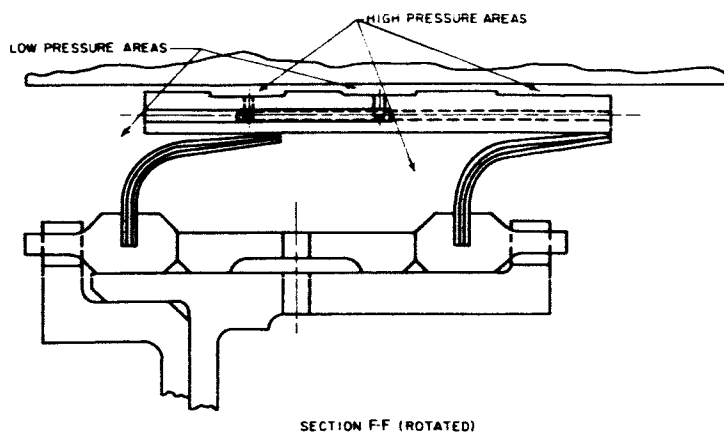
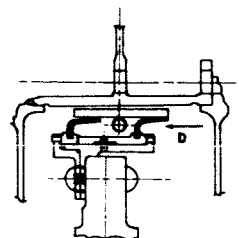


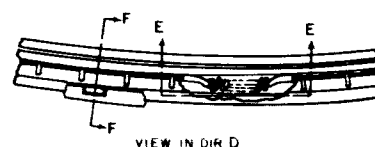
Figure 75 Stator Interstage Seal Concept Scheme A - Ref PWA Drawing No. L-67713 Ref MTI Sketch-D-2116



SECTION F-F (ROTATED)



SCHEME B

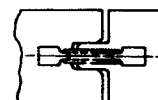


VIEW IN DIR D

# DESCRIPTION

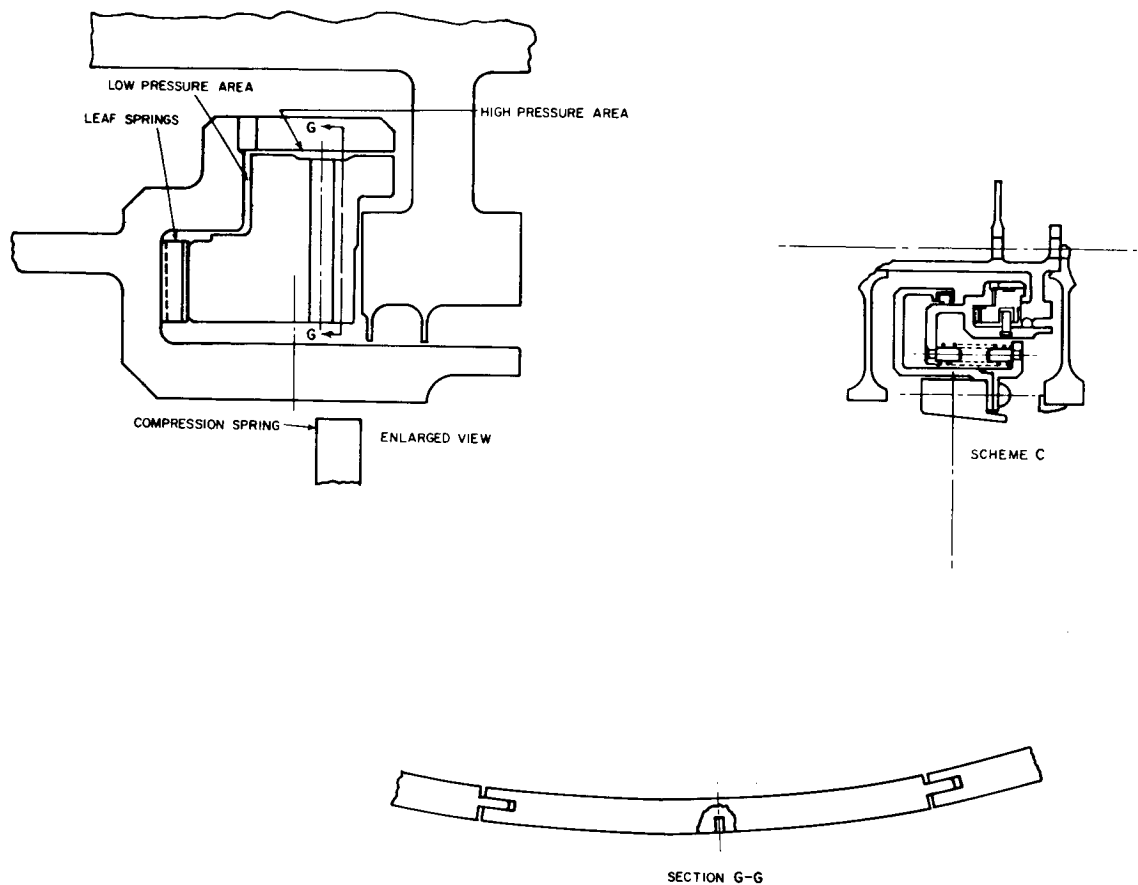
## Scheme B - Thin Strip Radial Seal

This design is a hydrostatic supported segmented ring seal in which the segments are thin flexible strips. Compression springs are located between the segments to make the seal retract at low air pressures. The secondary sealing is effected by using two rows of overlapping finger springs which also tie the segments to the fixed support.



SECT E-E

Figure 76 Stator Interstage Seal Concept Scheme B - Ref PWA Drawing No. L-67713 Ref MTI Sketch-D-2119

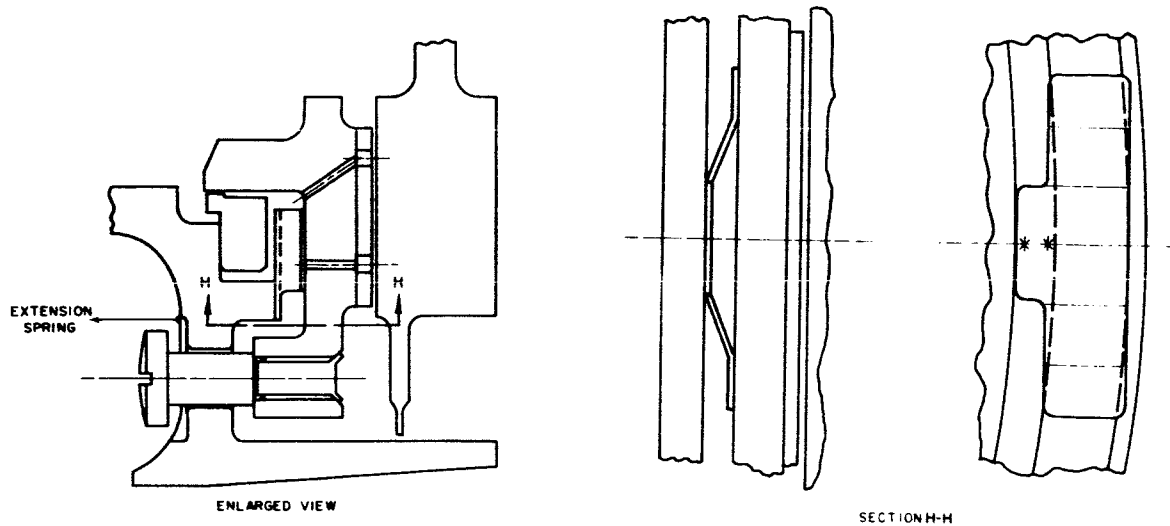


## DESCRIPTION

## Scheme C - One Side Floated Shoe

This seal is a hydrostatic supported segmented face seal in which the segments are rigid floating shoes. The floating shoes are retained in the seal carrier by an anti-rotation pin which also maintains a light extension load on the leaf springs. The light duty leaf springs and hydrostatic secondary sealing between the shoe and carrier allows the shoe to follow low magnitude high frequency motion. The seal carrier which has a piston ring for the secondary seal will follow the full 0.4 inches of axial motion required. The extension spring ties the seal carrier to the fixed housing and causes the seal carrier to retract at low air pressures. When the primary seal is open a labyrinth seal produces the required pressure differential to close the seal at the desired engine operating conditions.

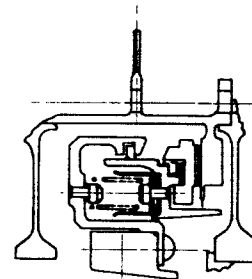
Figure 77 Stator Interstage Seal Concept Scheme C - Ref PWA Drawing No. L-67713 Ref MTI Sketch-D-2134



## DESCRIPTION

## Scheme D - Thin Strip - One Piece

The primary seal in this design is an orifice compensated hydrostatic supported one piece continuous thin strip face seal. A leaf spring is attached to the seal carrier and exerts a compressive force on the thin strip which is attached to the seal carrier by guide pins. Secondary sealing between the thin strip and the carrier consists of a fully floated piston ring which permits the thin strip to follow any runout or wobble of the face. A coating is shown which provides a better rubbing surface in case the thin strip contacts the face. The balance of the construction is similar to the one side floating shoe.



SCHEME D

Figure 78 Stator Interstage Seal Concept Scheme D - Ref PWA Drawing No. L-67713 Ref MTI Sketch-D-2132

Compressor End Seals - PWA Dwg. No. L-67714 Rev A<sub>4</sub>

| <u>Type of Seal</u>      | <u>Scheme</u> | <u>Ref. MTI<br/>Dwg. No.</u> | <u>Figure<br/>No.</u> | <u>Geom.<br/>Radial</u> | <u>Shape<br/>Face</u> |
|--------------------------|---------------|------------------------------|-----------------------|-------------------------|-----------------------|
| Two side floated shoe    | A             | SK-D-2116                    | 71                    | X                       |                       |
| One side floated shoe    | C             | SK-D-2134                    | 72                    |                         | X                     |
| Thin strip - 1 piece     | D             | SK-D-2132                    | 73                    |                         | X                     |
| Thin strip - C diaphragm | E             | SK-D-2118                    | 74                    |                         | X                     |

Stator Interstage Seals - PWA Dwg. No. L-67713 Rev A<sub>2</sub>

| <u>Type of Seal</u>   | <u>Scheme</u> | <u>Ref. MTI<br/>Dwg. No.</u> | <u>Figure<br/>No.</u> | <u>Geom.<br/>Radial</u> | <u>Shape<br/>Face</u> |
|-----------------------|---------------|------------------------------|-----------------------|-------------------------|-----------------------|
| Two side floated shoe | A             | SK-D-2116                    | 75                    | X                       |                       |
| Thin strip            | B             | SK-D-2119                    | 76                    | X                       |                       |
| One side floated shoe | C             | SK-D-2134                    | 77                    |                         | X                     |
| Thin strip - 1 piece  | D             | SK-D-2132                    | 78                    |                         | X                     |

Compressor end seal scheme B (SK-D-2119) is not included in this listing; it was replaced by scheme E (SK-D-2118), as indicated in the NASA letter of approval.

Dimensional Variance Considerations

The effects of the following dimensional variances on the compressor seal hydrostatic-hydrodynamic film thickness were considered.

1. Elastic

- a.) Centrifugal growth of rotating elements.
- b.) Changes in slope of surfaces of rotating elements due to combination of gas and centrifugal loads and variation in centrifugal effect in adjacent rotor stages.
- c.) Change in slope of seal supporting surfaces due to gas loads.
- d.) Vibration of rotor and seal supporting members.
- e.) Effect of gyroscopic loads.

2. Tolerance

- a.) Rotor runouts.
- b.) Squareness of seal supporting surfaces.



- c.) Flatness and surface finish of seal mating surfaces.
- d.) Tolerance build up.

3. Thermal

- a.) Distortion of seal mating surfaces due to thermal gradients.
- b.) Thermal growths.
- c.) Differential expansion.
- d.) Transient thermal effects.

It is Pratt & Whitney Aircraft's opinion that various elastic and thermal dimensional variances may prove to be a major obstacle to overcome in developing successful advanced compressor seals. The distortion of seal mating surfaces due to thermal gradients is a particular concern.

To maintain an effective hydrostatic or hydrodynamic air film between a seal and seal plate, it is necessary that the seal - seal plate interface surfaces remain essentially parallel. With a compressor seal operating at 850 ft/sec in 1200°F air, it has been estimated that several horsepower are developed in shearing the thin air film existing at the seal - seal plate interface. Localized heating of the interface surfaces provides a temperature gradient across the seal and seal plate causing them to curve ("heel") away from each other.

A possible solution to this problem being investigated by Pratt & Whitney Aircraft is the use of pyrolytic graphite having the anisotropic property of high thermal conductivity along one axis and low thermal conductivity along another axis. Rapid dissipation of heat away from the seal - seal plate interface should reduce the temperature gradient and minimize the "heeling" condition. It is recognized that pyrolytic graphite acting on itself as a seal - seal plate configuration may present excessive wear problem.

Analytical Program

Pratt & Whitney Aircraft has been monitoring the MTI analytical effort as specified in the prime contract.

## TASK II - COMPRESSOR END SEAL AND STATOR INTERSTAGE SEAL EXPERIMENTAL EVALUATION

This phase of the program provides for final design and procurement of compressor end seals and stator interstage seals, design and fabrication of a test rig, and experimental evaluation of the compressor seals.

A test rig will be designed and fabricated to evaluate the selected compressor end seals and stator interstage seals under simulated compressor operating conditions. The test apparatus will simulate the last stages of a full scale compressor including supporting members and bearing system in order to faithfully duplicate structural flexibility and thermal gradients.

The final design of the four compressor seal concepts selected for experimental evaluation includes all calculations, material determinations, analyses, and drawings necessary for seal optimization, procurement and experimental evaluation.

The compressor end seals and stator interstage seals will be calibrated in incremental steps at room temperature static conditions, room temperature dynamic conditions, and subsequently over the full ranges of temperature, speed, and pressure differential. Finally, the seals will be subjected to endurance testing and cyclic testing at simulated take-off and cruise conditions.

### PROGRESS

Design work was initiated in December on a full scale test rig.

### TASK III - COMPRESSOR STATOR PIVOT BUSHING AND SEAL CONCEPT FEASIBILITY ANALYSIS.

A feasibility analysis program is being conducted on stator vane pivot bushing and seal concepts for application in compressors for advanced air breathing propulsion systems. The first phase of this program is a preliminary analysis and a screening of various seal concepts prior to the selection of concepts for detailed feasibility analysis. The analytical effort includes a comparison of the selected concepts to current practice and all calculation, analyses, and drawings necessary to establish feasibility of these selected concepts. This analytical program is sub-contracted to Mechanical Technology Inc. (MTI) of Latham, New York and is being monitored by Pratt & Whitney Aircraft as required under the terms of the NASA contract.

#### MTI SCREENING OF VANE PIVOT SEAL DESIGNS

The screening study of stator pivot seal concepts conducted by MTI is presented in this section of the report. The material in this section was prepared by Dr. H.S. Cheng, J. Bjerklie, and Dr. D.F. Wilcock.

The high pressure stators of compressors for advanced engines will very likely incorporate variable vane stagger. The number of stages requiring them is as yet unknown but the total will probably exceed 500. Each variable vane utilizes a pivot which penetrates the compressor wall and even a little leakage out of each could represent a sizable efficiency loss.

This section discusses the design and screening of a number of vane pivot concepts. Some of these were in the original proposal, others have been conceived since then.

All potential seal designs are compared against a seal that was built and tested by Pratt & Whitney Aircraft (see Figure 79). That design was originated as a first modification of an existing design being used in practice. A test rig was built by Pratt & Whitney Aircraft consisting of this vane and its pivot in an airtight box. The only leakage possible was out of the seal, so leakage measurements could be made. Only one measurement was available during the term of the screening period, but it served to indicate the extent of the problem. Thus, the candidate seals could be rated as probably better or probably worse than the existing seal.

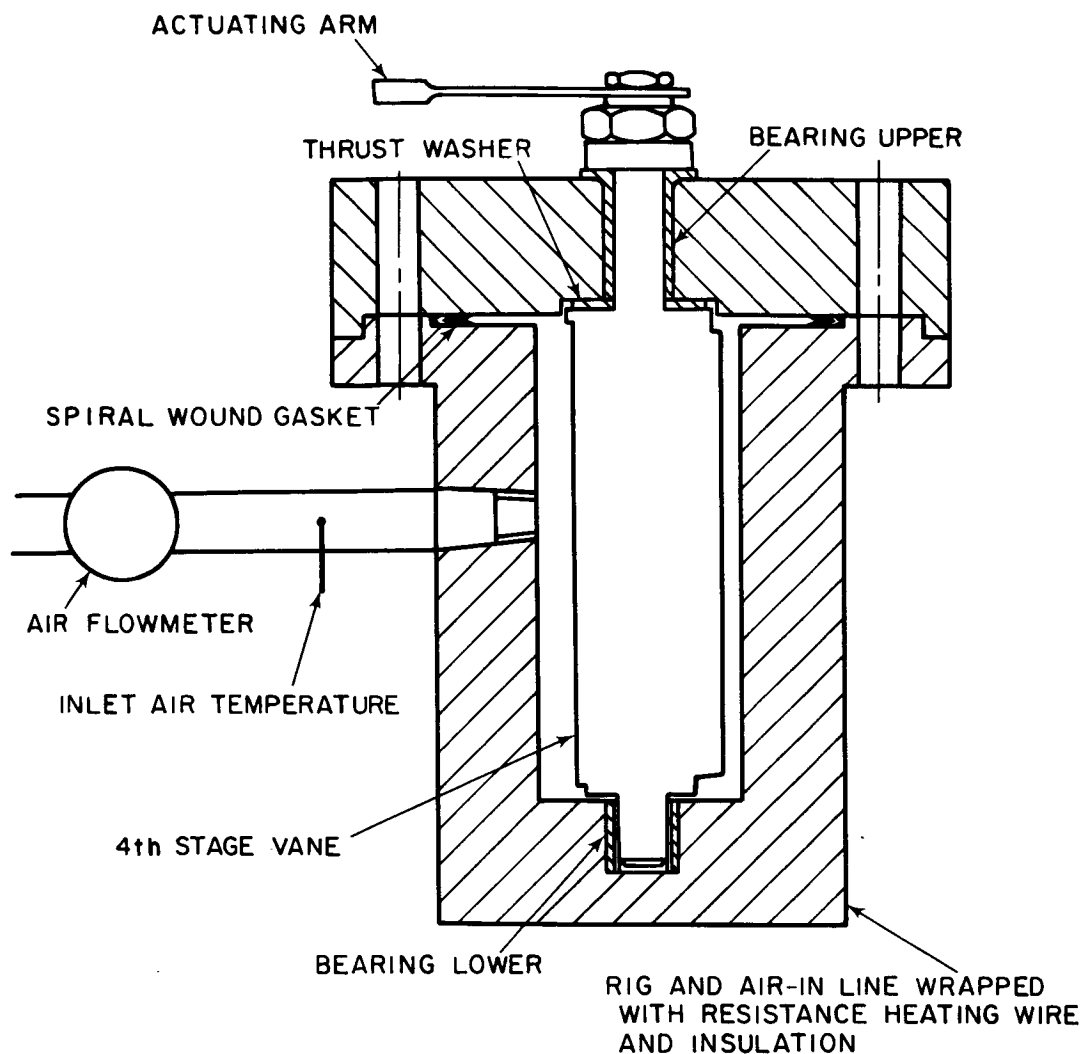


Figure 79 Vane Pivot Seal Test Rig

The seals considered in this study, sketched in Figure 80 are:

- Belleville washer
- Coned-carbon rings with gaps
- Fractured carbon rings
- Metal spring
- Seal packing
- Lamiflex

all from the proposal, plus:

Internal actuation

External covers

Bellows loaded face seals

Spring loaded spherical seat seal

Close clearance bushing

Variations of each basic type were examined when there appeared to be an advantage for a slightly changed design. First screening, however, was done on basic types only.

Considerations for the screening were of three primary types:

- (1) leakage rate
- (2) functional
- (3) logistics

Since the basic goal of the program was to reduce leakage, any candidate that could not lead to low leakage was discarded. Tolerance to dirt and load deflections plus inherent reliability were the two main parts of the functional considerations. If a candidate seal was considered poor in this respect, it was discarded. Finally, weight, space, actuation power, design simplicity, assembly, and servicing should show as much gain as possible for a candidate to be an advantageous type.

In all cases, comparison was made to the design used in the Pratt & Whitney Aircraft leakage tests. Those new seals showing the most potential gain over that design were considered the most promising candidates.

Eleven vane-pivot seal designs were compared on the basis of: (1) leakage rate, (2) functional capability, and (3) logistics or servicing capability.

From this screening analysis, two designs have been selected for the Feasibility Analysis Phase.

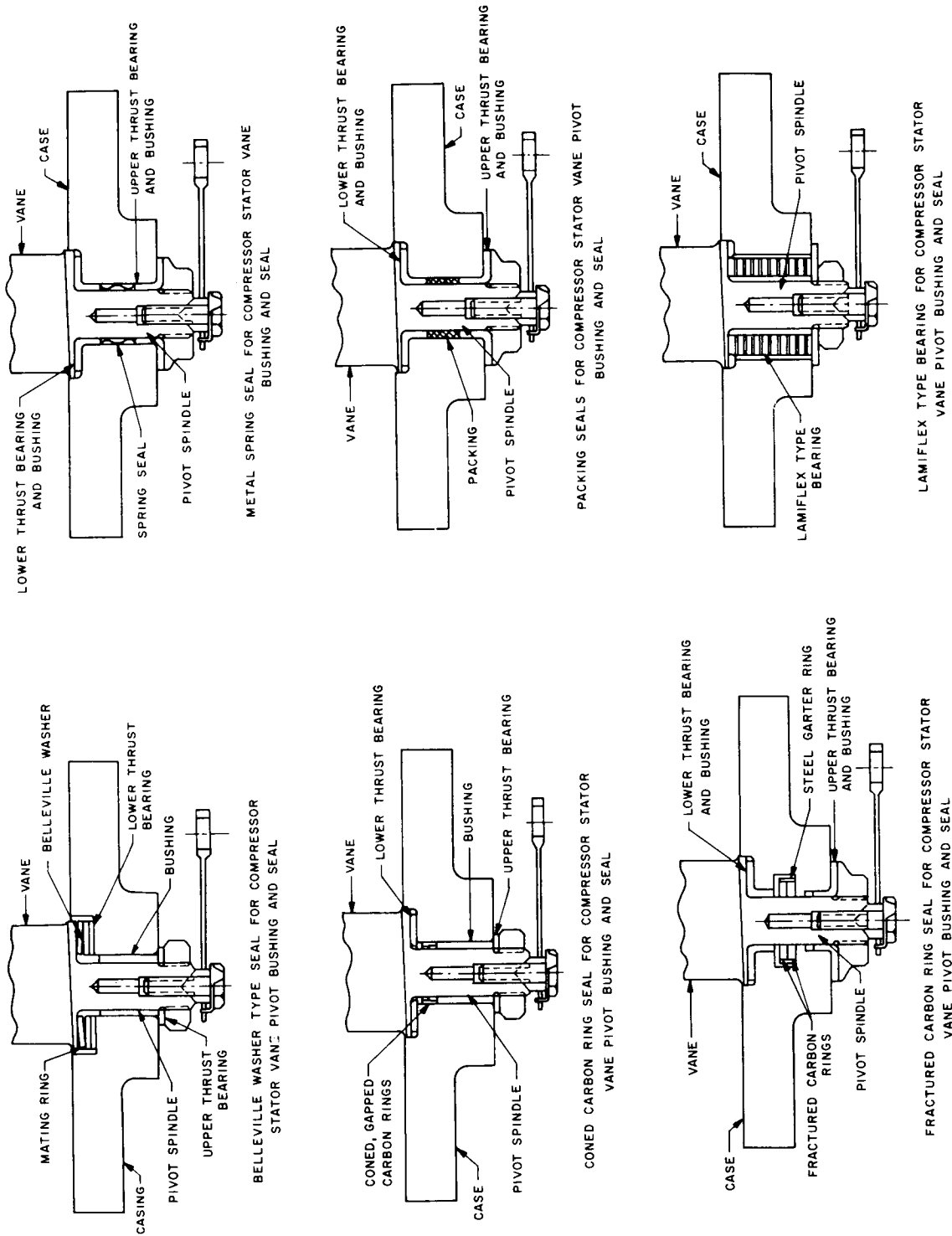


Figure 80 Vane Pivot Seal Concepts

### Concept I. Spherical Seat Face Seal

Primary sealing is accomplished by a spring loaded spherical seat face seal. The spherical face also acts as a thrust bearing to absorb the seating force of the Skinner type spring plus the thrust load created by the air pressure acting on the vane.

### Concept II. Single Bellows Face Seal

Primary sealing is expected by a bellows-supported face seal rubbing against the end of a bushing which is installed in the outer shroud with an interference fit. The thrust loads created by air pressure and spring forces are carried by a thrust bearing located at the tip of the vane.

### Screening

#### Leakage Improvement

Two candidate designs were discarded because it could not be shown that their leakage would be as little as the baseline design (the Pratt & Whitney Aircraft test pivot seal). The Belleville washer will have two leakage paths past the washer. Each path will be short, and the effective clearance will not be any less than the baseline design. The coned carbon ring seal with gaps has more leakage at a single gap than does the baseline design.

Pratt & Whitney Aircraft leakage measurement of a single vane during static, unloaded vane conditions was less than 0.004 SCFM at 94 psi and 400° F. The loading on the thrust washer, including initial torquing plus pressure load, is about 95 lbs. The leakage rate was used to calculate the effective gap width of each of two leakage paths, resulting in a calculated gap of 0.000088 inches.

To compare the above measurements and design with the Belleville washer, the load on the Belleville washer cannot be any greater than for the baseline design, otherwise the actuating power will be greater. Also, since

$$T_{\text{actuating}} = L \times F = L \times fN$$

Neither  $L$  nor  $f$  will be significantly different between designs, thus  $N$  (normal force) for the Belleville washer seal has to be equal to or less than that of the baseline seal to have equal or less actuating power.

With this loading, the effective gap between the washer and seal will be approximately the same as the scale of roughness. Assuming a good finish and a gap length equal to approximately 1/10 of the washer thickness, the calculated leakage for a non-loaded vane through the two paths is about 0.05 SCFM (63 micro inch finish), more than for the baseline system.

The gaps in the coned carbon rings can be as much as .010 inches. The leakage through such a gap can be as high as 0.1 SCFM at the same conditions as the baseline test. This is too great to allow its further consideration.

Functional Considerations - The baseline design has the possibility of getting dirt in the seal, encouraging cocking of the vane. Also, since the vane can be cocked, the leakage rate can become quite high under loaded vane conditions. Both of these possibilities pose problems for the baseline seal.

The close clearance bushing exhibits the same problems. In this case, however, the presence of particles between the bushing and vane pivot can contribute to severe wear because of the close clearance, and also can seriously increase the actuation power. Hence, this design was also rated as poorer than the baseline seal.

Reliability, as used in this report, relates to the opinion of the design engineers as to the possibility of failure of the seal during actuation of the vane. The fractured carbon ring, by its very nature, consists of relatively fragile parts. This is considered sufficient to rate it poorer than the baseline design.

The metal spring seal depends on close fit between the pivot and the spring for sealing. This essentially means that it will rub. Rubbing can lead to wear and eventual penetration of the spring material, especially since dirt can also deposit in the seal. Thus it was rated lower than the baseline seal in evaluating reliability.

The Lamiflex seal depends for its operation upon an elastomeric material bonding together a number of metallic washers. The stack of washers plus elastomer extends for most of the length of the pivot. However, the inner portion of the seal can be subjected to temperatures approaching 1200°F since this is the compressor exit temperature. Thus, at least a portion of some of the pivot seals will be exposed to temperatures which are considerably above the usable temperature of any available elastomer. Consequently, some of the pivots, if using the Lamiflex seal type, will not be reliable.

Internal actuation can potentially reduce leakage simply by reducing the number of compressor wall penetrations. However, internal actuation will necessitate the use of linkages exposed to hot oxidizing gases. Also, the actuating torque would have to be transmitted to the inner linkage through a limited number of vanes, potentially causing excessive stresses and deflections.

Multiple labyrinths can conceivably make a good seal. However, the number of segments of the seal must be large in number. The segments of the labyrinth must, then, be made of thin sheet (only a few thousandths of an inch thick). The probability of such labyrinths remaining non-rubbing is small when the vane is cocked while loaded. If



the segments rub, wear will occur, bending may occur, and generally unknown effects can take place. Consequently, the seal cannot be considered reliable for long life. The labyrinth seal was therefore rated a little lower than the baseline seal for reliability.

Logistic Considerations - The seal types which remain as candidates after eliminating the seals mentioned in Leakage and Functional considerations are:

- (1) packed seal
- (2) external covers
- (3) bellows or spring loaded face seals

However, these seals must be evaluated with respect to weight, space, actuation power, design simplicity, assembly, and servicing. These are factors which affect the installation and overall system, but which are not determinant as to the "workability" of the concept. The seal is acceptable to the degree that weight, space, and actuating power are kept down, and design simplicity, assembly, and servicing are kept uncomplicated. For want of a better single term, these are lumped under the word "logistics".

Weight of all the remaining concepts will be about the same except for the external cover type seal. This seal requires a separate "pressure skin" outside of the actuators and pivots. However, it is probably the most straightforward way of keeping leakage low, and despite the fact that it rates poorly on weight, space, and servicing, it may eventually be the least costly method.

Space requirements of all systems remaining under consideration are all about the same.

Only the packed seal will potentially exhibit higher actuating power than the baseline seal. Calculations indicate the possibility of low friction after "wear in", but past experience belies these results. Since design for packed seal actuating power depends upon an empirical design approach, past practice must be relied upon. Thus, it must be conceded that actuation power for packed seals may be too high to be acceptable.

The packed seal will also exhibit a difficult assembly and servicing requirement. The baseline seal is torqued down upon assembly so that unloaded actuating torque is 1.5 in-lbs. The packed seal must likewise be preloaded by torquing the seal upon assembly. However, the sealing ability of the packed seal depends upon the packing pressure against the vane shaft. The compressor pressure load does not markedly assist the sealing as it does for the tested seal. Thus the packed seal adjustment is slightly more sensitive to initial adjustment.

The packed seal must be "worn in" without loss of sealing ability. This, too, would complicate the assembly and servicing, however, since wearing in would have to occur before final installation.

External covers over the baseline seal would require additional time and effort in cover removal and replacement at each servicing. Since it is meant to be a reasonably tightly sealed unit itself, this does constitute assembly and servicing complexity.

Bellows loaded face seals do not have to be preloaded by torque adjustment; they can be assembled as a cartridge. Thus, they represent a gain in assembly and servicing ease.

The spring loaded, spherical seat face seal likewise need not be adjusted upon installation. However, its assembly is more sophisticated because one part of the seal has to be firmly assembled to the vane shaft. These two effects tend to counterbalance each other so far as assembly and servicing is concerned. Consequently, this seal was rated equal to the baseline seal.

### Screening Chart

The results of the foregoing considerations are displayed on the screening chart, Table XII. All seals are rated with respect to the baseline seal:

0 is the same rating

+ is a higher rating

- is a lower rating

TABLE XII

### COMPARISON OF VANE PIVOT SEAL CONCEPTS

| Seal Type                       | Leakage Control | Leakage Rating | Functional Considerations              |             | Functional Rating | Logistic Considerations |       |                 |  | Logistic Rating | Overall Rating |
|---------------------------------|-----------------|----------------|--|-------------|-------------------|-------------------------|-------|-----------------|--|-----------------|----------------|
|                                 |                 |                | Tolerance to Dirt and Load Deflections | Reliability |                   | Weight                  | Space | Actuation Power | Design Simplicity, Assembly, Servicing |                 |                |
| Baseline design                 | 0               | 0              | 0                                      | 0           | 0                 | 0                       | 0     | 0               | 0                                      | 0               | 0              |
| Belleville Washer               | -1/2            | *              |  |             |                   |                         |       |                 |  |                 |                |
| Coned carbon rings with gaps    | -1              | *              |  |             |                   |                         |       |                 |  |                 |                |
| Fractured carbon ring           | +1              |                | -1                                     | -1          | *                 |                         |       |                 |  |                 |                |
| Metal spring seal               | +1              |                | 0                                      | -1          | *                 |                         |       |                 |  |                 |                |
| Seal packing                    | +1              |                | +1                                     | +1          | +2                | 0                       | 0     | -1              | -1/2                                   | -1 1/2          | +1 1/2         |
| Close clearance bushing         | +1              |                | -1                                     | 0           | *                 |                         |       |                 |  |                 |                |
| Lamiflex                        | +2              |                | +1                                     | -1          | *                 |                         |       |                 |  |                 |                |
| Internal actuation              | +1              |                | +1                                     | -1          | *                 |                         |       |                 |  |                 |                |
| External covers                 | +1              |                | +1                                     | 0           | +1                | -1                      | 0     | 0               | -1                                     | -2              | 0              |
| Bellows or spring and face seal |                 |                |  |             |                   |                         |       |                 |  |                 |                |
| 1) single bellows               | +1              |                | +1                                     | 0           | +1                | 0                       | 0     | 0               | +1/2                                   | +1/2            | +2 1/2         |
| 2) 2 bellows                    |                 |                | +1                                     | +1          | +2                | 0                       | 0     | 0               | +1/2                                   | +1/2            | +3 1/2         |
| 3) Spherical seat               | +1              |                | +1                                     | +1          | +2                | 0                       | 0     | 0               | 0                                      | 0               | +3             |
| Multiple labyrinth              | +1/2            |                | +1/2                                   | -1/2        | *                 |                         |       |                 |  |                 |                |

\*Excluded from further consideration because of negative ratings

Most rating numbers are  $\pm 1$  since only a trend is meant to be indicated. Where an effect is known to be strong the rating can be  $\pm 2$ . Where an effect is suspected to be quite weak the rating is indicated as  $\pm 1/2$ .

As already implied, some seals were dropped from consideration as a result of specific negative rating. Any seal having a zero or negative leakage rating was not considered further - independent of how good it may be with respect to other considerations. Also, any seal having a negative rating for either of the functional considerations was dropped - independent of how good the seal might be from other considerations.

Logistic ratings could be either positive or negative and remain in contention since these considerations were not meant to be "go" - "no-go" ratings.

As a first approximation of the value of a seal, all rating numbers were summed to provide an overall rating. However, this was only done for those seals remaining in final contention. As indicated in Table XII, the order of preference among seals is as follows:

Double bellows loaded face seal

Spherical seat, spring loaded face seal

Single bellows loaded face seal

Packed seal

External covers

It should be re-emphasized here that the external covers would be the simplest overall solution if the additional weight, space, assembly, and servicing complexity can be tolerated. Since this study must consider these aspects, however, the external cover solution appears poorest of the acceptable designs.

It should also be pointed out that the slight difference in design between the single and double bellows seals really represents two variations of a single concept and should be considered as such.

The packed seal presents a gain at the expense of an uncertainty in its torque characteristics. Hence, it may not be as desirable as the rating number would indicate.

The seals with the highest rating numbers therefore represent the best initial concepts to be carried into the feasibility analysis.

1. bellows loaded face seal
2. spring loaded spherical seat face seals.

## MTI VANE-PIVOT SEAL FEASIBILITY ANALYSIS

The feasibility analysis of stator pivot bushing and seal concepts conducted to date by MTI is presented in this section of the report.

In the Screening Study just presented, it was mentioned that the two seals still under consideration are the bellows-loaded face seal and the spring-loaded spherical seat seal. Feasibility Analysis work since NASA approval of the Screening Study Concepts has involved refinement of the concepts and review for comments and suggestions with seal manufacturers. The final designs are being prepared in the light of these comments.

A sketch of a single bellows seal design, as shown in Figure 81, was sent to Sealol, Gits, and Cartriseal for comments and recommendations. Sealol responded with the sketch shown in Figure 82. This design incorporates a retaining ring over the seal rather than trapping the pivot between the housing rings. A final design will have to include the latter feature rather than the ring.

Sealol recommended the use of aluminum oxide or tungsten carbide rather than graphite as the face material. These materials will henceforth be considered as alternatives to graphite or boron nitride. Either of the latter will have much lower friction than the ceramics.

Because Sealol recommended the use of a larger bellows than desired, further consideration will be given to a machined bellows of only half or one convolution for the final design. This is made necessary because the circumferential spacing of the vane-pivots at a given stage is so tight.

Response from the other two vendors has been of marginal benefit.

Figure 83 shows another version of the bellows-loaded face seal, incorporating the thrust face at a point partway out on the pivot shaft. Some thermal advantage can be achieved by doing this because the temperature can be between 50°F and 100°F cooler than at the inside. This much temperature advantage could make graphite coating appear more feasible than at present. There would be no advantage gained for the other candidate face materials.

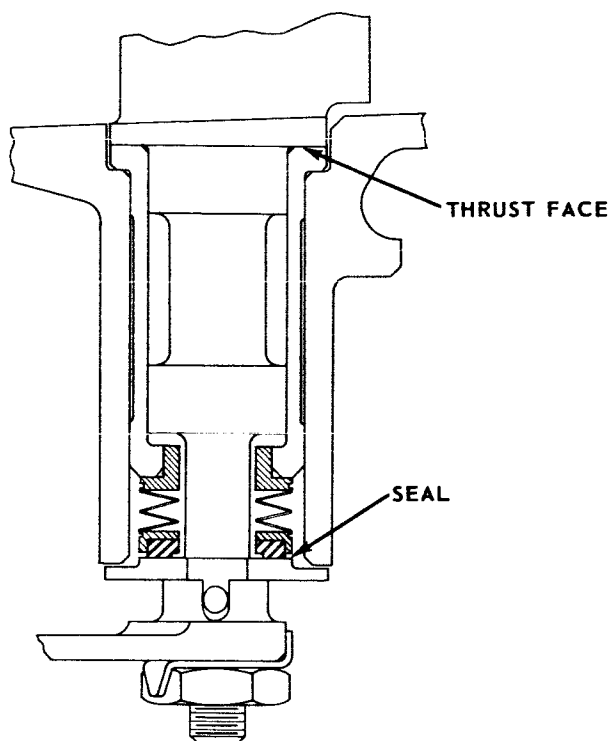


Figure 81 Single Bellows Seal

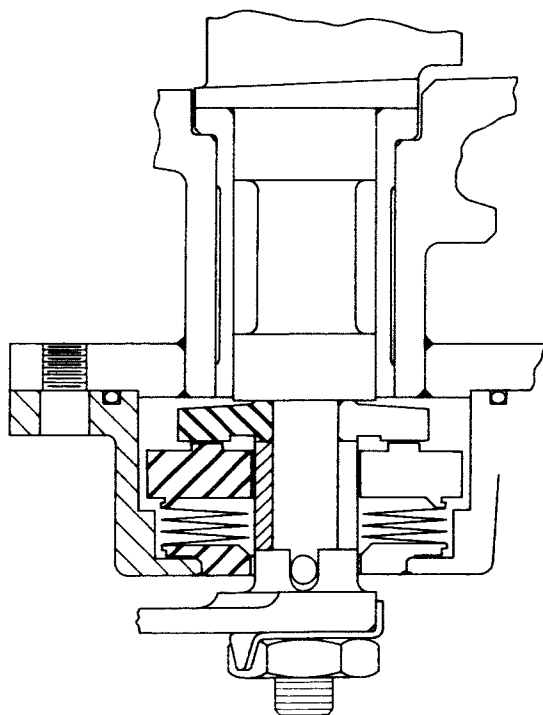


Figure 82 Single Bellows Seal, Sealol Design

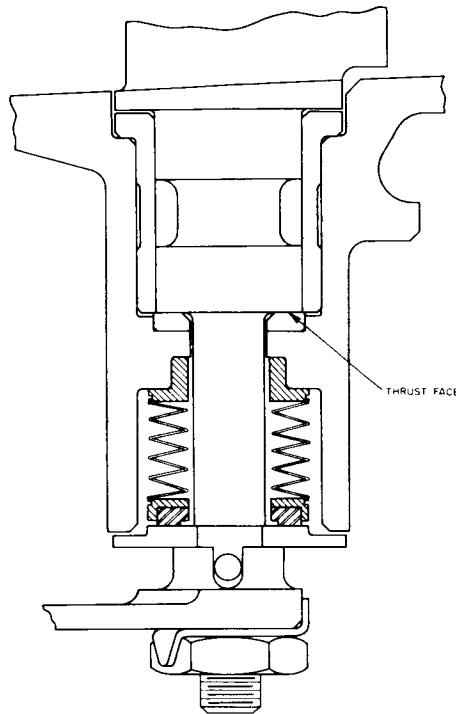


Figure 83 Single Bellows Seal, Relocated Thrust Face

A new scheme for the spherical seat face seal is being considered. The original one is shown in Figure 84. The thrust is now to be taken on a shoulder similar to that of Figure 83. The spherical seat seal is at the outer end of the pivot shaft, and a machined bellows is to be fitted between the housing and the seal.

All these variations of the two designs are to be considered in detail during the next report period. An attempt will be made to incorporate the use of graphite into these designs as the face material. Materials users and vendors will be contacted for further information as necessary. In the event that graphite is finally deemed impractical, the materials to be considered as alternatives will include:

- (1) Boron Nitride
- (2) Tungsten Carbide
- (3) Aluminum Oxide
- (4) Chrome Oxide

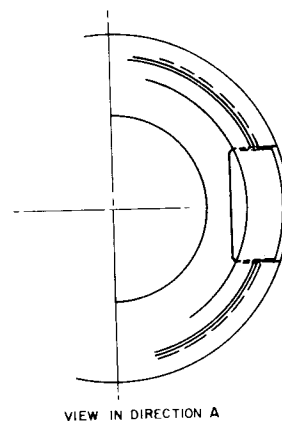
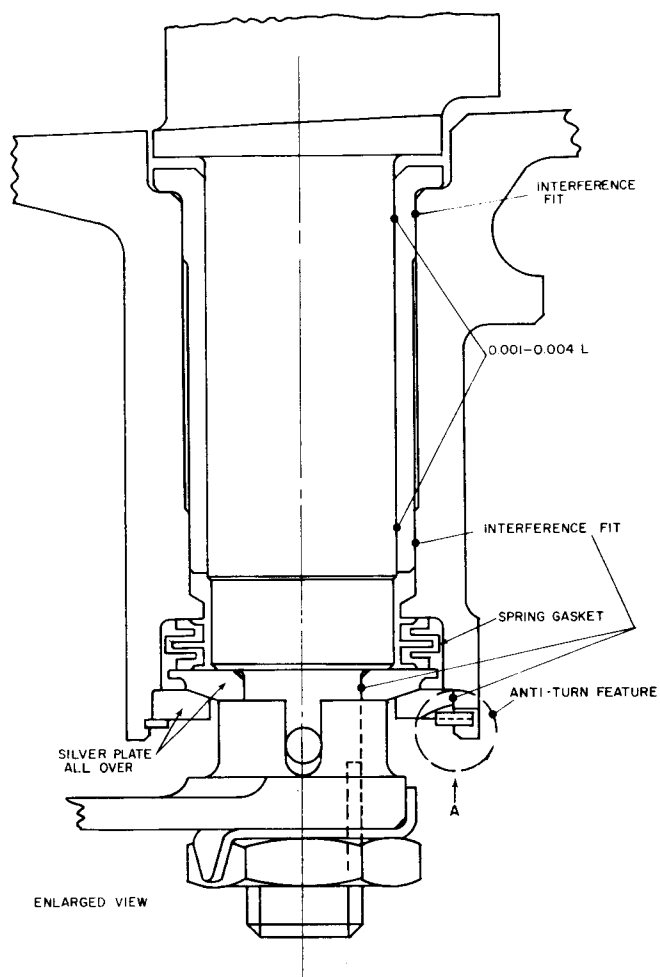
## PRATT &amp; WHITNEY AIRCRAFT PROGRAM

Two stator vane pivot bushing and seal screening study concepts were approved by NASA on October 7, 1965. This approval allowed the program to continue into the detailed feasibility analysis. The approved seal concepts listed below are shown in exploded views with accompanying descriptions in Figures 84 and 85. Scheme C (Figure 86) is an alternate for Scheme B.

|          |                          |
|----------|--------------------------|
| Scheme A | Spherical Seat Face Seal |
| Scheme B | Single Bellows Face Seal |
| Scheme C | Double Bellows Face Seal |

As directed by NASA, no feasibility analysis effort will be expended on the double-bellows seal design (Figure 86) unless it is determined that the sealing face surface in the single bellows seal is subject to distortion and leakage.

Pratt & Whitney Aircraft has been monitoring the MTI analytical effort, as specified in the prime contract.



## DESCRIPTION

## Scheme A - Spherical Seat Face Seal

In this design the primary seal is effected by a spring-loaded spherical seat face seal. The spherical face also acts as a thrust bearing to absorb the seating force of the Skinner spring plus the thrust load created by the air pressure acting on the vane. Both of the spherical surfaces will be plated with a material having a low coefficient of friction to reduce actuating torque and prevent galling.

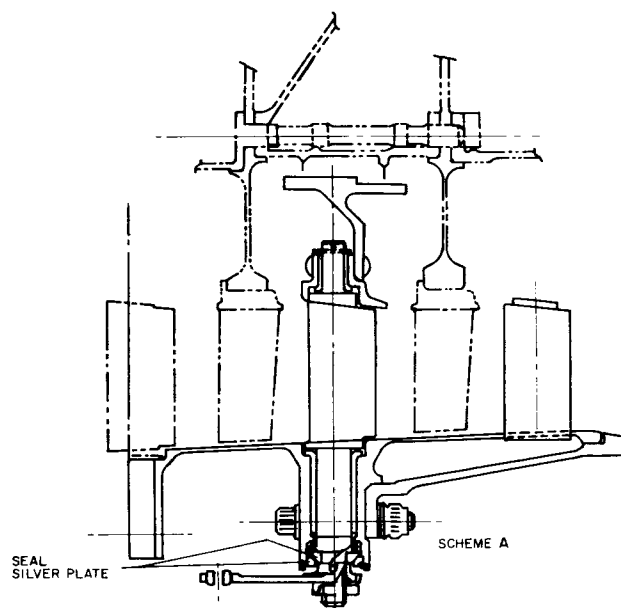
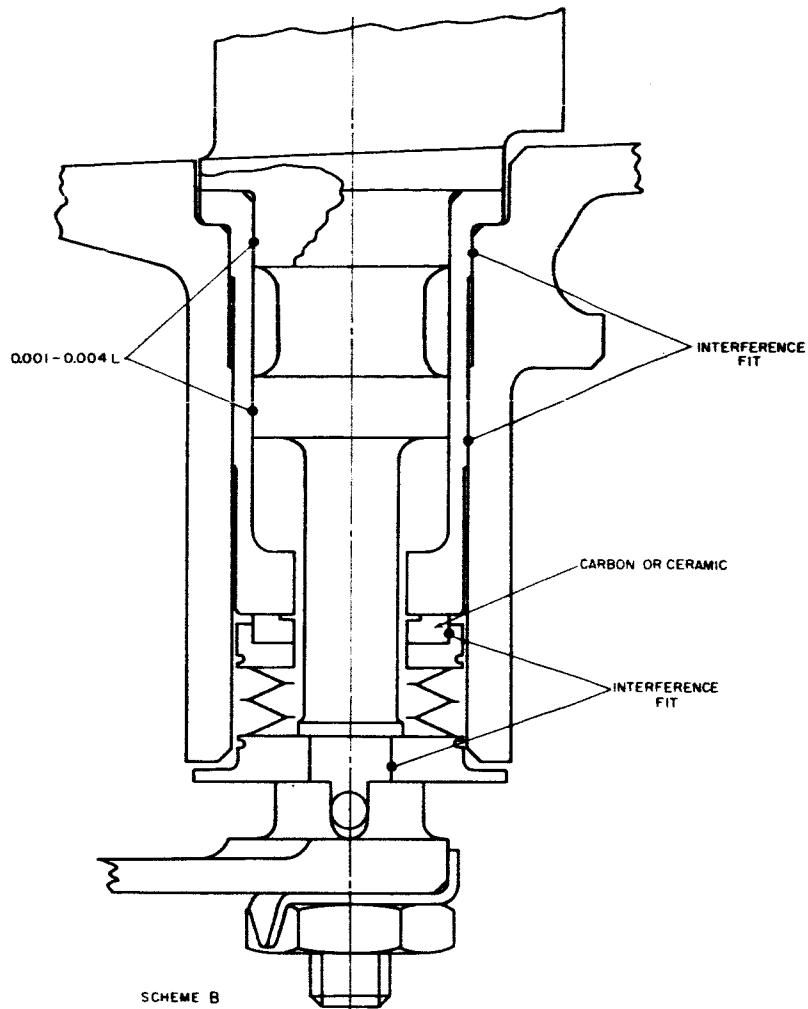


Figure 84 Stator Pivot Seal Concept Scheme A - Ref PWA Drawing No. L-67563 Ref MTI Sketch of 9-14-65 by H. Jones





## DISCRIPTION

## Scheme B - Single Bellows Face Seal

This design is similar to the double bellows seal, except that only one sealing face is bellows supported. The other sealing face is formed by the end of a bushing which is installed in the outer shroud with an interference fit. The main advantage of this design over the double bellows design is that it has fewer parts.

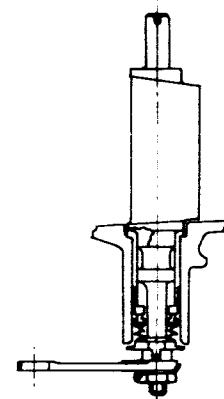
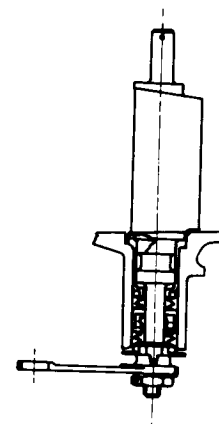
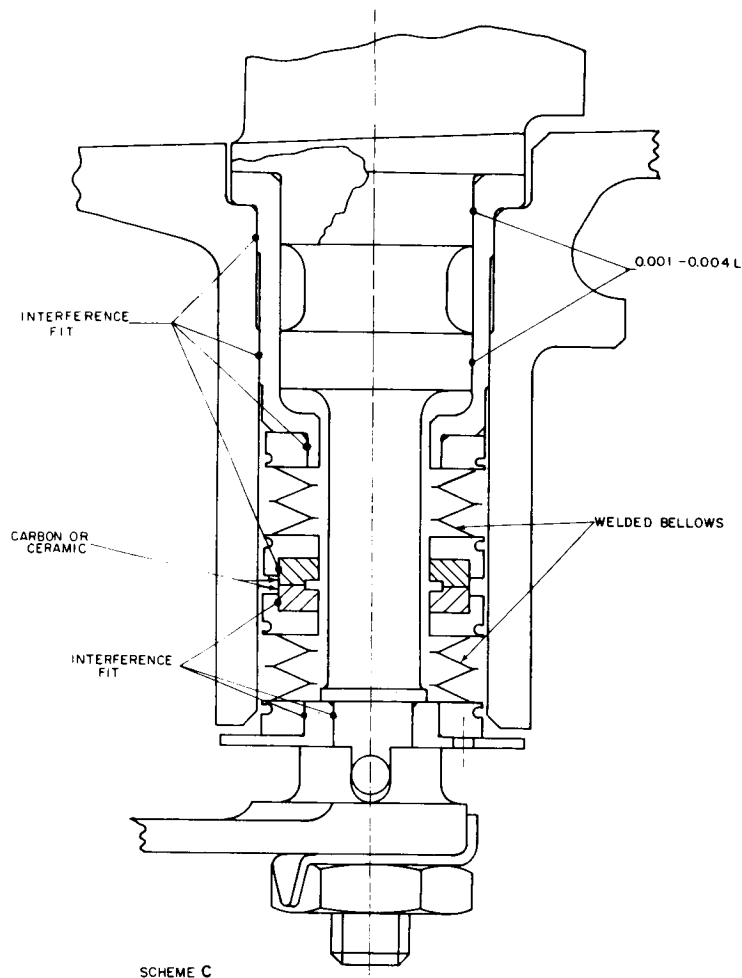


Figure 85 Stator Pivot Seal Concept Scheme B - Ref PWA Drawing No. L-67563 Ref MTI Sketch of 9-1-65 by E. Belawski



SCHEME C

## DESCRIPTION

## Scheme C - Double Bellows Face Seal

This design offers maximum tolerance to deflections in that both sealing surfaces are supported by a welded metal bellows. The seal pieces are made of a material such as carbon or ceramic and are retained in the bellows assembly by an interference fit. The thrust loads created by air pressure and spring forces are carried by a thrust bearing located at the tip of the vane.

Figure 86 Stator Pivot Seal Concept Scheme C - Ref PWA Drawing No. L-67563 Ref MTI Sketch of 9-5-65 by E. Belawski

#### TASK IV - PIVOT BUSHING AND SEAL EXPERIMENTAL EVALUATION

This phase of the program provides for final design and procurement of bushings and seals, design and fabrication of a test rig, and experimental evaluation of bushing and seal assemblies.

The final design of the two selected concepts for experimental evaluation includes all calculations, material determinations, analyses, and drawings necessary for pivot bushing and seal optimization, procurement, and experimental evaluation.

A single vane test rig will be designed and fabricated to evaluate the two selected pivot bushings and seal designs under simulated operating conditions for the last compressor stage. The vane and actuating mechanism are to be applicable to current advanced engine practice.

The pivot bushing and seal assemblies will be calibrated in incremental steps over the full pressure and temperature range, with a maximum pressure of 135 psi and a maximum temperature of 1200°F.

The seals will be subjected to a cyclic endurance run of at least 40 hours duration following a test program which provides for simulation of take-off (20 hours) and a cruise (20 hours) conditions typical of advanced engine designs through duplication of:

- Compressor stage air temperatures
- Supporting structure geometry
- Supporting structure temperatures
- Pivot movements as required for the vanes
- Pivot loading (mechanical loading to simulate air loading is acceptable)
- Compressor stage pressure drop

The pivot movement will be minimum of 13 degrees at 10 cycles per minute; the pivot loading will include a vibratory load to a convenient  $\pm 15\%$  of the steady load.

#### PROGRESS

Preliminary design work is continuing on a test rig in which the vane pivot bushing and seat experimental evaluation will be conducted. Further investigations were made of the methods of applying the required steady state and vibratory loads to the vane pivot seals. Since the air leakage rate is expected to be too low to maintain the test rig temperature of 1200°F, it appears desirable to incorporate electric cartridge-type heaters in the body of the rig.

An analysis of a current advanced engine has indicated that the minimum axis bending moment of the last stage stator vane was 19.8 inch-pounds at the outer diameter. The mechanical load required to simulate this air load was calculated, using the formula for a guided cantilevered beam, to be 21.85 pounds when applied to the lower pivot. The deflection of the vane at the lower pivot was calculated to be 0.0012 inches with the load applied perpendicular to the major axis. The load will be applied through a coil spring in the test rig. The steady state load will be set by compressing the spring to a predetermined height. The vibratory load will be superimposed by varying the deflection  $\pm$  by the use of an eccentric drive. The frequency of the vibratory load will be 30 cps. The stress in the vane will also be monitored during the test by attaching a strain gage to the upper part of the vane.

According to contractual agreement, no hardware will be procured until NASA approval of the design is obtained.

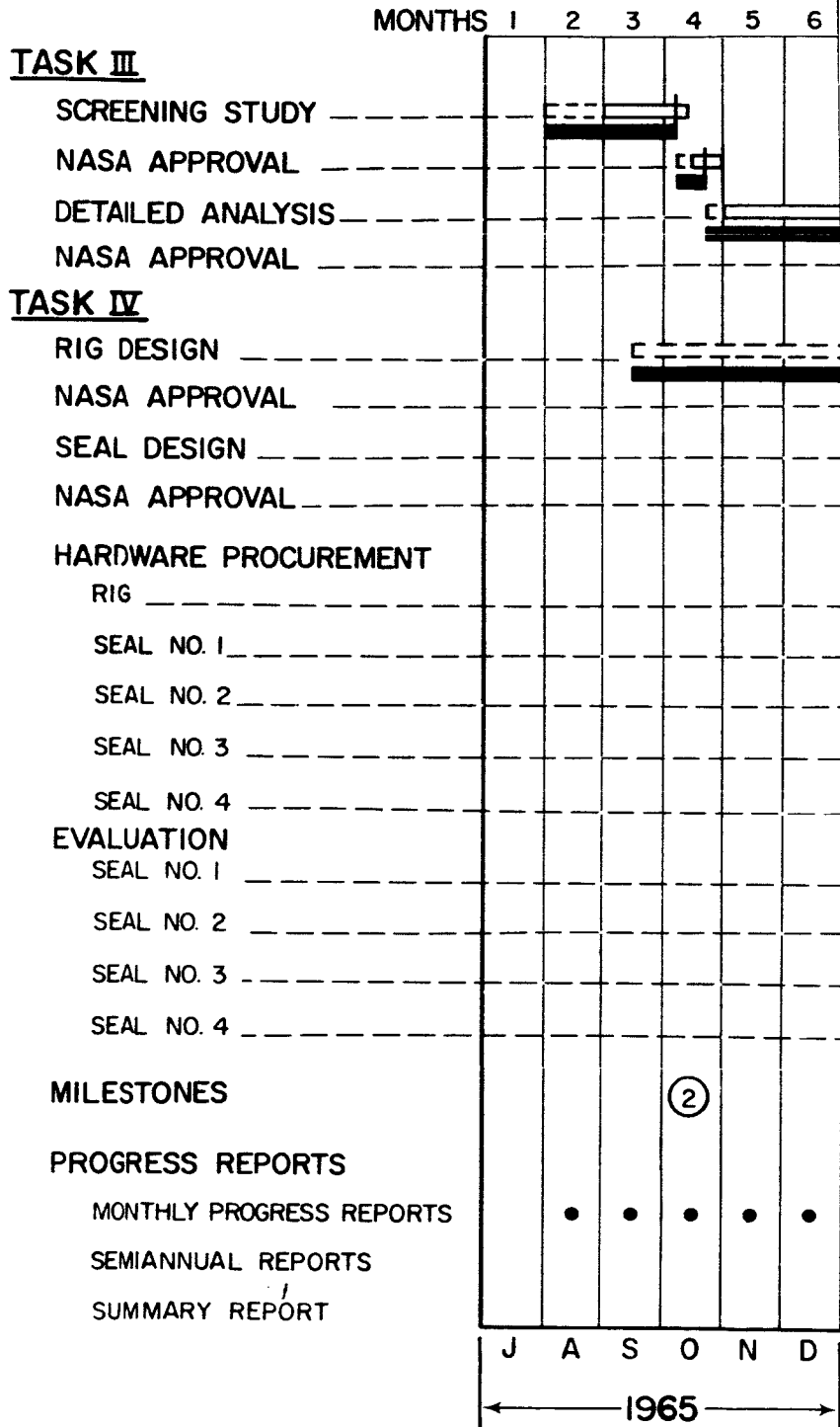
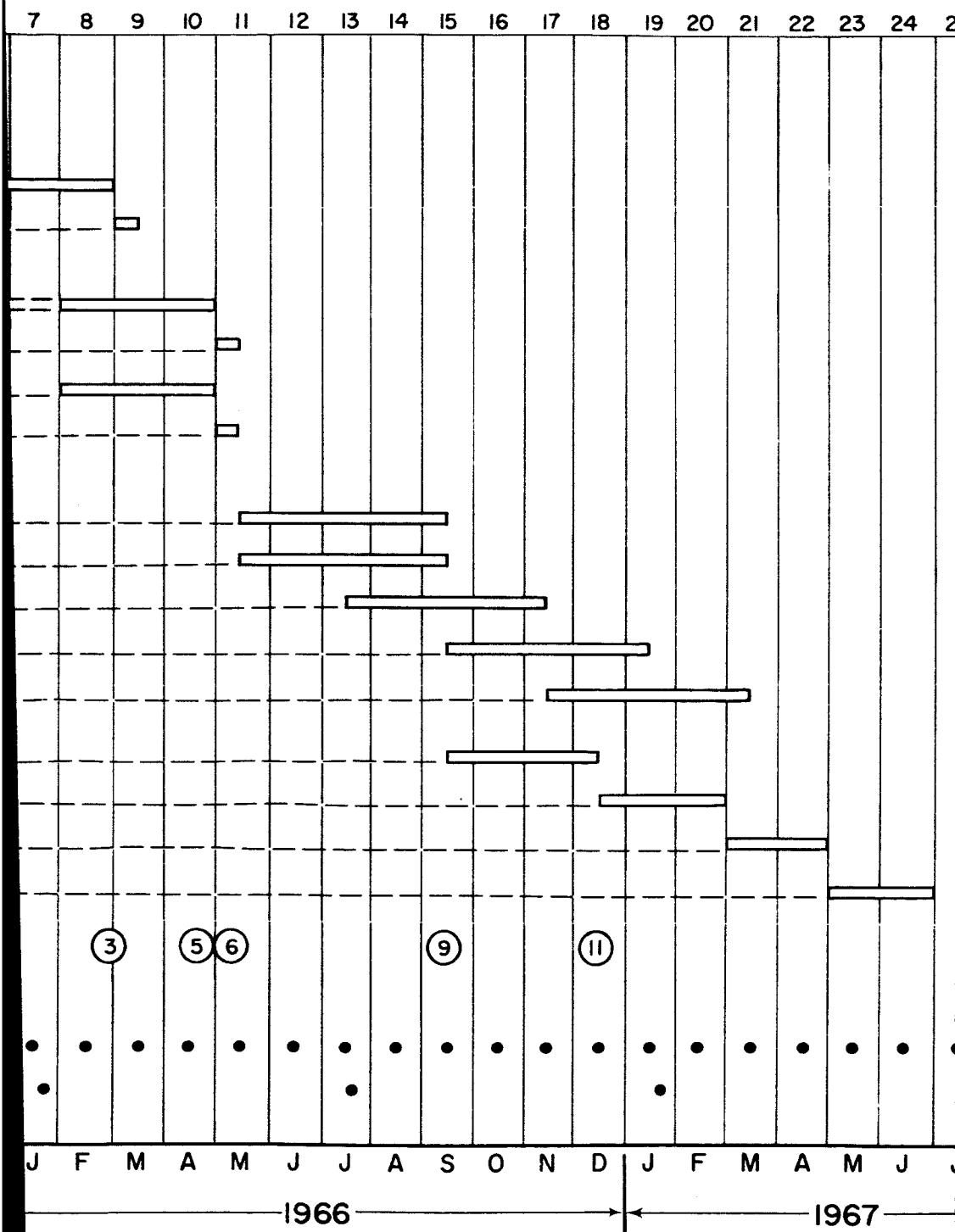


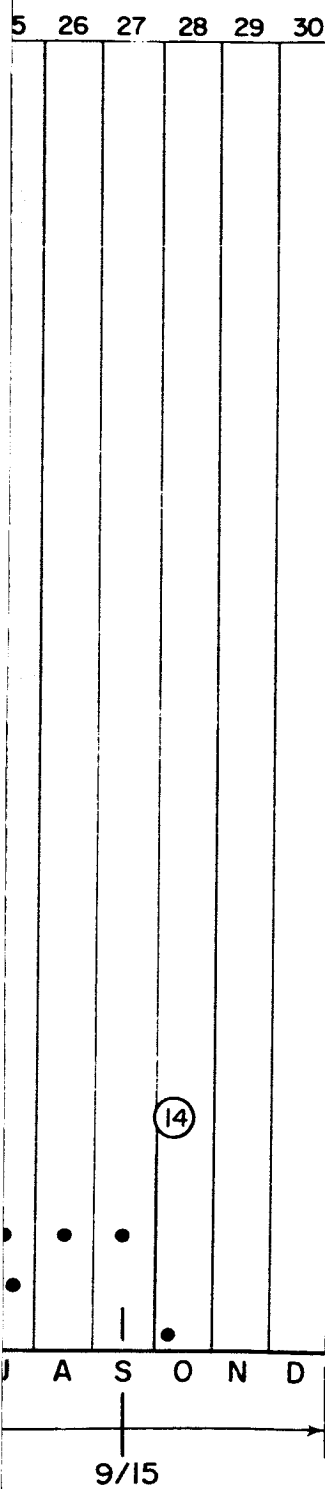
Figure 87 Compressor Seal

# COMPRESSOR SEAL DEVELOPMENT PROGRAM SCHEDULE AND MILESTONE CHART

CONTRACT NAS3-7605






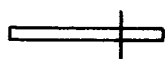
Development Program Schedule and Milestone Chart



### MILESTONES

1. TASK I - COMPLETE SCREENING STUDY
2. TASK III - COMPLETE SCREENING STUDY
3. TASK III - COMPLETE DETAILED ANALYSIS
4. TASK I - COMPLETE DETAILED ANALYSIS
5. TASK IV - COMPLETE RIG DESIGN
6. TASK IV - COMPLETE SEAL DESIGN
7. TASK II - COMPLETE RIG DESIGN
8. TASK II - COMPLETE SEAL DESIGN
9. INITIATE TASK IV TESTING
10. INITIATE TASK II TESTING
11. TASK IV - COMPLETE EVALUATION OF ONE STATOR PIVOT SEAL
12. TASK II - COMPLETE EVALUATION OF ONE COMPRESSOR END SEAL
13. TASK II - COMPLETE EVALUATION OF ONE STATOR INTERSTAGE SEAL
14. SUBMIT SUMMARY REPORT FOR NASA APPROVAL

### LEGEND

-  WORK PROJECTED
-  REVISED WORK PROJECTED
-  WORK ACCOMPLISHED
-  WORK COMPLETED EARLY

3

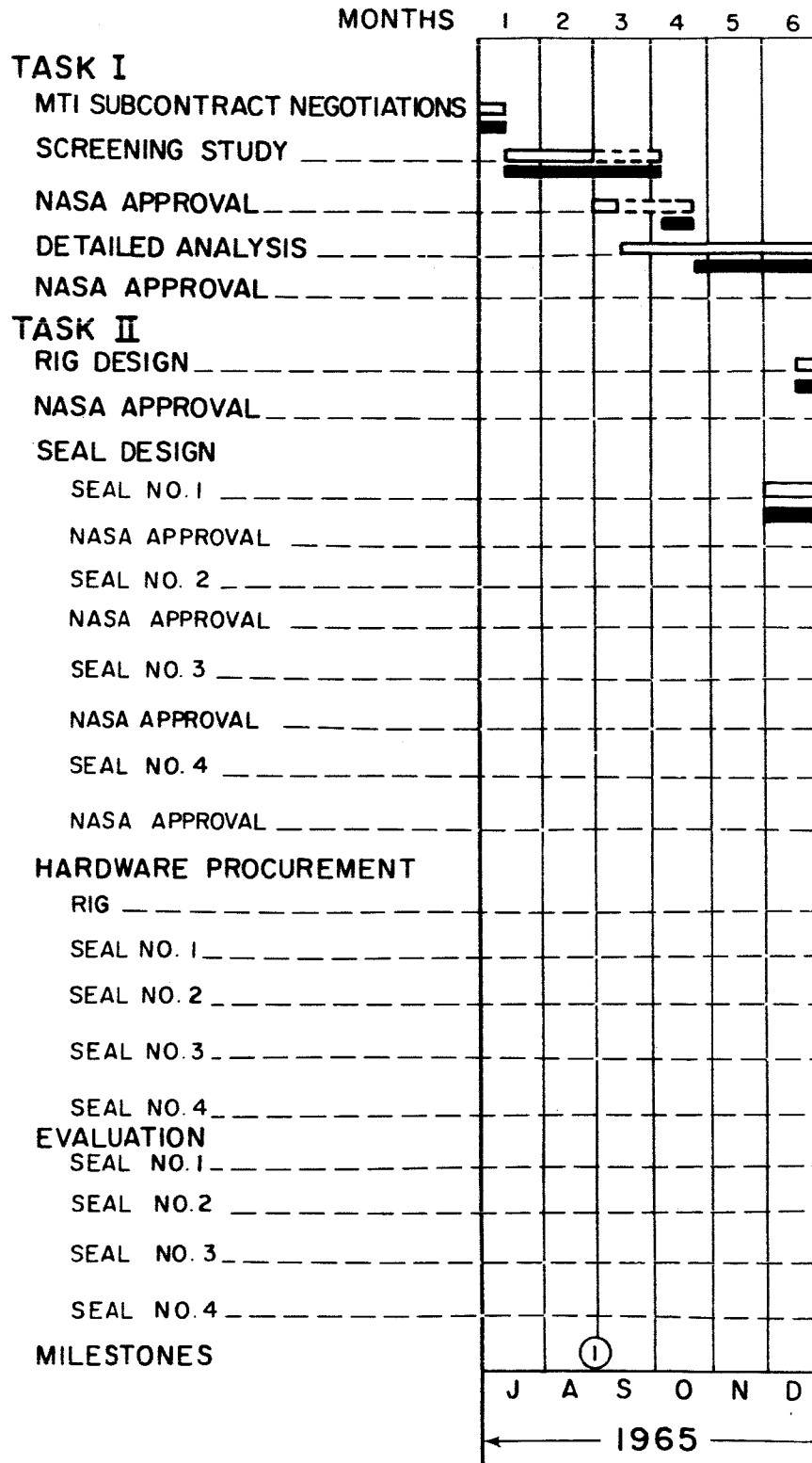
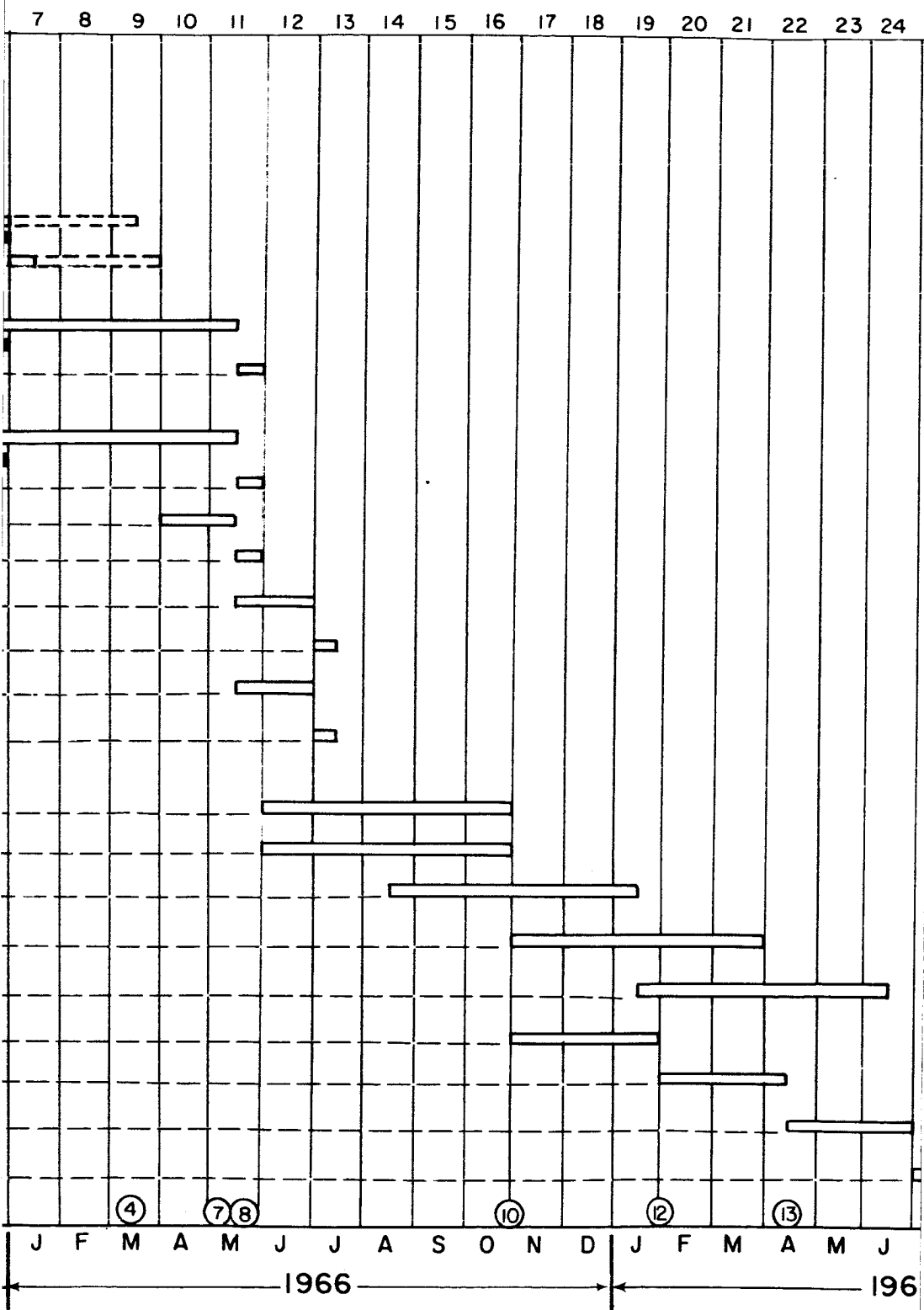


Figure 88 Compressor Seal



# COMPRESSOR SEAL DEVELOPMENT PROGRAM SCHEDULE AND MILESTONE CHART

CONTRACT NAS3-7605



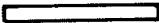



Development Program Schedule and Milestone Chart

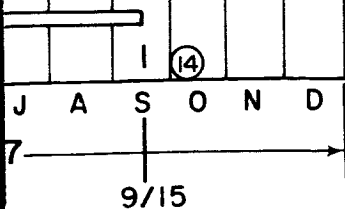
## MILESTONES

25 26 27 28 29 30

1. TASK I - COMPLETE SCREENING STUDY
2. TASK III - COMPLETE SCREENING STUDY
3. TASK III - COMPLETE DETAILED ANALYSIS
4. TASK I - COMPLETE DETAILED ANALYSIS
5. TASK IV - COMPLETE RIG DESIGN
6. TASK IV - COMPLETE SEAL DESIGN
7. TASK II - COMPLETE RIG DESIGN
8. TASK II - COMPLETE SEAL DESIGN
9. INITIATE TASK IV TESTING
10. INITIATE TASK II TESTING
11. TASK IV - COMPLETE EVALUATION OF ONE STATOR PIVOT SEAL
12. TASK II - COMPLETE EVALUATION OF ONE COMPRESSOR END SEAL
13. TASK II - COMPLETE EVALUATION OF ONE STATOR INTERSTAGE SEAL
14. SUBMIT SUMMARY REPORT FOR NASA APPROVAL

## LEGEND

-  WORK PROJECTED
-  REVISED WORK PROJECTED
-  WORK ACCOMPLISHED
-  WORK COMPLETED EARLY



3

## APPENDIX A

### FILM THICKNESS OPTIMIZATION STUDY

A seal of the type presented in this study permits a certain leakage flow. This leakage can be costly in both the power it takes to compress the air, as well as the reduction in turbine flow. In this project, the object of the study is to optimize the design in every respect. One of the obvious requirements is to reduce the leakage flow, while maintaining sufficient film thickness to assure successful mechanical operation without detrimental contact between rotating and stationary parts of the seals.

In opposition to this requirement is the fact that, as the film thickness is reduced, the drag power consumption of the seal increases. These are the factors that must be optimized.

#### LEAKAGE FLOW

In all seal designs the flow is computed on the basis that the leakage area is a slit as shown in Figure 89.

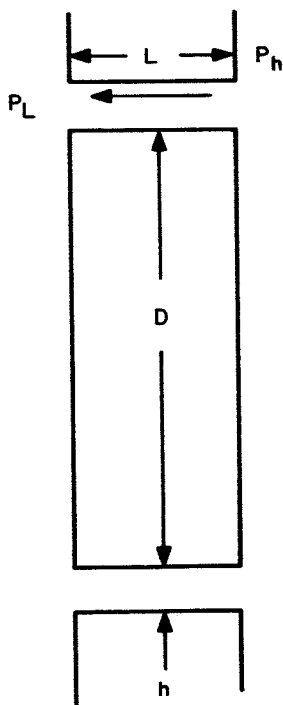


Figure 89 Schematic of Leakage Area Slit Assumed for Leakage Flow Computations

Then

$$Q = \frac{bh^3}{12\mu} \left( \frac{\Delta P}{L} \right) \quad (A-1)$$

where

$$Q = \text{Vol. of air at conditions } P_1 T_1 \quad \text{in}^3/\text{sec}$$

$$b = \text{length of slit} \quad \text{inches}$$

$$= 27.25 \pi$$

$$\Delta P = \text{Pressure difference} \quad \text{lb/in}^2$$

$$L = \text{length of leakage path} \quad \text{inches}$$

$$= 1/2 \text{ inch}$$

$$\mu = \text{viscosity of air at conditions } P_1 T_1 \quad \text{lb. sec/in}^2$$

$$= 5.69 \times 10^{-9} \quad \text{lb. sec/in}^2$$

$$h = \text{film thickness} \quad \text{inches}$$

$$= .0003 \text{ to } .001 \text{ inches}$$

Then

$$Q \frac{\text{in}^3}{\text{sec}} = \frac{27.25 \pi (\Delta P h^3)}{12 \times 5.69 \times 1/2} \times 10^9$$

$$Q = 2.5 \times 10^9 (\Delta P h^3) \frac{\text{in}^3}{\text{sec}} \quad (A-1a)$$

Convert the volume flow  $Q$  to weight flow by computing the density from the gas law

$$PV = RT \quad (A-2)$$

then

$$\text{Density } \rho = \frac{P_1}{RT_1} \text{ lbs/ft}^3$$

$R$  = Universal gas constant for air

$$= 53.3 \text{ (ft. lbs.) / (lbs. } ^\circ\text{R)}$$

$P_1$  = Inlet pressure lbs/in.<sup>2</sup>

$$= 144 P_1 \text{ lbs/ft}^2$$

$T_1$  = Inlet temp.  $^\circ\text{R}$

Finally, the leakage flow is

$W$  =  $\rho Q$  lbs/sec when the units are consistent

$$\therefore W = \frac{P_1 Q}{640 T_1} \text{ lbs/sec} \quad (\text{A-3})$$

#### COMPRESSION POWER

The pumping power required to compress the air from some lower pressure to the pressure level at the seal is given by the following equation

$$\text{HP} = \frac{W}{\eta} \times \frac{n}{n-1} \times R T_o \left[ R_c \frac{n-1}{n} - 1 \right] \times \frac{1}{550} \quad (\text{A-4})$$

where

$\text{HP}_{\text{comp}}$  = compression power - horsepower

$W$  = flow lbs/sec

$\eta$  = compression efficiency - dimensionless

$$= .86$$

$n$  = Exponent of the adiabatic compression process

$$= 1.4$$

$$R = 53.3 \frac{\text{ft} - \text{lb}}{\text{lb} - ^\circ\text{R}}$$

$$\begin{aligned} T_o &= \text{Initial air temperature } ^\circ\text{R} \\ &= 560 \end{aligned}$$

$$\begin{aligned} R_c &= \text{Compressor pressure ratio} \\ &= 20 \end{aligned}$$

$$550 = \text{Work rate } \frac{\text{ft lbs/sec}}{\text{H.P.}}$$

Then

$$\text{HP}_{\text{comp}} = \frac{1.4}{4} \times 53.3 \times 560 \left[ 20^{.286} - 1 \right] \times \frac{W}{550 \times 86}$$

$$\text{HP}_{\text{comp}} = 298 W \text{ lbs/sec} \quad (\text{A-4a})$$

#### SEAL DRAG POWER

The drag power of the seal is

$$\text{HP}_{\text{drag}} = \frac{\mu A U^2}{6600 h} \quad (\text{A-5})$$

$$A = \text{area of the seal surface, in}^2$$

$$= 27.25 \pi \times 1/2$$

$$U = \text{relative linear velocity of seal surface in/sec}$$

$$= \frac{\pi \times 27.25 \times 8000}{720} = 950 \text{ ft/sec}$$

$$h = \text{film thickness}$$

$$= .0003 \text{ to } .001 \text{ inches}$$

Then

$$\text{HP}_{\text{drag}} = \frac{5.69 \times 27.25 \pi \times 1/2 \times (950 \times 12)^2}{6600 \times 10^9 h} = \frac{5.2}{10^3 h}$$

Example

Compute the optimum film thickness for the compressor end seal, where the physical dimensions are as shown in Table XIII. First compute, (Ref. Equation A-1a)

$$Q = 2.5 \times 10^9 (\Delta P h^3) \text{ in}^3/\text{sec}$$

Assume that  $\Delta P = 150 \text{ lbs/in}^2$

Then

$$Q = 2.5 \times 10^9 \times 150 h^3$$

$$Q = 375 \times 10^9 h^3$$

And convert the volume flow to weight flow (Ref. Equation A-3)

$$W = \frac{P \cdot Q}{640 T_1} \quad \text{Assume } T_1 = 1600^\circ \text{R}$$

$$= \frac{150 \times Q}{640 \times 1600}$$

$$W = \frac{1.465 Q}{10^4}$$

Third, from this tabulated value, the compression power can be computed as follows, (Ref. Equation A-4a)

$$\text{HP}_{\text{comp.}} = 298W$$

Fourth, the drag power for the seal is

$$\text{HP}_{\text{drag}} = \frac{5.2}{10^3 h}$$

TABLE XIII.  
PHYSICAL DIMENSIONS-COMPRESSOR END SEAL

| $h$                  | $h^3$                  | $Q \text{ in}^3/\text{sec}$ | $W \text{ lbs/sec} = \frac{1465 Q}{104}$ | $HP_{\text{comp}} = \frac{HP_{\text{drag}}}{298W}$ | $HP_{\text{drag}} = \frac{5.2}{10^3 h}$ |
|----------------------|------------------------|-----------------------------|--|--|---|
| $3 \times 10^{-4}$   | $27 \times 10^{-12}$   | 10.13                       | .001485                                  | .443   | 17.3                                    |
| $5 \times 10^{-4}$   | $125 \times 10^{-12}$  | 46.9                        | .00688                                   | 2.05   | 10.4                                    |
| $7.5 \times 10^{-4}$ | $422 \times 10^{-12}$  | 158.2                       | .02315                                   | 6.9  | 6.93                                    |
| $10 \times 10^{-4}$  | $1000 \times 10^{-12}$ | 375.0                       | .0550                                    | 16.4   | 5.2                                     |



## APPENDIX B

SOLUTION OF A HYBRID LUBRICATION PROBLEM  
WITH RAYLEIGH STEPS AND CYCLIC BOUNDARY CONDITIONS

The problem is to solve Reynolds Equation in a field where the clearance function could present discontinuities. Also, the possibility of complicated boundary conditions should be easily accommodated.

The Reynolds Equation is written in two forms: the first, suitable for parts of the field where the clearance varies smoothly and the second, for clearance discontinuities. These are, respectively

$$\nabla \cdot \left( \frac{H^3}{2} \nabla Q - \Lambda \frac{QH}{P} \right) = 0 \quad (B-1)$$

and

$$\oint \left( \frac{H^3}{2} \nabla Q - \Lambda \frac{QH}{P} \right) \cdot \hat{n} \, d\ell = 0 \quad (B-2)$$

where

$$\nabla = i \frac{\partial}{\partial X} + j \frac{\partial}{\partial Y}$$

$i, j$  the base vectors of the coordinate system.

$$X, Y = \text{dimensionless coordinates} = \frac{X}{L}, \frac{Y}{L}$$

$L$  = typical length = length of side parallel to  $X$  axis

$$H = \text{dimensionless clearance} = \frac{h}{c}$$

$c$  = typical clearance

$$Q = P^2$$

$P$  = ambient pressure

$$\Lambda = \frac{6\mu L}{P_a c^2} V$$

$\mu$  = viscosity

$V$  = velocity =  $V_x i + V_y j$

$d\ell$  = element of a closed loop curve in the field

$\hat{n}$  = outward normal to above mentioned curve

The possible boundary conditions are:

- a. Fixed pressure such as at the outer boundaries exposed to atmosphere.
- b. Lines of symmetry where  $\frac{\partial P}{\partial X}$  or  $\frac{\partial P}{\partial Y} = 0$
- c. Periodicity conditions in X or Y.

The numerical solution of the problem is executed on a rectangular grid of  $M \times N$  points. Let  $i$  and  $j$  represent the matrix indices corresponding to the X and Y coordinates respectively.

Equation (B-1) is written in the following form:

$$3 \frac{\nabla H}{H} \cdot \nabla Q + \nabla^2 Q - \Lambda \frac{2Q}{PH^3} \cdot \nabla H - \frac{\Lambda \cdot \nabla Q}{PH^2} = 0 \quad (B-3)$$

By using the approximations

$$\nabla Q = (Q_{i+1,j} - Q_{i-1,j}) \frac{i}{2\Delta X} + (Q_{i,j+1} - Q_{i,j-1}) \frac{j}{2\Delta Y}$$

and

$$\nabla^2 Q = \frac{Q_{i+1,j} - 2Q_{ij} + Q_{i-1,j}}{(\Delta X)^2} + \frac{Q_{i,j+1} - 2Q_{ij} + Q_{i,j-1}}{(\Delta Y)^2},$$

and by computing H and its derivatives from analytical formulae, Equation (B-3) becomes

$$\mathcal{L}_1 (Q_{i,j}, Q_{i+1,j}, Q_{i-1,j}, Q_{i,j+1}, Q_{i,j-1}) = 0 \quad (B-4)$$

Where  $\mathcal{L}_1$  indicates a linear algebraic operator. The variable P is considered to be a coefficient so that the problem is solved by iteration. An initial distribution of P is selected, Q is solved for by linear methods, and then  $P = \sqrt{Q}$  provides an improved guess. This procedure is known to converge very rapidly.

For points on clearance discontinuities, Equation (B-2) must be used. The integration path is taken to be a rectangle of sides  $\Delta X$  and  $\Delta Y$  centered at the point in question. Equation (B-2) becomes

$$\left( \frac{H^3}{2} \frac{\partial Q}{\partial X} - \Lambda \frac{QH}{P} \right) \bigg|_{i-1/2, j}^{i+1/2, j} + \left( \frac{H^3}{2} \frac{\partial Q}{\partial Y} - \Lambda_y \frac{QH}{P} \right) \bigg|_{i, j-1/2}^{i, j+1/2} \Delta Y = 0 \quad (B-5)$$

where

$$\left. \frac{\partial Q}{\partial X} \right|_{i+1/2, j} = \frac{1}{\Delta X} (Q_{i+1, j} - Q_{ij}) \quad \text{etc.}$$

and variable values taken at half cell are obtained by averaging values at neighboring points.

Therefore, Equation (B-5) becomes

$$\mathcal{L}_2 (Q_{i, j}, Q_{i+1, j}, Q_{i-1, j}, Q_{i, j+1}, Q_{i, j-1}) = 0 \quad (B-6)$$

where  $\mathcal{L}_2$  is a linear algebraic operator.

Reynolds Equation is now reduced to a linear algebraic operator, (either  $\mathcal{L}_1$  or  $\mathcal{L}_2$ ), relating each point to its four neighbors.

The boundary conditions can now be treated. Points at which the pressure is known can be treated as field points where the governing equation is  $Q_{ij} = (\text{known pressure})^2$ . Points located on a line of symmetry can also be treated as field points with the symmetry condition incorporated in the proper form of Equation (B-4). Namely, if the symmetry line is normal to the X axis,  $Q_{i+1, j} = Q_{i-1, j}$  should be introduced in Equation (B-4) to eliminate whichever of the two quantities refers to a point outside the field mesh. An analogous operation may be carried out for symmetry lines normal to the Y axis.

Periodicity conditions are encountered in journal bearings and in thrust bearings having repetitive patterns. If the bearing clearance and running conditions are periodic in the X direction, one sees that  $Q$  and  $\partial Q / \partial X$  are the same at  $X = 0$  and  $X = 1$ . Numerically, this can be expressed by the relations

$$\left. \begin{aligned} Q_{1,j} &= Q_{M+1,j} \\ Q_{0,j} &= Q_{M,j} \end{aligned} \right\} \quad (B-7)$$

Similarly, periodicity in the Y direction can be expressed by

$$\left. \begin{aligned} Q_{i,1} &= Q_{i,N+1} \\ Q_{i,0} &= Q_{i,N} \end{aligned} \right\} \quad (B-8)$$

Relations (B-7) are used in Equation (B-4) when applied at  $i = M$  and  $i = 1$  respectively. Relations (B-8) are used in Equation (B-4) when applied at  $j = N$  and  $j = 1$  respectively. Thus  $Q_{M+1,j}$ ,  $Q_{0,j}$ ,  $Q_{i,N+1}$ ,  $Q_{i,0}$  are eliminated and a set of  $M \times N$  equations  $M \times N$  unknowns is obtained.

It should be noticed that all equations involve the function  $Q$  at a point and its immediate neighbors with the exception of the equations applicable to periodicity boundaries where relations (B-7) and (B-8) introduce values taken at the opposite extreme of the grid.

The problem is now completely formulated by a set of  $M \times N$  linear equations in  $M \times N$  unknowns which, due to the presence of the variable  $P$  as a coefficient, must be solved repeatedly. For this purpose, the technique of reference (9) is employed as generalized to handle the effect of periodic boundary conditions.

The equations are written in columns, thus

$$[A_i] \{Q_i\} + [B_j] \{Q_{j-1}\} + [C_j] \{Q_{j+1}\} = \{R_j\} \quad (B-9)$$

where  $[A_j]$ ,  $[B_j]$ ,  $[C_j]$  are  $M \times M$  matrices of coefficients obtained from the applications of the linear operators developed above.

The following relation must hold

$$Q_{j-1} = [E_j] \{Q_j\} + [D_j] \{Q_N\} + \{G_j\} \quad (B-10)$$

where

$$\begin{aligned} [D_1] &= \{1^0\} \quad \text{is not periodic in } Y \\ &\quad \text{(identity matrix) if periodic in } Y \\ [E_j] &= 0 \\ \{G_1\} &= 0 \end{aligned} \tag{B-11}$$

Substitution of Equation (B-10) in Equation (B-9) yields a set of recurrence relations

$$\left. \begin{aligned} [D_{j+1}] &= - [I]^{-1} [B_j] [D_j] \\ [E_{j+1}] &= - [I]^{-1} [C_j] \\ \{G_{j+1}\} &= [I]^{-1} \{ \{F_j\} - [B_j] \{G_j\} \} \end{aligned} \right\} \tag{B-12}$$

where

$$[I] = [A_j] + [B_j] [E_j]$$

Relations (B-12) can be applied for  $j = 1, N$  and the resulting values of the  $[D_j]$ ,  $[E_j]$  and  $\{G_j\}$  matrices stored.

Defining

$$\left. \begin{aligned} [R_N] &= \left[ \begin{bmatrix} 1 \\ \vdots \end{bmatrix} - [D_{N+1}] \right]^{-1} [E_{N+1}] \\ \text{and} \\ [S_{N+1}] &= \left[ \begin{bmatrix} 1 \\ \vdots \end{bmatrix} - [D_{N+1}] \right]^{-1} [G_{N+1}] \end{aligned} \right\} \tag{B-13}$$

The following recurrence relations hold

$$\left. \begin{aligned} [R_{j-1}] &= [D_j] [R_N] + [E_j] [R_j] \\ \text{and} \\ [S_{j-1}] &= [D_j] [S_N] + [D_j] [S_j] + [G_j] \end{aligned} \right\} \tag{B-14}$$

Relations (B-14) can be applied for values of  $j$  progressing from  $N$  to 2.

Then the solution is given by

$$\{Q_1\} = \left[ \begin{bmatrix} I \end{bmatrix} - [R_1] \right]^{-1} \{S_1\} \quad (B-15)$$

and

$$\{Q_j\} = [R_j] \{Q_1\} + \{S_j\} \quad (B-16)$$

applied for  $j = 2, 3, \dots, N$ .

The solution method as shown above is valid whether periodicity conditions in  $Y$  exist or not. If the periodicity in  $Y$  is not imposed, all  $D$  matrices are zero and saving can be realized both in storage and computation time.

Note that periodicity conditions in  $X$  still allow all  $D$  matrices to be zero and affect only the form of the  $A$  matrix.

#### APPLICATION DETAILS

In the present application of the solution method outlined above, the nature of all points in the grid is specified by a clue digit from 0 to 9. Three different values of specified pressure are allowed to accommodate two ambient pressures and possibly an internal feed.

The depressed area in the step is assumed to be uniformly depressed from the level of clearance given in Equation (B-17).

$$H = a + bX + cY + dX^2 + eXY + fY^2 + gX^3 + hY^3 \quad (B-17)$$

Upon convergence, the resulting pressure distribution is integrated to obtain; total load, moments about  $X = 0$ ,  $Y = 0$ , flow through a line parallel to the  $X$  axis. These quantities are specified by the following expressions:

$$W = \iint P \, dX \, dY \quad (B-18)$$

$$M_X = \iint P X \, dXdY \quad (B-19)$$

$$M_Y = \iint P Y \, dXdY \quad (B-20)$$

$$F_X = \int \left( H^3 P \frac{dP}{dX} - \Lambda_X HP \right) dY \quad (B-21)$$

$$F_Y = \int \left( H^3 P \frac{dP}{dY} - \Lambda_Y HP \right) dX \quad (B-22)$$

where

$$W = \frac{\text{load}}{PaL^2} : \text{for load per unit area } W' = \frac{\text{load}}{PaL^2} \left( \frac{L}{L^1} \right) = W \frac{L}{L^1}$$

where  $\frac{L}{L^1}$  is the ratio of X and Y dimensions

$$M_X = \frac{\text{moment about } X = 0}{PaL^3}$$

$$M_Y = \frac{\text{moment about } Y = 0}{PaL^3}$$

$$F_X = \frac{12\mu RT}{Pa^2 C^3} * (\text{flow in } -X \text{ direction})$$

$$F_Y = \frac{12\mu RT}{Pa^2 C^3} * (\text{flow in } -Y \text{ direction})$$

R = gas constant

T = absolute temperature

The values of the moments can be utilized to evaluate the location of the center of pressure.

The computer program is coded by the FORTRAN IV language and is subdivided in

|                                    |         |
|------------------------------------|---------|
| a) main program                    | RINØ 10 |
| b) subroutine for matrix inversion | MATINV  |
| c) integrating function            | SUM     |
| d) clearance function              | HFUN    |
| e) X derivative of clearance       | HXFUN   |
| f) Y derivative of clearance       | HYFUN   |

```

$      FORTRAN DECK,LSTOU
C      RINO10
C      PROGRAM TO SOLVE STEP COMPRESS. BEAR. PROB. WITH FIXED
C      BOUNDARIES, LINES OF SYMMETRY,JOINTS IN ANY DIRECTION.
C      EQUATIONS ARE WRITTEN FOR PARALLEL FACES
C      ONLY. CLEARANCE ALLOWS ONE DEPRESSED AREA
C      ONLY.
C      KUE=0 REGULAR POINT OR CORNER OF DEPRESSED AREA OR LINE OF SUMM
C      KUE=1,2,3 KNOWN PRESSURE= PFIX(1,2,OR 3)
C      KUE=4 VERTICAL LINE OF STEP
C      KUE=5 HORIZONTAL LINE OF STEP
C      KUE=6 TOP JOINT
C      KUE=7 BOTTOM JOINT
C      KUE=8 LEFT JOINT
C      KUE=9 RIGHT JOINT
C      PROBLEM IS SOLVED COLUMNWISE. M (FIRST INDEX)
C      SHOULD BE SMALLER THAN N(SECOND INDEX)
C      X IN I DIRECTION (VERT. DOWN)
C      Y IN J DIRECTION (HOR. LEFT TO RIGHT)
C      PLAMX,PLAMY=X,Y, COMPONENTS OF PLAM
C      (IH,JH),(IHH,JHH) ARE CORNERS OF STOP BOUNDARY
C      STEDE=STEP DEPTH. WHERE NO STEP H=1
C      NDIG= NO OF DIGITS WANTED REPEATED TO TRUNCATE SOLUTION
C      LKOUNT IS THE MAXIMUM ALLOWABLE NUMBER OF ITERATIONS
C      IFLO= I COORDINATE OF THE LINE ACROSS WHICH Y-FLOW IS COMPUTED.
C      JFLO= J COORDINATE OF THE LINE ACROSS WHICH X-FLOW IS COMPUTED.
C      QREP=.TRUE. PUT OUT P2 AFTEREACH ITERATION
C      PPOUT=.TRUE. OUTPUT OF P2 AFTER CONVERGENCE
C      POUT=.TRUE. WANTED OUTPUT OF P.AFTER CONVERGENCE
C      NEWKUE=.TRUE. IF NEW KUE ARRAY IS READ IN
C      DIMENSION PFIX(3),KUE(17,33),QFIX(3),H(17,33),PF(17,33),
1Q(17,33),FF(17,33),F(17),A(17,17),B(17),C(33),E(15,15,34),
1QSM(17,17),G(17,34),R(15,15,33),S(17,33),QQ(33),PP(33),PX(33),
1PY(33),D(15,15,34),QQQ(33)
      LOGICAL JOINT, QREP,PPOUT,POUT,NEWKUE
      NAMELIST/OUTPUT/QREP,PPOUT,POUT,NEWKUE/INPUT/M,N,PLAMX,
1 PLAMY,YOX,IH,JH,IHH,JHH,STEDE,NDIG,PFIX,NCASE ,LKOUNT,IFLO,JFLO
1 FORMAT(1X70I1)
2 FORMAT(70I1)
3 FORMAT( 25H MATRIX IS SINGULAR AT J= I3,16H,CASE ABANDONED./1H1)
4 FORMAT( / 10(1X,F11.7))
5 FORMAT( //18H CASE CONVERGES TO I3,14H DIGITS AFTER I3,11H ITERATI
1ONS)
6 FORMAT(//23H.FINAL RESULTS FOR CASE I5//13H FORCE/AREA =E14.7,
1 64HCOO. OF CENTER OF PRESSURE IN PERCENTAGE OF SIDE
2DIMENSIONS = (E14.7,1H, E14.7,2H).)
7 FORMAT(46H0FLOW PER UNIT LENGTH IN X AND Y DIRECTIONS =(
11PE14.7,2H, 1PE14.7,1H)/)
8 FORMAT(29H0FINAL PRESSURE DISTRIBUTION. //)
9 FORMAT(25H0FINAL P**2 DISTRIBUTION. //)
11 FORMAT (6H1INPUT)
      NR=5
      NW=6
10 READ(NR,INPUT)
      WRITE(NW,11)
      WRITE(NW,INPUT)
      READ(NR,OUTPUT)
      WRITE(NW,OUTPUT)
      IF(.NOT.NEWKUE)GO TO 35
      DO 20 I= 1,M
20 READ(NR,2)(KUE(I,J),J=1,N)

```



```

      DO 30 I=1,M
      WRITE(NW,1)(KUE(I,J),J=1,N)
      DO 30 J=1,N
30    KUE(I,J)=KUE(I,J)+1
35    KOUNT=0
      NN=N-1
      MM=M-1
      DO 40 K=1,3
40    QFIX(K)= PFIX(K)*PFIX(K)
      DX=1./FLOAT(MM)
      DY=YOX/FLOAT(NN)
      SA=1./DX
      SB=1./DY
      SAA= SA*SA
      SBB=SB*SB
      SC=SAA+SBB
      SD=-2.*SC
      SJ= 2.*SAA
      SE=PLAMX/(2.*DX)
      SG=PLAMY/(2.*DY)
      SH= 2.*SA
      SI=2.*SB
      SK=2.*SBB
      DO 50 I=1,M
      DO 50 J=1,N
50    H(I,J)=1.0
      DO 60 I=IH,IHH
      DO 60 J=JH,JHH
60    H(I,J)=H(I,J)+STEDE
      DO 70 I=1,M
      DO 70 J=1,N
      Q(I,J)= 1
      PF(I,J)=-1./(H(I,J)*H(I,J))
      JOINT=.FALSE.
80    DO 90 I=2,MM
      IF(KUE(I,1).EQ.9.OR.KUE(I,1).EQ.10) JOINT=.TRUE.
90    CONTINUE
100   DO 130 I=1,M
      G(I,1)=0.
      DO 110 K=1,M
110   E(I,K,1)=0.
      IF(.NOT.JOINT) GO TO 130
      DO 120 K=1,M
      D(I,K,1)=0.
      IF( I.EQ.K)D(I,K,1)=1.0
120   CONTINUE
130   CONTINUE
      DO 370 J=1,N
      DO 310 I=1,M
      FF(I,J)=PF(I,J)/SQRT(ABS(Q(I,J)))
      F(I)=0.
      KU= KUE (I,J)
      GO TO(140,210,210,230,250,270,270,140,140),KU
140   B(I)=SBB-SG*FF(I,J)
      C(I)=SBB+SG*FF(I,J)
      DO 150 K=1,M
      A(I,K)=0.0
      IF(K.EQ.I)A(I,K)=SD
150   CONTINUE
      IF(JOINT) GO TO 180
      IF(J.NE.1) GO TO 160

```

```

      B(I)=0.
      C(I)=SK
160  IF (J.NE.N) GO TO 170
      C(I)=0.
      B(I)=SK
170  IF(I.EQ.1) GO TO 190
      IF(I.EQ.M) GO TO 200
180  SR= SE*FF(I,J)
      A(I,I+1)= SAA+SR
      A(I,I-1)=SAA-SR
      GO TO 310
190  A(I,I+1)=SJ
      GO TO 310
200  A(I,I-1)=SJ
      GO TO 310
210  KKU=KUE(I,J)-1
      B(I)=0.
      C(I)=0.
      F(I)=QFIX(KKU)
      DO 220 K=1,M
      A(I,K)=0.
      IF(I.EQ.K) A(I,K)=1.0
220  CONTINUE
      GO TO 310
230  HHH= H(I,J+1)**3
      HH = H(I,J-1)**3
      B(I)= -SB * HH
      C(I)= - SB * HHH
      DO 240 K=1,M
240  A(I,K)= 0.
      A(I,I)=SB*(HH+HHH)+PLAMY*(H(I,J+1)-H(I,J-1))/SQRT(ABS(Q(I,J)))
      GO TO 310
250  HH= H(I-1,J)**3
      HHH= H(I+1,J)**3
      B(I)=0.
      C(I)=0.
      DO 260 K=1,M
260  A(I,K)=0.0
      A(I,I)=(HH+HHH)/DX-PLAMX*(H(I-1,J)-H(I+1,J))/SQRT(ABS(Q(I,J)))
      A(I,I+1)= -HHH/DX
      A(I,I-1)= -HH/DX
      GO TO 310
270  B(I)=SBB-SG*FF(I,J)
      C(I)=SBB+SG*FF(I,J)
      DO 280 K=1,M
      A(I,K)=0.0
      IF(K.EQ.1) A(I,K)=SD
280  CONTINUE
      SR= SE*FF(I,J)
      IF( KU. EQ.8) GO TO 290
      IF( KU.EQ.7) GO TO 300
      GO TO 310
290  A(I,1)=SAA+SR
      A(I,I-1)=SAA-SR
      GO TO 310
300  A(I,M)=SAA-SR
      A(I,I+1)=SAA+SR
      GO TO 310
310  CONTINUE
      DO 320 I=1,M
      DO 320 K=1,M

```

```

320 QSMA(I,K)=A(I,K) + B(I)*E(I,K,J)
    CALL MATINV(QSMA,M,BB,0,DET,ID)
    GO TO (340,330),ID
340 DO 360 I=1,M
    G(I,J+1)=0.
    DO 360 K=1,M
    G(I,J+1)=G(I,J+1)+QSMA(I,K)*(F(K)-B(K)*G(K,J))
    E(I,K,J+1)=-QSMA(I,K)*C(K)
    IF(.NOT.JOINT) GO TO 360
    DUM=0.0
    DO 350 KK=1,M
350 DUM=DUM-QSMA(I,KK)*B(KK)*D(KK,K,J)
    D(I,K,J+1)=DUM
360 CONTINUE
370 CONTINUE
    DMA=0.0
    IF(JOINT) GO TO 410
    DO 380 I=1,M
    DMA=AMAX1(DMA,ABS(Q(I,N)-G(I,N+1)))
380 Q(I,N)=G(I,N+1)
    DO 400 JJ=2,N
    J=N+2-JJ
    DO 400 I=1,M
    DUM=0.0
    DO 390 K=1,M
390 DUM=DUM+E(I,K,J)*Q(K,J)
    DUM=DUM+G(I,J)
    DMA=AMAX1(DMA,ABS(DUM-Q(I,J-1)))
400 Q(I,J-1)=DUM
    GO TO 560
410 DO 420 I= 1,M
    DO 420 K=1,M
    QSMA(I,K)= -D(I,K,N+1)
    IF(I.EQ.K)QSMA(I,K)=QSMA(I,K)+1.0
420 CONTINUE
    CALL MATINV(QSMA,M,BB,0,DET,ID)
    GO TO (430,330),ID
330 WRITE(NW,3) J
    GO TO 10
430 DO 460 I=1,M
    DU= 0.0
    DO 450 K=1,M
    DUM= 0.0
    DO 440 KK=1,M
440 DUM=DUM+QSMA(I,KK)*E(KK,K ,N+1)
    R(I,K,N)=DUM
450 DU=DU+QSMA(I,K)*G(K,N+1)
460 S(I,N)=DU
    DO 490 JJ=2,N
    J= N+2-JJ
    DO 490 I=1,M
    DU=0.0
    DO 480 K=1,M
    DUM=0.0
    DO 470 KK=1,M
470 DUM= D(I,KK,J)*R(KK,K,N)+E(I,KK,J)*R(KK,K,J)+DUM
    R(I,K,J-1)=DUM
480 DU=DU+D(I,K,J)*S(K,N)+E(I,K,J)*S(K,J)
490 S(I,J-1)=DU+G(I,J)
    DMA=0.0
    DO 500 I=1,M

```

```

DO 500 K=1,M
  QSMA(I,K)=-R(I,K,1)
  IF(I.EQ.K)QSMA(I,K)= QSMA(I,K)+1.0
500 CONTINUE
  CALL MATINV(QSMA,M,BB,0,DET,ID)
  GO TO(510,330),ID
510 DO 530 I=1,M
  DU=0.0
  DO 520 K=1,M
  DU=DU+QSMA(I,K)*S(K,1)
  DMA=AMAX1(DMA,ABS(DU-Q(I,1)))
530 Q(I,1)=DU
  DO 550 J=2,N
  DO 550 I=1,M
  DU=0.0
  DO 540 K=1,M
  DU=DU+R(I,K,J)*Q(K,1)
  DU=DU+S(I,J)
  DMA= AMAX1(DMA,ABS(DU-Q(I,J)))
550 Q(I,J)=DU
560 IF(QREP) WRITE(NW,4)Q
  KOUNT=KOUNT+1
  IF(KOUNT.GE.LKOUNT)GO TO 561
  IF(DMA .GT. 10.0**FLOAT(-NDIG)
561 WRITE(NW,5)NDIG,KOUNT
  WRITE(NW,11)
  IF(PPOUT)WRITE(NW,9)
  DO 575 I=1,M
  IF(PPOUT)WRITE(NW,4)(Q(I,J),J=1,N)
  DO 570 J=1,N
570 Q(I,J)=SQRT(ABS(Q(I,J)))
575 CONTINUE
  IF(POUT)WRITE(NW,8)
  DO 576 I=1,M
  IF(POUT)WRITE(NW,4)(Q(I,J),J=1,N)
576 CONTINUE
  DO 590 I=1,M
  X= DX*FLOAT(I-1)
  DO 580 J=1,N
580 QQQ(J)=Q(I,J)
  PP(I)= SUM(QQQ,N,DY)
590 PX(I)= PP(I)*X
  DO 610 J=1,N
  Y= FLOAT(J-1)*DY
  DO 600 I=1,M
600 QQQ(I)= Q(I,J)
610 PY(J)=SUM(QQQ,M,DX)*Y
  FP= SUM(PP,M,DX)
  FX= SUM(PX,M,DX)
  XF =FX/FP
  FY= SUM(PY,N,DY)
  YF=FY/FP/YOX
  FP=FP/YOX
  WRITE(NW,6) NCASE,FP,XF,YF
  DO 620 I=1,M
620 PP(I)=Q(I,JFLO)*H(I,JFLO)*(-PLAMY+H(I,JFLO)**2
  1*(Q(I,JFLO+1)-Q(I,JFLO-1))/(2.*DY))
  FLOY=SUM(PP,M,DX)
  DO 630 J=1,N
630 PP(J)=Q(IFLO,J)*H(IFLO,J)*(-PLAMX+H(IFLO,J)**2
  1*(Q(IFLO+1,J)-Q(IFLO-1,J))/(2.*DX))
  FLOX=SUM(PP,N,DY)/YOX
  WRITE(NW,7) FLOX,FLOY
  GO TO 10
END

```

)GO TO 100

```
S      FORTRAN DECK,LSTOU
S      INCODE  IBMF
      FUNCTION SUM(P,M,DX)
      DIMENSION P(33)
      K=2
      KK=M-1
      KKK=2
      SUM=0.0
10 DO 20 I=K, KK, KKK
20 SUM=SUM+P(I)
      GO TO (30,40,50),K
30 SUM=SUM*DX/3.0
      RETURN
40 K=3
45 SUM=2.0*SUM
      GO TO 10
50 K=1
      KK=M
      KKK=M-1
      GO TO 45
      END
```

```

$      FORTRAN DECK,LSTOU
$      INCODE  IBMF
C      MATRIX INVERSION WITH ACCOMPANYING SOLUTION OF LINEAR EQUATIONS  MA
C      NOVEMBER 1692  S GOOD  DAVID TAYLOR MODEL BASIN  AM MAT1  MA
C  MA
C      SUBROUTINE MATINV(A,N1,B,M1,DETERM,ID)  MA
C  MA
C      GENERAL FORM OF DIMENSION STATEMENT  MA
C  MA
C      DIMENSION A(17,17),B(17,1),INDEX(17,3)
C      EQUIVALENCE (IROW,JROW), (ICOLUMN,JCOLUMN), (AMAX, T, SWAP)  MA
C  MA
C      INITIALIZATION  MA
C  MA
C      M=M1
C      N=N1
C      10 DETERM=0.0
C      15 DO 20 J=1,N  MA
C      20 INDEX(J,3) = 0  MA
C      30 DO 550 I=1,N  MA
C  MA
C      SEARCH FOR PIVOT ELEMENT  MA
C  MA
C      40 AMAX=0.0
C      45 DO 105 J=1,N  MA
C      IF(INDEX(J,3)-1) 60, 105, 60  MA
C      60 DO 100 K=1,N  MA
C      IF(INDEX(K,3)-1) 80, 100, 715  MA
C      80 IF ( AMAX -ABS (A(J,K))) 85, 100, 100  MA
C      85 IROW=J  MA
C      90 ICOLUMN=K  MA
C      AMAX = ABS (A(J,K))  MA
C      100 CONTINUE  MA
C      105 CONTINUE  MA
C      INDEX(ICOLUMN,3) = INDEX(ICOLUMN,3) +1  MA
C      260 INDEX(I,1)=IROW  MA
C      270 INDEX(I,2)=ICOLUMN  MA
C  MA
C      INTERCHANGE ROWS TO PUT PIVOT ELEMENT ON DIAGONAL  MA
C  MA
C      130 IF (IROW-ICOLUMN) 140, 310, 140  MA
C      140 DETERM=-DETERM  MA
C      150 DO 200 L=1,N  MA
C      160 SWAP=A(IROW,L)  MA
C      170 A(IROW,L)=A(ICOLUMN,L)  MA
C      200 A(ICOLUMN,L)=SWAP  MA
C      IF(M) 310, 310, 210  MA
C      210 DO 250 L=1, M  MA
C      220 SWAP=B(IROW,L)  MA
C      230 B(IROW,L)=B(ICOLUMN,L)  MA
C      250 B(ICOLUMN,L)=SWAP  MA
C  MA
C      DIVIDE PIVOT ROW BY PIVOT ELEMENT  MA
C  MA
C      310 PIVOT =A(ICOLUMN,ICOLUMN)  MA
C      DETERM=DETERM*PIVOT  MA
C      330 A(ICOLUMN,ICOLUMN)=1.0  MA
C      340 DO 350 L=1,N  MA
C      350 A(ICOLUMN,L)=A(ICOLUMN,L)/PIVOT  MA
C      355 IF(M) 380, 380, 360  MA
C      360 DO 370 L=1,M  MA

```

PAGE NO. 166

## APPENDIX C

CENTER OF PRESSURE, HYDROSTATIC STEP  
COMPUTER PROGRAM

```

C      BASIC STEP-SEAL, ADDED CENTER OF PRESSURE, 1-12-66
C      NH=NO OF HBA, KCN=NO. OF SETS BAR=B1/B AND R
C      INP=CONTROL OF INPUT, INP=0 MORE CASES TO FOLLOW, INP=1, LAST CASE
C      HBA=H1/(H2-H1), R=P1/P2
C      TLC= LIMIT VALUE OF (1-PI) BELOW WHICH PRESS IS LINEARIZED
      DIMENSION HBA(50), BAR(50), RR(50)
12 READ 101
   READ 102, NH, KCN, INP
   READ 103, TLC
   READ 103, (HBA(I), I=1, NH)
   READ 103, (BAR(I), RR(I), I=1, KCN)
   PUNCH 100
   PUNCH 101
   PUNCH 104
   PUNCH 105, NH, KCN, INP
   DO 502 K=1, KCN
     B1B=BAR(K)
     R=RR(K)
     PUNCH 106, B1B, R
     R2=R*R
     FF=(1.0-R)*1.5
     FF=1.0/FF
     B2B=1.0-B1B
     BB2=B2B/B1B
     PUNCH 109
     DO 501 J=1, NH
       H=HBA(J)
503 H1=1.0+H
       H2=H1*H1
       H3=H2*H1
       B2=H*H
       B3=B2*H
       C1=BB2*B3
       DD=C1+H3
       EE=C1*R2+H3
       CC2=EE/DD
       CC=SQRTF(CC2)
       C3=CC+1.0
       C4=(CC2+C3)/C3
       C5=CC+R
       C6=(2.0*CC2-C5*R)/C5
       W=B2B*(C4*2.0-R*3.0)+B1B*C6
       W=W/2.0*FF
       FM1=CC2-R2
       FM=FM1/B1B
       RM1=1.-R
       B1BS=B1B*B1B
       B2BS=B2B*B2B
       PI3=CC2*CC
       DM1=R*B1B
       AM1=B1BS*((3.*R2-5.*CC2)*R2*R+2.*PI3*CC2)
       AM1=AM1*.2666666/ (FM1)**2-DM1*(2.-B1B)

```



```

1   +1.333333*B1B*B2B*(CC2+R*C5 )/C5
    AM1=AM1/RM1
    DIFC=1.-CC
    IF (DIFC-TLC) 30,30, 34
30  AM2=B2BS-DIFC*FF
    GO TO 36
34  AM2=((3.*CC2-5.)*PI3+2.)*.2666666/(1.-CC2)**2
    AM2=(AM2-R)*B2BS/RM1
36  XBAR=(AM1+AM2)/W*.5
    C1=BB2*B2
    DRH=(C1*R2+H2)*DD-(C1+H2)*EE
    DRH=DRH/DD*1.5/DD/CC
    C1=C3*C3
    C2=C5*C5
    C7=(CC2+2.0*CC)/C1*B2B
    WR=(CC2+2.0*CC*R)/C2*B1B
    WR=(C7+WR)*FF
    WH=DRH*WR
    IF (SENSE SWITCH 1 ) 40,42
40  PUNCH 103,AM1,AM2
42  PUNCH 103,H,W,WH,FM,XBAR,CC
501 CONTINUE
    PUNCH 108
502 CONTINUE
201 IF (INP) 202,12,202
202 STOP
100 FORMAT( 31H HYDRO-STATIC, BASIC STEP-SEAL /)
101 FORMAT(72H0
1
102 FORMAT(5I5)
103 FORMAT(6(1X1PE11.4))
105 FORMAT(3X14,6X14,6X14,6X14,6X14)
104 FORMAT(28HONO OF HBAR SETS B-R INP )
106 FORMAT(7H0 B1/B=,E13.6,6H R=,E13.6)
108 FORMAT(1H1)
109 FORMAT(66H H1/(H2-H1) WBAR DW/DHBAR MBAR XBAR
1 PI )
END

```

## APPENDIX D

PRESSURE AND FLOW, SPIRAL GROOVE  
COMPUTER PROGRAM

```

C      PRESSURE AND MASS FLOW RELATIONSHIP, SPIRAL-GROOVED SEAL
C      INPUT
C      AMK=LAMBDA*K1 (LAMBDA=COMPRESSIBILITY NUMBER, K1=GROOVE CONSTANT)
C      F3WW=DIMENSIONAL ARRAY OF F3W (F3W=MBAR/LAMBDA)*K1
C      EPS=CONVERGENCE CRITERION OF SOLVING P2/P1 IN AN IMPLICIT EQUATION
C      OF P2/P1 AND MBAR FOR A GIVEN MBAR
C      NRUN=NO. OF CASES TO BE CALCULATED, NF3W= NO. OF F3W TO BE CALCUL.
C      OUTPUT
C      AMK,K3W (K3W=F3W*K2/K1, K2=GROOVE CONSTANT), P2/P1, MBAR
C      MBAR=DIMENSIONLESS FLOW
C      DIMENSION F3WW(60)
      READ 2, EPS
      READ 1,NRUN
      PUNCH 3
      DO 32 NR=1,NRUN
      READ 4,NF3W,AMK
      READ 2,(F3WW(N),N=1,NF3W)
      DO 32 K=1,NF3W
      F3W=F3WW(K)/AMK
      I=1
      P=AMK*(1.0-F3W)+1.0
10    TEMP=(P-F3W)/(1.-F3W)
      IF(TEMP)35,11,11
11    FE=AMK-(P-1.0)-F3W*LOGF(TEMP)
      DFE= -1.0-F3W/(P -F3W)
      DP= -FE/DFE
      ADP= ABSF(DP/P)
      IF(ADP-EPS) 30,30,20
20    IF(I-50)22,36,36
22    I=I+1
      IF(SENSE SWITCH 1) 25,26
25    PUNCH 2,P,DP,FE,DFE
26    P=P+DP
      GO TO 10
30    PUNCH 2,AMK,F3W,P ,F3WW(K)
      GO TO 32
35    PUNCH 5,TEMP
      PUNCH 3
      GO TO 30
36    PUNCH 6,I
      PUNCH 3
      GO TO 30
32    CONTINUE
31    STOP
      1 FORMAT(1H ,15I5)
      2 FORMAT(1H ,6E12.5)
      3 FORMAT(8H K1LAMBDA 5X 3HK3W 9X 5HP2/P1 7X 4HMBAR)
      4 FORMAT(15, E12.5)
      5 FORMAT(34H NEGATIVE LOG (P-F3W)/(1.-F3W)=      ,E12.5)
      6 FORMAT(15H DIVERGE I=      ,15)
      END

```

## BIBLIOGRAPHY

Eckert, E.R. and Robert M. Drake, Jr., "Heat and Mass Transfer," McGraw-Hill Book Co., New York, 1959

Fuller, Dudley D., "Theory and Practice of Lubrication for Engineers," John Wiley & Sons, Inc., New York, 1956

Grassam, N.S. and J.W. Powell, "Gas Lubricated Bearings," Butterworth, Inc., London, 1964

Jakob, Max and George Hawkins, "Elements of Heat Transfer," third edition, John Wiley & Sons, Inc., New York, 1958

Lave, J.H., "Hydrostatic Gas Bearings," California Institute of Technology Progress Report No. 20-353 Pasadena, 1958

McAdams, William H., "Heat Transmission," McGraw-Hill Book Co., New York, 1942

Pinkus, Oscar and Beno Sternlicht, "Theory of Hydrodynamic Lubrication," McGraw-Hill Book Co., New York, 1961

Shapiro, A.H., "The Dynamics and Thermodynamics of Compressible Fluid Flow, Vol. 1" The Ronald Press Co., New York, 1953

Wildman, M., "Grooved Plate Gas Lubricated Thrust Bearings, with Special References to the Spiral Groove Bearing," Ampex Corporation, Prepared under Contract No. NoNR-3815(00), Fluid Dynamics Branch, ONR, RR 64-1, Jan. 1964

Keenan, J.H. and J. Kaye, "Gas Tables", John Wiley & Sons, New York 1961

Schlichting, H., "Boundary Layer Theory," Fourth Edition, McGraw-Hill, New York, 1960

Arwas, E.B. and Sternlicht, B., "Viscous Shear Compressor," Mechanical Technology Incorporated, Technical Report MTI 62TR21

Lund, J.W., "Gas Bearing Design Methods Vol. 2," Mechanical Technology Incorporated Technical Report, MTI 65TR5-II

Cheng, H.S., Chow, C.Y., and Murray S.F., "Gas Bearing Design Methods Vol. I", Mechanical Technology Incorporated Technical Report, MTI 65TR5-II

Tang, I.C., and Gross, W.A., "Analysis and Design of Externally Pressurized Gas Bearings", ASLE Trans. 5, 261-285 (1962)

## REFERENCES

1. Arwas, E. B., and B. Sternlicht, "Viscous Shear Compressor," MTI-62TR21, (September, 1962).
2. Timoshenko, S., Strength of Materials, Part II, D. Van Nostrand Co., Inc. Third Edition, 1956.
3. Hsing, F. and T. Chiang, "Discharge Coefficient of Orifices and Nozzles," Mechanical Technology Inc. Technical Memo MTI-65TM7.
4. Castelli, V. and J. Pirvics, "Equilibrium Characteristics of Axial-Groove Gas-Lubricated Bearings," ASME 65-LUB-16, (1965).
5. Arwas, E. B. and Sternlicht, B., "Viscous Shear Compressor", Mechanical Technology Incorporated, Technical Report MTI-62TR21.
6. Lund, J. W., "Gas Bearing Design Methods Vol. 2", Mechanical Technology Incorporated Technical Report, MTI-65TR5-II.
7. Cheng, H. S., Chow, C. Y., and Murray, S. F., "Gas Bearing Design Methods Vol. I", Mechanical Technology Incorporated Technical Report, MTI-65TR5-II.
8. Tang, I. C., and Gross, W. A., "Analysis and Design of Externally Pressurized Gas Bearings", ASLE Trans. 5, 261-285 (1962).

## Appendix B

9. Castelli, V. and J. Pirvics, "Equilibrium Characteristics of Axial-Groove Gas-Lubricated Bearings," ASME 65-LUB-16, (1965).

Semiannual Reports Distribution List  
NAS 3-7605Addressee

1. NASA-Lewis Research Center  
Spacecraft Technology  
Procurement Section  
Attention: John H. DeFord
2. NASA-Lewis Research Center  
Spacecraft Technology Division  
Attention: J. Howard Childs  
W.H. Roudebush  
D.P. Townsend (3)
3. NASA-Lewis Research Center  
Technical Utilization Office  
Attention: John Weber
4. NASA-Lewis Research Center  
Reports Control Office
5. NASA-Lewis Research Center  
Attention: Library
6. NASA-Scientific and Technical Information Facility (6)  
Box 5700  
Bethesda, Maryland  
Attention: NASA Representative
7. NASA-Lewis Research Center  
Fluid System Components Division  
Attention: I. I. Pinkel  
E. E. Disson  
R. L. Johnson  
W. R. Loomis  
L. P. Ludwig  
N. A. Swikert  
T. B. Shillito  
H. J. Hartmann
8. Air Force Materials Laboratory  
Wright-Patterson Air Force Base, Ohio  
Attention: MANL, R. Adamczak  
MANE, R. Headrick and J. N. Keible  
MAAE, P. House
9. Air Force Systems Engineering Group  
Wright-Patterson Air Force Base, Ohio  
Attention: SESMS, J. L. Wilkins  
SEJPF, S. Prete
10. Air Force Aero Propulsion Laboratory  
Wright-Patterson Air Force Base, Ohio  
Attention: AFAPL (APFL), K. L. Berkey & L.  
DeBrahum  
AFAPL (APTC), C. Simpson  
APTP, I. J. Gershon
11. FAA Headquarters  
800 Independence Avenue, S. W.  
Washington, D.C.  
Attention: J. Chavkin SS/120  
M. Lott FS/141
12. NASA Headquarters  
Washington, D.C. 20546  
Attention: N. F. Rekos (RAP)  
A. J. Evans (RAD)  
J. Maltz (RRM)
13. NASA-Langley Research Center  
Langley Station  
Hampton, Virginia 23365  
Attention: Mark R. Nichols
14. Mechanical Technology, Incorporated  
968 Albany-Shaker Road  
Latham, New York  
Attention: D. Wilcock
15. Clevite Corporation  
Cleveland Graphite Bronze Division  
17000 St. Clair Avenue  
Cleveland, Ohio 44110  
Attention: T. H. Koenig
16. Koppers Company, Incorporated  
Metal Products Division  
Piston Ring and Seal Department  
Baltimore 3, Maryland  
Attention: T. C. Kuchler
17. Stein Seal Company  
20th Street and Indiana Avenue  
Philadelphia 32, Pennsylvania  
Attention: Dr. P. C. Stein
18. Wright Aeronautical Division  
Curtiss-Wright Corporation  
333 West 1st Street  
Dayton 2, Ohio  
Attention: S. Lombardo
19. TRW, Incorporated  
23555 Euclid Avenue  
Cleveland, Ohio 44117  
Attention: O. Decker
20. General Electric Company  
Advanced Engine and Technology Department  
Cincinnati, Ohio 45215  
Attention: L. B. Venable  
G. J. Wile
21. Huyck Metals Company  
P.O. Box 30  
45 Woodmont Road  
Milford, Connecticut  
Attention: J. L. Fisher
22. Aerojet-General Corporation  
20545 Center Ridge Road  
Cleveland, Ohio 44116  
Attention: W. L. Snapp
23. Lycoming Division  
Avco Corporation  
Stratford, Connecticut  
Attention: R. Cuny
24. Battelle Memorial Institute  
505 King Avenue  
Columbus 1, Ohio  
Attention: C. M. Allen
25. Bendix Corporation  
Fisher Building  
Detroit 2, Michigan  
Attention: R. H. Isaccs
26. Boeing Aircraft Company  
224 N. Wilkinson  
Dayton, Ohio 45402  
Attention: H. W. Walker

Addressee

27. Douglas Aircraft Company  
Holiday Office Center  
16501 Brookpark Road  
Cleveland, Ohio 44135  
Attention: J. J. Pakiz
28. General Dynamics Corporation  
16501 Brookpark Road  
Cleveland, Ohio 44135  
Attention: George Vila
29. General Motors Corporation  
Allison Division  
Plant #8  
Indianapolis, Indiana  
Attention: E. H. Deckman
30. Lockheed Aircraft Company  
16501 Brookpark Road  
Cleveland, Ohio 44135  
Attention: Mr. L. Kelly
31. Martin Company  
16501 Brookpark Road  
Cleveland, Ohio 44135  
Attention: Z. G. Horvath
32. North American Aviation  
16501 Brookpark Road  
Cleveland, Ohio 44135  
Attention: George Bremer
33. Fairchild-Hiller Corporation  
Republic Aviation Division  
Farmingdale, Long Island  
New York 11735  
Attention: D. Schroeder
34. Westinghouse Electric Corporation  
55 Public Square  
Cleveland, Ohio 44113  
Attention: Lynn Powers
35. I.I.T. Research Foundation  
10 West 35 Street  
Chicago, Illinois 60616  
Attention: Dr. Strohmeler
36. Pesco Products Division  
Borg-Warner Corporation  
24700 N. Niles  
Bedford, Ohio
37. Stanford Research Institute  
Menlo Park, California  
Attention: R. C. Fey
38. Franklin Institute Laboratories  
20th and Parkway  
Philadelphia 3, Pennsylvania  
Attention: J. V. Carlson
39. Industrial Tectonics  
Box 401  
Hicksville, New York 11801  
Attention: J. Cherubin
40. Sealol Incorporated  
P.O. Box 2158  
Providence 5, Rhode Island  
Attention: Justus Stevens
41. Continental Aviation and Engineering  
12700 Kercheval  
Detroit 15, Michigan  
Attention: A. J. Fallman
42. Northrop Corporation  
1730 K. Street, N.W.  
Suite 903-5  
Washington 6, D.C.  
Attention: S. W. Fowler, Jr.
43. Chicago Rawhide Manufacturing Company  
1311 Elston Avenue  
Chicago, Illinois  
Attention: R. Blair
44. Midwest Research Institute  
425 Volker Blvd.  
Kansas City 10, Missouri  
Attention: V. Hopkins
45. Southwest Research Institute  
San Antonio, Texas  
Attention: P. M. Ku
46. E. I. DuPont de Nemours and Company  
1007 Market Street  
Wilmington 98, Delaware  
Attention: A. J. Cheney  
R. J. Laux
47. Fairchild Engine and Airplane Corporation  
Stratos Division  
Bay Shore, New York
48. Borg-Warner Corporation  
Roy C. Ingersoll Research Center  
Wolf and Algonquin Roads  
Des Plaines, Illinois
49. U.S. Naval Air Material Center  
Aeronautical Engine Laboratory  
Philadelphia 12, Pennsylvania  
Attention: A. L. Lockwood
50. Department of the Navy  
Bureau of Naval Weapons  
Washington, D.C.  
Attention: A. B. Nehman, RAAE-3  
C. C. Singleterry, RAPP-4
51. Department of the Navy  
Bureau of Ships  
Washington 25, D.C.  
Attention: Harry King, Code 634-A
52. SKF Industries, Incorporated  
1100 First Avenue  
King of Prussia, Pennsylvania  
Attention: L. B. Sibley
53. Crane Packing Company  
6400 W. Oakton Street  
Norton Groove, Illinois  
Attention: Harry Tankus
54. B. F. Goodrich Company  
Aerospace and Defense Products Division  
Troy, Ohio  
Attention: L. S. Blaikowski

Addressee

55. The University of Tennessee  
Department of Mechanical and Aerospace  
Engineering  
Knoxville, Tennessee  
Attention: Professor W. K. Stair
56. Hughes Aircraft Company  
International Airport Station  
P.O. Box 90515  
Los Angeles 9, California
57. U. S. Navy Marine Engineering Lab.  
Friction and Wear Division  
Annapolis, Maryland  
Attention: R. B. Snapp
58. Metal Bellows Corporation  
20977 Knapp Street  
Chatsworth, California  
Attention: Sal Artino
59. Rocketdyne  
6633 Canoga Avenue  
Canoga Park, California  
Attention: M. Butner
60. Carbon Products Division of Union Carbide  
Corporation  
270 Park Avenue  
New York 17, New York  
Attention: J. Cureau
61. Garlock, Incorporated  
Palmyra, New York 14522  
Attention: E. W. Fisher
62. Chemicals Division of Union Carbide Corp.  
Technical Service Lab.  
P.O. Box 65  
Tarrytown, New York  
Attention: J. C. Haaga
63. Durametallic Corporation  
Kalamazoo, Michigan  
Attention: H. Hummer
64. Morganite, Incorporated  
33-02 48th Avenue  
L.I.C. 1, New York  
Attention: S. A. Rokaw
65. United States Graphite Company  
1621 Holland  
Saginaw, Michigan  
Attention: F. F. Ruhl
66. Cartiseal Corporation  
3515 West Touhy  
Lincolnwood, Illinois  
Attention: R. Voitik
67. Department of the Army  
U. S. Army Aviation Material Laboratory  
Fort Eustis, Virginia 23604  
Attention: John W. White, Chief  
Propulsion Division